VNIVERSITAT DE VALÈNCIA Facultat de Ciències Biològiques

DOCTORAL THESIS
TESIS DOCTORAL

Sirena Soriano Rodríguez

2015

STUDY OF FRATAXIN DEFICIT IN DROSOPHILA

ESTUDIO DEL DÉFICIT DE FRATAXINA EN DROSOPHILA

Supervised by:
María Dolores Moltó Ruiz
María José Martínez Sebastián

VNIVERSITAT DE VALÈNCIA

PhD program In Biotechnology

VNIVERSITAT DE VALÈNCIA
Facultat de Ciències Biològiques
Departament de Genètica

La Dra M. Dolores Moltó Ruiz y la Dra M. José Martínez Sebastián, Profesoras Titulares del Departamento de Genética de la Facultad de Ciencias Biológicas de la Universitat de València,

INFORMAN:

Que Doña Sirena Soriano Rodríguez, licenciada en Ciencias Biológicas, ha realizado bajo su dirección en el departamento de Genética de la Facultad de Ciencias Biológicas de la Universitat de València, el trabajo titulado: **"Estudio del déficit de frataxina en *Drosophila*",** y consideran que reúne las condiciones necesarias para optar al grado de Doctora por la Universitat de València.

Valencia, 30 de Octubre de 2015

Fdo. Directora
M. Dolores Moltó Ruiz

Fdo. Codirectora
M. José Martínez Sebastián

This work was supported by grants from the European Community's Seventh Framework Program FP7/2007-2013 [grant agreement no. 242193 EFACTS] and from the Fundació la Marató TV3 of Spain [exp 101932].
The author, Sirena Soriano Rodríguez was the recipient of a fellowship from Ministerio de Ciencia e Innovación of Spain [AP2007-04050].

Table of contents

Resumen

Introducción

La ataxia de Friedreich (AF) es la ataxia hereditaria más común en la población de origen europeo, con una prevalencia de 2-4:100.000 (Palau y Espinós 2006). Se trata de una enfermedad neurodegenerativa que afecta principalmente al sistema nervioso central y periférico. Además de los síntomas neurológicos, los pacientes presentan cardiomiopatía hipertrófica, que constituye la causa frecuente de muerte prematura. También pueden presentar intolerancia a carbohidratos y diabetes mellitus en un 20% y 10% de los casos respectivamente. Actualmente no se dispone de cura ni de tratamiento efectivo para la enfermedad, pero diversas estrategias terapéuticas se encuentran en proceso de investigación y ensayo clínico.

La AF está causada por la expansión del triplete GAA en el primer intrón del gen *FXN* que produce una reducción importante de los niveles de la frataxina (Campuzano *et al.* 1996), cuya función se ejerce fundamentalmente en la mitocondria (Koutnikova *et al.* 1997). No obstante, no hay consenso en cuanto a la función exacta de esta proteína pero parece que está implicada en la homeostasis del hierro, en concreto en la formación de los grupos Fe-S (revisado en Pastore y Puccio 2013). De hecho, la falta de frataxina produce un déficit en la actividad de los enzimas que requieren un centro ferrosulfurado para su función. Otras características de la patología molecular de la AF incluyen la acumulación de hierro intramitocondrial acompañado de déficit de hierro en el citoplasma, disfunción mitocondrial y daño oxidativo (Babcock *et al.* 1997; Rötig *et al.* 1997; Puccio *et al.* 2001; Li *et al.* 2008).

La frataxina es una proteína altamente conservada en la evolución, con ortólogos en todos los eucariotas y gran parte de los procariotas (Gibson *et al.* 1996; Adinolfi *et al.* 2002). El mutante de frataxina en levadura es viable, pero la ausencia de esta proteína en organismos superiores es letal (Rötig *et al.* 1997). Se han obtenido distintos modelos de AF en ratón basados en estrategias de "knockout" condicional donde la falta de frataxina está limitada a ciertos tejidos como el neural o el cardiaco (Puccio *et al.* 2001), la inserción de una expansión del triplete GAA en el gen endógeno *Fxn* (Miranda *et al.* 2002), o mediante la transgénesis de alelos mutados del gen humano *FXN*

(Pook *et al.* 2001). También se dispone de diversos modelos celulares, incluyendo los desarrollados a partir de células de pacientes como linfoblastos y fibroblastos (Rötig *et al.* 1997).

El ortólogo de *FXN* en *Drosophila*, *fh* (*frataxin homolog*) codifica para una proteína de 190 amino ácidos que muestra una elevada similitud con el resto de ortólogos de frataxina (Cañizares *et al.* 2000). Actualmente hay dos modelos de AF en *Drosophila* que recapitulan las características patológicas y bioquímicas de la enfermedad. Estos modelos fueron obtenidos mediante el sistema de RNA de interferencia (RNAi) para el silenciamiento de *fh*, combinado con el sistema UAS-GAL4 que permite el control espacio temporal de su expresión. En el primero de ellos, la expresión ubicua del transgen *fh*RNAi-1 produce una reducción del 90% de los niveles de frataxina que causa letalidad en el estado pre-adulto (Anderson *et al.* 2005). El segundo de los modelos de AF en la mosca induce una reducción del 70% en los niveles de frataxina cuando se expresa ubicuamente la construcción *fh*RNAi-2. Estos mutantes funcionales de falta de frataxina presentan una disminución de supervivencia y de capacidad locomotora, que se agravan en condiciones de elevado estrés oxidativo (hiperoxia), y a nivel bioquímico, una reducción de la actividad aconitasa (Llorens *et al.* 2007).

Objetivos

El objetivo principal de esta tesis es continuar la caracterización del modelo de AF en *Drosophila* obtenido en nuestro laboratorio, para contribuir al estudio de la función de frataxina y de la fisiopatología de la enfermedad, así como para la búsqueda de marcadores biológicos y estrategias terapéuticas. Para ello, definimos los siguientes objetivos específicos en esta tesis: (1) demostrar la equivalencia funcional entre las frataxinas humana y de *Drosophila*; (2) evaluar la validez del modelo de AF en *Drosophila* para el rastreo de fármacos, mediante el análisis del efecto de los compuestos deferiprona e idebenona; (3) identificar modificadores de los fenotipos inducidos por la falta de frataxina por medio de un rastreo de genes candidatos y (4) determinar el efecto de la falta de frataxina en la homeostasis de los metales.

Metodología y resultados

1. Equivalencia funcional de las frataxinas humana y de *Drosophila* (Navarro *et al.* 2011, figuras 4 y 5)

Para demostrar la equivalencia funcional de ambas proteínas, en este trabajo se evaluó si la proteína humana podía reemplazar funcionalmente a la frataxina endógena en *Drosophila*. Para ello se generó un transgen que contiene la región codificante de *FXN* bajo el control de la secuencia UAS. Después se obtuvieron moscas que portaban esta construcción UAS-*FXN* y también la construcción de RNA de interferencia UAS-*fh*RNAi-1, expresadas de forma ubicua con *actina*-GAL4. La expresión de *FXN* en la mosca revirtió la reducción de la actividad aconitasa observada en las larvas *actina*-GAL4>UAS-*fh*RNAi-1 (Anderson *et al.* 2005), demostrando la equivalencia funcional de ambas proteínas.

La sobrexpresión de la frataxina endógena en *Drosophila* produce una reducción en la actividad aconitasa junto con otros fenotipos patogénicos como reducción de la supervivencia o de la habilidad motora. De forma similar, la sobrexpresión de la frataxina humana reduce la actividad aconitasa de las larvas *UAS*-FXN. Se ha descrito que la frataxina de levadura puede formar oligomeros de distintos tamaños y que un aumento de la oligomerización sería la responsable de los déficits funcionales de las proteínas con centros Fe-S (Seguin *et al.* 2009). Por ello, consideramos la posibilidad de que la frataxina humana estuviera produciendo oligomeros o quizá formando algún tipo de agregados tóxicos que redujeran la cantidad de proteína funcional en *Drosophila*. Para comprobar esta hipótesis se realizó una cromatografía de filtración en gel. Mediante esta técnica se recuperó el total de la frataxina humana expresada en *Drosophila* en forma de monómero. La ausencia de oligomeros o agregados indica que el mecanismo de toxicidad de la sobrexpresión de frataxina es de otro tipo, posiblemente una saturación del sistema por exceso de proteína o quizá el secuestro de proteínas que interaccionen con frataxina.

2. La deferiprona y la idebenona rescatan fenotipos inducidos por la falta de frataxina en *Drosophila* (Soriano *et al.* 2013).

Debido a la presencia de acúmulos de hierro en corazón, cerebro y otros tejidos de pacientes de AF (Bradley *et al.* 2000), se propuso la quelación de hierro como estrategia terapéutica para la enfermedad. El quelante de hierro deferiprona (DFP) produjo resultados prometedores en los primeros ensayos clínicos en pacientes en forma de reducción de la acumulación de hierro o mejoría de la ataxia (Boddaert *et al.* 2007; Kakhlon *et al.* 2008). Evaluamos el efecto de dos concentraciones de DFP (60 y 163 μM) administradas o bien en el estadio de larva o bien a los individuos adultos, sobre los fenotipos de nuestro modelo en *Drosophila* de AF. Cuando la DFP se administró de forma temprana, se observó una mejoría de la supervivencia y la habilidad motora de las moscas *actina*-GAL4>UAS-*fh*RNAi-2, siendo en general más efectiva la concentración más alta del compuesto. Dicha concentración de DFP también produjo la mejoría de la capacidad de escalada de los individuos *neuralized*-GAL4>UAS-*fh*RNAi-2, que presentan una reducción de los niveles de frataxina en el sistema nervioso periférico (Llorens *et al.* 2007). A continuación caracterizamos el efecto de la DFP sobre los niveles de hierro de las moscas modelo de AF. Encontramos que los niveles de hierro mitocondrial estaban aumentados en las moscas *actina*-GAL4>UAS-*fh*RNAi-2, mientras que la forma ferrosa del hierro en la fracción soluble se encontraba disminuida. Esto puede ser indicativo de la existencia de agregados de hierro insolubles. En cuanto al efecto de la DFP, el quelante produjo un aumento de los niveles de hierro férrico y ferroso solubles, lo que sugiere que evita la formación de la forma insoluble tóxica.

El aumento de los niveles de estrés oxidativo se ha descrito en pacientes de AF y en diversos modelos de la enfermedad (Rötig *et al.* 1997). Esto llevó a proponer el uso de antioxidantes como terapia que contrarrestara dicho daño oxidativo. La idebenona (IDE) es un antioxidante análogo a la coenzima Q10 que se utilizó en ensayos clínicos para la AF, en los que se describió una estabilización neurológica en pacientes pediátricos (Meier *et al.* 2012). Evaluamos también el efecto de la IDE sobre el fenotipo de las moscas modelo de AF, utilizando la misma estrategia que para la DFP, siendo en este caso las

concentraciones de 7 y 15 µM. Ambas concentraciones produjeron una mejora de la supervivencia y la capacidad de escalada tanto cuando el déficit de frataxina era ubicuo como cuando se restringió al sistema nervioso periférico. Como la actividad aconitasa es especialmente sensible al estrés oxidativo y se encuentra reducida en las moscas *actina*-GAL4>UAS-*fh*RNAi-2 en hiperoxia (Llorens *et al.* 2007), utilizamos este fenotipo para evaluar el efecto antioxidante de la IDE y observamos que dicho compuesto pudo recuperar la actividad aconitasa hasta los niveles del control. Estos resultados de rescate de los fenotipos de AF en el modelo de *Drosophila* constituyen una validación para su uso en futuros rastreos de moléculas terapéuticas.

3. Rastreo genético de modificadores de fenotipos inducidos por falta de frataxina en *Drosophila*

Una de las ventajas del uso de *Drosophila* como organismo modelo es la posibilidad de realizar rastreos genéticos a gran escala. Por este motivo, llevamos a cabo un rastreo de genes modificadores en nuestro modelo de AF en *Drosophila*. Seleccionamos 209 genes candidatos que incluían (1) rutas implicadas en la patogénesis de la enfermedad como la homeostasis de los metales, el estrés oxidativo y la autofagia; (2) proteínas que se encontraron diferencialmente expresadas en las moscas con déficit de frataxina en un estudio de proteómica realizado en el laboratorio y (3) modificadores obtenidos mediante rastreos genéticos en modelos en *Drosophila* de otras enfermedades neurodegenerativas. La línea *fh*RNAi-2 */ fh*RNAi-2 *; actin-GAL4 / TM6B , tub-GAL80* se cruzó con una serie de líneas disponibles comercialmente con mutaciones funcionales por RNAi (Vienna Drosophila Resource Center), falta de función y sobrexpresión (Bloomington Stock Center, Indiana University) de los genes elegidos. Los descendientes de estos cruces, de genotipo adecuado, fueron evaluados respecto a su capacidad de escalada en búsqueda de alelos modificadores que mejoraran o empeoraran dicho fenotipo. Entre los modificadores identificados se encontraron diversos genes que participan en la ruta de TOR (Target of Rapamycin) y en la homeostasis de metales y por tanto, seleccionamos estas dos rutas para un estudio más detallado de su participación en la patogénesis de la AF.

3.1. La ruta de TOR interacciona genéticamente con frataxina (Calap-Quintana *et al.* 2015, figura 1)

La ruta de TORC1 (Target of Rapamycin Complex 1) sirve como reguladora central del metabolismo celular, crecimiento, proliferación y supervivencia e integra señales intracelulares y extracelulares sobre la disponibilidad de nutrientes. La mayoría de estas señales se integran mediante el complejo TSC1/TSC2 (Tuberous Sclerosis Complex 1/2) que inhibe a Rheb (Rhas homolog enriched in brain ortholog) y este a su vez activa a TORC1. La síntesis proteica es promovida por la activación del factor de transcripción eIF-4E (eukaryotic translation initiation factor 4E) y de la kinasa S6K por medio de TORC1. Entre los modificadores del rastreo genético llevado a cabo en el modelo de AF en *Drosophila*, cuatro pertenecían a la ruta de TORC1: *Tsc1*, *S6K*, *eIF-4E* y *Lrrk* (Leucine-rich repeat kinase), activador de *eIF-4E*. En conjunto, se observó que la inhibición de la ruta de TORC1 producía una mejora del fenotipo motor del modelo de AF en mosca, señalando la implicación de esta ruta en la patogénesis de la enfermedad. Además, estos resultados sugieren una posible estrategia terapéutica para la AF mediante la inhibición de la ruta de TORC1, por ejemplo con compuestos como la rapamicina.

3.2. Rutas implicadas en la homeóstasis de los metales interaccionan genéticamente con frataxina (Soriano *et al.*, enviado para su publicación).

Debido a la participación del hierro en la fisiopatología de la AF, se incluyeron genes implicados en la homeostasis de los metales en la lista de candidatos para el rastreo genético. En este trabajo, para aumentar la confianza de los modificadores identificados, se incluyó un segundo fenotipo además de la capacidad de escalada. En concreto, se evaluó la mejoría o empeoramiento del defecto observado en el ojo de las moscas *GMR*-GAL4>UAS-*fh*RNAi-1. En concreto, en estos individuos la falta de frataxina se ha dirigido al ojo en desarrollo lo que produce un fenotipo de ojo “rugoso” que se puede observar externamente. Mediante esta estrategia se identificaron genes modificadores que participan en la homeostasis del hierro, transportadores de cobre y zinc así como en la detoxificación producida por metales. Al reducir la expresión de las proteínas reguladoras de hierro *Irp-1A* e

Irp-1B y de los transportadores de hierro regulados por ellas, transferrinas 1 y 2 y *malvolio*, mejoraron los fenotipos de ojo y de capacidad de escalada. También mejoraron ambos fenotipos al reducir los niveles de seis transportadores de zinc así como de la chaperona de cobre (Atox1) y del transportador de cobre (dCutC). La sobrexpresión de *MTF-1*, un factor de transcripción que regula la detoxificación de los metales, también rescataba los fenotipos de ojo y escalada. Sin embargo las metalotioneínas, que son activadas por MTF-1 actuaron como supresores cuando se reducía su expresión. Al haberse identificado genes modificadores de los fenotipos inducidos por falta de frataxina implicados en el transporte y la regulación de la homeóstasis de los metales, se procedió a estudiar esta ruta más en detalle.

4. Acumulación de metales en el modelo de AF en *Drosophila* (Soriano *et al.*, enviado para su publicación).

En muestras procedentes de pacientes de AF, se caracterizó una redistribución del hierro, cobre y zinc que no iba acompañada de un aumento de los niveles totales de estos metales. Sin embargo en el modelo de AF en *Drosophila* sí que observamos la acumulación de hierro, zinc, cobre y manganeso. Además, el quelante de zinc TPEN así como los quelantes de cobre TTM y BSC mejoraron la capacidad de escalada de las moscas *actina*-GAL4>UAS-*fh*RNAi-2.

Para estudiar el mecanismo por el cual los modificadores identificados en el rastreo genético producían la supresión de los fenotipos de las moscas con deficiencia de frataxina, estudiamos su efecto en la acumulación de hierro. Observamos que esta se reducía en el caso de malvolio, las transferrinas e Irp1 pero también para dos de los transportadores de zinc, *ZnT41F* y *fear of intimacy* (*foi*) y para la sobrexpresión de *MTF-1*.

Aunque las metalotioneinas se suelen asociar a la detoxificación de los metales y del daño oxidativo que producen éstos, también se las ha asociado con un efecto prooxidante (Suzuki *et al.* 1996). Los niveles de estrés oxidativo se encuentran incrementados en las moscas modelo de la AF. La reducción genética de la metalotioneína *MtnA,* al igual que la sobrexpresión de MTF-1,

además de mejorar la capacidad de escalada, rescataron los niveles de estrés oxidativo. Este resultado apoya la hipótesis del efecto prooxidante de las metalotioneínas. Y en conjunto, hemos identificado que la homeostasis de los metales está implicada en la patogénesis de la AF, y que la quelación del zinc y el cobre tiene potencial terapéutico para la enfermedad.

Conclusiones

1. La expresión del gen humano *FXN* rescata el déficit de actividad aconitasa producido por la falta de la frataxina endógena en *Drosophila*, indicando la equivalencia funcional de ambas proteínas.

2. El quelante de hierro deferiprona mejora los fenotipos inducidos por la falta de frataxina (supervivencia y habilidad motora) en el modelo de AF en *Drosophila* por medio de la quelación de la acumulación de hierro mitocondrial.

3. El antioxidante idebenona mejora los fenotipos inducidos por la falta de frataxina en el modelo de AF en *Drosophila* y rescata la reducción de la actividad aconitasa en hiperoxia.

4. Los niveles de zinc, cobre, manganeso y aluminio se encuentran aumentados en el modelo de AF en *Drosophila* y la quelación de zinc y cobre mejoran el fenotipo motor inducido por la falta de frataxina.

5. La reducción en la expresión de genes implicados en el transporte del hierro, cobre y zinc y la sobrexpresión del factor de transcripción *MTF-1* mejoran los fenotipos (desarrollo del ojo externo y habilidad motora) del modelo de AF en *Drosophila*.

6. Los miembros de la ruta de TORC1 TSC1, S6K, Lrrk y eIF-4E interaccionan genéticamente con frataxina de tal forma que la inhibición genética de dicha ruta suprime el déficit en la capacidad de escalada que muestran las moscas modelo de AF.

Bibliografía

Adinolfi S, Trifuoggi M, Politou AS, Martin S, Pastore A. 2002. A structural approach to understanding the iron-binding properties of phylogenetically different frataxins. Hum. Mol. Genet. 11:1865–1877.

Anderson PR, Kirby K, Hilliker AJ, Phillips JP. 2005. RNAi-mediated suppression of the mitochondrial iron chaperone, frataxin, in Drosophila. Hum. Mol. Genet. 14:3397–3405.

Babcock M, de Silva D, Oaks R, Davis-Kaplan S, Jiralerspong S, Montermini L, Pandolfo M, Kaplan J. 1997. Regulation of mitochondrial iron accumulation by Yfh1p, a putative homolog of frataxin. Science 276:1709–1712.

Boddaert N, Le Quan Sang KH, Rötig A, Leroy-Willig A, Gallet S, Brunelle F, Sidi D, Thalabard J-C, Munnich A, Cabantchik ZI. 2007. Selective iron chelation in Friedreich ataxia: biologic and clinical implications. Blood 110:401–408.

Bradley JL, Blake JC, Chamberlain S, Thomas PK, Cooper JM, Schapira AH. 2000. Clinical, biochemical and molecular genetic correlations in Friedreich's ataxia. Hum. Mol. Genet. 9:275–282.

Calap-Quintana P, Soriano S, Llorens JV, Al-Ramahi I, Botas J, Moltó MD, Martínez-Sebastián MJ. 2015. TORC1 Inhibition by Rapamycin Promotes Antioxidant Defences in a Drosophila Model of Friedreich's Ataxia. PloS One 10:e0132376.

Campuzano V, Montermini L, Moltò MD, Pianese L, Cossée M, Cavalcanti F, Monros E, Rodius F, Duclos F, Monticelli A, *et al.* 1996. Friedreich's ataxia: autosomal recessive disease caused by an intronic GAA triplet repeat expansion. Science 271:1423–1427.

Cañizares J, Blanca JM, Navarro JA, Monrós E, Palau F, Moltó MD. 2000. dfh is a Drosophila homolog of the Friedreich's ataxia disease gene. Gene 256:35–42.

Gibson TJ, Koonin EV, Musco G, Pastore A, Bork P. 1996. Friedreich's ataxia protein: phylogenetic evidence for mitochondrial dysfunction. Trends Neurosci. 19:465–468.

Kakhlon O, Manning H, Breuer W, Melamed-Book N, Lu C, Cortopassi G, Munnich A, Cabantchik ZI. 2008. Cell functions impaired by frataxin deficiency are restored by drug-mediated iron relocation. Blood 112:5219–5227.

Koutnikova H, Campuzano V, Foury F, Dollé P, Cazzalini O, Koenig M. 1997. Studies of human, mouse and yeast homologues indicate a mitochondrial function for frataxin. Nat. Genet. 16:345–351.

Li K, Besse EK, Ha D, Kovtunovych G, Rouault TA. 2008. Iron-dependent regulation of frataxin expression: implications for treatment of Friedreich ataxia. Hum. Mol. Genet. 17:2265–2273.

Llorens JV, Navarro JA, Martínez-Sebastián MJ, Baylies MK, Schneuwly S, Botella JA, Moltó MD. 2007. Causative role of oxidative stress in a Drosophila model of Friedreich ataxia. FASEB J. Off. Publ. Fed. Am. Soc. Exp. Biol. 21:333–344.

Meier T, Perlman SL, Rummey C, Coppard NJ, Lynch DR. 2012. Assessment of neurological efficacy of idebenone in pediatric patients with Friedreich's ataxia: data from a 6-month controlled study followed by a 12-month open-label extension study. J. Neurol. 259:284–291.

Miranda CJ, Santos MM, Ohshima K, Smith J, Li L, Bunting M, Cossée M, Koenig M, Sequeiros J, Kaplan J, *et al.* 2002. Frataxin knockin mouse. FEBS Lett. 512:291–297.

Navarro JA, Llorens JV, Soriano S, Botella JA, Schneuwly S, Martínez-Sebastián MJ, Moltó MD. 2011. Overexpression of human and fly frataxins in Drosophila provokes deleterious effects at biochemical, physiological and developmental levels. PloS One 6:e21017.

Palau F, Espinós C. 2006. Autosomal recessive cerebellar ataxias. Orphanet J. Rare Dis. 1:47.

Pastore A, Puccio H. 2013. Frataxin: a protein in search for a function. J. Neurochem. 126 Suppl 1:43–52.

Pook MA, Al-Mahdawi S, Carroll CJ, Cossée M, Puccio H, Lawrence L, Clark P, Lowrie MB, Bradley JL, Cooper JM, *et al.* 2001. Rescue of the Friedreich's ataxia knockout mouse by human YAC transgenesis. Neurogenetics 3:185–193.

Puccio H, Simon D, Cossée M, Criqui-Filipe P, Tiziano F, Melki J, Hindelang C, Matyas R, Rustin P, Koenig M. 2001. Mouse models for Friedreich ataxia exhibit cardiomyopathy, sensory nerve defect and Fe-S enzyme deficiency followed by intramitochondrial iron deposits. Nat. Genet. 27:181–186.

Rötig A, de Lonlay P, Chretien D, Foury F, Koenig M, Sidi D, Munnich A, Rustin P. 1997. Aconitase and mitochondrial iron-sulphur protein deficiency in Friedreich ataxia. Nat. Genet. 17:215–217.

Seguin A, Bayot A, Dancis A, Rogowska-Wrzesinska A, Auchère F, Camadro J-M, Bulteau A-L, Lesuisse E. 2009. Overexpression of the yeast frataxin homolog (Yfh1): contrasting effects on iron-sulfur cluster assembly, heme synthesis and resistance to oxidative stress. Mitochondrion 9:130–138.

Soriano S, Llorens JV, Blanco-Sobero L, Gutiérrez L, Calap-Quintana P, Morales MP, Moltó MD, Martínez-Sebastián MJ. 2013. Deferiprone and idebenone rescue frataxin depletion phenotypes in a Drosophila model of Friedreich's ataxia. Gene 521:274–281.

Suzuki KT, Rui M, Ueda J, Ozawa T. 1996. Production of hydroxyl radicals by copper-containing metallothionein: roles as prooxidant. Toxicol. Appl. Pharmacol. 141:231–237.

Introduction

1. Friedreich ataxia: clinical features and pathophysiology

Friedreich ataxia (FRDA), OMIM #229300, is the most commonly inherited ataxia in Western European population, with a prevalence of 2-4:100.000 and an estimated carrier frequency of 1:100 (reviewed in Palau and Espinós 2006).

The German pathologist Nikolaus Friedreich described in a series of papers between 1863 and 1877 the ataxic syndrome that now bears his name (reviewed in Koeppen 2013). The major clinical features of FRDA include age of onset around puberty, progressive ataxia, muscle weakness, sensory loss and non-neurological features such as skeletal defects and cardiomyopathy. Other clinical signs are diabetes mellitus and carbohydrate intolerance, affecting 10% and 20% of FRDA patients respectively [Table 1].

FRDA neuropathology starts with the degeneration of the large sensory neurons of the dorsal root ganglia (DRG) followed by atrophy of the dorsal columns that produces loss of proprioception and vibration sense. Degeneration of the spinocerebellar tracts of the spinal cord results in upper motor weakness. Atrophy is also observed in the dentate nuclei and accounts for the cerebellar component of ataxia. Most FRDA patients develop hypertrophic cardiomyopathy with thickened septum walls and iron deposits in the myocardium (reviewed in Parkinson *et al*. 2013).

Table 1: Clinical features of FRDA

Neurological features	Gait and limb ataxia Pyramidal weakness and wasting Areflexia Extensor plantar responses Loss of position and vibratory sense Dysarthria Abnormal eye movements (fixation instability) Vision and hearing loss
Non-neurological features	Scoliosis Foot deformity Diabetes mellitus Cardiomyopathy

2. Genetics of FRDA

2.1 The gene *FXN*

The human gene *FXN* (Frataxin gene) is located on the positive strand of chromosome 9 and contains seven exons: exons 1-4, 5a, 5b and 6 [Figure 1]. The major transcript is composed of the first five exons and produces the 210 amino acid mitochondrial protein frataxin (isoform A or FXN-1). Less abundant alternative transcripts of *FXN* have been identified. Exon 5b instead of 5a can be transcribed to produce a 171 amino acid isoform B or FXN-3 (Campuzano *et al*. 1996). Isoform A1 or FXN-2 contains an 8bp insertion by alternative splicing at intron 4 and encodes for a protein of 191 amino acids (Pianese *et al*. 2002). A recent study has identified two isoforms of frataxin that lack the mitochondrial targeting sequence and that are specifically expressed in the affected tissues in FRDA, cerebellum and heart (Xia *et al*. 2012).

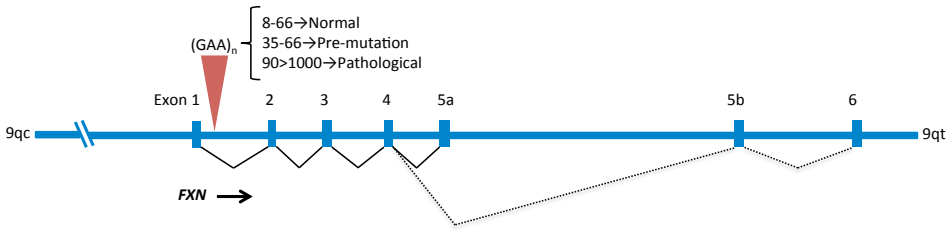

Figure 1: Structure of the gene *FXN*. *FXN*, localized in 9q21.11, contains seven exons and a GAA triplet repeat tract in the first intron. Alternative splicing of isoform A (solid line) and isoform B (discontinuous line) is represented. Adapted from Evans-Galea *et al*. 2014.

The gene *FXN* is transcribed from two main transcription start sites, TSS1 and TSS2, which are respectively 221 and 62 bp upstream the ATG translation start site (Campuzano *et al*. 1996; Kumari *et al*. 2011). The promoter seems to be contained in the 1255 bp region extending 5' from the open reading frame. The frataxin promoter is unusual among mammalian promoters by lacking a TATA sequence. The *FXN* locus is rich in repetitive DNA elements, particularly in this promoter region. These include retro-elements Alu (SINE, Short Interspersed Nuclear Elements) and L2 (LINE, Long Interspersed Nuclear Elements) as well as mammalian-wide interspersed repeats (MIR) and mariner

DNA transposon. The Alu and MIR elements have been found to function as enhancers of the promoter (Greene *et al*. 2005).

2.2 The GAA repeat expansion and genotype/phenotype correlation

In the center of an Alu element within the first intron of *FXN* is located a $(GAA)_n$ repeat tract that is polymorphic in the human population (Campuzano *et al*. 1996). Normal alleles contain from 8 to 66 GAA repeats whereas the FRDA associated alleles range from 90 up to 1700, most frequently between 600 and 900 (Campuzano *et al*. 1996; Dürr *et al*. 1996). Although most FRDA affected individuals are homozygous for the GAA expansion, approximately 4% are compound heterozygous for an expansion and a loss-of-function mutation (nonsense, missense, frameshift and splice-site point mutations or a deletion) (Cossée *et al*. 1999).

Alleles with interrupted GAA repeats are generally stable. Instability of the uninterrupted repeats gives rise to expansion mutations and start to occur when the number of repeats reaches the threshold of ~35 (Cossée *et al*. 1997; Sharma *et al*. 2002; Pollard *et al*. 2004). Paternal transmission is generally accompanied by a contraction of the repeats whereas when inherited from the mother, contractions or expansions are equally common (Monrós *et al*. 1997; Pianese *et al*. 1997). The expanded triplet repeat is not only unstable when transmitted from parent to child but also within somatic cells, what has been suggested to account for the selective vulnerability of specific cell types (De Biase *et al*. 2007).

The intronic GAA expansion produces partial gene silencing and results in a reduction of frataxin expression to 5-20% of normal levels (Campuzano *et al*. 1997). Two mechanisms of transcriptional repression of *FXN* by the triplet repeats have been proposed: (1) the generation of non-B DNA structures such as triplexes and sticky DNA or persistent DNA-RNA hybrids (Sakamoto *et al*. 1999; Grabczyk and Usdin 2000; Wells 2008) that would block the progress of the RNA polymerase II; (2) epigenetic mechanisms inducing the formation of heterochromatin (Saveliev *et al*. 2003).

The degree of *FXN* silencing is correlated with the length of the triplet repeat expansion in the shorter of the two alleles, as it is the severity, age of onset and progression of the disease. A higher number of GAA repeats is correlated with the cardiomyopathy and the neurological symptoms, including ataxia, sensory loss, dysarthria and scoliosis (Dürr *et al*. 1996; Isnard *et al*. 1997; Monrós *et al*. 1997; Montermini *et al*. 1997).

3. The protein frataxin

3.1 Cellular localization and structure

Human frataxin is translated by cytoplasmic ribosomes as a precursor of 210 amino acids that is imported into the mitochondria (Koutnikova *et al*. 1997). Then it is proteolytically cleaved by the mitochondrial processing peptidase (MPP) in a two-step process that leads to the successive generation of an intermediate form of 19 kDa (residues 42-210) and of the mature form of 14 kDa (residues 81-210) (Koutnikova *et al*. 1998; Condò *et al*. 2007)

Frataxin is a protein highly conserved among eukaryotes and some prokaryotes (Gibson *et al*. 1996; Adinolfi *et al*. 2002). Sequence alignment of the frataxin family shows two distinct regions: (1) an N-terminal block of 70-90 amino acids that is absent in prokaryotes and poorly conserved among eukaryotes and (2) a highly conserved block of 100-120 residues in the C-terminus of the protein [Figure 2a].

The structure of the human frataxin, the *Escherichia coli* homolog *CyaY* and the Yeast frataxin homolog 1 (*Yfh1*) have been characterized (Dhe-Paganon *et al*. 2000; Lee *et al*. 2000; Musco *et al*. 2000; He *et al*. 2004; Nair *et al*. 2004). The conserved C-terminal region folds in a unique α-β sandwich that consists of an antiparallel β-sheet flanked by two α helices assembled in a sequence alpha-$(beta)_{5-7}$-alpha. The N-terminal tail present in eukaryotes appears to be intrinsically unfolded [Figure 2b]. The presence of acidic residues within the first α-helix and the edge of the first β strand forms a negatively charged surface that is involved in iron binding, whereas a neutral flat area on

the β-sheet probably allows protein-protein interactions (Adinolfi *et al*. 2002; Foury *et al*. 2007).

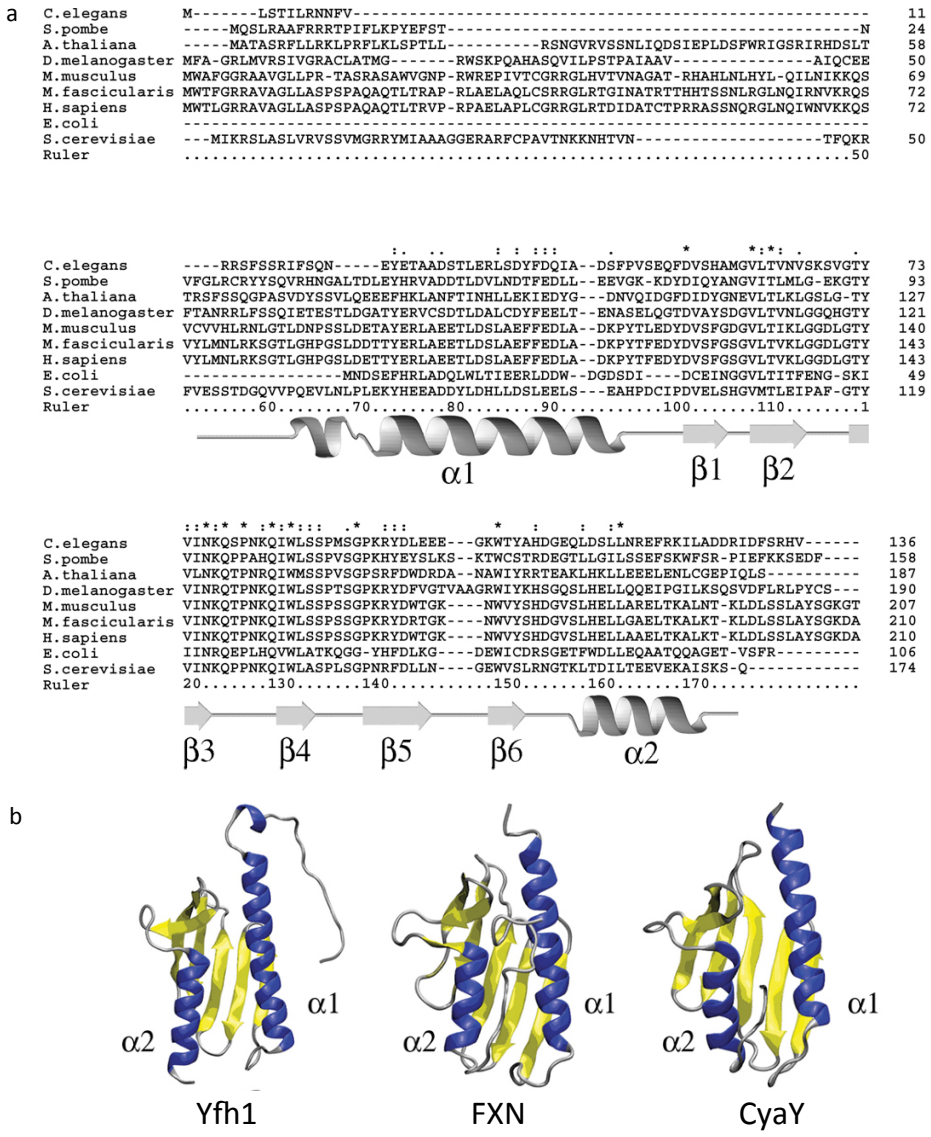

Figure 2: Conservation and structure of frataxin. a. Sequence alignment of nine frataxin orthologs. "*" indicates a fully conserved residue, ":" indicates conservation among groups of residues with strongly similar properties and "." indicates conservation among groups of residues with weakly similar properties. b. Three-dimensional structure of yeast, human and bacterial frataxins. Adapted from Bencze *et al*. 2006.

A difference among frataxin orthologs is their ability to undergo oligomerization reactions, and the functional relevance of these reactions is controversial. In the presence of excess iron, *Yfh1* has been shown to assemble into trimmers, hexamers and to larger 12-mers, 24-mers and 48-mers (Adamec *et al*. 2000; Gakh *et al*. 2002). Unlike CyaY and Yfh1, the mature form of the human frataxin (81-210) does not form oligomers and is able to rescue the viability of frataxin-deficient murine fibroblasts, indicating that the oligomerization is not a requisite for frataxin function (Schmucker *et al*. 2008).

3.2 Function of frataxin

The function of frataxin has been related to different mitochondrial pathways and still remains unclear. The most accepted hypothesis based on the data available supports the participation of frataxin in iron-sulfur cluster formation as the essential function of the protein (reviewed in Pastore and Puccio 2013).

Role of frataxin in the iron-sulfur cluster biogenesis

Fe-S clusters constitute one of the most ancient and ubiquitous of the biological prosthetic groups. More than 200 types of proteins contain Fe-S centers and exhibit a remarkable functional and structural diversity. Fe-S clusters are composed by two or more iron atoms bridged by sulfide centers, most frequently in a [2Fe-2S] or a [4Fe-4S] conformation. Three distinct types of biosynthetic machineries for Fe-S cluster assembly are present in prokaryotes: NIF, for maturation of nitrogenase in nitrogen-fixing bacteria; and ISC (Iron Sulfur Cluster) and SUF for generation of Fe-S proteins under normal and oxidative-stress conditions respectively (reviewed in Lill 2009). In higher eukaryotes, Fe-S biogenesis takes place in the mitochondria by means of homologous components of the bacterial ISC system that were transferred from the bacterial endosymbiotic ancestor of this organelle. Mitochondrial *de novo* Fe-S cluster biogenesis occurs in two steps. The first step involves the assembly of inorganic iron and sulfur on a scaffold protein, IscU in bacteria and Isu1 in yeast. It is known that this reaction needs a cysteine desulphurase as sulfur donor, IscS in bacteria and Nfs-1-Isd11 in yeast, whereas the origin of

the iron is still unclear. In the second step, the clusters are transferred from the scaffold to recipient apoproteins for incorporation within specific amino acid residues.

The involvement of frataxin in this biosynthetic process was first suggested by the deficient activity of proteins containing Fe-S clusters in FRDA patients (Rötig *et al*. 1997), and later in a cardiac mouse model of the disease (Puccio *et al*. 2001). Additional data supporting this hypothesis was provided by studies in the *Saccharomyces cerevisiae*. The absence of frataxin and the deficiency in the cysteine desulfurase Nfs1 in yeast result in a similar phenotype of mitochondrial iron accumulation and reduction of Fe-S protein activity (Chen *et al*. 2002). The observation of an iron-dependent interaction of yeast Yfh1 with the Nfs1/Isu1 complex further supported the participation of frataxin in Fe-S cluster assembly (Gerber *et al*. 2003). Work using mammalian recombinant proteins further characterized the interaction of human frataxin with a preformed complex composed of NFS1, ISCU and ISD11 (Tsai and Barondeau 2010; Schmucker *et al*. 2011).

The exact role of frataxin in the Fe-S cluster assembly process is as well a matter of debate. The iron-binding properties of the human protein indicated that frataxin was acting as the iron donor in the first step of the assembly reaction (Cavadini *et al*. 2002; Yoon and Cowan 2003). However, Tsai and Barondeau (2010) and Schmucker *et al*. (2011) demonstrated that iron is not required for the interaction between human frataxin and the NFS1/ISCU/ISD11 complex. Furthermore, frataxin has been proposed to function as an allosteric regulator that facilitates the transfer of sulfur from NFS1 for the assembly (Tsai and Barondeau 2010; Bridwell-Rabb *et al*. 2014) [Figure 3]. By contrast, results with the bacterial homolog of frataxin show the opposite situation from the mammalian system and establish a role for CyaY as inhibitor of the Fe-S cluster biogenesis (Adinolfi *et al*. 2009; Iannuzzi *et al*. 2011) .

Other functions proposed for frataxin

Frataxin has been shown to physically interact with the mitochondrial proteins aconitase (Bulteau *et al*. 2004), ferrochelatase (Yoon and Cowan

2004) and succinate dehydrogenase (González-Cabo *et al*. 2005). In addition to its primary role in Fe-S cluster biogenesis, frataxin has been proposed to act as iron chaperone that provides iron to aconitase and ferrochelatase or electrons to ubiquinone (SDH and putative Etf homologues) *via* direct protein-protein interaction.

Several studies reveal the existence of an extramitochondrial pool of frataxin, which has been proposed to participate in the cytosolic Fe-S cluster assembly (Acquaviva *et al*. 2005), interact with cytosolic aconitase/iron regulatory protein-1 (Condò *et al*. 2010) and promote cell survival (Condò *et al*. 2006).

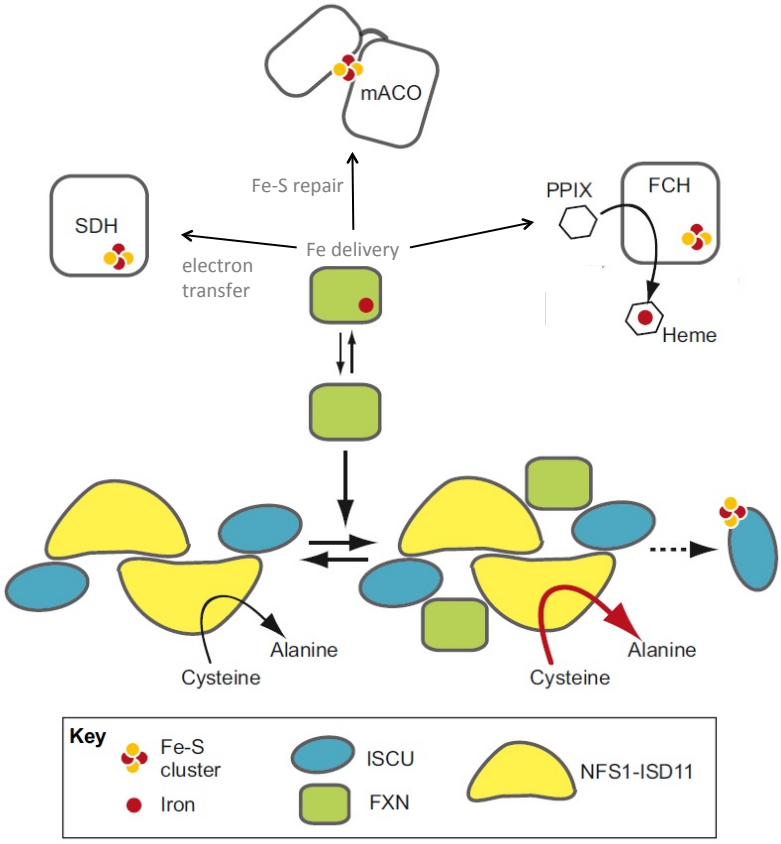

Figure 3: Possible functions of frataxin, as an iron donor to the Fe-S cluster assembly machinery or directly to some Fe-S proteins, or facilitating the transfer of sulfur from NFS1. Adapted from Martelli *et al*. 2012.

4. Molecular pathogenesis of FRDA

4.1 Fe-S protein dysfunction

Reduced levels of frataxin result in a dysfunction of the proteins containing Fe-S clusters, which participate in diverse pathways including heme biosynthesis, ribosome assembly or DNA replication and repair [Table 2].

Table 2: Fe-S cluster containing proteins

Functions	Examples
Respiratory chain	Complex I (NADH:ubiquinone dehydrogenase) Complex II (Succinate dehydrogenase) Complex III (Rieske protein)
TCA	Aconitase
Heme synthesis	Ferrochelatase
Catabolic pathways	ETFQO (aminoacid degradation and β-oxidation of fatty acids) Dihydropyrimidine dehydrogenase (Pyrimidine nucleotides) Xantine dehydrogenase (Purine nucleotides)
Ribosome assembly	RLI
DNA repair	FancJ XPD MUTYH
DNA replication	PRIM2
Regulation of gene expression	IRP

TCA: tricarboxylic acid cycle. ETFQO: electron-transfer flavoprotein-ubiquinone oxidoreductase. RLI: RNAse L inhibitor. FancJ: Fanconi anemia group J helicase. XPD: Xeroderma pigmentosum D helicase. MUTH: MutY DNA glycosylase. PRIM2: Primase 2. IRP: Iron Responsive Protein.

Fe-S clusters are also essential components of the respiratory electron transfer complexes and the TCA cycle [Table 2]. Energy production in the mitochondria is possible through the generation of a gradient of protons by the electron transport chain (ETC), which is later used to produce ATP by oxidative phosphorylation (OXPHOS). Disruption of the ETC and OXPHOS function due to frataxin deficiency results in impaired ATP production by FRDA mitochondria (Lodi *et al*. 1999).

4.2 Iron accumulation

Mitochondrial iron accumulation has been detected in heart, liver, spleen and the dentate nucleus of the cerebellum of FRDA patients as well as in yeast (Babcock *et al*. 1997), *C. elegans* (González-Cabo *et al*. 2011) and mouse models of the disease (Puccio *et al*. 2001; Al-Mahdawi *et al*. 2006).

The mechanism connecting frataxin deficiency to mitochondrial iron overload remains unclear. However, mitochondrial iron accumulation is observed for the deficiency of other genes involved in Fe-S cluster biogenesis, suggesting a shared mechanism (reviewed in Martelli and Puccio 2014). Proteins implicated in iron homeostasis such as the transcription factor IRP-1 require an Fe-S cluster for their function, providing a link between both processes (Huang *et al*. 2011). Furthermore, the mitochondrial iron overload in FRDA cells has been proposed to be in fact coupled with a relative iron depletion in the cytosol, which induces the cellular iron uptake (Li *et al*. 2008).

4.3 Oxidative stress

Markers of oxidative stress have been observed associated to frataxin deficiency in yeast (Babcock *et al*. 1997; Koutnikova *et al*. 1997; Radisky *et al*. 1999), *C. elegans* (Vázquez-Manrique *et al*. 2006), *Drosophila* (Llorens *et al*. 2007; Anderson *et al*. 2008; Navarro *et al*. 2010) and mouse (Puccio *et al*. 2001; Al-Mahdawi *et al*. 2006) as well as in FRDA patients (Rötig *et al*. 1997; Waldvogel *et al*. 1999).

Three mechanisms have been suggested to lead to the oxidative damage in FRDA (reviewed in Vaubel and Isaya 2013):

(a) Enhanced ROS production due to the uncoupling of the ETC (Rötig *et al*. 1997). The primary source of endogenous reactive oxygen species (ROS) is the OXPHOS. During the transfer of electrons to the molecular oxygen, there is a leak of electrons that generate superoxide anions (O_2^-). Reduced efficiency in the coupling of the ETC related to frataxin deficiency could be responsible of increasing the production of O_2^-.

(b) Increased ROS production through the Fenton chemistry (Isaya *et al*. 2004). The labile redox-active iron accumulated in FRDA cells can participate in the Fenton/Haber-Weiss reaction, giving rise to the highly oxidant hydroxyl radical (OH^-).

Haber-Weiss reaction:

$$Fe^{3+} + O_2^- \rightarrow Fe^{2+} + O_2$$

$$Fe^{2+} + H_2O_2 \rightarrow Fe^{3+} + OH^- + {}^{\cdot}OH \quad \text{(Fenton reaction)}$$

Net reaction $O_2^- + H_2O_2 \rightarrow O_2 + OH^- + {}^{\cdot}OH$

(c) Impaired antioxidant response. Several studies show that frataxin deficiency leads to the impairment of glutathione homeostasis. Increased glutathione bound to proteins has been observed in FRDA patient samples and frataxin deficient yeast (Piemonte *et al*. 2001; Auchère *et al*. 2008; Bulteau *et al*. 2012). In patient fibroblasts, the glutathionylation of actin was related to a deficient Nrf-2-dependent antioxidant response (Pastore *et al*. 2003).

4.4 The vicious circle hypothesis

The exact sequence of events that occur in FRDA has not been clarified yet. According to the classic vicious circle hypothesis, frataxin depletion results in impaired Fe-S cluster synthesis with intramitochondrial iron accumulation. This reactive iron would promote the formation of ROS by the Fenton chemistry that in turn destroys more Fe-S clusters [Figure 4].

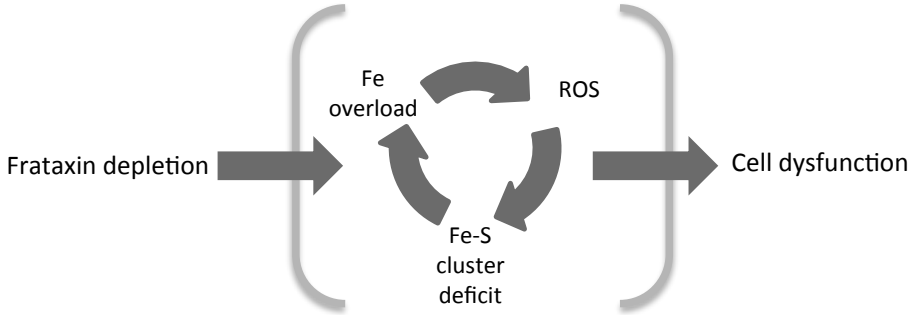

Figure 4: The vicious circle hypothesis of the molecular pathogenesis of FRDA. Adapted from Bayot *et al*. 2011.

However, some limitations to this hypothesis have been described. Cultured cells from FRDA patients exhibit increased sensitivity to oxidative stress but no decrease in Fe-S protein activity (Rötig *et al*. 1997). It has been suggested that the primary defect triggered by frataxin deficiency is a hypersensitivity to oxidative stress and a deficient activation of the antioxidant defenses rather than the increase in ROS production (Bayot *et al*. 2011). Regarding the mitochondrial iron accumulation, it also appears to be absent in patient-derived fibroblasts and lymphoblasts (Sturm *et al*. 2005) and has been reported to be a late event in mouse models of FRDA (Puccio *et al*. 2001), calling into question the role of the iron accumulation in the disease pathogenesis.

5. Therapeutic approaches

Currently, there is no cure or treatment approved for FRDA. However addressing the co-morbid symptoms may significantly improve the quality of life of the patients. Symptomatic treatments mainly consist in medications for the diabetes (insulin) and the heart disease (angiotensin-converting-enzyme inhibitors, diuretics and β-blockers), surgical procedures to correct the scoliosis and foot deformity, and physical therapy. Different therapeutic strategies for FRDA have been considered, directed to increase frataxin levels or to the downstream molecular defects of frataxin deficiency. The investigation on several candidate treatments is in different stages of the drug discovery process and can be followed in *www.curefa.org/pipeline*.

5.1 Iron chelation

Iron chelation is the treatment of choice for systemic iron overload arising from disorders such as in haemochromatosis and thalassemia intermedia or as a consequence of chronic blood transfusions. However, in FRDA the mitochondrial iron accumulation is coupled with cytosolic iron depletion and patients show normal serum iron and ferritin levels indicating no systemic iron overload. Therefore, an iron chelator for the treatment of FRDA should be able to redistribute iron from the mitochondria to other cellular compartments without causing overall iron depletion.

Deferiprone is an orally administered, lipid-soluble iron chelator that can easily cross the blood-brain barrier and the cellular membranes. Because of its low affinity for iron, it is less prone to cause iron depletion and may act as an iron donor for transferrin. In cell culture, deferiprone was indeed able to relocate iron from overloaded to depleted compartments, to extracellular transferrin and to the hemoglobin machinery (Sohn *et al*. 2008).

In a cellular model of FRDA, deferiprone at a concentration of 50 µM improved the phenotypes induced by frataxin knockdown. Specifically, deferiprone restored the mitochondrial membrane potential, ATP production, and aconitase activity, decreased ROS production and prevented apoptosis (Kakhlon *et al*. 2008). Furthermore, deferiprone has been established to increase *FXN* gene expression in a pharmacological screening in cell culture (Li *et al*. 2013). However, higher concentrations of deferiprone (150 µM) impaired aconitase activity and cell proliferation in patient's fibroblasts (Goncalves *et al*. 2008).

In a pilot open-label clinical trial, nine adolescent FRDA patients were treated with 20-30 mg of deferiprone/day during six months and exhibited reduced iron accumulation in the dentate nucleus and some improvement in ataxia scores (Boddaert *et al*. 2007). These results led to a subsequent randomized placebo-controlled phase 2 trial where three concentrations of deferiprone, 20, 40 and 60 mg/kg/day, were tested during 6 months (Pandolfo *et al*. 2014). Although worsening of the ataxia was reported for the two higher

concentrations, 20 mg/kg/day improved disease progression in patients with less severe condition. Interestingly, 20 and 40 mg/kg/day of deferiprone improved cardiac parameters. Taken together, the use of deferiprone for the treatment of FRDA looks promising but the results in the cell models and clinical trials indicate that concentrations have to be carefully considered. Moreover, deferiprone carries the risk of agranulocytosis, which has to be monitored with frequent blood counts (reviewed in Pandolfo and Hausmann 2013). Due to the overall conflicting results obtained, deferiprone has been removed from the clinical trials.

5.2 Decrease oxidative stress

Increased ROS levels have been observed in FRDA models and patients [see section 4]. The synthetic analog of coenzyme Q10, idebenone, was the first drug directed to decrease oxidative stress that reached Phase III clinical trials for FRDA. Idebenone is able to act both as antioxidant, decreasing intracellular ROS and preventing lipid peroxidation, and as electron carrier between damaged respiratory chain complexes, therefore improving mitochondrial function.

In an open-label trial with 5 mg/kg/day of idebenone during eight weeks, FRDA patients showed a decrease in the urinary oxidative stress marker 8-hydroxyl-2'-deoxyguanosine (Schulz *et al*. 2000). This study was followed by a randomized, double-blind, placebo controlled clinical trial in which adolescent FRDA patients received 5, 15 or 45 mg/kg/day during six months. Idebenone ameliorated the neurological symptoms of patients in a less severe stage but the increase in the urine oxidative stress marker could not be replicated (Di Prospero *et al*. 2007). A Phase III double-blind controlled trial was conducted over a pediatric cohort during 6 months to assess the efficacy of idebenone on neurological function and cardiomyopathy (Schulz *et al*. 2000; Schulz *et al*. 2009). Although idebenone failed this Phase III trial by not improving the neurological and the cardiac function, an open-label extension study of 12 months in these patients indicated a stabilization of the neurological symptoms. Similarly, a long-term open-label study with 5-20 mg/kg/day for 3-5 years indicated that idebenone prevents the progression of the neurological

dysfunction in the pediatric population together with the stabilization of cardiomyopathy in both pediatric and adult patients (Pineda *et al*. 2008).

Idebenone has also been removed from clinical trials for FRDA since the improvements observed using this compound could not been reproduced in larger clinical assays. However, other molecules aiming to reduce oxidative stress and improve mitochondrial function are being investigated. EPI-743 is an orally bioavailable small molecule that crosses the central nervous system and targets the enzyme NADPH quinone oxidoreductase. This compound has been established to increase antioxidant defenses in the mitochondrial disease Leber hereditary optic neuropathy (Ghelli *et al*. 2008) and is currently undergoing a Phase II clinical trial for FRDA.

5.3 Increase frataxin levels

A promising therapeutic strategy for FRDA is to increase the levels of frataxin, therefore preventing the downstream cascade of protein dysfunction and oxidative stress damage that ultimately leads to the clinical symptoms.

Histone deacetylase inhibitors (HDACi)

HDACi increase acetylation of histones, transcription factors and other proteins that regulate transcription. Because histone hypoacetylation has been associated to transcriptional silence in expanded *FXN* alleles, HDACi were proposed as candidates to restore frataxin levels (Herman *et al*. 2006). Sodium butyrate was the first HDACi shown to increase *FXN* expression in a reporter cell line (Sarsero *et al*. 2003). A screen of HDACi in FRDA lymphoblastoid cells revealed that BML-210 significantly increases frataxin expression (Herman *et al*. 2006). Several compounds with similar structures to BML-210 were synthesized and tested. Compound 109 (RG2833) was the most effective in up-regulating frataxin expression. RG2833 apparently increased frataxin mRNA in patient blood samples in an unpublished Phase I clinical trial but has been discarded as it can produce harmful metabolites upon degradation. Nicotinamide is a promising class III HDACi that also increases *FXN* expression,

in a transformed cell line, patient's lymphocytes and in an FRDA mouse model (Chan *et al*. 2013) and is being assessed in a Phase II clinical study.

Erythropoietin (EPO)

EPO is a hormone that controls erythropoiesis by primarily acting on erythrocyte precursors in the bone marrow. Recombinant human EPO (rhuEPO) was reported to increase frataxin levels in lymphocytes from FRDA patients, cultured cardiac cells and mouse neuronal cells (Sturm *et al*. 2005). EPO increases frataxin protein levels without affecting mRNA expression, suggesting a regulatory effect at the post-translational level (Acquaviva *et al*. 2008). In a pilot open-label clinical trial, 8 patients received subcutaneously 2000 IU of rhuEPO three times per week during 6 months. rhuEPO increased frataxin levels, improved ataxia scores and reduced oxidative stress markers (Boesch *et al*. 2008). Since EPO stimulates the production of erythrocytes, increase in hematocrit required phlebotomies in half of the patients treated. This side effect can be avoided with the use of the EPO derivate carbamylated EPO (CEPO) that increases frataxin protein levels in cell culture but has no erythropoietic activity (Sturm *et al*. 2010). In a clinical study where ten FRDA patients were treated with a first subcutaneous dose of 600 IU/kg and 1200 IU/kg three months later, CEPO induced an increase in frataxin that lasted up to 6 months after the latter dose (Saccà *et al*. 2011). However, in a double-blind, placebo-controlled Phase II trial, frataxin levels, oxidative stress or ataxia ratings did not change in 36 FRDA patients that received 325 μg of CEPO a total of six times during 2 weeks (Boesch *et al*. 2014) .

Interferon γ (IFNγ)

Frataxin levels have been shown to be transcriptionally upregulated by IFNγ in primary cell culture from FRDA patients. Furthermore, in a mouse model of FRDA, IFNγ increases frataxin expression in DRG neurons and ameliorates sensorimotor performance (Tomassini *et al*. 2012). IFNγ was administered via subcutaneous injection during 8 weeks in pediatric FRDA patients in a pilot open-label study, with some increase in frataxin levels and improvement in ataxia score (Seyer *et al*. 2015).

Protein replacement

Transactivator of transcription (TAT) is a short peptide derived from the human immunodeficiency virus capable of guiding a fusion protein across membranes (Del Gaizo *et al*. 2003). Therefore, a TAT fusion protein containing a mitochondrial targeting sequence can translocate into the mitochondria. Injection of TAT-FXN into conditional knockout mice extended their lifespan, increased aconitase activity and improved the cardiac phenotype (Vyas *et al*. 2011).

Gene therapy

An initial study in FRDA patient fibroblasts showed that either adeno-associated virus (AAV) or lentiviral vectors encoding the human *FXN* cDNA resulted in the expression of appropriately localized frataxin and increased the resistance to oxidative stress (Fleming *et al*. 2005). Intravenous injection of AAV expressing human *FXN* in a cardiac conditional mouse model (MCK mouse, Puccio *et al*. 2001) not only prevented the cardiac phenotype but also, when administered later, was able to revert the cardiomyopathy and the functional and structural defects of the cardiomyocytes (Perdomini *et al*. 2014).

High capacity herpes simplex virus type 1 (HSV-1) based vectors are promising for gene therapy in neurological diseases since they retain the neurotropic features of the HSV-1 virus, including being transported along axons and establishing latent infections with prolonged gene expression in both sensitive and motor neurons (reviewed in Manservigi *et al*. 2010). HSV-1 vectors containing the *FXN* genomic locus including the introns, the promoter and the flanking regulatory sequences were introduced in FRDA patient fibroblasts and also reduced their sensitivity to oxidative stress (Gomez-Sebastian *et al*. 2007). Interestingly, brainstem injection of the HSV-1 amplicon expressing human FXN on a neuronal conditional knockout mouse model rescued their motor coordination phenotype (Lim *et al*. 2007).

6. Models of FRDA

The use of models is essential to understand the pathophysiological mechanisms of human disease and to develop effective therapeutic approaches. The high degree of conservation of frataxin from bacteria to human enabled the development of models of FRDA using different organisms and cell types. The diverse FRDA models, which recapitulate to different extents the hallmarks of the disease, have been essential to investigate the function of frataxin and the underlying pathophysiological mechanisms, as well as for the development of therapeutic strategies.

6.1 Non-mammalian models

Saccharomyces cerevisiae and *Escherichia coli*

The models of frataxin deficiency in yeast have been essential for the study of the protein function [see section 3.2]. Yeast lacking *Yfh1* show iron accumulation and severe alteration of Fe-S enzyme activity including aconitase (Rötig *et al*. 1997). However, knocking out *CyaY* in *E. coli* did not affect bacterial growth, iron content or sensitivity to oxidative stress (Li *et al*. 1999).

Invertebrate models

Several transient knockdown models of FRDA in *C. elegans* have been published. Microinjection in L4 larvae of RNA interference (RNAi) targeting the *C. elegans* frataxin homolog *frh-1* led to a reduction in lifespan and increased sensitivity to oxidative stress. The *frh-1* (RNAi) worms also develop a pleiotropic phenotype of slow growth, lethargic behavior, egg-laying defects, abnormal pharyngeal pumping and defecation defects (Vázquez-Manrique *et al*. 2006). Equivalent results of decreased lifespan and impaired respiration were found with different RNAi constructs directed against *frh-1* (Zarse *et al*. 2007).

Intriguingly, *frh-1* RNAi knockdown administered in the adult stage (day 5) extended the lifespan of the worms, in addition to causing small body size, reduced fertility and altered response to oxidative stress (Ventura *et al*. 2005). This group developed an RNAi dilution strategy to titrate the reduction in expression of mitochondrial proteins including frataxin, and in fact they found that intermediate inhibition of these genes extended the lifespan whereas high inhibition leads to a decreased lifespan (Rea *et al*. 2007). Further investigation of the increased lifespan in response to frataxin suppression led to the hypothesis that mild mitochondrial stress may have pro-longevity effects through the induction of mitochondrial autophagy (Schiavi *et al*. 2013; Schiavi *et al*. 2015).

In the knockdown model generated by injection of RNAi in young worms (Vázquez-Manrique *et al*. 2006), lifespan and other physiological phenotypes were improved by supplementation with flavin adenine dinucleotide. These results prove the usefulness of the frataxin deficient model in *C. elegans* for drug screening in FRDA.

Frataxin knockdown models have also been generated in *Drosophila melanogaster*. Since it is the object of study of the present thesis, this topic will be further developed in section 7.3.

6.2 Mouse models (*Mus musculus*)

Conditional knockout mouse models

Complete deletion of *Fxn* in mouse results in lethality at embryonic day 6.5, demonstrating that frataxin is essential during early development (Cossée *et al*. 2000). Accordingly, no FRDA patients homozygous for point mutations with a total loss of frataxin have been identified.

Viable conditional knockout mouse models of FRDA were generated using the Cre-*lox*P recombination system. Deletion of the exon 4 of *Fxn* from a conditional floxed allele (Fxn^{L3}) was combined with tissue-specific or tissue-specific inducible Cre lines. Cardiac (MCK-Cre), neuronal (NSE-Cre and Prp-

CreER^T) and pancreatic (Ins2-Cre) mouse models reproduced the main features of FRDA, including hypertrophic cardiomyopathy, progressive spinocerebellar and sensory ataxia and diabetes (Puccio *et al*. 2001; Simon *et al*. 2004).

In the MCK-Cre mice, Cre recombinase is expressed under the muscle creatine kinase (MCK) promoter to drive the deletion of *Fxn* to heart and skeletal muscle. The MCK mice show a reduced lifespan and develop cardiac hypertrophy leading to cardiac failure, but not a muscle phenotype. Early deficit of Fe-S proteins occur before the mitochondrial iron accumulation (Puccio *et al*. 2001) No oxidative damage was observed, suggesting that oxidative stress is not involved at least in the early stages of the disease (Seznec *et al*. 2005).

In the NSE-Cre (neuron specific enolase) transgenic line, *Fxn* is deleted in neurons, but also in heart and liver due to leaky expression of the promoter. The NSE mutants exhibit a combined neurological and cardiac phenotype that includes progressive ataxia and loss of proprioception, cardiomyopathy and iron accumulation. The phenotype of this model is severe, with mice dying at around 25 days of age, and therefore does not reproduce the progressive aspect of FRDA (Puccio *et al*. 2001).

An inducible neural mouse model was generated where the Cre-recombinase is expressed under the control of the mouse prion protein promoter (Prp) only after injection of tamoxifen. This Prp-CreER^T model reproduces the neurodegenerative features observed in FRDA patients. Prp-CreER^T mice develop cerebellar and sensory ataxia together with a loss of proprioception. Histologically, degeneration of sensory neurons is observed in the DRG and the granular layer of the cerebellum (Simon *et al*. 2004).

In order to model the diabetes mellitus and glucose intolerance observed in FRDA patients, models lacking *Fxn* primarily in the β-cells of the pancreas were generated using Ins2-Cre. The Ins2-Cre mice develop glucose intolerance followed by diabetes. This phenotype is preceded by increased oxidative stress and apoptosis leading to a progressive reduction in the number of pancreatic islets (Ristow *et al*. 2003).

GAA expansion-based mouse models

The conditional knockout approach leads to a time and tissue-specific complete loss of frataxin. However, FRDA is a progressive disease that results from the presence of a residual amount of frataxin throughout life. Furthermore, the conditional models do not allow the study of the molecular mechanisms associated with the GAA-mediated silencing of frataxin and how it contributes to the disease. GAA repeat expansion-based models have been generated to address those issues, by means of two different strategies.

First was the generation of a knockin mouse model that carries a $(GAA)_{230}$ repeat expansion in the first intron of the endogenous mouse *Fxn* locus. The homozygous knockin mice (KIKI) were crossed with the frataxin knockout to obtain the double heterozygous knockin-knockout (KIKO). The KIKI and KIKO mice express 66-83% and 25-36% of wild-type frataxin levels, respectively (Miranda *et al*. 2002). After one year, the KIKO mice did not develop motor coordination defects, cardiomyopathy or iron deposits, suggesting that the decrease in frataxin levels did not reach the critical threshold required to induce pathology in mice. Although the KIKO mice had no signs of neurodegeneration, transcriptional analysis revealed changes in gene expression compared with controls, with most them occurring in the spinal cord (Coppola *et al*. 2006).

A second GAA repeat model was generated by using the human frataxin locus. Initially, transgenic mice containing the entire human *FXN* gene within a human yeast artificial chromosome (YAC) clone were crossed with the *Fxn* knockout. Offspring express only human frataxin in the appropriate tissues at levels comparable to the endogenous mouse protein and show a preserved respiratory chain function, indicating that the human protein is able to rescue the mouse frataxin deficit (Pook *et al*. 2001). Two mouse lines (YG22 and YG8) were subsequently obtained from a YAC containing GAA repeat expansions derived from FRDA patient DNA (GAA_{190} and GAA_{190+90} respectively). YG22 and YG8 mice were bred to the mouse frataxin knockout to generate the rescued mice YG22R and YG8R. These mice express comparatively reduced levels of human frataxin and show a progressive phenotype with mild locomotor

deficits, iron deposits, mild signs of oxidative stress and reduced aconitase activity in the heart. Histological abnormalities were observed as well including vacuolization and lipofuscin in the sensory neurons of the DRG (Al-Mahdawi *et al*. 2006). A new colony derived from YG8R named YG8sR contains a single pure GAA repeat expansion of more that 200 repeats due to intergenerational expansion, and develop a slightly more severe phenotype (Anjomani Virmouni *et al*. 2015).

Taken together, the GAA expansion-based murine models show a very mild phenotype and efforts are being made to obtain mouse lines with longer GAA repeats by either selecting founder mice with expanded repeats or by using a human *FXN* BAC (Bacterial Artificial Chromosome) to introduce very large GAA repeats from FRDA patients.

6.3 Mammalian cellular models

Patient-derived cells

Many studies have been conducted using patient-derived cells such as primary fibroblasts and lymphoblasts or, more recently, induced pluripotent stem cells (iPSCs). Primary fibroblasts and lymphoblasts derived from FRDA patients constitute a relevant model as they carry the complete frataxin locus including regulatory sequences and the GAA repeat expansions. Although these patient-derived cells have reduced levels of frataxin, the characteristic biochemical phenotype of FRDA is not present in normal conditions (Rötig *et al*. 1997; Brigitte Sturm *et al*. 2005). However, they are more sensitive to oxidative stress and this reduction in viability can be rescued by mitochondria-targeted antioxidants (Wong *et al*. 1999; Jauslin *et al*. 2003).

However, the most disease-relevant cellular types for the study of FRDA that are neurons and cardiomyocytes, are not accessible from patients. Somatic cells can be reprogrammed into iPSCs and then be differentiated into other cell types. Several iPSC lines derived from FRDA patient fibroblasts have been generated, using different sets of reprogramming transcription factors. These iPSCs recapitulate some characteristic molecular aspects of FRDA

including GAA repeat instability mediated by the mismatch repair mechanism and reduced frataxin levels but do not display deficits in Fe-S enzymes (Ku *et al*. 2010; Liu *et al*. 2011). FRDA iPSCs were differentiated into neurons and cardiomyocytes and in addition to reduced frataxin levels, displayed impaired mitochondrial function (Hick *et al*. 2013). A different model of FRDA-iPSC cardiomyocytes show disorganized mitochondrial network, mitochondrial DNA depletion, iron accumulation and cardiac hypertrophy cellular stress responses (Lee *et al*. 2014).

Frataxin silencing in cell lines

An alternative strategy to obtain FRDA cellular models consists in silencing frataxin, by means of siRNA or shRNAi, in different cell lines including embryonic carcinoma cells (Santos *et al*. 2001), HeLa cells (Stehling *et al*. 2004), oligodendroglioma cells (Napoli *et al*. 2007), Schwann cells (Lu *et al*. 2009), neuroblastoma cells (Bolinches-Amorós *et al*. 2014) or human astrocytes (Loría and Díaz-Nido 2015). These models reproduce to different extents the FRDA cellular phenotypes, probably due to the characteristics of the distinct cell lines and the variable knockdown efficiencies.

Murine cellular models

In an equivalent manner, non-human cellular models have been obtained either as primary culture from existing FRDA mouse models such as fibroblasts and neural stem cells from the YG8 mouse model (Sandi *et al*. 2014), or by frataxin silencing in murine cell lines such as rat myocytes (Obis *et al*. 2014). Another significant example is the generation of a humanized mouse fibroblast model carrying point mutations. Deletion of frataxin in a murine fibroblast cell line carrying the conditional allele Fxn^{L3} in combination with transient expression of Cre-recombinase led to inhibited cell division and cell death. Lethality can be rescued by stable transfection of human *FXN* or *FXN* carrying a point mutation. Interestingly, cells expressing the mutant alleles display Fe-S cluster deficit, mitochondrial iron accumulation and sensitivity to oxidative stress. Furthermore, the severity of the cellular phenotype correlates with the effect of the mutation observed in patients (Calmels *et al*. 2009).

7. *Drosophila melanogaster* as a model of FRDA

7.1 *Drosophila* as a model organism

The fruit fly, *D. melanogaste*r, constitutes a powerful animal model for research due to a combination of factors. First, *Drosophila* has a short life cycle of approximately 15 days from the lay of the egg to the eclosion of the adult from the pupae. This is especially critical for the study of aging and neurodegenerative diseases with a late developing phenotype. Additional benefits over the use of higher organisms include easy handling and cheap maintenance. These features allow the generation of large numbers of individuals that can be used for genetic screens.

However, the most important characteristic that substantiates the use of *Drosophila* as a model of human disease is that, not only at the cellular level, but also more complex pathways implicated in development, organogenesis or function of a complex nervous system are highly conserved between flies and vertebrates. The sequencing of the fly and human genomes revealed a large number of genes conserved in sequence and function between *Drosophila* and human, with an estimated 75% of known human disease-causing genes being present in the fly (Rubin 2000; Reiter *et al*. 2001). Besides, the *Drosophila* genome is smaller in size (1.23×10^8 bp *vs* 3.33×10^9 bp) and in number of genes (14.000 *vs* 20-25.000) compared to the human genome (Adams *et al*. 2000; International Human Genome Sequencing Consortium 2004). Accordingly, many human gene families composed of paralogues with redundant or overlapping functions correspond to a single gene or a smaller gene family in *Drosophila*, which facilitates the genetic studies.

The fruit fly has been used as model organism for a hundred years, starting with the work of Thomas Hunt Morgan who chose *Drosophila* to establish his chromosomal theory of heredity (Morgan 1915). Since, a variety of tools have been developed to manipulate and control *Drosophila* genetics. For instance, balancer chromosomes carrying inverted segments allow the maintenance of homozygous lethal mutations in heterozygosis by avoiding recombination.

Generation of transgenic lines

When the genetic cause of the human disease and the ortholog in the fly have been identified, several of these tools can be used to produce a transgenic model in *Drosophila*. Similarly, transgenic lines can be generated for genes known to be implicated in basic biological processes. Gain of function mutations typically involves transgenic individuals expressing mutant versions of the human gene. In addition, wild-type allele of the human gene or even the ortholog gene can be overexpressed in fly. Traditionally, methods of disrupting gene function to obtain loss of function mutations in *Drosophila* comprise chemical and transposable element mutagenesis. P element mobilization has been used for insertional inactivation and lead deletions in a gene by imprecise excision. P-element-mediated transformation also allows the insertion of single genes or constructs in the fly genome (Rubin and Spradling 1982). This methodology allows the overexpression of the gene of interest or the generation of a knockdown model by insertion of an RNAi construct. P[acman] is an improved transformation platform based on BACs that can introduce larger DNA fragments into specific "docks" of mapped in the genome (Venken *et al*. 2006).

There are also tools available for the spatial and temporal control of target genes or constructs. The UAS-GAL4 system, adapted from yeast, involves two transgenes [Figure 5]. One carries the GAL4 transcription factor under the control of a promoter of known expression pattern, and the other with the transgene of interest downstream of an upstream activating sequence (UAS) (Brand and Perrimon 1993). A large collection of GAL4 driver lines are available, carrying the promoters of genes such as *actin* (ubiquitous), *embryonal lethal abnormal vision* (*elav*, pan-neuronal), *neuralized* (*neur*, peripheral nervous system), *reverse polarity* (*repo*, glia) or *Glass Multimer Reporter* (GMR, eye). Other method to restrict the expression of a transgene is the flippase (FLIP)-flippase recognition target (FRT) recombination system that enables the generation of mutant patches in a heterozygous background, therefore allowing the expression of homozygous lethal mutations (Golic and Lindquist 1989).

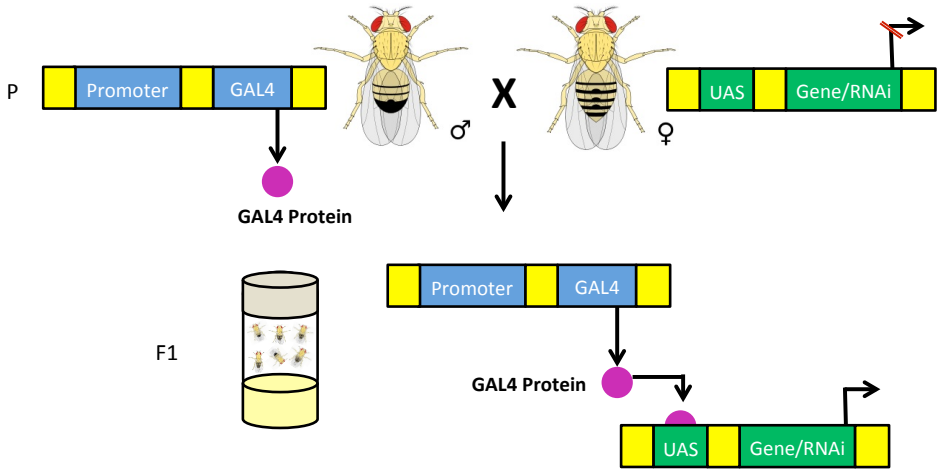

Figure 5: Schematic of the UAS-GAL expression system in *Drosophila.*

Genetic screens

One of the most powerful features of *Drosophila* as a model organism is the possibility to perform large-scale genetic screens for the characterization of signaling pathways and gene networks implicated in disease pathogenesis. Two main strategies can be used for this purpose. “Forward genetics” approaches go from the phenotype to the causative gene. Mutagenizing agents or transposable elements are used to generate large numbers of mutant flies that are subsequently screened for a phenotype relevant for the disease studied. For every mutant line selected out of the screen, the gene bearing the mutation is identified and constitutes a possible candidate to be involved in the disease of interest.

“Reverse genetics” can be applied to identify modifiers of the pathway or disease investigated. First, a mutant line for the gene of interest needs to be generated by any of the methodologies described above. Then comes the identification of a phenotype that can be easily assessed for improvement and worsening. Finally, the mutant line is crossed with a battery of loss of function, knockdown or overexpression lines, and the selected phenotype is evaluated. This strategy is possible thanks to the existence of a very high number of commercial mutant lines that are maintained in large repositories such as the

Bloomington Stock Center (Indiana University) or the Vienna Drosophila Resource Center.

7.2 *Drosophila* as a model of neurodegenerative diseases

An advantage from the cellular models is that *Drosophila* has a complex nervous system with neurons and glia, and protected by a blood brain barrier. Although overly less complicated, the fly brain is structurally and functionally very similar to the vertebrate brain. Furthermore, a number of assays have been developed to assess neural function and neurodegeneration in *Drosophila*. Some of them are (1) external morphology phenotypes such as eye and wing developmental defects, (2) histological such as retinal wasting, loss of eye rhabdomeres, brain vacuolization, neuronal loss or neuromuscular junction abnormalities and (3) behavioral like decreased lifespan or motor ability (reviewed in McGurk *et al*. 2015).

These features have enabled the study of the majority of the human neurodegenerative diseases in *Drosophila* models, including Alzheimer's disease, Parkinson's disease, fragile X syndrome and a number of polyQ diseases [Table 3]. The use of *Drosophila* as a model has enabled the identification of modifiers for many of these pathologies by means of unbiased and candidate-based genetic screens. One example is the identification of the transcriptional regulator CREB-binding protein (CBP) as a suppressor of the polyQ-associated degeneration in a model of Huntington's disease (Steffan *et al*. 2001). The histone acetyltransferase function of CBP is inhibited by interaction of its active site with the expanded huntingtin and therefore the use of HDACi was suggested to mitigate poliQ toxicity (Bodai *et al*. 2003; Ferrante *et al*. 2003; Hockly *et al*. 2003). A more recent example is the combination of two screens in parallel, in a cellular and a *Drosophila* model of Spinocerebellar ataxia-1, that established the involvement of the RAS-MAPK-MSK1 signaling pathway as a regulator of Ataxin-1 levels and toxicity (Park *et al*. 2013). Moreover, *Drosophila* models of neurodenegerative diseases have been used as a platform for the identification of new therapeutic compounds. Recently, mutants for the vesicular monoamine transporter (dVMAT) as a model of Parkinson's disease were screened for more than 1000 known drugs.

By assessing larval locomotion and adult fertility phenotypes, one compound was identified and suggested for the treatment of Parkinson's disease (Lawal *et al*. 2014).

Table 3: *Drosophila* models of neurodegenerative diseases. Adapted from McGurk *et al*. 2015.

Disease / protein	Some initial references
Alzheimer's disease models	
APP	(Fossgreen *et al*. 1998; Greeve *et al*. 2004)
A-beta peptide	(Finelli *et al*. 2004; Iijima *et al*. 2004)
PSEN 1, PSEN 2	(Ye and Fortini 1999)
MAPT (Tau)	(Wittmann *et al*. 2001; Jackson *et al*. 2002)
Parkinson's disease models	
DJ-1	(Menzies *et al*. 2005; Meulener *et al*. 2005; Park *et al*. 2005; Yang *et al*. 2005; Lavara-Culebras *et al*. 2010)
LRRK2	(Liu *et al*. 2008)
Parkin (loss of function)	(Greene *et al*. 2003)
PINK1 (loss of function)	(Clark *et al*. 2006; Park *et al*. 2006; Yang *et al*. 2006)
SNCA (α-synuclein)	(Feany and Bender 2000)
PolyQ disease models	
HD	(Jackson *et al*. 1998; Romero *et al*. 2008)
SCA1	(Fernandez-Funez *et al*. 2000)
SCA2/ALS	(Satterfield *et al*. 2002; Kim *et al*. 2014)
SCA3/MJD	(Warrick *et al*. 1998; Warrick *et al*. 2005)
SCA7	(Jackson *et al*. 2005; Latouche *et al*. 2007)
SCA8	(Mutsuddi *et al*. 2004)
SCA17	(Hsu *et al*. 2014)
Some additional disease models	
FXTAS	(Jin *et al*. 2003)
Prion disease (PrP)	(Gavin *et al*. 2006; Thackray *et al*. 2012)

APP: Amyloid precursor protein. PSEN: presenilin. LLRK2: Leucine-rich repeat kinase 2. PINK1: PTEN-induced putative kinase 1. HD: Huntington's disease. SCA: Spinocerebellar ataxia. ALS: Amyotrophic lateral sclerosis. MJD: Machado Joseph disease. FXTAS: Fragile X-associated tremor/ataxia syndrome. PrP: prion protein.

7.3 Models of FRDA in *Drosophila*

Frataxin homolog (*fh*) is the *Drosophila* homolog of human *FXN*. The gene *fh,* of 965 bp, is located in 8C/D of the X chromosome. It is composed of one intron flanqued by two exons, encoding for the 190 amino acid *Drosophila* frataxin protein. Frataxin is a highly conserved protein [see section 3.1], and the *Drosophila* protein shares that conservation in both sequence and structure. Preliminary *in silico* analysis predicted the presence of signal peptide for mitochondrial import (Cañizares *et al*. 2000). The mitochondrial localization of frataxin was corroborated by a co-localization experiment in cell culture (Llorens *et al*. 2007). The physical characteristics and the iron binding properties of the *Drosophila* frataxin were later resolved by (Kondapalli *et al*. 2008).

A first *Drosophila* model of FRDA was generated by RNAi knockdown (Anderson *et al*. 2005). Expression of the UAS-*fh*RNAi transgene with the ubiquitous driver *daughterless*-GAL4 induced a 90% reduction of frataxin levels. Frataxin-depleted larvae show retarded development and reduced viability. There are a 1-2% of adult escapers, which have a shortened lifespan. Activity of the Fe-S enzymes mitochondrial aconitase and respiratory complexes II, III and IV is reduced in both the frataxin deficient larvae and adults, and larvae exhibit hypersensitivity to iron as well. Frataxin knockdown directed to the peripheral nervous system with the C96-GAL4 driver does not affect pre-adult development but reduces adult lifespan. To test whether oxidative damage was contributing to the deleterious effects of frataxin deficiency, they ectopically expressed enzymes implicated in oxidative stress scavenging. They found that the enzymes that scavenge H_2O_2 but not the ones that scavenge superoxide rescue the phenotypes induced by frataxin knockdown in the peripheral nervous system, suggesting that this oxidative stress scavenging pathway has a critical role in FRDA pathogenesis (Anderson *et al*. 2008). Defects in mitochondrial axonal transport and membrane potential have been characterized in the neuromuscular junctions of the frataxin-deficient larvae, but increased of ROS is not observed (Shidara and Hollenbeck 2010).

A second RNAi knockdown model of FRDA was established in our laboratory (Llorens *et al*. 2007). Ubiquitous expression of this new *fh*RNAi transgene with the actin-*GAL4* driver led to a moderate reduction of 70%, closer to patient frataxin levels. This situation is compatible with normal embryonic development. However, the frataxin-deficient adult flies show a reduction in lifespan and motor ability. Hyperoxia exacerbated the difference in lifespan between the *fh*RNAi flies compared with the controls and induced a reduction in aconitase activity, indicating an increased sensitivity to oxidative stress (Llorens *et al*. 2007). Frataxin knockdown flies also exhibit an increase in fatty acids leading to toxic lipid peroxidation. When the loss of frataxin is driven to glial cells, the animals show reduced lifespan and locomotor activity, increased sensitivity to oxidative insult, neurodegeneration and lipid droplets in glial cells (Navarro *et al*. 2010). Taken together, these results support the implication of oxidative stress and lipid peroxidation, and the importance of the glia, in the pathogenesis of FRDA. The study of the iron homeostasis in the frataxin-deficient flies revealed a hypersensitivity to dietary iron mediated by an impaired activation of ferritin translation. Moreover, the upregulation of mitoferrin leads to increased mitochondrial iron uptake. Interestingly, mitoferrin downregulation rescued several of the phenotypes caused by the loss of frataxin (Navarro *et al*. 2015).

Recently, a *Drosophila* heart model of FRDA was published, showing impaired heart function. The authors did not find that oxidative stress was involved in the heart phenotype. However, methylene blue, an alternative electron carrier that bypasses mitochondrial complexes I-III, rescued the heart dysfunction (Tricoire *et al*. 2014).

Although they are not exactly models of FRDA, frataxin overexpression in model organisms might be useful to study the protein function. In particular, overexpressing frataxin in the mitochondria extended the lifespan and increased the resistance to oxidative stress in *Drosophila*, suggesting a role for frataxin in the protection against oxidative stress and the subsequent cell damage (Runko *et al*. 2008)

Objectives

The main objective of this thesis is to further characterize the *Drosophila* model of FRDA previously obtained in our laboratory (Llorens *et al*. 2007), in order to contribute to the study of the function of frataxin and the physiopathology of the disease, and to the finding of biological markers and therapeutic approaches. From this main objective, we defined the following specific objectives for this thesis:

1. To determine whether the human frataxin and its homolog in *Drosophila* share an equivalent function.

2. To evaluate the validity of the *Drosophila* model of FRDA as a drug-screening tool by testing the effect of deferiprone and idebenone on the frataxin-deficiency induced phenotypes.

3. To identify modifiers of FRDA pathogenesis by means of a candidate pathway genetic screen.

4. To determine the effect of frataxin depletion in the metal homeostasis of the *Drosophila* model of FRDA.

Articles

Article 1. Overexpression of human and fly frataxins in *Drosophila* provokes deleterious effects at biochemical, physiological and developmental levels (Navarro *et al*. 2011)

OPEN ACCESS Freely available online

PLoS one

Overexpression of Human and Fly Frataxins in Drosophila Provokes Deleterious Effects at Biochemical, Physiological and Developmental Levels

Juan A. Navarro[1☯], José V. Llorens[2,3*☯], Sirena Soriano[2], José A. Botella[1], Stephan Schneuwly[1], María J. Martínez-Sebastián[2], María D. Moltó[2,4]

1 Institute of Zoology, University of Regensburg, Regensburg, Germany, **2** Departament de Genètica, Universitat de València, Burjassot, Valencia, Spain, **3** Instituto de Biomedicina, CSIC, Valencia, Spain, **4** CIBERSAM (Centro de Investigación Biomédica en Red de Salud Mental), Madrid, Spain

Abstract

Background: Friedreich's ataxia (FA), the most frequent form of inherited ataxias in the Caucasian population, is caused by a reduced expression of frataxin, a highly conserved protein. Model organisms have contributed greatly in the efforts to decipher the function of frataxin; however, the precise function of this protein remains elusive. Overexpression studies are a useful approach to investigate the mechanistic actions of frataxin; however, the existing literature reports contradictory results. To further investigate the effect of frataxin overexpression, we analyzed the consequences of overexpressing human (FXN) and fly (FH) frataxins in *Drosophila*.

Methodology/Principal Findings: We obtained transgenic flies that overexpressed human or fly frataxins in a general pattern and in different tissues using the UAS-GAL4 system. For both frataxins, we observed deleterious effects at the biochemical, histological and behavioral levels. Oxidative stress is a relevant factor in the frataxin overexpression phenotypes. Systemic frataxin overexpression reduces *Drosophila* viability and impairs the normal embryonic development of muscle and the peripheral nervous system. A reduction in the level of aconitase activity and a decrease in the level of NDUF3 were also observed in the transgenic flies that overexpressed frataxin. Frataxin overexpression in the nervous system reduces life span, impairs locomotor ability and causes brain degeneration. Frataxin aggregation and a misfolding of this protein have been shown not to be the mechanism that is responsible for the phenotypes that have been observed. Nevertheless, the expression of human frataxin rescues the aconitase activity in the *fh* knockdown mutant.

Conclusion/Significance: Our results provide *in vivo* evidence of a functional equivalence for human and fly frataxins and indicate that the control of frataxin expression is important for treatments that aim to increase frataxin levels.

Citation: Navarro JA, Llorens JV, Soriano S, Botella JA, Schneuwly S, et al. (2011) Overexpression of Human and Fly Frataxins in Drosophila Provokes Deleterious Effects at Biochemical, Physiological and Developmental Levels. PLoS ONE 6(7): e21017. doi:10.1371/journal.pone.0021017

Editor: Mel B. Feany, Brigham and Women's Hospital, Harvard Medical School, United States of America

Received February 28, 2011; **Accepted** May 16, 2011; **Published** July 11, 2011

Funding: This work was supported by grants from Fondo Investigaciones Sanitarias (ISCIII06- PI0677) and La Fundació la Marató TV3 (exp 101932) of Spain. JVL is supported by the European Friedreich's Ataxia Consortium for Translational Studies. SS is a recipient of a fellowship from Ministerio de Ciencia e Innovación of Spain. The funders had no role in study design, data collection and analysis, decision to publish, or preparation of the manuscript.

Competing Interests: The authors have declared that no competing interests exist.

* E-mail: jose.vicente.llorens@uv.es

☯ These authors contributed equally to this work.

Introduction

Friedreich's ataxia (FA), an autosomal recessive disease, is the most frequent form of inherited ataxias in the Caucasian population (1:50000) [1]. The major cause of this disease is the presence of a large GAA repeat expansion in the first intron of the *FXN* gene [2]. This large GAA repeat decreases the level of transcription of the mRNA that encodes the protein frataxin [3,4], resulting in levels that range from 5% to 30% of the normal level of this protein [5]. The clinical manifestations of FA involve spinal cord and cerebellum neurodegeneration, which cause gait and limb ataxia, muscular weakness and speech impairments [6,7]. Other manifestations of FA include scoliosis, diabetes and hypertrophic cardiomyopathy, which is the main cause of death [8].

Frataxin is a highly conserved protein throughout evolution [9]. This degree of conservation has enabled the development of FA models in many organisms, from *E.coli* to the mouse, that have contributed to a better understanding of this protein's function; however, the exact function of frataxin remains elusive. Seminal findings by a number of key studies have suggested potential roles for frataxin in iron homeostasis [10–14], as an activator of the respiratory chain [15–17], as a regulator of Fe-S cluster assembly through activation [12,18–23] or inhibition [24] and/or by promoting cellular defense against reactive oxygen species [25–32].

In *Drosophila*, the frataxin homolog (*fh*) shares a high degree of sequence conservation and projected folding with other frataxin orthologs [33]. Moreover, a reduction in the level of frataxin expression in *Drosophila* has been established as an effective model to study frataxin function and the pathological mechanisms that underlie frataxin deficiency. In fact, the loss of *fh* recapitulates important behavioral and biochemical features of human disease

[31,34]. Furthermore, *Drosophila* models have provided support for the crucial involvement of oxidative stress, particularly peroxides, in the development of FA [31,32,35]. These models have also indicated that frataxin is relevant in glial cells and that these cells play a role in FA [35]. In addition, these models have revealed that mitochondrial depolarization is an initial element in the axonal transport defects that lead to a concomitant dying-back neuropathy [36]. Overexpression studies in the fruit fly have been greatly used to study the gene's function and to provide insight into the human inherited pathologies. Among these studies, several reports of investigations of the ectopic expression of human genes in *Drosophila* have provided highly valuable information regarding Alzheimer's disease [37], polyglutamine diseases [38], Parkinson's disease [39,40] and dominant spinocerebellar ataxias (SCAs) [41,42].

For frataxin overexpression, the existing literature presents contradictory results. Experiments in mice [17,43] or in cultured cells [15,44,45] have revealed that frataxin overexpression was innocuous or had a positive effect on the cell's biology, stimulating the production of ATP or inducing the recruitment of antioxidant defenses. Similarly, Runko *et al.* [46] reported that the overexpression of *Drosophila* frataxin promoted cellular resistance to oxidative stress. However, we have previously reported that *Drosophila* frataxin overexpression [31] leads to detrimental phenotypes in the fly, including developmental defects, a decrease in the level of aconitase activity and hypersensitivity to oxidative stress. Notably, the overexpression of frataxin in yeast has also been shown to critically affect aconitase activity [47].

In the present study, we analyzed the effects of the overexpression of two frataxins in a multicellular organism, *Drosophila melanogaster*. To achieve this aim, we generated transgenic flies that overexpressed human (*FXN*) and fly (*fh*) frataxins through the UAS/GAL4 system. We also studied whether FXN can functionally replace endogenous *Drosophila* frataxin. In the present paper, we report that the increased expression of human or fly frataxin in *Drosophila* leads to deleterious effects at biochemical, histological and behavioral levels. We also show that FXN can rescue the reduction in the aconitase activity that is associated with the loss of frataxin in the fly. Our results provide *in vivo* evidence of a functional equivalence between human and fly frataxins and indicate that the regulation of frataxin expression is a key factor that underlies frataxin function.

Materials and Methods

Drosophila stocks

The w^{1118} strain of *Drosophila* was used as the control line and for the injection of the UAS-*FXN* construct. The UAS-*fh* line, which carried the *fh* coding sequence under the control of UAS, was previously generated in our laboratory [31]. The UAS-*fh* line induced a 9-fold increase in the level of *fh*-mRNA at 29°C. The *UD1R2* line was kindly provided by J.P. Phillips (University of Guelp, Guelp, ON). *UD1R2* induced a strong interference of *fh*, and the FH protein was reduced to undetectable levels [34]. The MitoCat flies were a gift from W. Orr (Southern Methodist University, Dallas, USA). The *actin*-GAL4, da^{G32}-GAL4, *24B*-GAL4, *neur*-GAL4, *repo*-GAL4 and *Appl*-GAL4 driver lines were obtained from the Bloomington Stock Center. The stocks were maintained at 25°C using standard cornmeal agar medium. The crosses between the GAL4 drivers and the UAS responder lines were conducted at either 25°C or 29°C. The rescue experiments were conducted by generating the following stocks: *mitoCat* / CyO; UAS-*FXN* / TM3; and *UDIR2* / CyO; UAS-*FXN* / TM3.

Construction of the UAS-*FXN* transgene and the generation of the fly transformants

The cDNA for *FXN* was obtained from human fetal brain poli-(A)+ mRNA (Invitrogen). A 645 bp fragment, which included the entire coding region of the gene, was amplified using the following primers: *FXN*-pUASTf (CTCGAGATGTGGACTCTCGGGC-GCCG) and *FXN*-pUASTr (GGTACCTCAAGCATCTTTT-CCGGAATAGGCCAAG). This fragment was inserted into the pCR2.1-TOPO vector and was then subcloned into the pUAST vector to generate the UAS-*FXN* transgene.

The transgenic flies were generated using standard embryo injection protocols [48]. Seven independent lines were obtained, and the presence of the transgene was verified in each line using PCR with vector-specific primers. The sequencing of the PCR products revealed that there were no mutations present in the *FXN* sequence. The lines were examined for the expression of *FXN* by crossing each of these lines with the *actin*-GAL4 driver line. A line that contained the UAS-*FXN* transgene on the second chromosome was selected to perform our experiments.

Western blotting

The total protein extraction from the *Drosophila* larvae was performed as previously described [49]. The protein levels were determined using the Bradford assay. The samples were separated on 5% stacking, 15% separating SDS polyacrylamide gels. The resolved proteins were electroblotted to a Hybond-ECL nitrocellulose membrane (GE Healthcare) and were probed using mouse anti-FXN (Chemicon, Millipore, 1:2000), mouse anti-NDUFS3 (Mitosciences MS112, 1:2000) or mouse anti-α-tubulin (Sigma-Aldrich, 1:2500) antibodies. Fluorescent goat anti-mouse was used as the secondary antibody in these cases. Detection and quantification was conducted using the Odyssey system (Li-cor Inc.). Alternatively, goat anti-mouse IgG horseradish peroxidase conjugate (Sigma-Aldrich) was used as a secondary antibody and was detected using ECL Detection Reagent (GE Healthcare).

Immunohistochemistry staining

The whole mount embryo staining technique with horseradish peroxidase was conducted as previously described [50]. The embryos were incubated with the following primary antibodies: mouse mAb anti-myosin heavy chain (anti-MHC), 1:8 dilution, a gift from D. Kiehart; mouse mAb 22C10 anti-peripheral nervous system neurons (anti-PNS), 1:50 dilution; mouse mAb BP102 anti-central nervous system axons (anti-CNS), 1:200 dilution, from the Developmental Studies Hybridoma Bank; and rabbit anti-even-skipped protein, 1:2000 dilution, kindly provided by M. Frasch. The Ab-antigen complexes were detected using biotinylated horse anti-mouse IgG (Pierce, Rockford, IL) or biotinylated goat anti-rabbit IgG (Pierce) antibodies.

Brain histology

For the examination of the adult fly brains using light and electron microscopy, ultrathin Epon plastic sections were post-stained with 2% uranyl acetate, which was followed by Reynolds' lead citrate. Next, the sections were stabilized for transmission electron microscopy using carbon coating. The examination was conducted using a Zeiss EM10C/VR electron microscope at 80 kV. The glial cell material was identified by its characteristically higher electron density.

Life span determination and climbing assay

For the life span determination, the male flies were collected within 24 h of eclosion and were raised at 25°C under a 12 h:12 h

light/dark cycle. These flies were transferred to fresh food vials every 2–3 days. The climbing assay was conducted as described in Botella *et al.* [51].

Assay of the aconitase activity

The total aconitase activity was determined from L3 larvae using the Bioxytech Aconitase-340^{TM} Spectrophotometric Assay Kit (Oxis International Inc, Portland, OR).

Hyperoxia treatment

The hyperoxia treatment was started one day post-eclosion and was performed as previously described [31]. To measure the aconitase activity, L3 larvae were maintained in hyperoxia conditions for a 24 h period before performing the assay.

Gel filtration chromatography

The mitochondria from the *actin*-GAL4>UAS-*FXN* larvae were isolated (MITOISO1, Sigma), lysed in hypotonic buffer (HEPES 10 mM, pH 7.0) and sonicated (three times for 30 sec) before being centrifuged at 20,000 *g* for 30 min. The mitochondrial matrix proteins were subjected to size exclusion chromatography on a Superdex 200 10/300 GL column with a fractionation range of 10 to 600 kDa (GE Healthcare) and were eluted with 50 mM HEPES and 140 mM NaCl, pH 8.0, at a flow rate of 0.5 ml/min. Blue Dextran 2000 (1 mg/ml) was used to estimate the void volumes, and gel filtration molecular weight standards (GE Healthcare) were used to calibrate the column. An equal volume of each fraction was analyzed using SDS-PAGE and western blotting.

Statistical analysis

A Kaplan-Meier analysis of the survival data with a semi-parametric log rank test was performed using Graph Pad Prism 4.0 software. The differences in the locomotor and aconitase activities were tested using a one-way ANOVA test, using the Statistical Packages for the Social Sciences (SPSS) v17.0. A value of $p<0.05$ was considered to be statistically significant.

Results

Human frataxin is correctly expressed and targeted to the mitochondria in *Drosophila*

To investigate the effect of human *FXN* expression in *D. melanogaster*, we generated transgenic flies that carried the UAS-*FXN* construct. These flies were crossed with the *da*-GAL4 driver line at 25°C to reach the ubiquitous expression of the human gene. Because the *da*-GAL4>UAS-*FXN* individuals exhibited lethality before adult eclosion, the presence of human frataxin was confirmed in the transgenic larvae using western blotting. As expected, human frataxin was only detected in the *da*-GAL4>UAS-*FXN* larvae; no signal was observed in the driver and responder controls (Figure 1A). To test whether *FXN* was transported into the mitochondria, we analyzed the relative amount of frataxin in the mitochondrial and cytosolic fractions. We used an anti-actin antibody as a control for cytosolic contamination. In three independent experiments, the amount of frataxin was consistently found to be 8-10 times higher in the mitochondrial fraction in comparison to the cytosolic fraction, with only a residual amount of frataxin being present in the cytoplasm. The quantity of actin was similar in both fractions. Therefore, our results indicate that human frataxin is mainly localized within the mitochondria in *Drosophila* cells, as it exhibits the same subcellular localization as endogenous *Drosophila* frataxin [31].

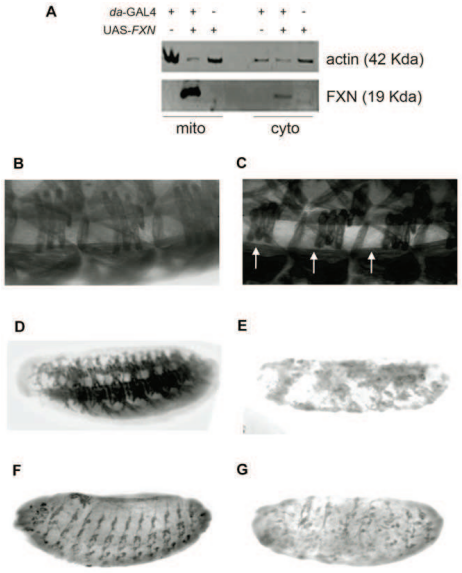

Figure 1. Effect of *FXN* overexpression in the embryonic development. (A) Detection of the FXN protein in *da*-GAL4>UAS-*FXN* (+,+) larvae in the mitochondrial (mito) and the cytosolic (cyto) fractions. The control genotypes of the larvae were *da*-GAL4>*yw* (+,−) and *yw*>UAS-*FXN* (−,+). The human frataxin protein was localized in the mitochondria. Anti-actin was used as a control for cytosolic contamination. (B–G) Muscular and nervous system defects in *da*-GAL4>UAS-*FXN* and *actin*-GAL4>UAS-*FXN* embryos at stage 16. In these panels, anterior is toward the left, and all of the views are lateral views. Anti-myosin staining revealed abnormalities in the junctions of lateral transversal muscles 1, 2 and 3 and the ventral longitudinal muscle 1 (C) compared with the control (B). Moreover, a few embryos exhibited abnormalities in the muscular development of mutant (E) versus control (D) embryos. Staining with 22C10 detected strong abnormalities in the axonal path finding of the sensory nerves (G) with respect to the control (F).
doi:10.1371/journal.pone.0021017.g001

Human frataxin overexpression reduces *Drosophila* viability

We have previously reported the consequences of increasing the amount of *fh* expression in *Drosophila* [31]. We found that the general and mesodermal overexpression of *fh* at 29°C resulted in lethality during the pre-adult stages and restricted the expression of *fh* in the nervous system, which had no effect on viability.

To test whether the effect of *FXN* overexpression on *Drosophila* viability was similar to the effect of the overexpression of *fh*, we first investigated systemic *FXN* expression with the ubiquitous *da*-GAL4 and *actin*-GAL4 drivers by mating the flies at 25°C and 29°C. Full lethality was observed with both drivers at both temperatures. These results were similar to those after the *fh* overexpression (Table 1); however, deaths were observed earlier in the individuals with *FXN* expression than in those with *fh* overexpression.

Next, we examined the consequences of a tissue-specific expression of *FXN*. The *FXN* expression was specifically driven

Table 1. The effect of general and tissue-specific expression of human and fly frataxins on *Drosophila* viability at 25°C and 29°C.

Expression pattern	GAL4 drivers	*FXN* expression	*fh* overexpression
Ubiquitous	*actin*	Lethal	Lethal
	da	Lethal	Lethal
Muscular system	*24B*	Lethal	Lethal
Nervous system	*Appl*	Viable at 25°C	Viable
		Lethal at 29°C	
	neur	Viable	Viable
	repo	Viable	Viable

doi:10.1371/journal.pone.0021017.t001

in the nervous system and in the muscles, which are two of the most affected tissues in patients with FA. The *FXN* expression in the embryonic mesoderm (*24B*-GAL4) led to the death of all of the individuals that were early to late pupae. However, we observed viable progeny that expressed *FXN* in the central nervous system (CNS), in the sensory organs and their precursors and in the glial cells, using the *Appl*-GAL4, *neur*-GAL4 and *repo*-GAL4 drivers, respectively. In contrast, the expression of *FXN* at 29°C with the neuronal post-mitotic driver *Appl*-GAL4 resulted in pre-adult lethality (Table 1).

Collectively, these results demonstrate that tissues respond similarly to *Drosophila* and human frataxin overexpression and that an adequate balance of the systemic synthesis of frataxin is critical for fly viability.

The general expression of *FXN* disrupts normal *Drosophila* development

Inmunohistochemical staining was conducted in *da*-GAL4>UAS-*FXN* and *actin*-GAL4>UAS-*FXN* embryos to identify the underlying defects that were associated with the lethal phenotypes. Anti-myosin staining of the muscular system revealed defects in the junctions of lateral transversal muscles 1, 2 and 3 with ventral longitudinal muscle 1, which was likely due to deficient muscle growth (Figure 1C). Defects in several muscles were also reported after *fh* overexpression [31]. In a few cases, we observed *FXN*-expressing embryos that exhibited a disrupted muscular system (Figure 1E). After the embryo's PNSs were stained using the 22C10 antibody, a strong disorganization of the sensory axons was detected (Figure 1G). Similar alterations were described for the *da*-GAL4 driven overexpression of *fh* [31]. No abnormalities were found in the CNS of the *FXN*-expressing embryos when they were stained using the BP102 antibody (as in *da*-GAL4>UAS-*fh* embryos; data not shown).

We observed that the lethal phenotypes that were associated with the general overexpression of human or fly frataxin mainly resulted from the impairment of correct muscle and PNS development, whereas the CNS was not affected. The high degree of similarity between the defects that were observed with the overexpression of human and fly frataxins supports the involvement of the overexpression of FXN in the same developmental mechanisms than FH overexpression. In addition, these results indicate that the frataxin level is critical for the normal embryonic development of muscle and the PNS.

Nervous system expression of *FXN* shortens life span, impairs locomotor performance and causes brain degeneration

We further assessed whether human frataxin expression in neural tissues affects *Drosophila* fitness during adulthood. The length of the life span was examined using the *Appl* -GAL4, *neur* -GAL4 and *repo*-GAL4 drivers. The *FXN* flies exhibited a statistically significant decline in the mean (75%, 80% and 50%, respectively) and maximum life spans (74%, 75% and 56%, respectively). These decreases were larger than those that were observed after the overexpression of endogenous fly frataxin (Figure 2A–C).

To study the effect of frataxin overexpression on the nervous system functioning in *Drosophila*, the locomotor activity of the flies was analyzed. The overexpression of human or fly frataxin reduced the climbing ability of the flies in an age-dependent manner for all three of the drivers used. The larger reduction was observed for *FXN* with *neur*-GAL4 driver, which exhibited a 70% reduction in the 5-day-old flies and a 90% reduction in the 10-day-old flies (Figure 2E). *Appl* (Figure 2D) and *repo*-GAL4 (Figure 2F) also induced locomotor dysfunctions, although to a lesser extent (55% and 25% in 5-day-old flies, respectively). The findings indicate that aging appears to exacerbate the reduction in locomotor ability that results from frataxin overexpression.

To identify the cellular pathology underlying the life span and locomotor phenotypes that have been associated with frataxin overexpression, the brain sections from flies that overexpressed human frataxin were analyzed using light and electron microscopy. The selective *FXN* expression in glial cells induced a strong age-related degeneration in the cortex and a neuropil vacuolization with the presence of droplet-like structures (Figure 3D). An ultrastructural analysis revealed a complete morphological disruption of the glial cells and the concomitant formation of lipid droplets (Figure 3E). Notably, a very similar phenotype was observed in the glial cells that lacked *Drosophila* frataxin [35]. Moreover, as shown in Figure 3F, several regions of the brain exhibited clear mitochondrial phenotypes, such as an abnormal morphology or vacuolization. Although the *Appl*-GAL4 > UAS-*FXN* flies exhibited a clear locomotor deficit and a shortened life span, these flies did not display brain abnormalities compared to the control age-matched individuals (data not shown).

These results indicate that an excess of frataxin impairs embryonic development and negatively affects fly fitness. Remarkably, our results from glial cells may suggest that frataxin overexpression alters cellular homeostasis in a similar manner to frataxin knock-down. These data indicate that a balance of frataxin levels is critical for the correct functioning of several cell types in the *Drosophila* nervous system.

Overexpression of human frataxin enhances susceptibility to oxidative stress

One of the most characteristic biochemical defects that is associated with a loss of frataxin is the reduction of aconitase activity [18,19,31]. Therefore, we tested whether the overexpression of human frataxin in *Drosophila* would also affect the activity of this enzyme. Aconitase activity was measured in *actin*-GAL4>UAS-*FXN* L3 larvae because the ubiquitous expression of *FXN* caused lethality before adult eclosion (Table 1). Notably, these larvae exhibited a 50% reduction in aconitase activity under normoxia conditions (Figure 4A).

Several FA models have also resulted in a strong reduction of other Fe-S-cluster-containing proteins, such as the complex I subunit, SdhA, SdhB or the Rieske protein [52,53]. Thus, we

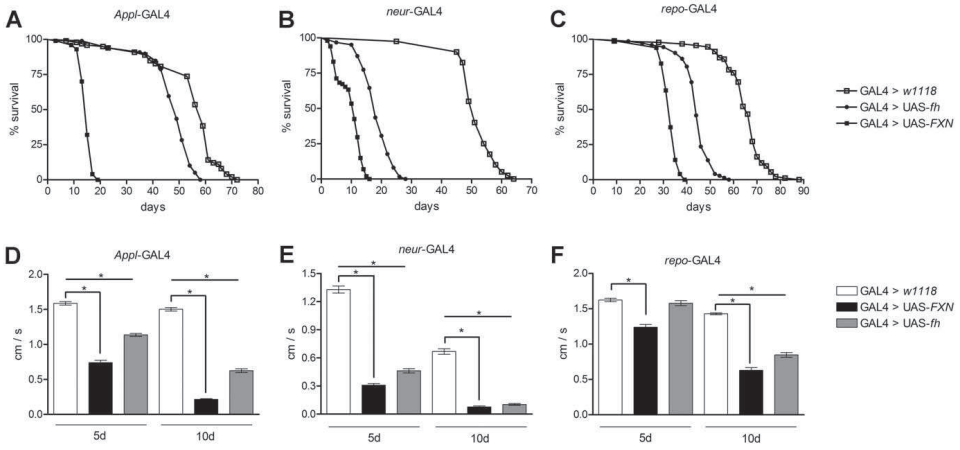

Figure 2. Physiological and behavioral defects induced by frataxin overexpression in nervous system. (A–C) Life span under normoxia conditions. Overexpression of human (black square) or *Drosophila* (black circle) frataxin in a pan-neural fashion (A), in the sensory organs and their precursors (B) or the glial cells (C) dramatically shortens the mean and maximum life span compared to control flies (white square). (D–F) Negative geotaxis experiment with 5- and 10-day-old individuals. Overexpression of frataxin in all 3 nervous system cell types strongly reduced the walking ability of the flies. The strongest effect was observed when the PNS driver (*neur*-GAL4) was applied. The statistical differences between the survival curves in A, B and C were analyzed using the Kapplan-Meier test, and both of the frataxins exhibited a statistically significant reduction ($p<0.001$) compared to that of the control individuals. The level of significance in D, E and F was determined using a one-way ANOVA with the *post hoc* Newman-Keuls test (* $p<0.05$). The error bars represent the standard error.
doi:10.1371/journal.pone.0021017.g002

examined whether frataxin overexpression would produce a similar effect on the NDUFS3 levels. In agreement with the results of other studies [52,53], we observed that FXN overexpression triggered a 40% reduction in the amount of NDUFS3 protein expression (Figure 4B) without a change in the mRNA levels (data not shown), which excludes the possibility of a transcriptional regulatory mechanism. The reduction of the aconitase activity and the decrease in the amount of NDUFS3 expression are direct evidence of a reduction in the Fe-S cluster formation in our overexpression model.

Given that aconitase is a specific target of oxidative stress [54,55], we assessed the functional integrity of aconitase in *FXN* larvae after oxidative stress injury. As expected, the ubiquitous expression of *FXN,* combined with a hyperoxia treatment, also resulted in a two-fold reduction in aconitase activity compared to hyperoxia-treated controls (Figure 4A). Moreover, aconitase was seriously affected in flies with general *fh* overexpression that was combined with hyperoxia [31].

To test whether oxidative stress was involved in the phenotypes that were observed in the nervous system, we exposed flies that overexpressed *FXN* to a highly oxidative atmosphere (99.5% O_2). Under these conditions, we observed a strong decrease in the mean (65%) and maximum life span (50%) when compared to those of the controls (Figure 4C–E). Again, the *FXN* flies displayed stronger phenotypes than the flies that overexpressed *fh*.

In *Drosophila*, a constitutive increase in the mitochondrial-driven catalase (*mitoCat*) activity is known to improve the resistance to oxidative damage [56]. Moreover, the expression of this enzyme has been reported to extend the life span of frataxin-deficient flies and to improve the resistance of these flies to oxidative insult [32]. Therefore, we examined the effect of this free radical scavenger on life span and locomotor performance in our frataxin overexpressing flies. As illustrated in Figure 4F, *mitoCat* produced a significant prolongation of life span when frataxin was overexpressed using *neur*-GAL4 and caused a statistically non-significant increase for repo-GAL4 (Figure 4G). In addition, *mitoCat* ameliorated the climbing deficiency that was induced by *FXN* or *fh* overexpression in glial cells (Figure 4H).

These results clearly identify oxidative stress and mainly hydrogen peroxides as key factors in the frataxin overexpression phenotypes that have been observed.

Overexpressed FXN do not form aggregates or misfold in *Drosophila*

The overexpression of human or *Drosophila* frataxins produce a phenotype that is surprisingly similar to the phenotype that is observed in frataxin-depleted mutants. Thus, we assessed whether the overexpression of frataxin would induce neomorph phenotypes and lead to a loss of function phenocopy *via* protein aggregation or misfolding.

Heat shock proteins have been reported to display rescuing effects in *Drosophila* neurodegenerative models of protein misfolding or aggregation [57–59]. Therefore, we assessed whether the co-expression of heat-shock proteins would lead to beneficial effects in our frataxin overload scenarios. Human heat-shock cognates were used in combination with *FXN,* and *Drosophila Hsp70* and *Hsp22* were co-expressed with *fh*; however, these heat-shock proteins were not able to improve the climbing performance of the frataxin-overexpressing flies (data not shown).

Size exclusion chromatography was conducted for the mitochondrial matrix proteins from the *FXN*-overexpressing larvae, and the fractions that were obtained were analyzed using western blotting for the presence of *FXN*. In our experiments, after the overexpression of *FXN* in *Drosophila*, human frataxin was recovered

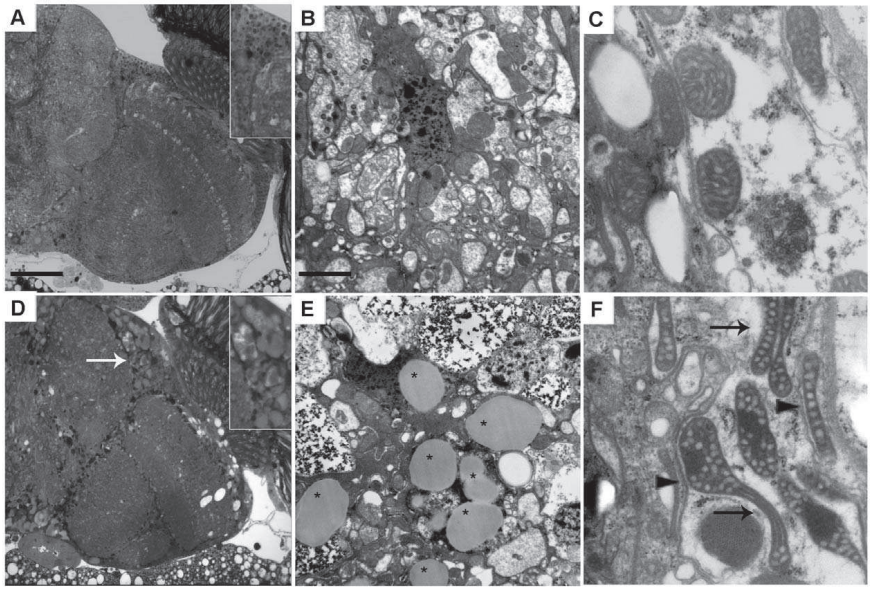

Figure 3. Strong degeneration and lipid droplet accumulation in glial cells overexpressing frataxin. (A–C) 25-day-old *Repo*-GAL4 / + controls; (D–F) 25-day-old *Repo*-GAL4 / UAS-*FXN*. (D) Overexpression of human frataxin induced a strong degeneration in the cortex (white arrow and 3X magnification box). (E, F) The electron microscopy analysis revealed an accumulation of lipid droplets (denoted by asterisks; E) in the glial cells of the frataxin-overexpressing brains and revealed mitochondria with altered morphologies (arrows; F) and internal vacuolization (arrow heads; F). The scale bar represents 50 μm (A, D) and 2.5 μm (B, C, E, F).
doi:10.1371/journal.pone.0021017.g003

as a monomeric form (Figure 5A), and no high molecular weight frataxin aggregates (dimers, trimers or multimeric forms of frataxin) were detected in the void volume (fraction 14). It was nevertheless possible that frataxin protein aggregates were not solubilized with the mitochondrial matrix proteins. Insoluble cellular proteins were solubilized, and the western blot did not reveal the presence of frataxin in this solubilized fraction (data not shown).

Collectively, these results indicate that frataxin aggregation or misfolding is unlikely to be the mechanism behind the phenotypes that have been observed.

FXN overexpression restores the aconitase activity in *fh* deficient individuals

In terms of their sequences and other structural properties, the degree of conservation between FH and FXN [33,60] indicates a possible similarity in the function of these proteins. In support of this hypothesis, we have shown that *Drosophila* and human frataxin overexpression produce similar phenotypes. Lastly, we investigated the consequences of expressing *FXN* in *fh*-knockdown flies. To accomplish this task, we generated flies by combining *FXN* and *UDIR2* transgenes, and the latter transgene induced a 90% reduction in the level of *fh* expression [34].

A decrease in the level of aconitase activity appears to be the most sensitive biological and biochemical marker in the FA fly models [31–35]. As a result, we tested whether aconitase could be rescued in *fh* knockdown flies expressing *FXN*. In agreement with previously published results [34], the depletion of fly frataxin led to a two-fold reduction in aconitase activity in larvae compared to controls. Remarkably, the expression of *FXN* prevented aconitase inactivation, and the aconitase activity was recovered to levels that were comparable with those of the controls (Figure 4A).

Considering the possibility that the rescue of the aconitase activity was related to degradation of the *FXN* mRNA that was induced by the RNAi transgene directed to *fh*, we assessed the human frataxin protein levels using western blotting. Comparable levels of FXN were observed in the *actin*-GAL4>UAS-*FXN* and *actin*-GAL4>UAS-*UDIR2*;UAS-*FXN* larvae (Figure 4B).

We can conclude that human frataxin is able to replace the endogenous *Drosophila* frataxin, which suggests that these proteins play an equivalent role in the cell biology of these organisms.

Discussion

Friedreich's ataxia is the most common autosomal recessive ataxia in the Caucasian population. This disease exhibits an irreversible progression that confines a patient to a wheelchair and leads to an early death. Moreover, although different treatments are currently being developed and assessed in clinical trials, there is no cure available. To generate effective and adequate therapies for Friedreich's ataxia, it is imperative to define the function of the frataxin protein. Unfortunately, the precise function of this protein is still a matter of debate. Although overexpression studies do not represent a disease model for FA, these studies are a useful approach to decipher the mechanism of action of frataxin.

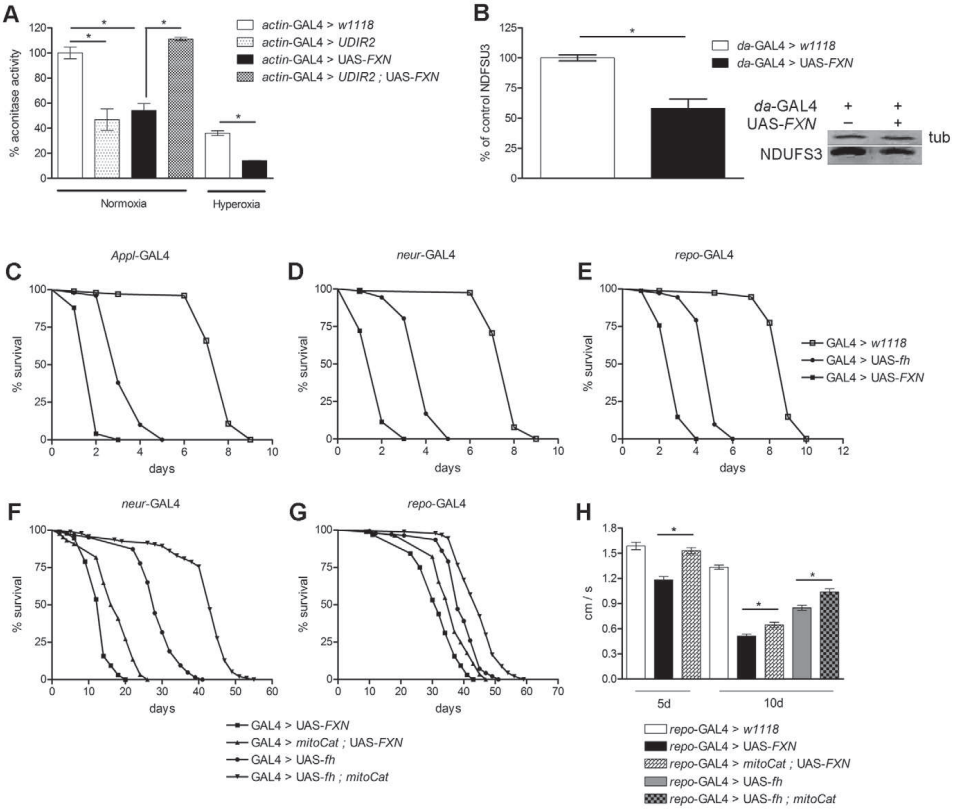

Figure 4. Molecular effects of frataxin overexpression and the involvement of oxidative stress. (A) The negative effects of human-frataxin overexpression on aconitase activity under normoxia and hyperoxia (99.5% O_2) conditions. (B) Human frataxin overexpression triggered a reduction in the synthesis of the complex I subunit (amount normalized to the internal control α-tubulin). (C–E) Increased susceptibility to hyperoxia-mediated oxidative damage in flies overexpressing human and fly frataxin in the nervous system. (F,G) Constitutive expression of mitochondrial catalase (*mitoCat*) led to an extension of the mean and maximum life span of the flies with increased frataxin expression. This effect was strong in the peripheral nervous system (*neur*-GAL4) and moderate in the glial cells (*repo*-GAL4). (H) Co-expression of mitochondrial catalase (*mitoCat*) rescues (5d) and alleviates (10d) the locomotor deficits in the flies with an increased level of frataxin expression in the glial cells. The survival curves were analyzed using the Kapplan-Meier test. The level of significance in A, B and H was determined using a one-way ANOVA with a *post hoc* Newman-Keuls test (*$p<0.05$). The error bars represent the standard error.
doi:10.1371/journal.pone.0021017.g004

Furthermore, these models may provide insight into the effects of an excess of frataxin, which is a critical factor for the validation of treatments that are based on an increase in this protein's expression.

Frataxins are a highly conserved family of proteins. *In silico* analyses have shown that *Drosophila* frataxin and frataxin proteins that are found in other species share large percentages of identity and similarity in their sequence and a common secondary structure [33]. The closest match between the human and the fly frataxins involves a stretch of 38 amino acids at the C-terminus, which is encoded by *fh* exon 2, and exons 4 and 5a of the *FXN* gene, respectively. This highly conserved region is very likely to form a functional domain with a β-sheet structure that is flanked by α-helices, where the sequence is less conserved [33]. Moreover, *Drosophila* frataxin has similar biophysical properties to human frataxin [60] and exhibits a mitochondrial localization [31]. In agreement with mouse models of FA [19], a strong systemic depletion of *fh* induces lethality during early development [31,34], whereas the moderate reduction of *fh* produces phenotypes that parallel the symptoms of FA patients [31]. In addition, the tissue-specific silencing of frataxin leads to the mimicking of human phenotypes [31,34–36]. Collectively, these data indicate that these proteins may be playing identical roles; however, their functional equivalence had not yet been demonstrated experimentally.

In the present work, we generated a *Drosophila* strain that overexpressed the human frataxin (*FXN*). Flies with an increased

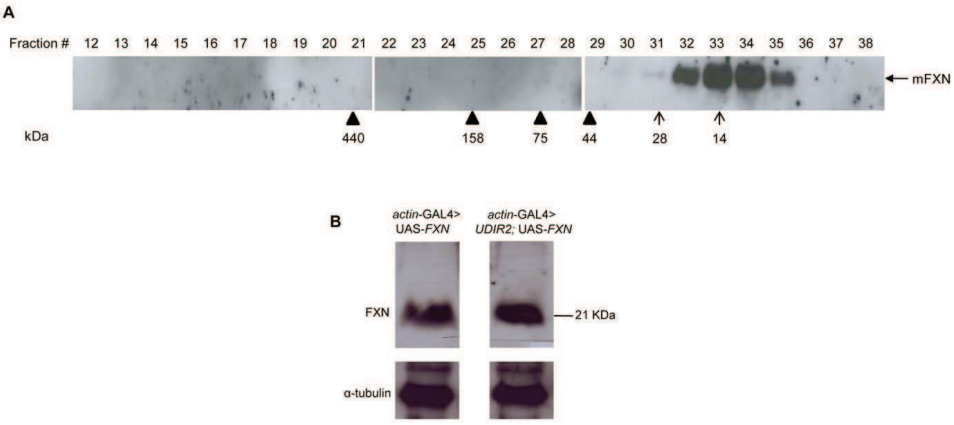

Figure 5. FXN does not form aggregates in *Drosophila,* and its expression is not diluted when it is coexpressed with the interference of *fh*. (A) Mitochondrial cell extracts were obtained from *actin*-GAL4>UAS-*FXN* larvae and were size fractionated. The fractions were subsequently analyzed using SDS-PAGE and western blotting with an anti-human frataxin antibody. The positions of ferritin (440 kDa), aldolase (158 kDa), conalbumin (75 kDa), and ovalbumin (44 kDa) and the estimated position for the frataxin monomer and dimer are indicated as arrowheads and arrows, respectively. (B) Detection of FXN protein in *actin*-GAL4>UAS-*FXN* and *actin*-GAL4>*UDIR2*; UAS-*FXN* larvae. The FXN protein is not diluted when it is co-expressed with an RNA interference construct of *fh*. α-tubulin was used as a loading control.
doi:10.1371/journal.pone.0021017.g005

level of expression of *FXN* exhibited similar defects to those found after endogenous frataxin overexpression, such as an alteration of development, a reduction in viability, life span and motor ability [31] and clear manifestations of nervous system degeneration, impaired Fe-S cluster formation and an enhanced susceptibility to oxidative stress. These results support the hypothesis that these frataxins are functionally equivalent. In the present work, we have shown that *FXN* was able to recover aconitase activity, the most sensitive biochemical marker of FA, in frataxin-deficient larvae.

Although the effect of frataxin overproduction has been investigated in several models, our studies using *Drosophila* as a model are the only studies to show deleterious defects. Human frataxin overexpression has been reported to be innocuous in mice [43] or to stimulate energy production [17]. Frataxin promotes OXPHOS activation in cell culture [15,45] and increases cellular antioxidant defense in cell culture and yeast [44,47]. In agreement with these findings, the overexpression of frataxin in *Drosophila* that was conducted by Runko *et al.* [46] increased the resistance to oxidative stress and extended the life span of the flies. These differences may be related to the characteristics of the models but may also result from quantitative differences in the level of frataxin overproduction. A closer look at the data from these studies reveals that a slight overexpression of frataxin was reported, from 2 to 6 times that of baseline, depending on the model and/or the tissue that was used. Conversely, in the present work, and in Llorens *et al.* [31], a minimum of 9-fold increase in frataxin production was induced. Therefore, it is possible that moderate overproduction of this protein may lead to beneficial effects, whereas the expression of frataxin beyond a given threshold may have multiple effects inducing toxicity. Taken together, these results indicate that frataxin requires an optimal balance of its expression level to carry out its function properly. To date, very little is known about the regulation of frataxin expression. It has been reported that the transcription factors *Hypoxia-inducible Factor 2alpha* [61], SRF and TFAP2 [62] are involved in regulating the expression of frataxin, as may be the iron content of the cell [63]. Analyzing the mechanism of this regulatory network is a new field that will provide new targets for future therapies.

In agreement with the results of the present study, the overproduction of yeast frataxin has been shown to impair Fe-S cluster formation and to lead to a reduction in aconitase and SDH activities [47]. These authors proposed that the trimeric form of frataxin may be responsible for the interaction with the complex of iron-sulfur cluster machinery. Thus, the increase in frataxin oligomerization due to its overexpression would lower the amounts of trimers that restrict the production of the cluster. To clarify the toxic mechanism that is responsible for frataxin overexpression in *Drosophila*, we considered the possibility that FXN was also inducing protein aggregation or misfolding, leading to a reduction in the level of functional frataxin. However, the results of our gel filtration assays did not show any shift in FXN to higher molecular masses, and the protein was recovered in the monomeric form. In addition, the overexpression of human or fly heat-shock proteins did not lead to any improvement in the frataxin overexpression phenotypes. These results indicate that protein aggregation and misfolding are not the central factors leading to the frataxin overexpression defects. Notably, our results do not reproduce the data from the experiments using bacterial [64,65] or yeast [47,66] models in which frataxin forms multimers. These findings indicate that oligomerization does not occur in *Drosophila*. Our results are in agreement with the findings of Kondapalli *et al.* [60], who reported that FH seems to be less prone to aggregation *in vitro* than the yeast protein, which appeared as a monomer in most of the conditions that were tested.

In our overexpression model, we observed aconitase inactivation and a reduction in the NDUFS3 levels, indicating an alteration in Fe-S cluster formation. These results argue in favor of the role of frataxin as an inhibitor of the Fe-S cluster assembly machinery, as previously suggested by Adinolfi *et al.* [24]. However, this inhibitory function is not consistent with the

stimulation of the respiratory chain that has been described by other authors [15,17,45]. Therefore, we propose that a moderate overexpression of frataxin may promote the synthesis of clusters or promote their stabilization when they are incorporated into apoproteins, as has been previously suggested [16,28]. In contrast, a larger increase in the overexpression of frataxin may lead to a reduction in Fe-S cluster formation, regardless of this proteins function as an activator [12,18–23] or suppressor [24], by saturating the ISC machinery or by sequestering the proteins from the machinery that interact with frataxin. Frataxin has been recently proposed to maintain the ISCU/NFS1/ISD11 interaction [23]; however, an increase of frataxin may over-stabilize this complex and cause an Fe-S cluster deficiency.

Our results that show the constitutive expression of mitochondrial catalase demonstrate that oxidative stress and hydrogen peroxides are key factors in the frataxin overexpression phenotypes. Notably, the positive effect of mitochondrial catalase in counteracting frataxin defects has been previously reported [32]. These results suggest a common mechanism in the loss-of-function and gain-of-function phenotypes that are induced by frataxin. Remarkably, in Llorens *et al.* [31] and in the present study, other similar phenotypes between strong frataxin overproduction and frataxin depletion have been described, such as structural defects that lead to a reduction in longevity and locomotor capabilities and an increased sensitivity to oxidative damage. Moreover, the overexpression of *FXN* in glial cells leads to the presence of the lipid droplets and the brain degeneration that have been exhibited by glial-frataxin deficient flies [35].

In conclusion, we demonstrate that overexpression of *Drosophila* and human frataxins induces severe developmental problems in flies, a shortening of life span, brain degeneration and reduced aconitase activity. Moreover, the control of frataxin expression emerges as a crucial element for present and future treatments, such as gene therapy approaches, aimed at increasing frataxin levels.

Acknowledgments

The authors thank Dr. Dan Kiehart and Dr. Francesc Palau for the generous gifts of the anti-MHC and anti-Frataxin, respectively. The hybridoma antibodies 22C10 and BP102, which were developed by S. Benzer and C. Goodman, respectively, were obtained from the Developmental Studies Hybridoma Bank, developed under the auspices of the NICHD, and maintained by the University of Iowa, Department of Biological Sciences, IA 52242. We also thank the Bloomington Stock Center for the fly stocks. The authors would like to thank Uschi Roth for their technical assistance, and Dr. Juan Ferré and Dr. Emmanuel Lesuisse for their technical assistance and protocol for the gel filtration experiment. We also thank the Servicio Central de Soporte a la Investigación Experimental de la Universitat de València for access to the DNA analysis resources and databases.

Author Contributions

Conceived and designed the experiments: JAN JVL S. Soriano MJM JAB S. Schneuwly MDM. Performed the experiments: JAN JVL S. Soriano. Analyzed the data: JAN JVL S. Soriano MJM MDM. Contributed reagents/materials/analysis tools: JAB S. Schneuwly MJM MDM. Wrote the paper: JAN JVL S. Soriano MJM MDM.

References

1. Palau F, Espinós C (2006) Autosomal recessive cerebellar ataxias. Orphanet J Rare Dis 1: 47. doi:10.1186/1750-1172-1-47.
2. Campuzano V, Montermini L, Moltò MD, Pianese L, Cossée M, et al. (1996) Friedreich's ataxia: autosomal recessive disease caused by an intronic GAA triplet repeat expansion. Science 271: 1423–1427.
3. Ohshima K, Montermini L, Wells RD, Pandolfo M (1998) Inhibitory effects of expanded GAA.TTC triplet repeats from intron I of the Friedreich ataxia gene on transcription and replication in vivo. J. Biol. Chem 273: 14588–14595.
4. Sakamoto N, Chastain PD, Parniewski P, Ohshima K, Pandolfo M, et al. (1999) Sticky DNA: self-association properties of long GAA.TTC repeats in R.R.Y triplex structures from Friedreich's ataxia. Mol. Cell 3: 465–475.
5. Campuzano V, Montermini L, Lutz Y, Cova L, Hindelang C, et al. (1997) Frataxin is reduced in Friedreich ataxia patients and is associated with mitochondrial membranes. Hum. Mol. Genet 6: 1771–1780.
6. Harding AE (1981) Friedreich's ataxia: a clinical and genetic study of 90 families with an analysis of early diagnostic criteria and intrafamilial clustering of clinical features. Brain 104: 589–620.
7. Harding AE (1993) Clinical features and classification of inherited ataxias. Adv Neurol 61: 1–14.
8. Harding AE, Hewer RL (1983) The heart disease of Friedreich's ataxia: a clinical and electrocardiographic study of 115 patients, with an analysis of serial electrocardiographic changes in 30 cases. Q J Med 52: 489–502.
9. Gibson TJ, Koonin EV, Musco G, Pastore A, Bork P (1996) Friedreich's ataxia protein: phylogenetic evidence for mitochondrial dysfunction. Trends Neurosci 19: 465–468.
10. Babcock M, de Silva D, Oaks R, Davis-Kaplan S, Jiralerspong S, et al. (1997) Regulation of mitochondrial iron accumulation by Yfh1p, a putative homolog of frataxin. Science 276: 1709–1712.
11. Cavadini P, Gellera C, Patel PI, Isaya G (2000) Human frataxin maintains mitochondrial iron homeostasis in Saccharomyces cerevisiae. Hum. Mol. Genet 9: 2523–2530.
12. Mühlenhoff U, Gerber J, Richhardt N, Lill R (2003) Components involved in assembly and dislocation of iron-sulfur clusters on the scaffold protein Isu1p. EMBO J 22: 4815–4825. doi:10.1093/emboj/cdg446.
13. Park S, Gakh O, O'Neill HA, Mangravita A, Nichol H, et al. (2003) Yeast frataxin sequentially chaperones and stores iron by coupling protein assembly with iron oxidation. J. Biol. Chem 278: 31340–31351. doi:10.1074/jbc.M303158200.
14. Moreno-Cermeño A, Obis E, Belli G, Cabiscol E, Ros J, et al. (2010) Frataxin Depletion in Yeast Triggers Up-regulation of Iron Transport Systems before Affecting Iron-Sulfur Enzyme Activities. J. Biol. Chem 285: 41653–41664. doi:10.1074/jbc.M110.149443.
15. Ristow M, Pfister MF, Yee AJ, Schubert M, Michael L, et al. (2000) Frataxin activates mitochondrial energy conversion and oxidative phosphorylation. Proc. Natl Acad Sci U S A 97: 12239–12243. doi:10.1073/pnas.220403797.
16. González-Cabo P, Vázquez-Manrique RP, García-Gimeno MA, Sanz P, Palau F (2005) Frataxin interacts functionally with mitochondrial electron transport chain proteins. Hum. Mol. Genet 14: 2091–2098. doi:10.1093/hmg/ddi214.
17. Schulz TJ, Westermann D, Isken F, Voigt A, Laube B, et al. (2010) Activation of mitochondrial energy metabolism protects against cardiac failure. Aging (Albany NY) 2: 843–853.
18. Rötig A, de Lonlay P, Chretien D, Foury F, Koenig M, et al. (1997) Aconitase and mitochondrial iron-sulphur protein deficiency in Friedreich ataxia. Nat. Genet 17: 215–217. doi:10.1038/ng1097-215.
19. Puccio H, Simon D, Cossée M, Criqui-Filipe P, Tiziano F, et al. (2001) Mouse models for Friedreich ataxia exhibit cardiomyopathy, sensory nerve defect and Fe-S enzyme deficiency followed by intramitochondrial iron deposits. Nat. Genet 27: 181–186. doi:10.1038/84818.
20. Ramazzotti A, Vanmansart V, Foury F (2004) Mitochondrial functional interactions between frataxin and Isu1p, the iron-sulfur cluster scaffold protein, in Saccharomyces cerevisiae. FEBS Lett 557: 215–220.
21. Vivas E, Skovran E, Downs DM (2006) Salmonella enterica strains lacking the frataxin homolog CyaY show defects in Fe-S cluster metabolism in vivo. J Bacteriol 188: 1175–1179. doi:10.1128/JB.188.3.1175-1179.2006.
22. Stemmler TL, Lesuisse E, Pain D, Dancis A (2010) Frataxin and mitochondrial FeS cluster biogenesis. J. Biol. Chem 285: 26737–26743. doi:10.1074/jbc.R110.118679.
23. Schmucker S, Martelli A, Colin F, Page A, Wattenhofer-Donzé M, et al. (2011) Mammalian Frataxin: An Essential Function for Cellular Viability through an Interaction with a Preformed ISCU/NFS1/ISD11 Iron-Sulfur Assembly Complex. PLoS ONE 6: e16199. doi:10.1371/journal.pone.0016199.
24. Adinolfi S, Iannuzzi C, Prischi F, Pastore C, Iametti S, et al. (2009) Bacterial frataxin CyaY is the gatekeeper of iron-sulfur cluster formation catalyzed by IscS. Nat. Struct. Mol. Biol 16: 390–396. doi:10.1038/nsmb.1579.
25. Emond M, Lepage G, Vanasse M, Pandolfo M (2000) Increased levels of plasma malondialdehyde in Friedreich ataxia. Neurology 55: 1752–1753.
26. Schulz JB, Dehmer T, Schöls L, Mende H, Hardt C, et al. (2000) Oxidative stress in patients with Friedreich ataxia. Neurology 55: 1719–1721.
27. Ristow M, Mulder H, Pomplun D, Schulz TJ, Müller-Schmehl K, et al. (2003) Frataxin deficiency in pancreatic islets causes diabetes due to loss of beta cell mass. J. Clin. Invest 112: 527–534. doi:10.1172/JCI18107.
28. Bulteau A, O'Neill HA, Kennedy MC, Ikeda-Saito M, Isaya G, et al. (2004) Frataxin acts as an iron chaperone protein to modulate mitochondrial aconitase activity. Science 305: 242–245. doi:10.1126/science.1098991.

29. Bulteau A, Dancis A, Gareil M, Montagne J, Camadro J, et al. (2007) Oxidative stress and protease dysfunction in the yeast model of Friedreich ataxia. Free Radic. Biol. Med 42: 1561–1570. doi:10.1016/j.freeradbiomed.2007.02.014.
30. Vázquez-Manrique RP, González-Cabo P, Ros S, Aziz H, Baylis HA, et al. (2006) Reduction of Caenorhabditis elegans frataxin increases sensitivity to oxidative stress, reduces lifespan, and causes lethality in a mitochondrial complex II mutant. FASEB J 20: 172–174. doi:10.1096/fj.05-4212fje.
31. Llorens JV, Navarro JA, Martínez-Sebastián MJ, Baylies MK, Schneuwly S, et al. (2007) Causative role of oxidative stress in a Drosophila model of Friedreich ataxia. FASEB J 21: 333–344. doi:10.1096/fj.05-5709com.
32. Anderson PR, Kirby K, Orr WC, Hilliker AJ, Phillips JP (2008) Hydrogen peroxide scavenging rescues frataxin deficiency in a Drosophila model of Friedreich's ataxia. Proc. Natl Acad Sci U S A 105: 611–616. doi:10.1073/pnas.0709691105.
33. Cañizares J, Blanca JM, Navarro JA, Monrós E, Palau F, et al. (2000) dfh is a Drosophila homolog of the Friedreich's ataxia disease gene. Gene 256: 35–42.
34. Anderson PR, Kirby K, Hilliker AJ, Phillips JP (2005) RNAi-mediated suppression of the mitochondrial iron chaperone, frataxin, in Drosophila. Hum. Mol. Genet 14: 3397–3405. doi:10.1093/hmg/ddi367.
35. Navarro JA, Ohmann E, Sanchez D, Botella JA, Liebisch G, et al. (2010) Altered lipid metabolism in a Drosophila model of Friedreich's ataxia. Hum. Mol. Genet 19: 2828–2840. doi:10.1093/hmg/ddq183.
36. Shidara Y, Hollenbeck PJ (2010) Defects in mitochondrial axonal transport and membrane potential without increased reactive oxygen species production in a Drosophila model of Friedreich ataxia. J Neurosci 30: 11369–11378. doi:10.1523/JNEUROSCI.0529-10.2010.
37. Finelli A, Kelkar A, Song H, Yang H, Konsolaki M (2004) A model for studying Alzheimer's Abeta42-induced toxicity in Drosophila melanogaster. Mol. Cell. Neurosci 26: 365–375. doi:10.1016/j.mcn.2004.03.001.
38. Marsh JL, Pallos J, Thompson LM (2003) Fly models of Huntington's disease. Hum. Mol. Genet 12 Spec No 2: R187–193. doi:10.1093/hmg/ddg271.
39. Feany MB, Bender WW (2000) A Drosophila model of Parkinson's disease. Nature 404: 394–398. doi:10.1038/35006074.
40. Venderova K, Kabbach G, Abdel-Messih E, Zhang Y, Parks RJ, et al. (2009) Leucine-Rich Repeat Kinase 2 interacts with Parkin, DJ-1 and PINK-1 in a Drosophila melanogaster model of Parkinson's disease. Hum. Mol. Genet 18: 4390–4404. doi:10.1093/hmg/ddp394.
41. Fernandez-Funez P, Nino-Rosales ML, de Gouyon B, She WC, Luchak JM, et al. (2000) Identification of genes that modify ataxin-1-induced neurodegeneration. Nature 408: 101–106. doi:10.1038/35040584.
42. Mutsuddi M, Marshall CM, Benzow KA, Koob MD, Rebay I (2004) The spinocerebellar ataxia 8 noncoding RNA causes neurodegeneration and associates with staufen in Drosophila. Curr. Biol 14: 302–308. doi:10.1016/j.cub.2004.01.034.
43. Miranda CJ, Santos MM, Ohshima K, Tessaro M, Sequeiros J, et al. (2004) Frataxin overexpressing mice. FEBS Lett 572: 281–288. doi:10.1016/j.febslet.2004.07.022.
44. Shoichet SA, Bäumer AT, Stamenkovic D, Sauer H, Pfeiffer AFH, et al. (2002) Frataxin promotes antioxidant defense in a thiol-dependent manner resulting in diminished malignant transformation in vitro. Hum. Mol. Genet 11: 815–821.
45. Schulz TJ, Thierbach R, Voigt A, Drewes G, Mietzner B, et al. (2006) Induction of oxidative metabolism by mitochondrial frataxin inhibits cancer growth: Otto Warburg revisited. J. Biol. Chem 281: 977–981. doi:10.1074/jbc.M511064200.
46. Runko AP, Griswold AJ, Min K (2008) Overexpression of frataxin in the mitochondria increases resistance to oxidative stress and extends lifespan in Drosophila. FEBS Lett 582: 715–719. doi:10.1016/j.febslet.2008.01.046.
47. Seguin A, Bayot A, Dancis A, Rogowska-Wrzesinska A, Auchère F, et al. (2009) Overexpression of the yeast frataxin homolog (Yfh1): contrasting effects on iron-sulfur cluster assembly, heme synthesis and resistance to oxidative stress. Mitochondrion 9: 130–138. doi:10.1016/j.mito.2009.01.007.
48. Rubin GM, Spradling AC (1982) Genetic transformation of Drosophila with transposable element vectors. Science 218: 348–353.
49. Kirby K, Hu J, Hilliker AJ, Phillips JP (2002) RNA interference-mediated silencing of Sod2 in Drosophila leads to early adult-onset mortality and elevated endogenous oxidative stress. Proc Natl Acad Sci U S A 99: 16162–16167. doi:10.1073/pnas.252342899.
50. Patel NH (1994) Imaging neuronal subsets and other cell types in whole-mount Drosophila embryos and larvae using antibody probes. Methods Cell Biol 44: 445–487.
51. Botella JA, Ulschmid JK, Gruenewald C, Moehle C, Kretzschmar D, et al. (2004) The Drosophila carbonyl reductase sniffer prevents oxidative stress-induced neurodegeneration. Curr. Biol 14: 782–786. doi:10.1016/j.cub.2004.04.036.
52. Sutak R, Xu X, Whitnall M, Kashem MA, Vyoral D, et al. (2008) Proteomic analysis of hearts from frataxin knockout mice: marked rearrangement of energy metabolism, a response to cellular stress and altered expression of proteins involved in cell structure, motility and metabolism. Proteomics 8: 1731–1741. doi:10.1002/pmic.200701049.
53. Guillon B, Bulteau A, Wattenhofer-Donzé M, Schmucker S, Friguet B, et al. (2009) Frataxin deficiency causes upregulation of mitochondrial Lon and ClpP proteases and severe loss of mitochondrial Fe-S proteins. FEBS J 276: 1036–1047. doi:10.1111/j.1742-4658.2008.06847.x.
54. Das N, Levine RL, Orr WC, Sohal RS (2001) Selectivity of protein oxidative damage during aging in Drosophila melanogaster. Biochem J 360: 209–216.
55. Delaval E, Perichon M, Friguet B (2004) Age-related impairment of mitochondrial matrix aconitase and ATP-stimulated protease in rat liver and heart. Eur. J Biochem 271: 4559–4564. doi:10.1111/j.1432-1033.2004.04422.x.
56. Orr WC, Sohal RS (1992) The effects of catalase gene overexpression on life span and resistance to oxidative stress in transgenic Drosophila melanogaster. Arch. Biochem. Biophys 297: 35–41.
57. Warrick JM, Chan HY, Gray-Board GL, Chai Y, Paulson HL, et al. (1999) Suppression of polyglutamine-mediated neurodegeneration in Drosophila by the molecular chaperone HSP70. Nat. Genet 23: 425–428. doi:10.1038/70532.
58. Auluck PK, Chan HYE, Trojanowski JQ, Lee VMY, Bonini NM (2002) Chaperone suppression of alpha-synuclein toxicity in a Drosophila model for Parkinson's disease. Science 295: 865–868. doi:10.1126/science.1067389.
59. Fernandez-Funez P, Casas-Tinto S, Zhang Y, Gómez-Velazquez M, Morales-Garza MA, et al. (2009) In vivo generation of neurotoxic prion protein: role for hsp70 in accumulation of misfolded isoforms. PLoS Genet 5: e1000507. doi:10.1371/journal.pgen.1000507.
60. Kondapalli KC, Kok NM, Dancis A, Stemmler TL (2008) Drosophila frataxin: an iron chaperone during cellular Fe-S cluster bioassembly. Biochemistry 47: 6917–6927. doi:10.1021/bi800366d.
61. Oktay Y, Dioum E, Matsuzaki S, Ding K, Yan L, et al. (2007) Hypoxia-inducible factor 2alpha regulates expression of the mitochondrial aconitase chaperone protein frataxin. J. Biol. Chem 282: 11750–11756. doi:10.1074/jbc.M611133200.
62. Li K, Singh A, Crooks DR, Dai X, Cong Z, et al. (2010) Expression of human frataxin is regulated by transcription factors SRF and TFAP2. PLoS ONE 5: e12286. doi:10.1371/journal.pone.0012286.
63. Li K, Besse EK, Ha D, Kovtunovych G, Rouault TA (2008) Iron-dependent regulation of frataxin expression: implications for treatment of Friedreich ataxia. Hum. Mol. Genet 17: 2265–2273. doi:10.1093/hmg/ddn127.
64. Bou-Abdallah F, Adinolfi S, Pastore A, Laue TM, Dennis Chasteen N (2004) Iron binding and oxidation kinetics in frataxin CyaY of Escherichia coli. J. Mol. Biol 341: 605–615. doi:10.1016/j.jmb.2004.05.072.
65. Layer G, Ollagnier-de Choudens S, Sanakis Y, Fontecave M (2006) Iron-sulfur cluster biosynthesis: characterization of Escherichia coli CYaY as an iron donor for the assembly of [2Fe-2S] clusters in the scaffold IscU. J. Biol. Chem 281: 16256–16263. doi:10.1074/jbc.M513569200.
66. Aloria K, Schilke B, Andrew A, Craig EA (2004) Iron-induced oligomerization of yeast frataxin homologue Yfh1 is dispensable in vivo. EMBO Rep 5: 1096–1101. doi:10.1038/sj.embor.7400272.

Article 2. Deferiprone and idebenone rescue frataxin depletion phenotypes in a *Drosophila* model of Friedreich's ataxia (Soriano *et al*. 2013)

Gene 521 (2013) 274–281

Contents lists available at SciVerse ScienceDirect

Gene

journal homepage: www.elsevier.com/locate/gene

Deferiprone and idebenone rescue frataxin depletion phenotypes in a *Drosophila* model of Friedreich's ataxia

Sirena Soriano [a,1], José V. Llorens [a,b,1], Laura Blanco-Sobero [a], Lucía Gutiérrez [c], Pablo Calap-Quintana [a], M. Puerto Morales [c], M. Dolores Moltó [a,d,*], M. José Martínez-Sebastián [a]

[a] Departament de Genètica, Universitat de València, Burjassot, Valencia, Spain
[b] Instituto de Biomedicina, CSIC, Valencia, Spain
[c] Instituto de Ciencia de Materiales de Madrid/CSIC, Madrid, Spain
[d] CIBERSAM (Centro de Investigación Biomédica en Red de Salud Mental), INCLIVA, Spain

ARTICLE INFO

Article history:
Accepted 25 February 2013
Available online 28 March 2013

Keywords:
Frataxin
Aconitase
Mitochondria
Oxidative stress
Life span
Climbing capability

ABSTRACT

Friedreich's ataxia (FRDA), the most common inherited ataxia, is a neurodegenerative disease caused by a reduction in the levels of the mitochondrial protein frataxin, the function of which remains a controversial matter. Several therapeutic approaches are being developed to increase frataxin expression and reduce the intramitochondrial iron aggregates and oxidative damage found in this disease. In this study, we tested separately the response of a *Drosophila* RNAi model of FRDA (Llorens et al., 2007) to treatment with the iron chelator deferiprone (DFP) and the antioxidant idebenone (IDE), which are both in clinical trials. The FRDA flies have a shortened life span and impaired motor coordination, and these phenotypes are more pronounced in oxidative stress conditions. In addition, under hyperoxia, the activity of the mitochondrial enzyme aconitase is strongly reduced in the FRDA flies. This study reports that DFP and IDE improve the life span and motor ability of frataxin-depleted flies. We show that DFP eliminates the excess of labile iron in the mitochondria and thus prevents the toxicity induced by iron accumulation. IDE treatment rescues aconitase activity in hyperoxic conditions. These results validate the use of our *Drosophila* model of FRDA to screen for therapeutic molecules to treat this disease.

1. Introduction

Friedreich's ataxia (FRDA) is an autosomal recessive neurodegenerative disorder (Harding, 1981, 1993) that constitutes the most common form of hereditary ataxia, with a prevalence of 1:50,000 in Caucasian populations. This disabling condition usually manifests in childhood or adolescence with progressive gait and limb ataxia, dysarthria, lower limb areflexia, muscle weakness and sensory loss. Besides the central and peripheral nervous systems, extraneural organs are also affected in FRDA. A significant proportion of patients develop hypertrophic cardiomyopathy, which is the major contributor to morbidity and mortality risks in this disease. Other manifestations include diabetes mellitus and carbohydrate intolerance (reviewed in Pandolfo, 2009).

FRDA arises from a deficit in the mitochondrial protein frataxin caused by loss-of-function mutations in the gene *FXN* (Campuzano et al., 1996; Koutnikova et al., 1997). Most patients are homozygous for expansions of a GAA triplet-repeat within the first intron of this gene (Monrós et al., 1997), which produces gene silencing (Al-Mahdawi et al., 2008). Frataxin is a highly conserved protein, and its deficiency leads to several biochemical disturbances such as impaired iron–sulfur (Fe–S) cluster synthesis resulting in the dysfunction of the respiratory chain complexes and aconitase, mitochondrial iron overload coupled to cellular iron deregulation and oxidative stress hypersensitivity (reviewed in Schmucker and Puccio, 2010). Initially, excess of iron was reported in the hearts of FRDA patients (Lamarche et al., 1980; Sanchez-Casis et al., 1976) and was later found in several other tissues (Bradley et al., 2000; Waldvogel et al., 1999) where the iron deposit pattern was consistent with mitochondrial localization. Increased iron content in the mitochondria was previously described in the yeast knockout of the frataxin homolog (*Yfh1*) (Foury and Cazzalini, 1997). Similar to the *Yfh1* yeast model and conditional knockout mice (Puccio et al., 2001), significant deficiencies of mitochondrial Fe–S cluster containing enzymes within the respiratory chain and Krebs cycle were also found in FRDA tissues, especially in the heart (Bradley et al., 2000; Rötig et al., 1997). Patient samples present increased levels of oxidative stress biomarkers such as lipid peroxidation products (Emond et al., 2000) and lesions in nuclear and mitochondrial DNA (Haugen et al., 2010). Furthermore, cultured fibroblasts from

Abbreviations: BPS, bathophenanthroline disulfonate; DFP, deferiprone; 6-FAM, 6-carboxyfluorescein; *fh*, *Drosophila* frataxin homolog; FRDA, Friedreich's ataxia; GFP, green fluorescent protein; IDE, idebenone; *neur*-GAL4, *neuralized*-GAL4; PNS, peripheral nervous system; ROS, reactive oxygen species; RT-qPCR, Real-Time Polymerase Chain Reaction; *Yfh*, yeast frataxin homolog.

* Corresponding author at: Department of Genetics, Universitat de València, Dr. Moliner, 50 46100-Burjassot, Valencia, Spain. Tel.: +34 963543400; fax: +34 963543029.
E-mail address: dmolto@uv.es (M.D. Moltó).
[1] These authors contributed equally to this work.

0378-1119/$ – see front matter © 2013 Elsevier B.V. All rights reserved.
http://dx.doi.org/10.1016/j.gene.2013.02.049

FRDA patients have a reduced capacity to mobilize antioxidant defenses, which makes them very vulnerable to oxidative insult (Paupe et al., 2009).

Several therapies are currently being examined for the treatment of FRDA (González-Cabo et al., 2009). Drugs in advanced phases of clinical trials target the pathogenic cascade downstream of frataxin deficiency. On this basis, administrations of iron chelators such as deferiprone (DFP) and antioxidants such as idebenone (IDE) are considered rational therapeutic approaches. The orally active, blood–brain barrier-permeable DFP is a small molecule that preferentially binds iron and prevents its reaction with reactive oxygen species (ROS). It shows the ability to relocate iron accumulated in cell compartments to extracellular transferrin and to the hemoglobin machinery (Sohn et al., 2008). In a preliminary clinical trial, it was shown that DFP diminishes brain iron accumulation in FRDA patients, which is associated with neurological improvement (Boddaert et al., 2007). IDE is a synthetic analog of coenzyme Q10 and, similar to it, can undergo reversible redox reactions. The rationale for its use in FRDA is its capability to act both as a potent antioxidant, protecting membranes from damage by inhibiting lipid peroxidation in mitochondria, and as an electron carrier, supporting mitochondrial function. In several clinical trials, treatment with IDE has been proven to ameliorate cardiac and neurological function (reviewed in Meier and Buyse, 2009; Schulz et al., 2009). Phase 3, double-blind, controlled trials have already been conducted in FRDA subjects to assess the efficacy of IDE on neurological function (Lynch et al., 2010) and on cardiomyopathy (Lagedrost et al., 2011). Authors concluded that IDE did not significantly improve the neurological and cardiac status of the pediatric cohort treated over a 6-month period compared with placebo treatment. Nevertheless, an open-label extension study in these patients for 12 months, combined with the previous double-blind study indicated that IDE at a high dose stabilizes the overall neurological function and improves fine motor skills and speech (Meier et al., 2012). In addition, an open-label study combining IDE and DFP indicated a stabilizing effect in neurological dysfunction, an improvement in heart hypertrophy parameters and a statistically significant reduction of iron deposits in the dentate nucleus (Velasco-Sánchez et al., 2011).

We have previously developed a *Drosophila* model for FRDA (Llorens et al., 2007) that takes advantage of the GAL4/UAS transgene-based RNAi methodology to down-regulate the *Drosophila* frataxin homolog (*fh*). In this model, *fh* knockdown recapitulates several hallmarks of FRDA including poor motor coordination, reduced aconitase activity, reduced life span and enhanced sensitivity to oxidative stress. In the study reported here, we validated the *Drosophila* model of FRDA as a useful tool to screen for chemical compounds that ameliorate or prevent the disease. Treatment with either DFP or IDE improved the survival and the climbing ability of the frataxin-depleted flies. We also found that DFP eliminates the excess of labile iron in the mitochondria preventing its toxic effects, and IDE rescued aconitase activity of the *fh*RNAi flies under hyperoxic conditions.

2. Materials and methods

2.1. Drosophila stocks

The *fh*RNAi strain was previously generated in our laboratory and induces a knockdown in frataxin of up to 30% (Llorens et al., 2007). The *yw* strain was used as a control for the assays performed. The UAS-GFP strain and the driver lines *actin*-GAL4 and *neuralized*-GAL4 (*neur*-GAL4), which promote expression in a ubiquitous and peripheral nervous system (PNS) pattern, respectively, were obtained from the Bloomington Stock Center (Indiana University).

2.2. Culture media, drugs and culture conditions

Drosophila stocks were maintained at 25 °C on standard cornmeal agar medium. The experimental crosses between the GAL4 drivers and the *fh*RNAi lines were performed on Instant *Drosophila* Medium Formula 4–24 Blue (Carolina Biological Supply Company) at 25 °C. Drugs were administered at two starting points: [1] the eggs were collected and transferred into vials containing the *Drosophila* medium supplemented with the compound to be tested, and adults were transferred to fresh vials with the drug 3 times per week (early treatment); and [2] one-day post-eclosion flies were transferred into vials with the respective treatment and moved to fresh vials containing the drug 3 times per week (adult treatment). DFP, kindly provided by Apopharma, was dissolved in H_2O to concentrations of 65 μM and 163 μM. IDE was supplied by BIOMOL International and dissolved in 0.1% DMSO to concentrations of 7 μM and 15 μM. These concentrations were calculated from previously reported clinical doses of such compounds (Cohen, 2006; Voncken et al., 2004), and the flies' weights were taken into account.

2.3. Life span and negative geotaxis

For life span determination, flies of the appropriate genotype were collected within 24 h after eclosion from the puparium and were raised at 25 °C under a 12 hour light/dark cycle with transfer of survivors to fresh vials 3 times per week. A total of 250 adult individuals were tested per treatment. In the case of negative geotaxis assays, we followed the experimental procedure described in Botella et al. (2004). This test was always performed at the same time of the day. A total of 25 individuals of appropriate genotypes were tested and 3 measurements were performed per individual.

2.4. Assay of aconitase activity

To measure aconitase activity, flies were maintained in hyperoxic conditions for 24 h as described previously (Llorens et al., 2007) before performing the assay. Aconitase activity was determined from whole individuals using the Bioxytech Aconitase-340™ Spectrophotometric Assay Kit (Oxis International Inc.). Measurements were performed in a 96 well plate by scaling down the volumes indicated in the manufacturer's protocol. Absorbance at 340 nm was measured for 20 min at 37 °C with a Tekan Spectra-Fluor microplate reader. Data obtained were normalized to protein sample levels determined using a Bradford assay.

2.5. Measurement of total, mitochondrial and soluble iron

Flies were freeze-dried, weighed and digested with nitric acid for 2 days (24 h at room temperature and 24 h at 90 °C). Atomic absorption spectroscopy was used to measure the iron levels, calibrated against standard solutions. In the case of mitochondrial iron, the mitochondrial-enriched fraction from fresh flies was obtained with the MITOISO1 kit (Sigma-Aldrich). The mitochondrial pellets obtained were acid digested prior to the measurement of iron levels.

To determine the content of soluble iron, we used the iron assay kit (BioVision). Mitochondrial pellets were tested for ferrous (Fe^{2+}) and total ($Fe^{2+} + Fe^{3+}$) soluble iron following the manufacturer's instructions.

2.6. Green fluorescent protein (GFP) quantification

Total protein extraction from *Drosophila* adults was performed as described previously (Kirby et al., 2002). The supernatant was used to measure the GFP fluorescence in a 96 well plate with excitation at 485 nm and emission at 535 nm in a VICTOR spectrophotometer (Perkin-Elmer). The GFP fluorescence levels were normalized to the quantity of protein of the sample, determined using a Bradford assay.

2.7. Real-Time Polymerase Chain Reaction (RT-qPCR)

Total RNA was isolated from 100 adult flies using the QuickPrep mRNA Purification kit (GE Healthcare). cDNA was synthesized with Expand Reverse Transcriptase (Roche Diagnostics) and oligo-dT primers. RT-qPCR was performed with TaqMan probes for *fh* and *rp49* as a control, containing 6-carboxyfluorescein (6-FAM) at the 5′ end (Applied Biosystems). Thermocycling was performed in the ABI PRISM 7500 Sequence Detection System (Applied Biosystems). The relative quantification of each cDNA was calculated in triplicate experiments using the comparative Ct method.

2.8. Statistical analysis

Statistical analyses were performed with the GraphPad Prism 4.0 software. Kaplan–Meier survival plots were analyzed with semiparametric log rank tests. For comparison of means, we performed an unpaired non-parametric Student's *t* test or one-way ANOVA. In all cases, values of $P < 0.05$ were considered statistically significant.

3. Results

3.1. Deferiprone improves the life span and motor ability of frataxin knockdown mutants

The mitochondrial iron accumulation described in FRDA models and in patients (Babcock et al., 1997; Bradley et al., 2000; Puccio et al., 2001) provides the rationale for the use of the iron chelator DFP for FRDA in clinical trials (Boddaert et al., 2007). To evaluate the effect of DFP on the life span of the frataxin-depleted flies, DFP was administered to the *actin*-GAL4 > UAS-*fh*RNAi flies at two concentrations, 65 and 163 μM, and with two regimens termed early and adult treatments, respectively.

A ubiquitous reduction of frataxin in flies led to a shortened life span; the maximum life span was reduced from 90 days in the control to 60 days in the *fh*RNAi flies (Llorens et al., 2007). Early treatment with the highest concentration of DFP moderately improved survival of the frataxin deficient flies ($P = 0.0004$) (Fig. 1A). The treatment extended the life span of the *fh*RNAi flies by approximately 80 days, which is close to the value observed for the controls. No significant differences were observed in the early treatment with 65 μM of DFP or with any of the DFP concentrations in the adult treatment (data not shown).

Because the motor ability of the *actin*-GAL4 > UAS-*fh*RNAi flies is also seriously impaired (Llorens et al., 2007), we tested the effect of DFP on this phenotype using negative geotaxis assays. Early treatment with 163 μM of DFP improved the climbing ability of FRDA flies both at the first ($P < 0.01$) and the second week ($P < 0.001$) after the emergence from the puparium (Fig. 1B). A similar tendency was observed with the 65 μM treatment of DFP in both time points, but it was not statistically significant. In contrast, when the compound was added only at the adult stage, significant differences were not observed in climbing ability (data not shown). DFP treatment did not affect the climbing ability of control flies (Fig. 1B).

Because the PNS is one of the most affected tissues in FRDA patients, the reduction of frataxin was directed to the *Drosophila* sensory organs and their precursors using the driver *neur*-GAL4. Early treatment with 163 μM of DFP significantly improved the climbing ability of the *neur*-GAL4 > UAS-*fh*RNAi flies in the first ($P < 0.001$) and the second week ($P < 0.01$) after adult emergence from the puparium (Fig. 1C). Specifically, two-week-old treated *fh*RNAi flies exhibited similar climbing ability than the treated control flies (Fig. 1C). DFP had no effect on control flies in both time points. Treatment with 65 μM of DFP caused some recovery but it was not statistically significant. No significant differences were detected when DFP was administered only in the adult stage (data not shown).

3.2. Deferiprone improves frataxin-depleted phenotypes by specifically chelating mitochondrial iron

Because frataxin depletion produces mitochondrial iron overload, we measured the total iron content of *fh*RNAi flies by atomic absorption spectroscopy. No significant differences in the total iron content between the *fh*RNAi and control flies were found (data not shown). However we observed a trend towards an increase of iron levels in the FRDA flies. Consistent with previous reports, we found that mitochondrial iron was significantly increased in the *fh*RNAi flies with respect to the controls ($P < 0.01$) (Fig. 1D).

Next, we determined the relative amounts of ferrous (Fe^{2+}) and total iron in the soluble pool of mitochondrial samples using a colorimetric assay. Ferric iron (Fe^{3+}) concentration was established by subtracting total minus ferrous. There were no significant differences between Fe^{2+} and total iron in the mitochondrial samples from control and *fh*RNAi flies, indicating that all soluble iron is mainly present in the Fe^{2+} form (Fig. 1E). Soluble mitochondrial iron showed a tendency to decrease in FRDA flies compared to controls (Fig. 1E). This is in contrast with the observation made using atomic absorption spectroscopy where mitochondrial iron levels were increased (Fig. 1D). This finding could be interpreted as a relative increase in insoluble iron, which would accumulate and form iron aggregates, similar to results previously described in the MCK mouse model of FRDA (Puccio et al., 2001) and in human tissues (Bradley et al., 2000).

DFP has been shown to act on the labile iron pools in subcellular compartments, such as in mitochondria (Sohn et al., 2008). Therefore, we assessed the effect of DFP on the mitochondrial iron content of *fh*RNAi flies. We found that early treatment with 163 μM of DFP caused a further increase in the mitochondrial iron content of the FRDA flies ($P < 0.01$) but not in controls (Fig. 1D), indicating that its effect on the model flies is specific. DFP treatment increased Fe^{2+} levels in the *fhRNAi* flies ($P < 0.05$), reverting back to normal levels, while the same treatment caused a further increase in total iron levels in *fhRNAi* flies ($P < 0.05$) (Fig. 1E). The difference between the total and Fe^{2+} measurements after DFP treatment indicates an increase in the Fe^{3+}. DFP might be binding the ferric iron and preventing its accumulation as an insoluble form. As a result, DFP might reduce cellular iron toxicity improving phenotype in the FRDA flies.

3.3. Idebenone recovers the life span and motor abilities of frataxin-depleted mutants

Oxidative stress has been suggested to be a major cause of the pathophysiology of FRDA. From our previous results in which hyperoxia highly decreased the life span and climbing ability of *fh*RNAi flies (Llorens et al., 2007), we hypothesized that the shortened life span and the locomotor impairment also observed during aging of these flies result from the harmful effects of ROS. Because the use of antioxidants should alleviate these phenotypes, we tested the effects of the antioxidant IDE at concentrations of 7 and 15 μM, at the two starting points (early and adult treatments as indicated above).

When IDE was administered to one-day post-eclosion adults (Figs. 2A–B), both concentrations improved the life span of the *fh*RNAi flies ($P < 0.001$) with respect to non-treated flies with the same genotype. No significant changes in life span were found in the early treatment on any of the concentrations tested (data not shown). In addition, 7 μM and 15 μM of IDE significantly improved the climbing ability in two-week-old *fh*RNAi flies ($P < 0.01$ and $P < 0.05$, respectively) when the treatment was started early (Fig. 2D). No significant differences in climbing were observed either in the first week of early treatment (Fig. 2D) or when IDE was added to adult individuals (data not shown). When the frataxin reduction was restricted to the PNS, 7 μM IDE induced an improvement in the life span on *neur*-GAL4 > UAS-*fh*RNAi early treated flies ($P < 0.0001$) (Fig. 2C) but not for the rest of the conditions tested (data not shown).

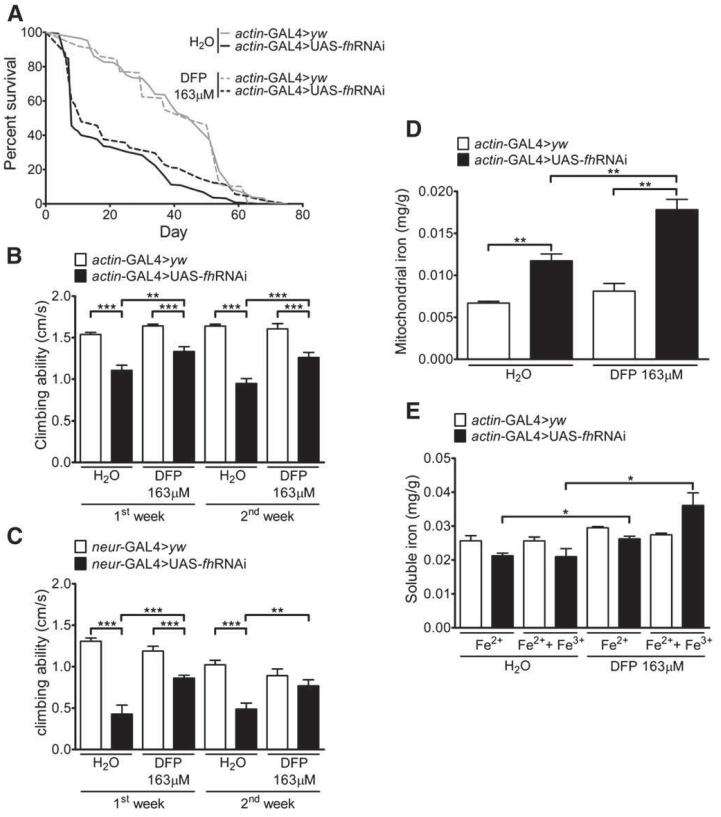

Fig. 1. Deferiprone recovers FRDA-like phenotypes by chelating mitochondrial iron. (A) Effect of DFP on the life span of systemic frataxin-depleted flies. Early treatment with 163 μM of DFP moderately improved the life span of *actin*-GAL4 > UAS-*fh*RNAi flies. (B) Effect of DFP on negative geotaxis assays in 5- (first week) and 10-day old adults (second week) with ubiquitous reduction in *fh* expression. In all cases, the *fh*RNAi flies showed reduced climbing capabilities when compared to controls ($P < 0.001$). Early treatment with 163 μM of DFP ameliorated this phenotype in the first ($P < 0.01$) and the second week ($P < 0.001$). (C) Effect of DFP on climbing capabilities of individuals with reduction in *fh* expression limited to the PNS. In almost all cases, the *fh*RNAi flies behaved differently than controls ($P < 0.001$). Early 163 μM DFP treatment improved the strong reduction of the climbing abilities of the *fhRNAi* flies in the first ($P < 0.001$) and the second week ($P < 0.01$). (D) Mitochondrial iron measurements by atomic absorption spectroscopy in 5-day-old *actin*-GAL4 > UAS-*fh*RNAi flies. Mitochondrial iron showed a significant increment in the *fh*RNAi flies with respect to the control flies ($P < 0.01$). FRDA flies treated with 163 μM DFP showed a further increase in the mitochondrial iron content ($P < 0.01$). (E) Measurement of mitochondrial soluble iron in 5-day-old *actin*-GAL4 > UAS-*fh*RNAi flies. DFP treatment increased Fe^{2+} levels in the FRDA flies ($P < 0.05$) and caused a further increase in total iron levels in these flies ($P < 0.05$) indicating an increase in Fe^{3+}. (*$P < 0.05$, **$P < 0.01$, ***$P < 0.001$. Error bars represent the standard error.)

3.4. Idebenone recovers the reduction of aconitase activity under hyperoxia

Aconitase activity is considered to be a sensor of oxidative damage and is diminished in the *fh*RNAi flies under hyperoxic conditions (Llorens et al., 2007), as well as in patients (Rötig et al., 1997) and other models of the disease (Al-Mahdawi et al., 2006; Puccio et al., 2001; Rötig et al., 1997). We tested the effect of IDE and DFP treatments on aconitase activity in the FRDA flies after they were subjected to an environment with 99.5% oxygen for 24 h. Only 163 μM DFP and 7 μM IDE were evaluated as these concentrations yielded the best results in the survival and climbing tests. When IDE was administered early, the aconitase activity was recovered to nearly normal levels in *fh*RNAi flies (Fig. 2E). When this compound was administered at the adult stage, there was also an increase of aconitase activity, but it was not statistically significant (data not shown). We did not find any change in the aconitase activity of *fh*RNAi flies when treated with DFP (Fig. 2E).

To ensure that the improvement in the mutant phenotypes observed was not an artifact caused by an interaction between DFP or IDE and the UAS-GAL4 system, we analyzed the expression of the green fluorescent protein (GFP) using the construct UAS-GFP under the control of the *actin*-GAL4 driver. Fluorescence of flies that hatched on H_2O, DMSO, 163 μM DFP and 7 μM IDE was measured, and no significant differences were observed between any of the treatments (Fig. 3A). Therefore, the drugs affected the pathophysiological mechanisms underlying the mutant phenotype resulting from frataxin depletion.

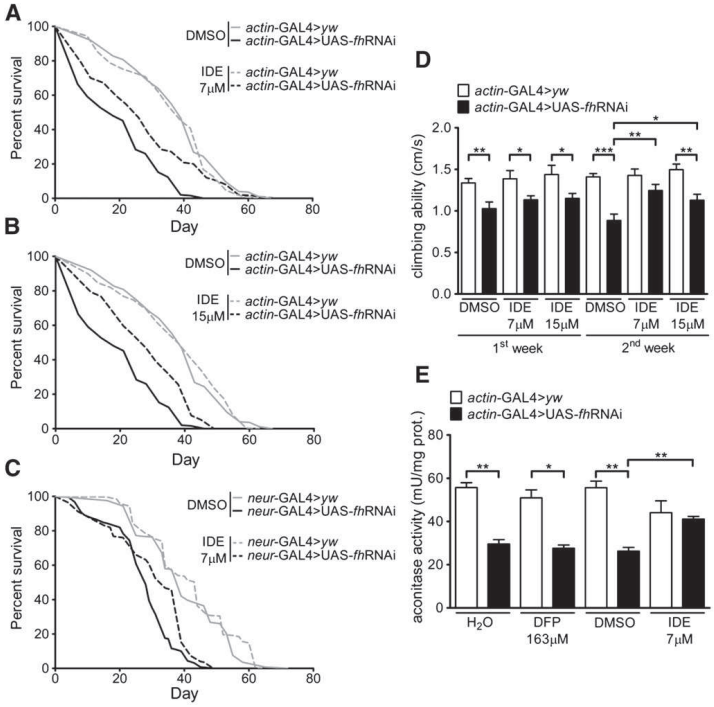

Fig. 2. Idebenone recovers behavioral and biochemical defects induced by frataxin depletion. (A–C) Effect of IDE on the life span of frataxin-depleted flies. IDE treatments at concentrations of 7 μM (A) and 15 μM (B) applied to one-day post-eclosion *fhRNAi* adults enhanced the life span of systemic frataxin-depleted flies. IDE at 7 μM improved this phenotype in the flies with a frataxin deficit in the PNS (C). (D) Effect of early treatment of IDE on climbing test evaluated at 5-(first week) and 10-day-old adults (second week). In almost all cases *fh*RNAi flies exhibited less climbing ability than control flies (P values from 0.05 to 0.001). This phenotype was improved during the second week after IDE treatments at 7 μM ($P < 0.01$) and 15 μM ($P < 0.05$). (E) Aconitase activity in hyperoxia after treatment with IDE. Consistent with previous results, aconitase activity is reduced in FRDA flies ($P < 0.01$). The negative effect of frataxin depletion on aconitase activity under hyperoxia is recovered with the early treatment with IDE ($P < 0.01$) but not with DFP. (*$P < 0.05$, **$P < 0.01$, ***$P < 0.001$. Error bars represent the standard error.)

Iron chelation has been previously correlated with changes in frataxin expression (Boddaert et al., 2007; Li et al., 2008). To assess whether DFP affects the expression of *fh*, we performed qRT-PCR in control adults treated early with 163 μM DFP. We observed that frataxin mRNA levels were not changed in flies treated with DFP versus H_2O (Fig. 3B). These data show that DFP did not affect the expression of the *fh* gene and that the improvement of phenotypes observed with this drug was not due to changes in frataxin expression.

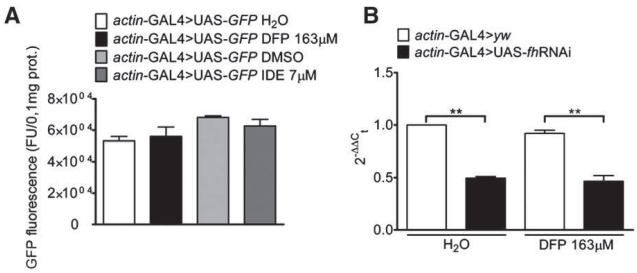

Fig. 3. DFP and IDE do not interfere with the UAS-GAL4 system and DFP does not affect *fh* expression. (A) Fluorescence values normalized to protein concentration from *actin*-GAL4 > UAS-GFP flies were not affected by treatment with DFP or IDE. (B) Frataxin mRNA levels of control flies did not show statistically significant differences after treatment with DFP. The same result is observed in *fh*RNAi flies. (**$P < 0.01$. Error bars represent the standard error.)

4. Discussion and conclusions

Friedreich's ataxia is the most prevalent inherited ataxia in the Caucasian population. It is a disease that typically affects young people and exhibits an irreversible progression that confines the patient to a wheelchair approximately 15 years after onset. Life expectancy averages between 40 and 50 years. Although different treatments are currently being developed and assessed in clinical trials, there is no cure for this disease at the present time. Therefore, it is imperative that new promising molecules are evaluated for their therapeutic potential and to obtain better knowledge of frataxin function and the molecular pathways affected in FRDA patients. *Drosophila* models of human diseases are acquiring increased significance for medical and pharmacological research due to their ease, rapid generation time and low cost of maintenance. These models powerfully bridge the gap between cell culture and vertebrate systems in modeling human genetic diseases.

Our *Drosophila* model for FRDA parallels the situation observed in patients of this disease. Namely, the flies have a moderate systemic reduction of frataxin expression to levels that are 30% of normal *fh*-mRNA, which is compatible with normal embryonic development (Llorens et al., 2007). In this model, RNAi-induced silencing of frataxin leads to a shortened life span and impaired motor coordination. These phenotypes are more severe under oxidative stress conditions, in which the activity of the mitochondrial enzyme aconitase is also strongly reduced (Llorens et al., 2007). The phenotypes of this model organism resemble the motor function impairment, the decreased life expectancy and the enhanced sensitivity to oxidative stress present in FRDA patients. In the present work, we tested the effects of two drugs that are currently in clinical trials for FRDA, an iron chelator (DFP) and an antioxidant (IDE), on our *fh*-RNAi flies to probe the usefulness of this model for further drug screening. The rationale for their use in FRDA was based on the basic pathophysiological features of frataxin depletion: mitochondrial iron accumulation and oxidative damage.

In a pilot study with FRDA patients, DFP was shown to improve ataxia and to reduce iron accumulation in the dentate nucleus as assessed by magnetic resonance imaging (Boddaert et al., 2007). Consistent with these observations, we here report that treatment with DFP improved the life span and motor ability of FRDA flies. This improvement could be explained by the ability of DFP to sequester the excess labile iron in the mitochondria that results from frataxin deficiency. As a result, DFP might eliminate cellular iron toxicity blocking Fenton's reaction in which Fe^{3+} is reduced back to Fe^{2+}, thereby preventing generation of powerful oxidizing molecules. DFP not only acts as a chelator but also functions as an iron donor for metabolic reutilization. It is known that DFP acts as an iron relocating agent at the cellular level, and due to its low affinity for iron, DFP can transfer it to biologically relevant molecules for physiological reuse (Sohn et al., 2008). This is crucial in FRDA in which intracellular iron is incorrectly distributed and mitochondrial iron overload is coupled with cytosolic depletion of iron, leading to compromised cellular function. Therefore, DFP might render the chelated iron bioavailable to restore cell functions affected by the deficit of frataxin.

Intramitochondrial iron deposits have been observed in the heart and central nervous system in patients (Lamarche et al., 1980; Waldvogel et al., 1999) and as a late event in conditional mouse models (Puccio et al., 2001) whereas intramitochondrial iron accumulation has not been observed either in FRDA patient cells (Sturm et al., 2005) or in the frataxin knockout mouse model (Cossée et al., 2000). In this study we did not find mitochondrial iron deposits in the muscular tissue of FRDA flies by electron microscopy despite the presence of excess iron levels in the mitochondria. These iron deposits may be present in our *Drosophila* model in tissues other than the muscle or they might appear later in life.

Changes in frataxin expression have been previously associated with cellular iron availability. Li et al. (2008) demonstrated that the expression of human *frataxin* is regulated by the cellular iron levels and that treatment with the cytosolic iron chelator deferoxamine decreased the expression of this gene in multiple human cell lines, which raises the possibility that DFP may cause a decrease in frataxin expression. In this regard, moderate concentrations of DFP (50 μM) did not affect frataxin levels in cultured cells (Kakhlon et al., 2008). Similarly, frataxin mRNA levels did not change in *Drosophila* upon treatment with 163 μM DFP.

Because oxidative stress is central in the pathogenesis of FRDA (reviewed in Armstrong et al., 2010), several antioxidant molecules have been suggested for therapeutic purposes. IDE is a potent antioxidant that penetrates membranes and enters mitochondria. It protects against mitochondrial damage and enhances respiration by improving the electron flux along the electron transport chain. Existing clinical data have provided broad evidence that IDE can ameliorate cardiac hypertrophy in patients with FRDA. However, data on the improvement of neurological symptoms are less clear (Artuch et al., 2002; Di Prospero et al., 2007; Lynch et al., 2010; Mariotti et al., 2003; Pineda et al., 2008; Ribaï et al., 2007). In this work, we show that IDE treatment ameliorates the motor ability in frataxin-depleted flies and improves the life span when *fh* silencing is targeted to the PNS. These results support a beneficial effect of IDE on neurological function.

Aconitase is a four iron–four sulfur (4Fe–4S) cluster enzyme that is often used as a marker of oxidative stress because it is inactivated by ROS through the removal of its labile iron atom. A decrease in aconitase activity has been described in patients and in several models of FRDA (Al-Mahdawi et al., 2006; Puccio et al., 2001; Rötig et al., 1997), including our model in *Drosophila* (Llorens et al., 2007). We have shown that IDE recovers aconitase activity in *fh*-RNAi flies, as is expected due to its antioxidant capacity. However, in the presence of DFP, the activity of this enzyme was still reduced in the FRDA flies. Both findings of increased and further reduced aconitase activity under DFP treatment can be found in the literature (Goncalves et al., 2008; Kakhlon et al., 2008, respectively). It has been described that moderate concentrations of DFP (50 μM) increase the activity of this enzyme (Kakhlon et al., 2008), but high doses of this compound (150 μM) inhibit aconitase activity (Goncalves et al., 2008). However, our results are more in agreement with the work of Foury (1999) regarding the effect of the iron chelator bathophenanthroline disulfonate (BPS) in a frataxin-deficient strain of yeast. They found that aconitase activity is not restored by BPS, which is similar to what occurs in our *Drosophila* model treated with DFP. These results suggest that aconitase might be impaired in a manner that is not directly linked to iron toxicity. Alternatively, deferiprone treatment was not effective enough to reduce oxidative stress in the conditions tested and therefore aconitase activity could not be rescued in such conditions. This enzyme is selectively inactivated by ROS (Das et al., 2001; Delaval et al., 2004) and, in contrast to other mitochondrial Fe–S enzymes, is the most vulnerable enzyme to ROS in our FRDA model (Llorens et al., 2007).

Finally, we found that both DFP and IDE were significantly effective in improving the mutant phenotypes in our FRDA fly model. In most cases, the compounds were most effective when added to larvae (early treatment). However, it has been reported that drugs incorporated prior to metamorphosis lose their efficacy during this stage of fly development (Hirth, 2010). Therefore, the beneficial effects of the drug may be suppressed in the adult flies. Nevertheless, there have been several successful examples of the use of *Drosophila melanogaster* in the drug discovery process for a wide range of human diseases, in which chemical compounds are administered at larval stages and result in significant improvement of adult phenotypes (Garcia-Lopez et al., 2008, 2011; Pandey and Nichols, 2011). These findings indicate that *Drosophila* is a useful model to test drug effects in different developmental stages. Particularly, in the context of FRDA, our results propose that early treatments of DFP and IDE might be more advantageous in this disease. In fact, the age at which IDE treatment is initiated has been suggested to be an important factor in the effectiveness of this therapy (Pineda et al., 2008).

In conclusion, the results presented in this paper demonstrate that the effects of two drugs that are currently in clinical trials for the treatment of FRDA are comparable between patients and the frataxin-deficient flies. Therefore, we have validated the use of the *Drosophila* model for the identification of new therapeutic molecules and the analysis of the molecular pathways implicated in FRDA. In addition, these therapeutic molecules might also be useful to treat other disorders, such as Parkinson's disease and Alzheimer's disease, which are also associated with an abnormal distribution of iron due to regional iron accumulation coupled with increased oxidative stress (reviewed in Crichton et al., 2011). With this work, we provide new evidence for the use of flies as experimental human disease models. *Drosophila* models allow for exploration of the normal function of the human genes involved in disease by studying the endogenous counterparts in flies. Moreover, these models offer the opportunity to address specific hypotheses concerning disease pathology. Finally, fly mutants can be also used to test new approaches for the treatment of such diseases.

Funding

This work was supported by a grant from La Fundació la Marató TV3 [exp 101932] of Spain.

S.S. is a recipient of a fellowship from Ministerio de Ciencia e Innovación of Spain; J.V.L. is supported by the European Friedreich's Ataxia Consortium for Translational Studies; L.B-S. was a recipient of the fellowship "Cinc Segles-Empresa" from Valencia University, Spain; P.C-Q. is supported by a grant from La Fundació la Marató TV3 of Spain and L.G. holds a Sara Borrell contract from the Spanish ISCIII-MSPS [CD09/00030].

Conflict of interest

The authors declare no competing financial interests.

Acknowledgments

The authors would like to thank ApoPharma for kindly donating the deferiprone used in this study. We also thank Mª Carmen García González and Carolina Chaparro Ronda from the Chemical Analysis Support Laboratory of the ICMM, Francisco R. Urbano Olmos and Covadonga Aguado Ballano from the Laboratory of Electron Microscopy of UAM for their help in iron measurements and TEM imaging, respectively and Ismael Al-Ramahi for critical reading of the manuscript.

References

Al-Mahdawi, S., et al., 2006. GAA repeat expansion mutation mouse models of Friedreich ataxia exhibit oxidative stress leading to progressive neuronal and cardiac pathology. Genomics 88, 580–590.

Al-Mahdawi, S., et al., 2008. The Friedreich ataxia GAA repeat expansion mutation induces comparable epigenetic changes in human and transgenic mouse brain and heart tissues. Hum. Mol. Genet. 17, 735–746.

Armstrong, J.S., Khdour, O., Hecht, S.M., 2010. Does oxidative stress contribute to the pathology of Friedreich's ataxia? A radical question. FASEB J. 24, 2152–2163.

Artuch, R., et al., 2002. Friedreich's ataxia: idebenone treatment in early stage patients. Neuropediatrics 33, 190–193.

Babcock, M., et al., 1997. Regulation of mitochondrial iron accumulation by Yfh1p, a putative homolog of frataxin. Science 276, 1709–1712.

Boddaert, N., et al., 2007. Selective iron chelation in Friedreich ataxia: biologic and clinical implications. Blood 110, 401–408.

Botella, J.A., et al., 2004. The *Drosophila* carbonyl reductase sniffer prevents oxidative stress-induced neurodegeneration. Curr. Biol. 14, 782–786.

Bradley, J.L., Blake, J.C., Chamberlain, S., Thomas, P.K., Cooper, J.M., Schapira, A.H., 2000. Clinical, biochemical and molecular genetic correlations in Friedreich's ataxia. Hum. Mol. Genet. 9, 275–282.

Campuzano, V., et al., 1996. Friedreich's ataxia: autosomal recessive disease caused by an intronic GAA triplet repeat expansion. Science 271, 1423–1427.

Cohen, A.R., 2006. New advances in iron chelation therapy. Hematology Am. Soc. Hematol. Educ. Program 42–47.

Cossée, M., et al., 2000. Inactivation of the Friedreich ataxia mouse gene leads to early embryonic lethality without iron accumulation. Hum. Mol. Genet. 9, 1219–1226.

Crichton, R.R., Dexter, D.T., Ward, R.J., 2011. Brain iron metabolism and its perturbation in neurological diseases. J. Neural Transm. 118, 301–314.

Das, N., Levine, R.L., Orr, W.C., Sohal, R.S., 2001. Selectivity of protein oxidative damage during aging in *Drosophila melanogaster*. Biochem. J. 360, 209–216.

Delaval, E., Perichon, M., Friguet, B., 2004. Age-related impairment of mitochondrial matrix aconitase and ATP-stimulated protease in rat liver and heart. Eur. J. Biochem. 271, 4559–4564.

Di Prospero, N.A., Baker, A., Jeffries, N., Fischbeck, K.H., 2007. Neurological effects of high dose idebenone in patients with Friedreich's ataxia: a randomised, placebo-controlled trial. Lancet Neurol. 6, 878–886.

Emond, M., Lepage, G., Vanasse, M., Pandolfo, M., 2000. Increased levels of plasma malondialdehyde in Friedreich ataxia. Neurology 55, 1752–1753.

Foury, F., 1999. Low iron concentration and aconitase deficiency in a yeast frataxin homologue deficient strain. FEBS Lett. 456, 281–284.

Foury, F., Cazzalini, O., 1997. Deletion of the yeast homologue of the human gene associated with Friedreich's ataxia elicits iron accumulation in mitochondria. FEBS Lett. 411, 373–377.

Garcia-Lopez, A., Monferrer, L., Garcia-Alcover, I., Vicente-Crespo, M., Alvarez-Abril, M.C., Artero, R.D., 2008. Genetic and chemical modifiers of a CUG toxicity model in *Drosophila*. PLoS One 3, e1595.

García-López, A., Llamusí, B., Orzáez, M., Pérez-Payá, E., Artero, R.D., 2011. In vivo discovery of a peptide that prevents CUG-RNA hairpin formation and reverses RNA toxicity in myotonic dystrophy models. Proc. Natl. Acad. Sci. U. S. A. 108, 11866–11871.

Goncalves, S., Paupe, V., Dassa, E.P., Rustin, P., 2008. Deferiprone targets aconitase: implication for Friedreich's ataxia treatment. BMC Neurol. 8, 20.

González-Cabo, P., Llorens, J.V., Palau, F., Moltó, M.D., 2009. Friedreich ataxia: an update on animal models, frataxin function and therapies. Adv. Exp. Med. Biol. 652, 247–261.

Harding, A.E., 1981. Friedreich's ataxia: a clinical and genetic study of 90 families with an analysis of early diagnostic criteria and intrafamilial clustering of clinical features. Brain 104, 589–620.

Harding, A.E., 1993. Clinical features and classification of inherited ataxias. Adv. Neurol. 61, 1–14.

Haugen, A.C., et al., 2010. Altered gene expression and DNA damage in peripheral blood cells from Friedreich's ataxia patients: cellular model of pathology. PLoS Genet. 6, e1000812.

Hirth, F., 2010. *Drosophila melanogaster* in the study of human neurodegeneration. CNS Neurol. Disord. Drug Targets 9, 504–523.

Kakhlon, O., et al., 2008. Cell functions impaired by frataxin deficiency are restored by drug mediated iron relocation. Blood 112, 5219–5227.

Kirby, K., Hu, J., Hilliker, A.J., Phillips, J.P., 2002. RNA interference-mediated silencing of Sod2 in *Drosophila* leads to early adult-onset mortality and elevated endogenous oxidative stress. Proc. Natl. Acad. Sci. U. S. A. 99, 16162–16167.

Koutnikova, H., Campuzano, V., Foury, F., Dollé, P., Cazzalini, O., Koenig, M., 1997. Studies of human, mouse and yeast homologues indicate a mitochondrial function for frataxin. Nat. Genet. 16, 345–351.

Lagedrost, S.J., et al., 2011. Idebenone in Friedreich ataxia cardiomyopathy results from a 6-month phase III study (IONIA). Am. Heart J. 161 (639–645.e1).

Lamarche, J.B., Côté, M., Lemieux, B., 1980. The cardiomyopathy of Friedreich's ataxia morphological observations in 3 cases. Can. J. Neurol. Sci. 7, 389–396.

Li, K., Besse, E.K., Ha, D., Kovtunovych, G., Rouault, T.A., 2008. Iron-dependent regulation of frataxin expression: implications for treatment of Friedreich ataxia. Hum. Mol. Genet. 17, 2265–2273.

Llorens, J.V., et al., 2007. Causative role of oxidative stress in a *Drosophila* model of Friedreich ataxia. FASEB J. 21, 333–344.

Lynch, D.R., Perlman, S.L., Meier, T., 2010. A phase 3, double-blind, placebo-controlled trial of idebenone in Friedreich ataxia. Arch. Neurol. 67, 941–947.

Mariotti, C., Solari, A., Torta, D., Marano, L., Fiorentini, C., Di Donato, S., 2003. Idebenone treatment in Friedreich patients: one-year-long randomized placebo-controlled trial. Neurology 60, 1676–1679.

Meier, T., Buyse, G., 2009. Idebenone: an emerging therapy for Friedreich ataxia. J. Neurol. 256 (Suppl. 1), 25–30.

Meier, T., Perlman, S.L., Rummey, C., Coppard, N.J., Lynch, D.R., 2012. Assessment of neurological efficacy of idebenone in pediatric patients with Friedreich's ataxia: data from a 6month controlled study followed by a 12-month open-label extension study. J. Neurol. 259, 284–291.

Monrós, E., et al., 1997. Phenotype correlation and intergenerational dynamics of the Friedreich ataxia GAA trinucleotide repeat. Am. J. Hum. Genet. 61, 101–110.

Pandey, U.B., Nichols, C.D., 2011. Human disease models in *Drosophila melanogaster* and the role of the fly in therapeutic drug discovery. Pharmacol. Rev. 63, 411–436.

Pandolfo, M., 2009. Friedreich ataxia: the clinical picture. J. Neurol. 256 (Suppl. 1), 3–8.

Paupe, V., et al., 2009. Impaired nuclear Nrf2 translocation undermines the oxidative stress response in Friedreich ataxia. PLoS One 4, e4253.

Pineda, M., et al., 2008. Idebenone treatment in paediatric and adult patients with Friedreich ataxia: long-term follow-up. Eur. J. Paediatr. Neurol. 12, 470–475.

Puccio, H., et al., 2001. Mouse models for Friedreich ataxia exhibit cardiomyopathy, sensory nerve defect and Fe–S enzyme deficiency followed by intramitochondrial iron deposits. Nat. Genet. 27, 181–186.

Ribaï, P., et al., 2007. Neurological, cardiological, and oculomotor progression in 104 patients with Friedreich ataxia during long-term follow-up. Arch. Neurol. 64, 558–564.

Rötig, A., et al., 1997. Aconitase and mitochondrial iron–sulphur protein deficiency in Friedreich ataxia. Nat. Genet. 17, 215–217.

Sanchez-Casis, G., Cote, M., Barbeau, A., 1976. Pathology of the heart in Friedreich's ataxia: review of the literature and report of one case. Can. J. Neurol. Sci. 3, 349–354.
Schmucker, S., Puccio, H., 2010. Understanding the molecular mechanisms of Friedreich's ataxia to develop therapeutic approaches. Hum. Mol. Genet. 19, R103–R110.
Schulz, J.B., et al., 2009. Diagnosis and treatment of Friedreich ataxia: a European perspective. Nat. Rev. Neurol. 5, 222–234.
Sohn, Y.-S., Breuer, W., Munnich, A., Cabantchik, Z.I., 2008. Redistribution of accumulated cell iron: a modality of chelation with therapeutic implications. Blood 111, 1690–1699.
Sturm, B., et al., 2005. Friedreich's ataxia, no changes in mitochondrial labile iron in human lymphoblasts and fibroblasts: a decrease in antioxidative capacity? J. Biol. Chem. 280, 6701–6708.
Velasco-Sánchez, D., et al., 2011. Combined therapy with idebenone and deferiprone in patients with Friedreich's ataxia. Cerebellum 10, 1–8.
Voncken, M., Ioannou, P., Delatycki, M.B., 2004. Friedreich ataxia-update on pathogenesis and possible therapies. Neurogenetics 5, 1–8.
Waldvogel, D., van Gelderen, P., Hallett, M., 1999. Increased iron in the dentate nucleus of patients with Friedrich's ataxia. Ann. Neurol. 46, 123–125.

Article 3. TORC1 inhibition by rapamycin promotes antioxidant defences in a *Drosophila* model of Friedreich's ataxia (Calap-Quintana *et al*. 2015)

PLOS | ONE

RESEARCH ARTICLE

TORC1 Inhibition by Rapamycin Promotes Antioxidant Defences in a *Drosophila* Model of Friedreich's Ataxia

Pablo Calap-Quintana[1], Sirena Soriano[1,2], José Vicente Llorens[1¤], Ismael Al-Ramahi[2], Juan Botas[2], María Dolores Moltó[1,3]*, María José Martínez-Sebastián[1]

1 Department of Genetics, University of Valencia, Burjassot, Valencia, Spain, **2** Department of Molecular and Human Genetics, Baylor College of Medicine, Houston, Texas, United States of America, **3** CIBERSAM, INCLIVA, Valencia, Spain

¤ Current address: Evolutionary Biology Center, Uppsala University, Uppsala, Sweden
* dmolto@uv.es

OPEN ACCESS

Citation: Calap-Quintana P, Soriano S, Llorens JV, Al-Ramahi I, Botas J, Moltó MD, et al. (2015) TORC1 Inhibition by Rapamycin Promotes Antioxidant Defences in a *Drosophila* Model of Friedreich's Ataxia. PLoS ONE 10(7): e0132376. doi:10.1371/journal.pone.0132376

Editor: Francesc Palau, Sant Joan de Déu Children's Hospital, SPAIN

Received: February 10, 2015

Accepted: June 14, 2015

Published: July 9, 2015

Data Availability Statement: All relevant data are within the paper and its Supporting Information files.

Funding: This work was supported by grants from the European Community's Seventh Framework Program FP7/2007-2013 [grant agreement no. 242193 EFACTS] and the Fundació la Marató TV3 of Spain [exp 101932]. Work in the Botas laboratory was supported by the R01-NS42179 NIH grant. P.C.-Q. is a recipient of a research contract from La Fundació la Marató TV3 of Spain; S.S. was a recipient of a fellowship from Ministerio de Ciencia e Innovación of Spain; and J.V.L. was supported by a

Abstract

Friedreich's ataxia (FRDA), the most common inherited ataxia in the Caucasian population, is a multisystemic disease caused by a significant decrease in the frataxin level. To identify genes capable of modifying the severity of the symptoms of frataxin depletion, we performed a candidate genetic screen in a *Drosophila* RNAi-based model of FRDA. We found that genetic reduction in TOR Complex 1 (TORC1) signalling improves the impaired motor performance phenotype of FRDA model flies. Pharmacologic inhibition of TORC1 signalling by rapamycin also restored this phenotype and increased the lifespan and ATP levels. Furthermore, rapamycin reduced the altered levels of malondialdehyde + 4-hydroxyalkenals and total glutathione of the model flies. The rapamycin-mediated protection against oxidative stress is due in part to an increase in the transcription of antioxidant genes mediated by *cap-n-collar* (*Drosophila* ortholog of *Nrf2*). Our results suggest that autophagy is indeed necessary for the protective effect of rapamycin in hyperoxia. Rapamycin increased the survival and aconitase activity of model flies subjected to high oxidative insult, and this improvement was abolished by the autophagy inhibitor 3-methyladenine. These results point to the TORC1 pathway as a new potential therapeutic target for FRDA and as a guide to finding new promising molecules for disease treatment.

Introduction

Friedreich's ataxia (FRDA), an autosomal recessive disease, is the most common inherited ataxia among Caucasians [1]. It is a multisystemic disease affecting the central and peripheral nervous systems and other non-neural organs, resulting in multiple signs and symptoms [2]. This incapacitating condition exhibits an irreversible progression that confines a patient to a wheelchair and leads to early death. FRDA is caused by a partial loss of *FXN* function [3], with the vast majority of patients carrying an intronic GAA expansion mutation in both alleles of

research contract from the European Community's Seventh Framework Program FP7/2007-2013 [grant agreement no. 242193 EFACTS]. This work was supported by a grant of the Prometeo Program from Generalitat Valenciana [PROMETEOII/2014/067].

Competing Interests: The authors have declared that no competing interests exist.

this gene [4]. *FXN* codifies frataxin, a mitochondrial protein that is highly conserved through evolution [5] and whose deficiency results in several biochemical disturbances. Major alterations include impaired iron-sulphur cluster biogenesis, dysfunction of respiratory chain complexes and aconitase, mitochondrial iron accumulation and increased oxidative stress sensitivity [6].

A growing amount of data from patient samples and different model organisms of the disease suggest that oxidative stress plays an important role in the pathophysiology of FRDA. Biomarkers of oxidative damage, such as lipid peroxidation products, have been frequently found in patient samples and in a *Drosophila* model of the disease [7,8]. Increased levels of reactive oxygen species (ROS) have also been reported in FRDA lymphoblasts [9] and in mouse, *Drosophila* and yeast models [10–12]. In addition, frataxin depletion enhances the sensitivity to different pro-oxidant agents in FRDA cells, mice, *Drosophila melanogaster*, *Caenorhabditis elegans* and yeast [13–17]. Furthermore, a reduction in the ability to promote antioxidant defences has been reported in cultured fibroblasts from FRDA patients [18] and in the dorsal root ganglia from YG8R frataxin-deficient mice [19].

To date, there is no cure for FRDA, but several strategies for the discovery of effective therapeutics are being developed or tested in clinical trials (http://www.curefa.org/pipeline.html). These strategies seek to increase frataxin expression and to reduce the biochemical consequences of its deficiency, such as oxidative damage. Important progress has been achieved in frataxin replacement therapies [20,21], as well as in treatments directed to increasing protein levels [22]. Genetically manipulable organisms such as *Drosophila* are acquiring increased significance for medical and pharmaceutical research as valuable tools for testing potential therapies. The identification of the *Drosophila FXN* ortholog, *fh*, [23] led to the development of fly models of FRDA that can be used to explore frataxin function [24] and to provide *in vivo* evidence of a functional equivalence for human and fly frataxins [25]. These models have contributed to a comprehensive characterisation of the phenotype associated with frataxin deficiency [8,11,15,26–28]. Recently, we have validated the use of *Drosophila* as an experimental tool to screen for therapeutic molecules to treat FRDA and proposed that early treatments using the antioxidant idebenone and the iron chelator deferiprone may be advantageous to slow down the disease progression [29]. In addition the molecule methylene blue has been suggested for the treatment of the heart dysfunction in FRDA [30]. These findings stimulate further work using *Drosophila* to find new pharmacological drugs that may be relevant to this disease.

Here, we conducted a genetic screen of candidate genes related to FRDA pathophysiology to identify new therapeutic targets for this disease. We found that downregulation of TOR Complex 1 (TORC1) function suppresses the impaired motor performance of our *Drosophila* model of FRDA [15]. To evaluate the therapeutic efficacy of TORC1 inhibition, we used rapamycin, a lipophilic macrolide that acts as an inhibitor of the TOR kinase [31]. This treatment was able to increase the motor performance and survival of frataxin knockdown flies and could also induce an improvement in the oxidative status and an increase in the ATP levels.

Materials and Methods

Drosophila melanogaster strains

The *UAS-fh*RNAi line was previously generated in our laboratory and produces a reduction of up to 70% of frataxin mRNA when expressed ubiquitously using the *actin-Gal4* driver; this reduction is compatible with a normal development [15]. The y^1w^*, w^{1118}, *UAS-GFP*, *actin-Gal4*, *nos-Gal4*; *UAS-GFP-LC3*, *UAS-foxo-GFP*, *cnc-EGFP*, *UAS-S6k*^{STDETE} (here referred as *S6k*^{CA}) and *Thor*^{2} (here referred as *4E-BP*^{LOF}) strains were obtained from the Bloomington

Stock Center. y^1w^*; *actin-Gal4* and w^{1118}; *actin-Gal4* flies were used as controls, while *UAS-fh*RNAi; *actin-Gal4* flies were used as FRDA model flies (here referred as *fh*RNAi).

Culture conditions and drug treatments

Drosophila stocks were maintained at 25°C under a 16/8 hour light/dark cycle on standard cornmeal agar medium. The media named "RAP", "3-MA" and "RAP + 3-MA" were prepared with, respectively rapamycin at 1 μM (LC Laboratories), 3-methyladenine at 67 μM (Sigma-Aldrich), and both rapamycin at 1 μM and 3-MA at 67 μM. All compounds were previously dissolved in dimethylsulfoxide (DMSO; Sigma-Aldrich) at a final concentration of 0.1% (v/v). The medium named "DMSO" only contained this compound at 0.1% (v/v) and was used as control medium. Crosses were conducted at 25°C in the supplemented media. F_1 flies of the appropriate genotype were transferred to fresh vials containing the compound every 3 days.

Genetic screen

The *UAS-fh*RNAi; *actin-Gal4* flies (*fh*RNAi flies) were crossed at 28°C with approximately 300 lines, including RNAi lines from the Vienna Drosophila Resource Center and loss-of-function and overexpression lines for candidate genes from the Bloomington Stock Center. We focused on candidate pathways implicated in FRDA pathophysiology comprising metal homeostasis, response to oxidative stress, apoptosis and autophagy. Motor performance tests were conducted as described previously [32] for the identification of genetic modifiers of frataxin depletion. We recorded the number of flies that climbed to a height of 11.5 cm.

Climbing and survival assays

Groups of fifteen 7-day-old males were transferred into vials of 1.5 cm in diameter and 25 cm in height. The height reached from the bottom of the vial by each fly in a period of 10 s was recorded with a camera. For each genotype, approximately 100 flies were tested. The results are expressed in percentage, taking as 100% the mean climbing speed of control flies in the DMSO medium. Lifespan was measured starting with 100 adult males of each genotype and by recording the number of living flies every 3 days. Survival under hyperoxia was measured using 30 adult males exposed to a constant flux of 99.5% oxygen under a low positive pressure from day 1 to day 4 after eclosion from the puparium. Three replicates were performed, and the results showed the percentage of dead flies after 4 days of hyperoxia.

GFP-LC3 quantification in larvae

The *UAS-fh*RNAi and y^1w^* lines were crossed with the *nos-Gal4*; *UAS-GFP-LC3* strain, which expresses the microtubule-associated protein 1A/1B-light chain 3 (LC3) as a fusion protein with GFP under the control of the *nanos* promoter (a marker for autophagy [33]). Fat bodies of third instar larvae were imaged with a fluorescence microscope (Leica DM 2500; Leica Microsystems) using a x40 objective. Larvae were maintained in normoxia or subjected to one day of hyperoxia before the dissections. The number of fluorescent dots per field was counted automatically using the tools of ImageJ software (National Institutes of Health, USA). The results are expressed in percentage, taking as 100% the average number of dots for control flies in the DMSO medium.

Biochemical assays

Biochemical assays were conducted in triplicate or quadruplicate with thirty 7-day-old males of the appropriate genotype. ATP levels were determined using the ATP Detection Reagent of

the Mitochondrial ToxGlo Assay (Promega). Flies were homogenised in a buffer of 0.25 M Sucrose; 10 mM HEPES-NaOH pH 7.4; 0.1% Triton X-100 (v/v), Na_3VO_4 5 mM, and the extract was centrifuged at 1000 g for 10 min at 4°C. The luminescence of the supernatant was measured using a Tecan Infinite M200 PRO luminometer (Tecan Group). ATP levels were normalised to the total protein, which was measured using the BCA assay. The results are expressed in percentage, taking as 100% the ATP level of control flies in the DMSO medium.

The concentration of malondialdehyde (MDA) + 4-hydroxyalkenals (HAE) was measured using the Bioxytech LPO-586 Kit (Oxis International). Flies were homogenised in a buffer of 50 mM Tris-HCl at pH 7.4 with 5 mM butylated hydroxytoluene, and the extract was centrifuged at 3000 g for 10 min at 4°C. A_{586} measurements were performed in a Spectronic Genesys 5 spectrophotometer (Milton Roy). MDA + HAE levels were normalised to the protein amount determined by the Bradford assay. The results are expressed in nmol of MDA + HAE per μg of protein.

The total concentration of GSH, including both the reduced and oxidised forms, was measured using a Bioxytech GSH-420 Spectrophotometric Assay Kit (Oxis International). Flies were homogenised in trichloroacetic acid, and the extract was centrifuged at 3000 g for 10 min at 4°C. A_{420} was measured in a Spectronic Genesys 5 spectrophotometer (Milton Roy). The obtained data were normalised to the total protein determined by the Bradford assay, and the results are expressed in mmol of total GSH per μg of protein.

For measurements of the aconitase activity in hyperoxia, flies were incubated in normoxia for 5 days and then treated with 99.5% oxygen for 2 days. Aconitase activity was determined from the whole-fly extracts using the Bioxytech Aconitase-340 Spectrophotometric Assay Kit (Oxis International) as previously described [29]. A_{340} was measured using a Tecan Infinite M200 PRO luminometer (Tecan Group), and the results are expressed in percentage, taking as 100% the aconitase activity of control flies in DMSO medium.

Quantitative real-time PCR (RT-qPCR)

Total RNA was extracted from 7-day-old males using a miRNeasy Mini Kit (Qiagen). RNA was converted into cDNA with Expand Reverse Transcriptase (Roche) and oligo-dT primers. Amplification was conducted using the Step One Plus Real-Time PCR System (Applied Biosystems) and Power SYBR Green (Applied Biosystems). The following primers were used for the transcript amplification of the different genes: *frataxin homolog (fh)*, 5′ACACCCTGGACGCACTGT3′ and 5′CCAGGTTCACGGTTAGCAC3′; *Adenylyl cyclase 76E* (*Ac76E*), 5′ CGATCAAATAGCTCAGGAGAACCA3′ and 5′ CATTTATGCCGGTCGCCTCA3′ ; *cap-n-collar* (*cnc*), 5'CACGTTTTCAAGCTCACCAC3' and 5'TCCCTGCAGCACACACAAT3'; *Catalase (Cat)*, 5'GTTCGAGTGTTTCTAAATTCTGGTT3' and 5'GTGGTAATGGCACCAGG AGAA3'; *forkhead box sub-group O (foxo)*, 5'CCCACCGGCAAAATCAACAA3' and 5'CCTCGCCAGCCCAAAAGATA3'; *Glutamate-cysteine ligase catalytic subunit (Gclc)*, 5'GAGAGCGAAACAGAGTGACGA3' and 5'GAACTGATTGACGCCATGCT3'; *Glutathione S transferase D1* (*GstD1*), 5'TACATCGCGAGTTTCACAACAG3' and 5'CAGGTTGAG CAGCTTCTTGTT3'; *Peroxiredoxin 3* (*Prx3*), 5'CCGATTTCAAGGGTCTGGCT3' and 5'CAACAATTTCGGTGGGGCAA3'; *Sestrin* (*Sesn*), 5'CCCCAGTTCCACGATCACTT3' and 5'CGCTTCACCAGATACGGACA3'; *Superoxide dismutase* (*Sod*), 5' GAACAGGAGAG CAGCGGTA3' and 5'TACGGATTGAAGTGCGGTCC3'; *Superoxide dismutase 2* (*Sod2*), 5'CAGATATGTTCGTGGCCCGT3' and 5'CGGCAGATGATAGGCTCCAG3'. The *Ribosomal protein L32* gene (*RpL32*) was used as an internal control and was amplified using the 5′CCAAGCACTTCATCCGCCACC3′ and 5′GCGGGTGCGCTTGTTCGATCC3′ primers. The results were analysed using the Step One Plus software v2.0 (Applied Biosystems). The gene

expression levels are relative to the internal control, and the relative quantification of each cDNA was calculated in quadruplicate experiments using the Ct method. The results are expressed as the fold change of relative gene expression compared with that for control flies in the DMSO medium.

Nuclear isolation and GFP quantification

*fh*RNAi flies were crossed with the *UAS-foxo-GFP* and *cnc-EGFP* lines. For *UAS-foxo-GFP*, third instar larvae were collected as the co-expression with *fh*RNAi resulted in adult semi-lethality; whereas 7-day-old males were analysed for *cnc-EGFP*. Flies with the genotypes *actin-Gal4; UAS-foxo-GFP* and *actin-Gal4; cnc-EGFP*, respectively, were used as controls. Total extractions and nuclear fractions were isolated following the procedure described previously [34], and GFP fluorescence was measured using a Tecan Infinite M200 PRO luminometer (Tecan Group). The results are expressed as the nuclear/total fluorescence ratio, considering the ratio of the control flies in the DMSO medium as 1.

Statistical Analysis

Statistical analyses were performed using GraphPad Prism 5.03 software (GraphPad software). Kaplan-Meier survival plots were analysed using semiparametric log rank tests. For the comparison of means, we performed an unpaired nonparametric Student's *t* test. In all cases, values of $P<0.05$ were considered statistically significant. Error bars represent standard error of the mean (SEM).

Results

TORC1 pathway genetically interacts with frataxin

To identify genetic modifiers that might modulate the phenotypes caused by frataxin knockdown in *Drosophila*, we conducted a genetic screen of candidate pathways implicated in FRDA pathophysiology. Specifically, we examined the effect of knockdown, loss and gain-of-function alleles corresponding to metal homeostasis, response to oxidative stress, apoptosis and autophagy pathways. We then conducted motor performance tests to determine whether these alleles suppress the motor impairment of the *fh*RNAi flies. The screen revealed four modifiers from the TORC1 signalling pathway: the tuberous sclerosis complex protein 1 (*Tsc1*), the protein kinase S6K (*S6k*), the eukaryotic translation initiation factor 4E (*eIF-4E*) and the Leucine-rich repeat kinase (*Lrrk*) (Fig 1A).

One of the most important regulators of TORC1 activity is the tuberous sclerosis complex (TSC), which is a heterodimer that comprises the proteins TSC1 and TSC2. TSC1/2 negatively regulates TORC1 signalling by inactivating the Ras homolog enriched in brain ortholog (*Rheb*) GTPase. The simultaneous knockdown of *Tsc1* and frataxin resulted in semi-lethality, whereas the expression of the RNAi for *Tsc1* with the *actin-Gal4* driver had no effect on viability in control flies. *S6k* and *eIF-4E* are downstream targets of TORC1. Expression of a dominant-negative form of S6K [35] improved the motor performance of the *fh*RNAi flies (Fig 1B). In contrast, the expression of a constitutively active version of S6K [35] produced a detrimental effect when combined with frataxin knockdown by inducing semi-lethality. Regarding *eIF-4E*, a loss of function mutation suppressed the impaired motor performance phenotype of the *fh*RNAi flies (Fig 1C). In all cases, the *S6k* and *eIF-4E* alleles on their own had no effect on the viability or motor performance of control flies. We also demonstrated that knocking down the *Lrrk* suppresses the frataxin knockdown phenotype (Fig 1D). *Lrrk* is the *Drosophila* ortholog of the human *LRRK2*, and dominant pathogenic mutations in this gene cause the most common

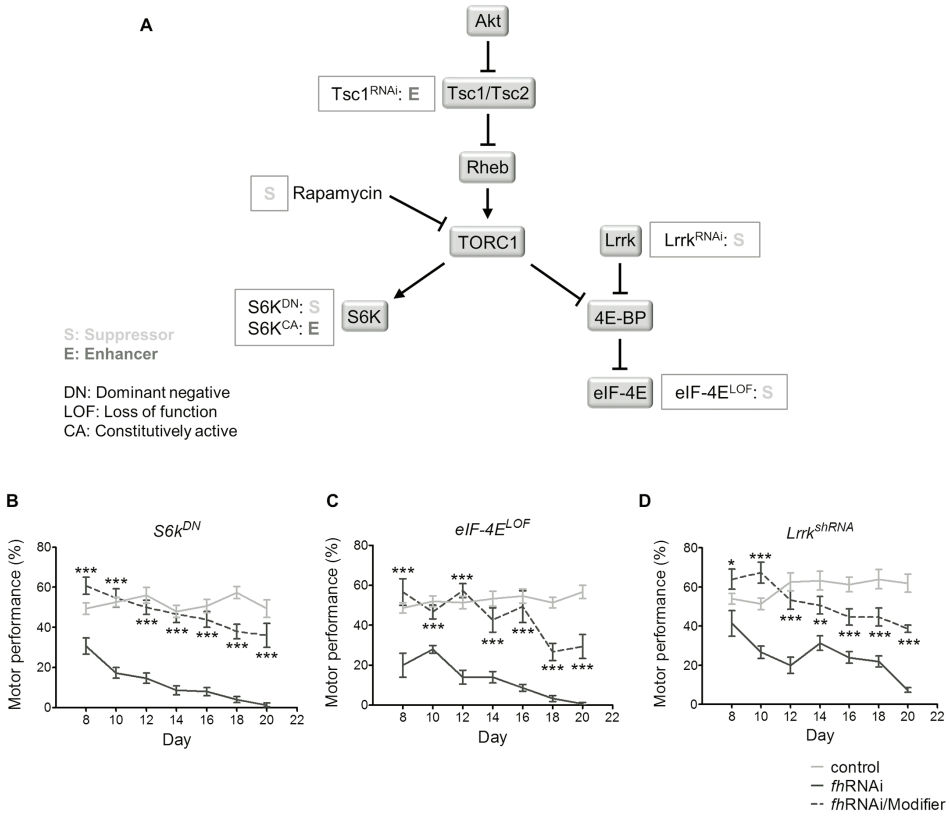

Fig 1. Genetic reduction of TORC1 signalling improves the motor performance of frataxin knockdown flies. (A) Gene modifiers of frataxin knockdown identified in *Drosophila* and their position within the TORC1 signalling pathway. (B-D) Improvement of motor performance of *fh*RNAi flies by the effect of a dominant negative allele of *S6k* (B), a loss of function allele of *eIF-4E* (C) and a shRNA against *Lrrk* (D). Motor performance is expressed as the percentage of flies that climbed to a height of 11.5 cm. Control (w^{1118}; *actin-Gal4* flies), *fh*RNAi (*UAS-fh*RNAi; *actin-Gal4* flies), *fh*RNAi/Modifier (*fh*RNAi flies carrying the corresponding allele of the modifier). Asterisks represent the statistical significance between the *fh*RNAi and *fh*RNAi/Modifier flies for every day. **P*<0.05, ***P*<0.01, ****P*<0.001. Error bars represent SEM.

doi:10.1371/journal.pone.0132376.g001

familial forms and some sporadic cases of Parkinson's disease [36]. In *vitro* studies show that the eIF-4E binding protein (4E-BP) is a substrate of *Lrrk* [37], (Fig 1A). Genotypes of the *Drosophila* strains corresponding to these genetic interactors are shown in S1 Table.

Rapamycin improves the motor performance and lifespan deficits of the *fh*RNAi flies

Because the reduction of TORC1 activity decreases S6K and eIF-4E activities [38], we tested whether pharmacologic inhibition of this complex with rapamycin would also improve the

phenotypes of our *Drosophila* FRDA model. First, we tested the effect of 1 μM rapamycin on the motor performance of the frataxin knockdown flies. This concentration had been previously proved effective in *Drosophila* [39] and did not provoke the negative effect on viability that we found for the higher concentrations. Here, we used the climbing speed of flies as it provides a more accurate assessment of the motor performance. In DMSO medium, 7-day-old *fh*RNAi flies showed a 25% decrease in climbing speed compared with controls raised in the same medium. Rapamycin induced the recovery of the motor performance phenotype of the frataxin knockdown flies up to control levels (Fig 2A). Because another feature of our *Drosophila* model of FRDA is a shortened lifespan [15], we also tested the effect of rapamycin on this phenotype. It has been reported that rapamycin increases the lifespan in *Drosophila* and other organisms [40]. Accordingly, 1 μM rapamycin produced a slight but statistically significant increase in the lifespan of both control ($P = 0.0116$) and *fh*RNAi ($P = 0.0004$) flies (Fig 2B).

To confirm the inhibitory effect of rapamycin on TORC1 activity, we measured the developmental time needed by flies to reach the adult stage. It has been shown that, in conjunction with the insulin/IGF signalling pathway, TORC1 controls the larval development in *Drosophila*, matching the speed of growth to the nutrient availability. A reduction in the amount of food reduces TORC1 signalling in the fat body and the prothoracic gland and increases the time needed by the individuals to reach the pupae stage [41]. We observed that the rapamycin treatment increased, by approximately one day, the mean time needed by both control and *fh*RNAi individuals to reach the adult stage (S1 Fig). This result indicated that rapamycin reduces TORC1 signalling similarly to the food restriction effect and that the rapamycin concentration used could efficiently modify the TORC1 activity.

Finally, to test whether the suppression by rapamycin of the motor performance and lifespan phenotypes of *fh*RNAi flies was an artefact caused by interference with the GAL4/UAS system, we verified that rapamycin had no effect on the expression of a GFP reporter (S2 Fig). RT-qPCR of the transcript for frataxin showed that rapamycin did not alter the level of the *fh* mRNA either in the control or in the frataxin knockdown flies (S3 Fig).

Rapamycin protects against oxidative stress in the FRDA model

Oxidative stress plays a central role in the pathophysiology of FRDA, as shown in patients and in cellular and animal models of the disease [7–12], including our *Drosophila* model. In this context, the impairment of motor performance and survival exhibited by the *fh*RNAi flies were ameliorated after treatment using the antioxidant idebenone [29]. *fh*RNAi flies also show an increased sensitivity to external oxidative stress, as indicated by an enhanced reduction in motor performance and lifespan [15]. Taking into account these data, we asked whether rapamycin might be suppressing the FRDA toxicity in part by decreasing oxidative stress.

We monitored the effect of rapamycin on the levels of malondialdehyde (MDA) + 4-hydroxyalkenals (HAE) and total glutathione, two markers of oxidative stress. As expected, *fh*RNAi flies show a higher amount of MDA + HAE compared with that of control flies in the DMSO medium (Fig 3A). Interestingly, rapamycin restored the MDA + HAE levels in the *fh*RNAi flies, whereas rapamycin had no effect on the controls. As shown in Fig 3B, *fh*RNAi flies had higher levels of total glutathione than did control flies and rapamycin produced a significant reduction in the total amount of glutathione in the *fh*RNAi flies but did not affect the total glutathione levels in the controls. Therefore, the inhibition of TORC1 with rapamycin seems to

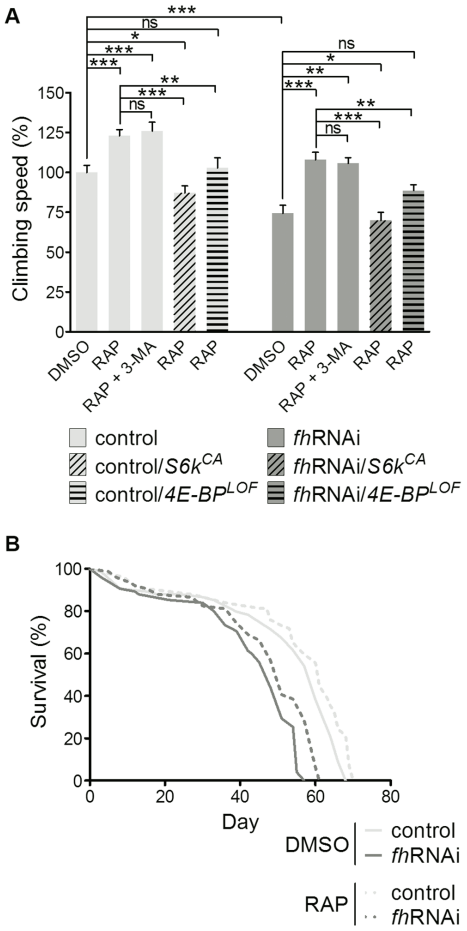

Fig 2. Rapamycin increases climbing speed and survival. (A) Rapamycin treatment increases the climbing speed of 7-day-old males in both the control and FRDA fly groups, and this effect is not affected by the addition of the autophagy inhibitor 3-MA. A constitutively active allele of S6K ($S6k^{CA}$) and a loss of function allele of 4E-BP ($4E\text{-}BP^{LOF}$) prevent rapamycin from increasing the climbing speed. Climbing speed is expressed in percentage (mean climbing speed of control flies in the DMSO medium is 100%). ns: non-significant, $^{*}P<0.05$, $^{**}P<0.01$, $^{***}P<0.001$. Error bars represent SEM. (B) Survival is also increased in control ($P = 0.0116$) and FRDA flies ($P = 0.0004$) after the drug treatment. Control ($y^{1}w^{*}$; *actin-Gal4* flies), control/$S6k^{CA}$ (control flies carrying the $S6k^{CA}$ allele), control/$4E\text{-}BP^{LOF}$ (control flies carrying the $4E\text{-}BP^{LOF}$ allele), *fh*RNAi (*UAS-fh*RNAi; *actin-Gal4* flies), *fh*RNAi /$S6k^{CA}$ (model flies carrying the $S6k^{CA}$ allele), *fh*RNAi /$4E\text{-}BP^{LOF}$ (model flies carrying the $4E\text{-}BP^{LOF}$ allele).

doi:10.1371/journal.pone.0132376.g002

ameliorate the oxidative stress injury in frataxin knockdown flies, resulting in a decrease in the altered MDA + HAE and total glutathione levels.

Autophagy induction by rapamycin is not critical except in hyperoxic conditions

It is well established that rapamycin treatment leads to the activation of autophagy through the inhibition of TORC1 [31]. Thus, we asked whether autophagy might play a role in the protection against oxidative stress conferred to the *fh*RNAi flies by rapamycin. For this purpose, we used the 3-MA compound, which inhibits Vps34 (vacuolar protein sorting 34), a class III phosphoinositide 3-kinase that is essential for autophagosome biogenesis [42]. First, we confirmed that at the concentrations used in this study, rapamycin and 3-MA were effective as inducers and inhibitors of autophagy, respectively. As shown in S4 Fig, rapamycin induces the formation of autophagosomes, which were labelled with GFP-LC3, in control and frataxin knockdown flies, and the addition of 3-MA decreased the number of GFP-LC3 dots.

Next, we tested the effect of autophagy inhibition on the levels of MDA + HAE and total glutathione. No changes were detected between the RAP and the RAP + 3-MA media (Fig 3A

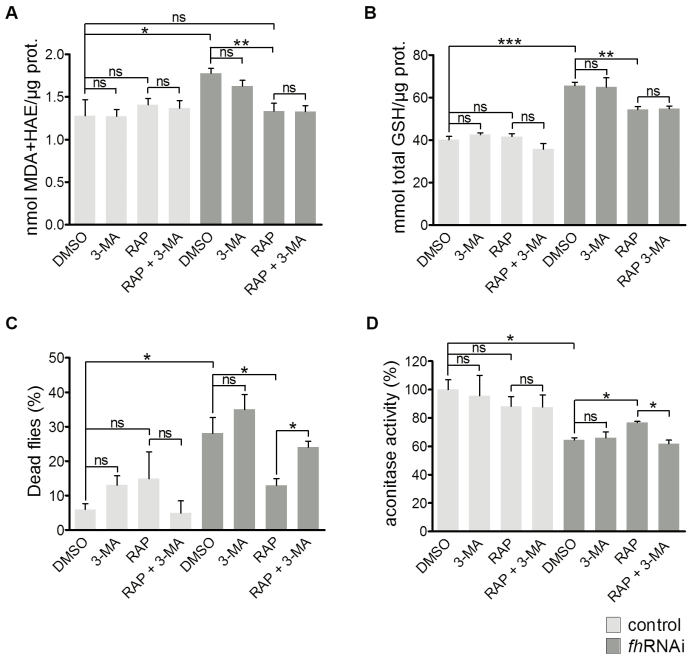

Fig 3. Rapamycin increases oxidative stress protection. In the normoxic condition, rapamycin reduces the altered levels of malondialdehyde + 4-hydroxyalkenals (A) and total glutathione (B) of model flies without requiring autophagy induction as the addition of 3-MA has no effect. In hyperoxia, rapamycin improves the survival of FRDA flies (C) and increases the aconitase activity (D). The addition of 3-MA abolishes these effects in model flies, highlighting the relevance of autophagy in this highly oxidative condition. Control (y^1w^*; *actin-Gal4* flies), *fh*RNAi (*UAS-fh*RNAi; *actin-Gal4* flies). ns: non-significant, **P*<0.05, ***P*<0.01, ****P*<0.001. Error bars represent SEM.

doi:10.1371/journal.pone.0132376.g003

and 3B), indicating an autophagy-independent effect for rapamycin. In addition, the beneficial effect of rapamycin on the motor performance was also autophagy-independent (Fig 2A). These data show that even though autophagy is induced by rapamycin, autophagy has no important protective effect in these conditions.

Then, we asked whether autophagy induction by rapamycin is beneficial for flies under external oxidative stress. We assessed the effect of rapamycin on the survival of *fh*RNAi flies incubated in a hyperoxic atmosphere for 4 days. In the DMSO medium, we observed higher mortality in *fh*RNAi flies (28%) than in controls (6%). Rapamycin reduced the number of dead *fh*RNAi flies but had no significant effect on the survival of the controls (Fig 3C). Interestingly, the decreased lethality observed in hyperoxia conditions was abolished by the addition of 3-MA (Fig 3C), suggesting that autophagy is indeed necessary for the protective effect of rapamycin on *fh*RNAi flies in hyperoxia. In this condition, rapamycin and 3-MA were also effective as an inducer and inhibitor of autophagy, respectively (S4 Fig).

To further confirm this hypothesis, we measured the activity of aconitase during hyperoxia. Under this experimental condition, the reduction of enzyme activity was significantly higher in the *fh*RNAi flies than in the control flies [15]. We observed that the aconitase activity increased in the rapamycin-treated *fh*RNAi flies and that this increase was also abolished by the addition of 3-MA (Fig 3D). Together, these data suggest that the autophagy induction by rapamycin is required for the protection against highly oxidative conditions; however, other mechanisms downstream of TORC1 should act in conditions of endogenous production of ROS in the FRDA model.

Rapamycin enhances antioxidant defences increasing the nuclear translocation of Cnc

TORC1 modulates the function of several transcription factors that, in turn, control the transcription of important antioxidant genes [43,44]. To determine whether rapamycin transcriptionally induces endogenous antioxidant defences, we analysed the expression of two key transcription factors implicated in antioxidant protection (*foxo* and *cnc*) and four well-known target genes (*Sesn* and *Ac76E* for FOXO; *Gclc* and *GstD1* for Cnc). In the DMSO medium, we observed higher levels of the *foxo* (53% increase) and *cnc* (38% increase) transcripts in the *fh*RNAi flies than in the controls. Rapamycin did not modify the expression of these genes at the transcriptional level (Fig 4A and 4D). The FOXO target genes *Sesn* and *Ac76E* showed no differences between the control and *fh*RNAi flies in both DMSO and RAP medium (Fig 4E and 4F). In contrast, the transcript levels of the Cnc target genes were higher in the *fh*RNAi flies than in the controls when both were cultured in the DMSO medium (40% for *Gclc* and 34% for *GstD1*). Rapamycin increased the expression of these genes in both the control and *fh*RNAi flies (Fig 4B and 4C). Rapamycin also increased the mRNA level of *Cat*, *Prx3*, *Sod* and *Sod2* (Fig 4G–4J]), which encode important enzymes that protect the cell from oxidative damage and are subjected to overlapping regulation of FOXO and Cnc transcription factors.

To explain the augmented expression of the Cnc target genes by rapamycin, we searched for cellular localisation of Cnc using an EGFP-tagged *cnc* allele. We found a higher nuclear/cellular fluorescence ratio of Cnc-EGFP after rapamycin treatment in both the control and *fh*RNAi flies (Fig 4K). No differences were observed in the case of a FOXO-GFP fused protein (S5 Fig). These results indicate that rapamycin enhances the protection against oxidative stress by inducting endogenous antioxidant defences and that this effect is mediated, at least in part, by an increase in the nuclear translocation of the transcription factor Cnc.

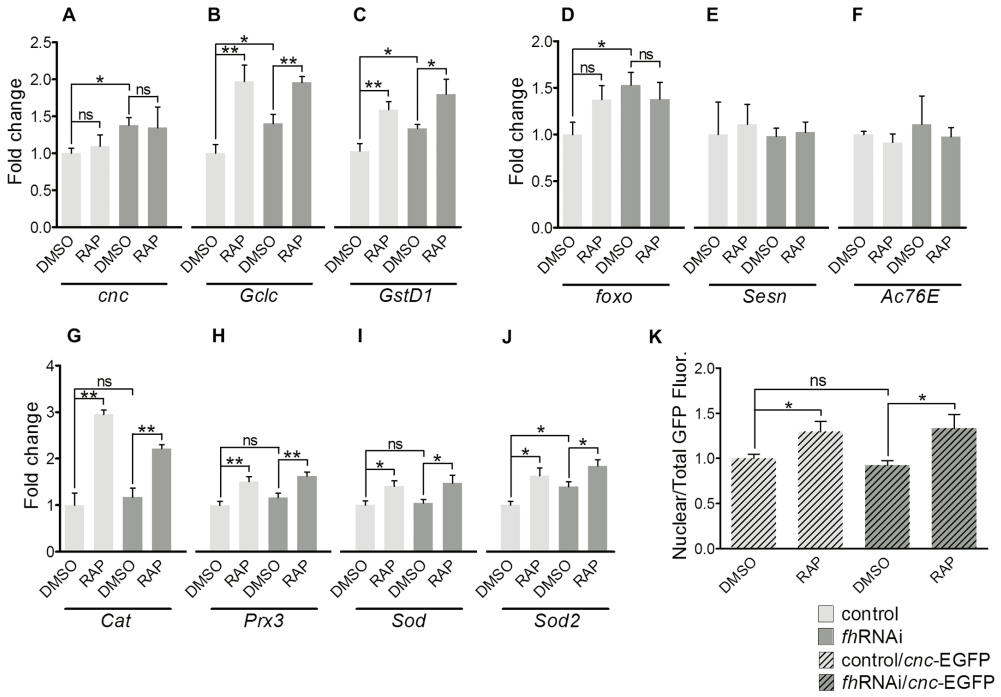

Fig 4. Rapamycin increases the expression of antioxidant genes under the control of Cnc. (A) *cnc* expression is not affected by rapamycin, but the transcription of two Cnc targets, *Gclc* (B) and *GstD1*(C), is higher in flies treated with the compound. (D-F) Rapamycin does not affect neither *foxo* expression nor the expression of the two FOXO targets *Sesn* and *Ac76E*. (G-J) Rapamycin increases the mRNA level of *Cat*, *Prx3*, *Sod* and *Sod2*, which are subjected to overlapping regulation from FOXO and Cnc transcription factors. (K) Rapamycin also increases the fraction of Cnc located in the nucleus. Control (y^1w^*; *actin-Gal4* flies), *fh*RNAi (*UAS-fh*RNAi; *actin-Gal4* flies), control/*cnc*-EGFP (control flies expressing a *cnc* allele tagged with the EGFP) and *fh*RNAi/*cnc*-EGFP: (*fh*RNAi flies expressing a *cnc* allele tagged with the EGFP). ns: non-significant, **P*<0.05, ***P*<0.01. Error bars represent SEM.

doi:10.1371/journal.pone.0132376.g004

Rapamycin increases the availability of ATP through 4E-BP

A pathological reduction of frataxin levels results in an impairment of ATP synthesis [45,46]. We measured the ATP levels in whole-fly extracts, and we did not find significant differences when comparing *fh*RNAi and control flies in the DMSO medium (Fig 5). Because different *Drosophila* tissues have distinct sensitivity to frataxin depletion [15], it is possible that the reduced ATP levels may be restricted to these tissues. Interestingly, rapamycin treatment increased the ATP levels (Fig 5) in both the control (41% increase) and frataxin knockdown flies (37% increase). This increase may contribute to the beneficial effect of rapamycin on the FRDA phenotype. To identify the pathway downstream of TORC1 involved in the ATP increase, we combined the rapamycin treatment with 3-MA, a constitutively active allele of S6K or a loss of function allele of 4E-BP, and we measured the ATP levels in the three cases. We observed that the 4E-BP mutation prevented rapamycin from increasing the ATP levels,

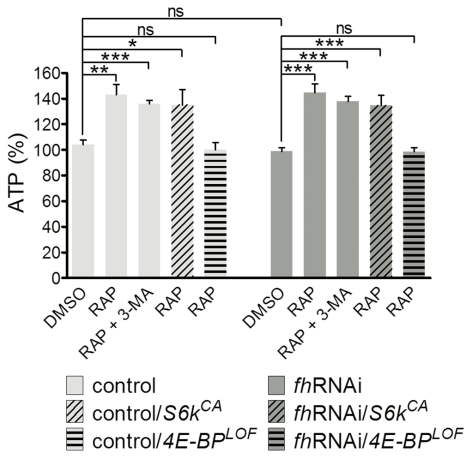

Fig 5. Rapamycin increases ATP levels both in control and *fh*RNAi flies. Rapamycin is able to increase ATP levels in control and *fh*RNAi flies even with the addition of the autophagy inhibitor 3-MA or in flies carrying a constitutively active allele of S6K ($S6k^{CA}$). In flies carrying a 4E-BP loss of function allele ($4E\text{-}BP^{LOF}$), rapamycin cannot increase ATP levels. Control (y^1w^*; *actin-Gal4* flies), *fh*RNAi (*UAS-fh*RNAi; *actin-Gal4* flies), control/$S6k^{CA}$ (control flies carrying the $S6k^{CA}$ allele), control/ $4E\text{-}BP^{LOF}$ (control flies carrying the $4E\text{-}BP^{LOF}$ allele), *fh*RNAi /$S6k^{CA}$ (model flies carrying the $S6k^{CA}$ allele), *fh*RNAi/$4E\text{-}BP^{LOF}$ (model flies carrying the $4E\text{-}BP^{LOF}$ allele). ns: non-significant, **P*<0.05, ***P*<0.01, ****P*<0.001. Error bars represent SEM.

doi:10.1371/journal.pone.0132376.g005

while the expression of the constitutively active S6K and the inhibition of autophagy had no effect on that increase. These results indicate that rapamycin ameliorates the ATP availability in flies through the 4E-BP and that inactivation of S6K or autophagy induction after TORC1 inhibition is not critical in this process [47,48]. Nevertheless, the modulation of the activity of both S6K and 4E-BP by TORC1 but not autophagy is indeed required for the rapamycin-mediated recovery of motor performance of *fh*RNAi flies (Fig 2A).

Discussion

TOR is an evolutionarily conserved protein that senses and integrates various environmental and intracellular signals to regulate growth and homeostasis in all eukaryotic cells. It functions by forming two structurally and functionally different multiprotein complexes, TORC1 and TOR Complex 2 (TORC2). TORC1 is better described and regulates many major cellular functions, including protein synthesis, lipid biogenesis and autophagy. TORC1 is sensitive to inhibition by rapamycin treatment [49].

In this study, we identified several components of the TORC1 pathway as modifiers of frataxin knockdown phenotypes in *Drosophila melanogaster*. We found that a genetic reduction in TORC1 signalling activity suppresses the impaired motor performance phenotype of the *fh*RNAi flies. Accordingly, genetic activation of TORC1 signalling produced a detrimental effect when combined with frataxin knockdown by inducing semi-lethality. Thus, we tested the therapeutic usefulness of a pharmacologic inhibition of TORC1 in the *fh*RNAi flies, using the

natural macrolide rapamycin [31]. We observed that rapamycin restored the motor performance of frataxin knockdown flies to normal levels, in agreement with the genetic reduction of *S6k* and *eIF-4E*. Rapamycin also increased the mean and maximum survival of the *fh*RNAi flies similarly as it did in controls. It is well known that TORC1 inhibition prolongs the lifespan of different species [40,50] and such effect is extended to *fh*RNAi flies.

The expression of dominant-negative forms of TOR and S6K and TOR inhibition by rapamycin provides flies with resistance to oxidative stress, whereas increased Rheb-TOR-S6K signalling sensitises flies to this type of stress and promotes early senescence of locomotor activity [50, 51]. Furthermore, it has also been reported in *Drosophila* that 4E-BP is important for survival under different types of stress, including oxidative insult [52]. In particular, high levels of oxidative stress markers have been found in FRDA patient samples as well as in several models of the disease [9,53–55]. In agreement with these results, we found an increased amount of MDA and HAE in the *fh*RNAi flies; these lipid peroxidation compounds are produced after the breakdown of unstable polyunsaturated fatty acid peroxides. The *fh*RNAi flies also showed increased levels of total GSH, a molecule with antioxidant function that reduces hydrogen and lipid peroxides when it is oxidised to its disulphide form, GSSG. Interestingly, rapamycin reduced significantly the MDA + HAE and total glutathione levels in the *fh*RNAi flies, restoring to some extent the normal situation observed in control flies. Recently, a similar result has been reported in the yeast frataxin knockout model in which rapamycin reduces ROS production [56].

The inhibition of TOR signalling by rapamycin has been shown to be protective against toxicity in several cell and animal models of neurodegenerative diseases. In some cases, this protective effect of rapamycin appears to be autophagy-dependent, particularly in neurodegenerative diseases associated with aggregation-prone mutant proteins [57]. However, our results indicated that in a normoxic condition, autophagy is not the main mechanism by which rapamycin protects *fh*RNAi flies against the ROS injury caused by frataxin deficiency. Our data show that neither the rescue of motor performance nor the protection against ROS induced by rapamycin were affected by the chemical inhibitor of autophagy 3-MA in normoxia.

TORC1 inhibition by rapamycin increases the transcript levels of genes involved in the free radical scavenging and Nrf2-mediated oxidative stress response in mouse adult stem cells [43] and in *C. elegans* [44]. We studied the possible effect of rapamycin on the activity of the transcription factors FOXO and Cnc (the *Drosophila* ortholog of the mammalian Nrf2), which control the expression of many genes involved in resistance against different types of stresses [44,58]. Our results showed that rapamycin increased the transcription of antioxidant genes dependent upon Cnc but not FOXO, and that this effect is mediated by an increase in the nuclear translocation of Cnc. Therefore, it may be the origin of the protective effect of rapamycin against oxidative stress caused by frataxin reduction in the *fh*RNAi flies. There are still many aspects of Nrf2 regulation that remain poorly understood. Nevertheless, several regulation mechanisms have been already described, both dependent and independent of the Keap1 protein (recently reviewed in [59]). Some of these mechanisms could explain the increase in Cnc activity mediated by rapamycin. Protein kinase C is able to disrupt the association between Nrf2 and Keap1, promoting the translocation of Nrf2 into the nucleus. GSK3β promotes Nrf2 ubiquitination and the degradation of the protein by the proteasome; thus, GSK3β inhibition can also contribute to Nrf2 activity. Both Protein kinase C activation and GSK3β inhibition can be triggered by an increase in PI3K-Akt signalling, and rapamycin is able to produce this effect by means of a negative feedback loop in TORC1 regulation [60,61] (S6 Fig). However, the actual mechanism by which rapamycin increases Cnc activity in FRDA model flies needs further research.

Interestingly, we found that autophagy becomes an important protective mechanism in *fh*RNAi flies subjected to a strong external oxidative insult. *fh*RNAi flies cultured in a hyperoxic environment show an enhanced reduction of motor performance and lifespan [15]. In this work, we observed that rapamycin improves the survival and aconitase activity of *fh*RNAi flies subjected to hyperoxia and that the beneficial effect of rapamycin decreases when 3-MA is added. Our results agree with other studies [39,50,62] in which autophagy is induced by rapamycin or by overexpressing/interfering *Atg* genes or components of the TORC1 signalling cascade to protect flies against strong external oxidative stress. Altogether, these data suggest that the autophagy induction by rapamycin operates as a cellular mechanism to protect against strong oxidative insults. However, in the oxidative conditions resulting from the endogenous ROS production in the *fh*RNAi flies, the protective effects of rapamycin are more likely to reside in its antioxidant properties rather than autophagy induction.

In conditions of frataxin depletion, several deficiencies in the mitochondrial electron transport chain result in impaired generation of ATP [45,46]. Reducing TORC1 activity may be beneficial for the energy status of frataxin-depleted cells because this signalling pathway activates specific regulatory mechanisms that can increase mitochondrial efficiency. Bonawitz et al. [47] reported that *tor*1 null yeast exhibit a higher rate of mitochondrial translation and steady-state abundance of several mitochondria-encoded OXPHOS components. In *Drosophila*, dietary restriction, whose effects are mediated to a great extent by TORC1, is capable of increasing the translation of genes involved in oxidative phosphorylation to ensure continued ATP generation, and this effect has been attributed to the TORC1 target 4E-BP [48]. In support of this idea, we found that inhibition of TORC1 by rapamycin increases the total ATP levels of both control and *fh*RNAi flies, which may contribute to the recovery of the motor performance and the slight increase in lifespan of the *fh*RNAi flies. We also found that 4E-BP is the key mediator in the increase of ATP levels after TORC1 inhibition by rapamycin. Finally, although much progress has been made in the understanding of TORC1 function, we cannot exclude the possibility that other unknown molecular mechanisms regulated by this critical signalling complex may be contributing to the recovery of the motor dysfunction of the rapamycin-treated *fh*RNAi flies.

Rapamycin is a well-described drug approved for human uses. This drug and its analogues (rapalogs) have important clinical applications in oncology and transplantation medicine. Ongoing clinical trials using rapalogs to treat different malignancies are providing an extensive body of data about the safety, tolerability and side effects of rapalogs [63]. In FRDA, lower doses of rapamycin may be beneficial combined with other drugs as antioxidants and iron chelators. It may enhance the advantages of either compound acting alone because none of the tested antioxidants or chelators has been proven to be sufficiently effective on the neurological symptoms of FRDA [64].

Our results show that the reduction of TORC1 signalling activity in the Drosophila model of FRDA rescues several phenotypes (impairment of motor abilities and reduced lifespan) that mimic the clinical features of this disease. These results point to the TORC1 pathway as a new potential therapeutic target for FRDA and as a guide to finding new promising molecules for disease treatment.

Supporting Information

S1 Fig. TORC1 inhibition by rapamycin increases development time to adulthood in control and *fh*RNAi flies. The time needed by individuals to eclose from the puparium was measured. The day the crosses were made was established as day zero. Parental flies were maintained in these vials for 2 days and then were removed. The results indicate the average

time, in days, needed by individuals of F_1 to complete the preadult development. Control (y^1w^*; *actin-Gal4* flies), *fh*RNAi (*UAS-fh*RNAi; *actin-Gal4* flies). ns: non-significant, $^{***}P<0.001$.
(TIF)

S2 Fig. Rapamycin does not interfere with the GAL4/UAS system. Fluorescence from thirty 7-day-old males expressing GFP in a ubiquitous pattern (*UAS-GFP*; *actin-Gal4*) was measured as previously described in [29].
(TIF)

S3 Fig. Rapamycin does not alter the level of *fh* mRNA neither in control nor in *fh*RNAi flies. Control (y^1w^*; *actin-Gal4* flies), *fh*RNAi(*UAS-fh*RNAi; *actin-Gal4* flies). ns: non-significant.
(TIF)

S4 Fig. Effect of rapamycin and 3-MA on the induction and inhibition, respectively, of autophagosome formation. ns: non-significant, $^{*}P<0.05$, $^{**}P<0.01$, $^{***}P<0.001$. control/GFP-LC3 (UAS-GFP-LC3/+; Nos-Gal4/+) and *fh*RNAi/GFP-LC3: (UAS-GFP-LC3/UAS-*fh*RNAi; Nos-Gal4/+)
(TIF)

S5 Fig. Rapamycin does not alter the fraction of FOXO-GFP located in the nucleus. control/*foxo*-GFP (control flies expressing a *foxo* allele tagged with the GFP) and *fh*RNAi/*foxo*-EGFP: (*fh*RNAi flies expressing a *foxo* allele tagged with the GFP).
(TIF)

S6 Fig. Hypothesis of Nrf2 activation by rapamycin. Rapamycin might increase Nrf2 activity by mechanisms depending on PKC and GSK3β, triggered by a TORC1 negative feedback loop which may increase PI3K-Akt signalling.
(TIF)

S1 Table. Genotypes of the *Drosophila* strains corresponding to the genetic interactors in the TORC1 pathway.
(TIF)

Acknowledgments

Authors thank the Servicio Central de Soporte a la Investigación Experimental de la Universitat de València for access to the DNA analysis resources and databases.

Author Contributions

Conceived and designed the experiments: PC-Q SS JVL IA-R JB MDM MJM-S. Performed the experiments: PC-Q SS JVL. Analyzed the data: PC-Q SS JVL IA-R JB MDM MJM-S. Contributed reagents/materials/analysis tools: IA-R JB MDM MJM-S. Wrote the paper: PC-Q SS MDM MJM-S. Revised the manuscript critically: JVL IA-R JB.

References

1. Palau F, Espinós C. Autosomal recessive cerebellar ataxias. Orphanet J Rare Dis. 2006; 1: 47–65. PMID: 17112370
2. Delatycki MB, Corben LA. Clinical features of Friedreich ataxia. J Child Neurol. 2012; 27: 1133–1137. doi: 10.1177/0883073812448230 PMID: 22752493

3. Campuzano V, Montermini L, Moltò MD, Pianese L, Cossée M, Cavalcanti F, et al. Friedreich's ataxia: autosomal recessive disease caused by an intronic GAA triplet repeat expansion. Science. 1996; 271: 1423–1427. PMID: 8596916
4. Monrós E, Moltó MD, Martínez F, Cañizares J, Blanca J, Vílchez JJ, et al. Phenotype correlation and intergenerational dynamics of the Friedreich ataxia GAA trinucleotide repeat. Am J Hum Genet. 1997; 61: 101–110. PMID: 9245990
5. Gibson TJ, Koonin EV, Musco G, Pastore A, Bork P. Friedreich's ataxia protein: phylogenetic evidence for mitochondrial dysfunction. Trends Neurosci. 1996; 19: 465–468. PMID: 8931268
6. Schmucker S, Puccio H. Understanding the molecular mechanisms of Friedreich's ataxia to develop therapeutic approaches. Hum Mol Genet. 2010; 19: R103–110. doi: 10.1093/hmg/ddq165 PMID: 20413654
7. Emond M, Lepage G, Vanasse M, Pandolfo M. Increased levels of plasma malondialdehyde in Friedreich ataxia. Neurology. 2000; 55: 1752–1753. PMID: 11113241
8. Navarro JA, Ohmann E, Sanchez D, Botella JA, Liebisch G, Moltó MD, et al. Altered lipid metabolism in a Drosophila model of Friedreich's ataxia. Hum Mol Genet. 2010; 19: 2828–2840. doi: 10.1093/hmg/ddq183 PMID: 20460268
9. Napoli E, Taroni F, Cortopassi GA. Frataxin, iron-sulfur clusters, heme, ROS, and aging. Antioxid Redox Signal. 2006; 8: 506–516. PMID: 16677095
10. Ristow M, Mulder H, Pomplun D, Schulz TJ, Muller-Schmehl K, Krause A, et al. Frataxin deficiency in pancreatic islets causes diabetes due to loss of beta cell mass. J Clin Invest. 2003; 112: 527–534. PMID: 12925693
11. Anderson PR, Kirby K, Orr WC, Hilliker AJ, Phillips JP. Hydrogen peroxide scavenging rescues frataxin deficiency in a Drosophila model of Friedreich's ataxia. Proc Natl Acad Sci. U.S.A. 2008; 105: 611–616. doi: 10.1073/pnas.0709691105 PMID: 18184803
12. Irazusta V, Cabiscol E, Reverter-Branchat G, Ros J, Tamarit J. Manganese is the link between frataxin and iron-sulfur deficiency in the yeast model of Friedreich ataxia. J Biol Chem. 2006; 281: 12227–12232. PMID: 16510442
13. Wong A, Yang J, Cavadini P, Gellera C, Lonnerdal B, Taroni F, et al. The Friedreich's ataxia mutation confers cellular sensitivity to oxidant stress which is rescued by chelators of iron and calcium and inhibitors of apoptosis. Hum Mol Genet 1999; 8: 425–30. PMID: 9949201
14. Al-Mahdawi S, Pinto RM, Varshney D, Lawrence L, Lowrie MB, Hughes S, et al. GAA repeat expansion mutation mouse models of Friedreich ataxia exhibit oxidative stress leading to progressive neuronal and cardiac pathology. Genomics 2006; 88: 580–590. PMID: 16919418
15. Llorens JV, Navarro JA, Martínez-Sebastián MJ, Baylies MK, Schneuwly S, Botella JA, et al. Causative role of oxidative stress in a Drosophila model of Friedreich ataxia. FASEB J. 2007; 21: 333–344. PMID: 17167074
16. Vázquez-Manrique RP, González-Cabo P, Ros S, Aziz H, Baylis HA, Palau F. Reduction of Caenorhabditis elegans frataxin increases sensitivity to oxidative stress, reduces lifespan, and causes lethality in a mitochondrial complex II mutant. FASEB J. 2006; 20: 172–174. PMID: 16293572
17. Lefevre S, Sliwa D, Auchre F, Brossas C, Ruckenstuhl C, Boggetto N, et al. The yeast metacaspase is implicated in oxidative stress response in frataxin-deficient cells. FEBS Lett. 2012; 586: 143–148. doi: 10.1016/j.febslet.2011.12.002 PMID: 22155640
18. Paupe V, Dassa EP, Goncalves S, Auchère F, Lönn M, Holmgren A, et al. Impaired nuclear Nrf2 translocation undermines the oxidative stress response in Friedreich ataxia. PLoS One. 2009; 4: e4253. doi: 10.1371/journal.pone.0004253 PMID: 19158945
19. Shan Y, Schoenfeld RA, Hayashi G, Napoli E, Akiyama T, Iodi Carstens M, et al. Frataxin deficiency leads to defects in expression of antioxidants and Nrf2 expression in dorsal root ganglia of the Friedreich's ataxia YG8R mouse model. Antioxid Redox Signal. 2013; 19: 1481–1493. doi: 10.1089/ars.2012.4537 PMID: 23350650
20. Gimenez-Cassina A, Wade-Martins R, Gomez-Sebastian S, Corona JC, Lim F, Diaz-Nido J. Infectious delivery and long-term persistence of transgene expression in the brain by a 135-kb iBAC-FXN genomic DNA expression vector. Gene Ther. 2011; 18: 1015–1019. doi: 10.1038/gt.2011.45 PMID: 21490681
21. Perdomini M, Belbellaa B, Monassier L, Reutenauer L, Messaddeq N, Cartier N, et al. Prevention and reversal of severe mitochondrial cardiomyopathy by gene therapy in a mouse model of Friedreich's ataxia. Nat Med. 2014; 20: 542–547. doi: 10.1038/nm.3510 PMID: 24705334
22. Soragni E, Xu C, Plasterer HL, Jacques V, Rusche JR, Gottesfeld JM. Rationale for the development of 2-aminobenzamide histone deacetylase inhibitors as therapeutics for Friedreich ataxia. J Child Neurol. 2012; 27: 1164–1173. doi: 10.1177/0883073812448533 PMID: 22764181

23. Cañizares J, Blanca JM, Navarro JA, Monrós E, Palau F, Moltó MD. dfh is a Drosophila homolog of the Friedreich's ataxia disease gene. Gene. 2000; 256: 35–42. PMID: 11054533

24. Kondapalli KC, Kok NM, Dancis A, Stemmler TL. Drosophila frataxin: an iron chaperone during cellular Fe-S cluster bioassembly. Biochemistry. 2008; 47: 6917–6927. doi: 10.1021/bi800366d PMID: 18540637

25. Navarro JA, Llorens JV, Soriano S, Botella JA, Schneuwly S, Martínez-Sebastián MJ, et al. Overexpression of human and fly frataxins in Drosophila provokes deleterious effects at biochemical, physiological and developmental levels. PLoS One. 2011; 6: e21017. doi: 10.1371/journal.pone.0021017 PMID: 21779322

26. Anderson PR, Kirby K, Hilliker AJ, Phillips JP. RNAi-mediated suppression of the mitochondrial iron chaperone, frataxin, in Drosophila. Hum Mol Genet. 2005; 14: 3397–3405. PMID: 16203742

27. Runko AP, Griswold AJ, Min KT. Overexpression of frataxin in the mitochondria increases resistance to oxidative stress and extends lifespan in Drosophila. FEBS Lett. 2008; 582: 715–719. doi: 10.1016/j.febslet.2008.01.046 PMID: 18258192

28. Shidara Y, Hollenbeck PJ. Defects in mitochondrial axonal transport and membrane potential without increased reactive oxygen species production in a Drosophila model of Friedreich ataxia. J Neurosci. 2010; 30: 11369–11378. doi: 10.1523/JNEUROSCI.0529-10.2010 PMID: 20739558

29. Soriano S, Llorens JV, Blanco-Sobero L, Gutiérrez L, Calap-Quintana P, Morales MP, et al. Deferiprone and idebenone rescue frataxin depletion phenotypes in a Drosophila model of Friedreich's ataxia. Gene. 2013; 521: 274–281. doi: 10.1016/j.gene.2013.02.049 PMID: 23542074

30. Tricoire H, Palandri A, Bourdais A, Camadro JM, Monnier V. Methylene blue rescues heart defects in a Drosophila model of Friedreich's ataxia. Hum Mol Genet. 2014; 23: 968–979. doi: 10.1093/hmg/ddt493 PMID: 24105471

31. Loewith R, Hall MN. Target of rapamycin (TOR) in nutrient signaling and growth control. Genetics. 2011; 189: 1177–1201. doi: 10.1534/genetics.111.133363 PMID: 22174183

32. Park J, Al-Ramahi I, Tan Q, Mollema N, Diaz-Garcia JR, Gallego-Flores T, et al. RAS-MAPK-MSK1 pathway modulates ataxin 1 protein levels and toxicity in SCA1. Nature. 2013; 498: 325–331. doi: 10.1038/nature12204 PMID: 23719381

33. Rusten TE, Lindmo K, Juhász G, Sass M, Seglen PO, Brech A, et al. Programmed autophagy in the Drosophila fat body is induced by ecdysone through regulation of the PI3K pathway. Dev Cell. 2004; 7: 179–192. PMID: 15296715

34. Kawasaki H, Hirose S, Ueda H. A Simple and Quick Method to Isolate Nuclear Extracts from Pupae of Drosophila melanogaster. Cytotechnology. 2005; 49: 67–70. doi: 10.1007/s10616-005-5414-3 PMID: 19003064

35. Barcelo H, Stewart MJ. Altering Drosophila S6 kinase activity is consistent with a role for S6 kinase in growth. Genesis. 2002; 34: 83–85. PMID: 12324955

36. Healy DG, Falchi M, O'Sullivan SS, Bonifati V, Durr A, Bressman S, et al. Phenotype, genotype, and worldwide genetic penetrance of LRRK2-associated Parkinson's disease: a case-control study. Lancet Neurol. 2008; 7: 583–590. doi: 10.1016/S1474-4422(08)70117-0 PMID: 18539534

37. Imai Y, Gehrke S, Wang HQ, Takahashi R, Hasegawa K, Oota E, et al. Phosphorylation of 4E-BP by LRRK2 affects the maintenance of dopaminergic neurons in Drosophila. EMBO J. 2008; 27: 2432–2443. doi: 10.1038/emboj.2008.163 PMID: 18701920

38. Katewa SD, Kapahi P. Role of TOR signaling in aging and related biological processes in Drosophila melanogaster. Exp Gerontol. 2011; 46: 382–390. doi: 10.1016/j.exger.2010.11.036 PMID: 21130151

39. Ravikumar B, Berger Z, Vacher C, O'Kane CJ, Rubinsztein DC. Rapamycin pre-treatment protects against apoptosis. Hum Mol Genet. 2006; 15: 1209–1216. PMID: 16497721

40. Kapahi P, Chen D, Rogers AN, Katewa SD, Li PW, Thomas EL, et al. With TOR, less is more: a key role for the conserved nutrient-sensing TOR pathway in aging. Cell Metab. 2010; 11: 453–465. doi: 10.1016/j.cmet.2010.05.001 PMID: 20519118

41. Layalle S, Arquier N, Léopold P. The TOR pathway couples nutrition and developmental timing in Drosophila. Dev Cell. 2008; 15: 568–577. doi: 10.1016/j.devcel.2008.08.003 PMID: 18854141

42. Petiot A, Ogier-Denis E, Blommaart EF, Meijer AJ, Codogno P. Distinct classes of phosphatidylinositol 3'-kinases are involved in signaling pathways that control macroautophagy in HT-29 cells. J Biol Chem. 2000; 275: 992–998. PMID: 10625637

43. Kofman AE, McGraw MR, Payne CJ. Rapamycin increases oxidative stress response gene expression in adult stem cells. Aging. 2012; 4: 279–289. PMID: 22529334

44. Robida-Stubbs S, Glover-Cutter K, Lamming DW, Mizunuma M, Narasimhan SD, Neumann-Haefelin E, et al. TOR Signaling and Rapamycin Influence Longevity by Regulating SKN-1/Nrf and DAF-16/FoxO. Cell Metab. 2012; 15: 713–724. doi: 10.1016/j.cmet.2012.04.007 PMID: 22560223

45. Lodi R, Hart PE, Rajagopalan B, Taylor DJ, Crilley JG, Bradley JL, et al. Antioxidant treatment improves in vivo cardiac and skeletal muscle bioenergetics in patients with Friedreich's ataxia. Ann Neurol. 2001; 49: 590–596. PMID: 11357949

46. Lynch DR, Lech G, Farmer JM, Balcer LJ, Bank W, Chance B, et al. Near infrared muscle spectroscopy in patients with Friedreich's ataxia. Muscle Nerve. 2002; 25: 664–673. PMID: 11994959

47. Bonawitz ND, Chatenay-Lapointe M, Pan Y, Shadel GS. Reduced TOR Signaling Extends chronological Life Span via Increased Respiration and Upregulation of Mitochondrial Gene Expression. Cell Metab. 2007; 5: 265–277. PMID: 17403371

48. Zid BM, Rogers AN, Katewa SD, Vargas MA, Kolipinski MC, Lu TA, et al. 4E-BP extends lifespan upon dietary restriction by enhancing mitochondrial activity in Drosophila. Cell. 2009; 139: 149–60. doi: 10.1016/j.cell.2009.07.034 PMID: 19804760

49. Wullschleger S, Loewith R, Hall MN. TOR signaling in growth and metabolism. Cell. 2006; 124: 471–484. PMID: 16469695

50. Bjedov I, Toivonen JM, Kerr F, Slack C, Jacobson J, Foley A, et al. Mechanisms of life span extension by rapamycin in the fruit fly Drosophila melanogaster. Cell Metab. 2010; 11: 35–46. doi: 10.1016/j.cmet.2009.11.010 PMID: 20074526

51. Patel PH, Tamanoi F. Increased Rheb-TOR signaling enhances sensitivity of the whole organism to oxidative stress. J Cell Sci. 2006; 119: 4285–4292. PMID: 17038544

52. Tettweiler G, Miron M, Jenkins M, Sonenberg N, Lasko PF. Starvation and oxidative stress resistance in Drosophila are mediated through the eIF4E-binding protein, d4E-BP. Genes Dev. 2005; 19: 1840–1843. PMID: 16055649

53. Auchère F, Santos R, Planamente S, Lesuisse E, Camadro JM. Glutathione dependent redox status of frataxin-deficient cells in a yeast model of Friedreich's ataxia. Hum Mol Genet. 2008; 17: 2790–2802. doi: 10.1093/hmg/ddn178 PMID: 18562474

54. Pastore A, Tozzi G, Gaeta LM, Bertini E, Serafini V, Di Cesare S, et al. Actin glutathionylation increases in fibroblasts of patients with Friedreich's ataxia: a potential role in the pathogenesis of the disease. J Biol Chem. 2003; 278: 42588–42595. PMID: 12915401

55. Tozzi G, Nuccetelli M, Lo Bello M, Bernardini S, Bellincampi L, Ballerini S, et al. Antioxidant enzymes in blood of patients with Friedreich's ataxia. Arch Dis Child. 2002; 86: 376–379. PMID: 11970939

56. Marobbio CM, Pisano I, Porcelli V, Lasorsa FM, Palmieri L. Rapamycin reduces oxidative stress in frataxin-deficient yeast cells. Mitochondrion. 2012; 12: 156–161. doi: 10.1016/j.mito.2011.07.001 PMID: 21782979

57. Sarkar S. Regulation of autophagy by mTOR-dependent and mTOR-independent pathways: autophagy dysfunction in neurodegenerative diseases and therapeutic application of autophagy enhancers. Biochem Soc Trans. 2013; 41: 1103–1130. doi: 10.1042/BST20130134 PMID: 24059496

58. Turpaev KT. Keap1-Nrf2 signaling pathway: mechanisms of regulation and role in protection of cells against toxicity caused by xenobiotics and electrophiles. Biochemistry (Mosc). 2013; 78: 111–126.

59. Bryan HK, Olayanju A, Goldring CE, Park BK. The Nrf2 cell defence pathway: Keap1-dependent and-independent mechanisms of regulation. Biochem Pharmacol. 2013; 85: 705–717. doi: 10.1016/j.bcp.2012.11.016 PMID: 23219527

60. Carracedo A, Pandolfi PP. The PTEN-PI3K pathway: of feedbacks and cross-talks. Oncogene. 2008; 27: 5527–5541. doi: 10.1038/onc.2008.247 PMID: 18794886

61. O'Reilly KE, Rojo F, She QB, Solit D, Mills GB, Smith D, et al. mTOR inhibition induces upstream receptor tyrosine kinase signaling and activates Akt. Cancer Res. 2006; 66: 1500–1508. PMID: 16452206

62. Simonsen A, Cumming RC, Brech A, Isakson P, Schubert DR, Finley KD. Promoting basal levels of autophagy in the nervous system enhances longevity and oxidant resistance in adult Drosophila. Autophagy. 2008; 4: 176–184. PMID: 18059160

63. Kaplan B, Qazi Y, Wellen JR. Strategies for the management of adverse events associated with mTOR inhibitors. Transplant Rev. 2014; 28: 126–133.

64. Kearney M, Orrell RW, Fahey M, Pandolfo M. Antioxidants and other pharmacological treatments for Friedreich ataxia. Cochrane Database Syst Rev. 2012; 4: CD007791. doi: 10.1002/14651858.CD007791.pub3 PMID: 22513953

Supporting information

S1 Table. Genotypes of the *Drosophila* strains corresponding to the genetic interactors in the TORC1 pathway.

Strain	Genotype	Effect	Reference
Tsc1^{shRNAi}	w^{1118}; P{GD11836}v22252/TM3	Knockdown	
S6K^{DN}	w^{1118}; P{UAS-S6k.KQ}2	Dominant negative	Barceló and Stewart, 2002
S6K^{CA}	w^{1118}; P{UAS-S6k.STDETE}2	Constitutively active	Barceló and Stewart, 2002
eIF-4E^{LOF}	y^1 w^*; P{lacW}eIF-4E^{5058911}/TM3, Sb^1	Loss of function	
Lrrk^{shRNA}	P{KK100916}VIE-260B	Knockdown	

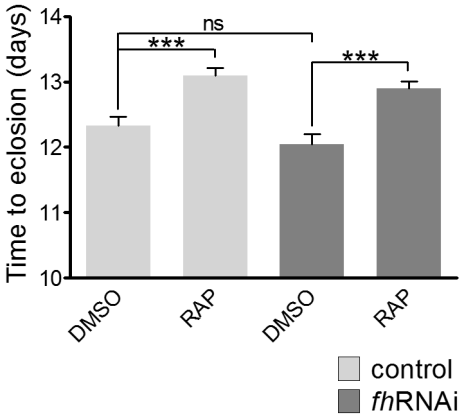

S1 Fig. TORC1 inhibition by rapamycin increases development time to adulthood in control and fhRNAi flies. The time needed by individuals to eclose from the puparium was measured. The day the crosses were made was established as day zero. Parental flies were maintained in these vials for 2 days and then were removed. The results indicate the average time, in days, needed by individuals of F1 to complete the preadult development. Control (y^1w^*; actin-Gal4 flies), *fh*RNAi (UAS-*fh*RNAi; *actin*-Gal4 flies). ns: non-significant, ***P<0.001.

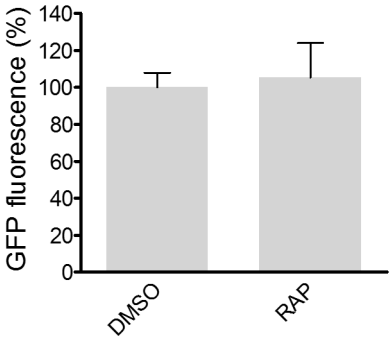

S2 Fig. Rapamycin does not interfere with the GAL4/UAS system. Fluorescence from thirty 7-day-old males expressing GFP in a ubiquitous pattern (*UAS*-GFP; *actin*-Gal4) was measured as previously described in [29].

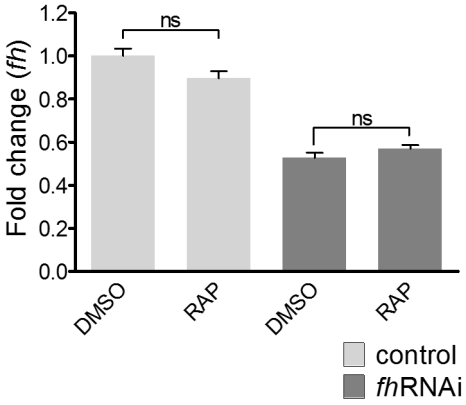

S3 Fig. Rapamycin does not alter the level of *fh* mRNA neither in control nor in *fh*RNAi flies. Control (y^1w^*; *actin-Gal4* flies), *fh*RNAi(*UAS-fh*RNAi; *actin-Gal4* flies). ns: non-significant.

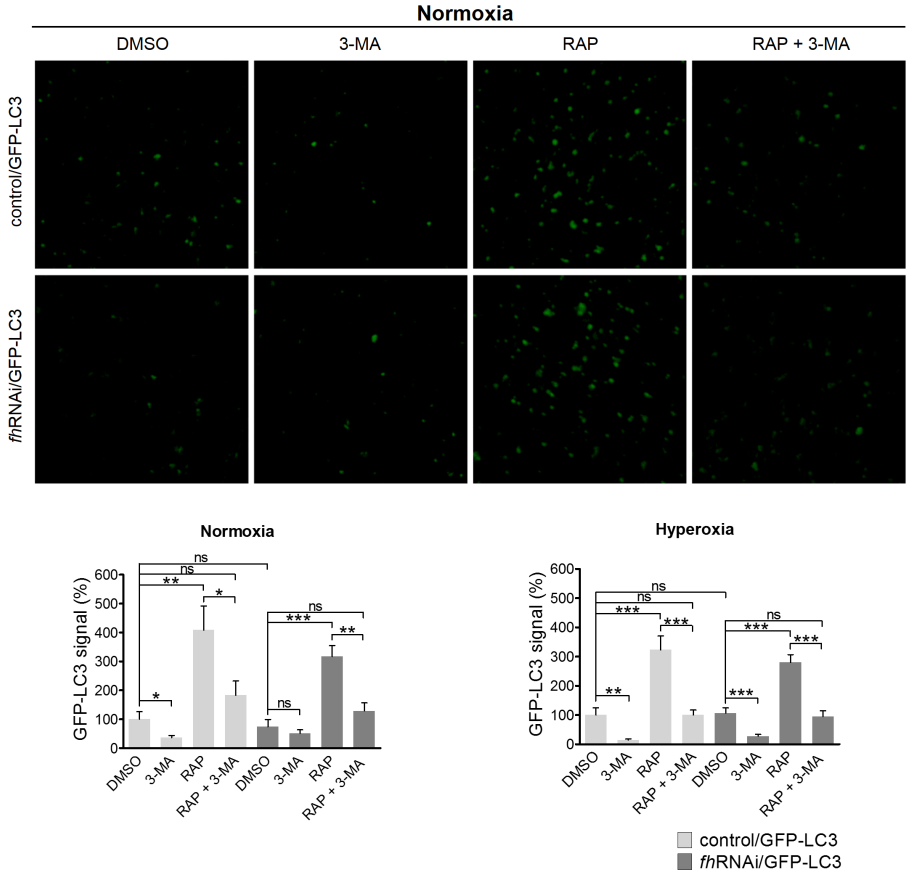

S4 Fig. Effect of rapamycin and 3-MA on the induction and inhibition, respectively, of autophagosome formation. ns: non-significant, **P*<0.05, ***P*<0.01, ****P*<0.001. control/GFP-LC3 (UAS-GFP-LC3/+; Nos-Gal4/+) and *fh*RNAi/GFP-LC3: (UAS-GFP-LC3/UAS-*fh*RNAi; Nos-Gal4/+).

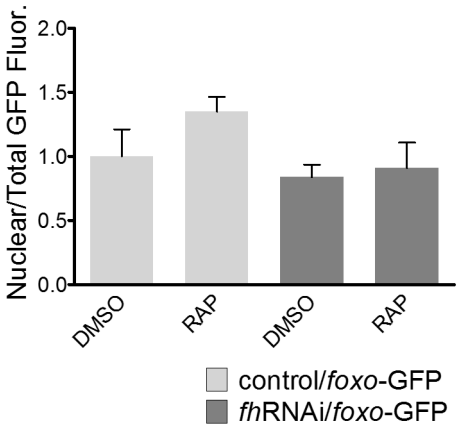

S5 Fig. Rapamycin does not alter the fraction of FOXO-GFP located in the nucleus. Control/*foxo*-GFP (control flies expressing a *foxo* allele tagged with the GFP) and *fh*RNAi/*foxo*-EGFP: (*fh*RNAi flies expressing a *foxo* allele tagged with the GFP).

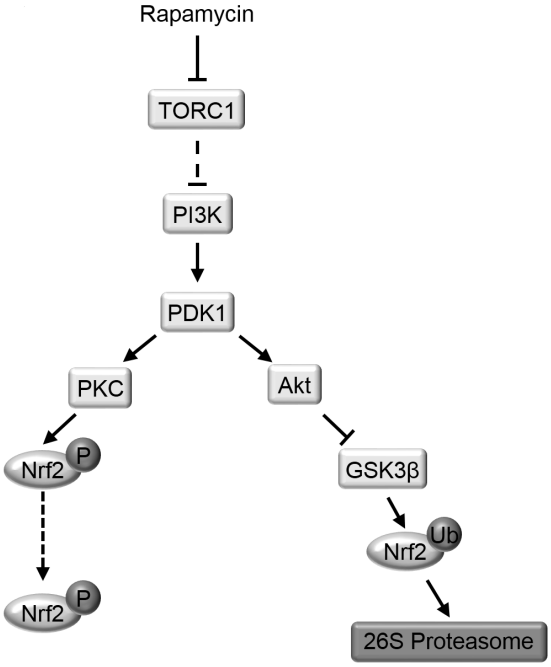

S6 Fig. Hypothesis of Nrf2 activation by rapamycin. Rapamycin might increase Nrf2 activity by mechanisms depending on PKC and GSK3β, triggered by a TORC1 negative feedback loop which may increase PI3K-Akt signalling.

Article 4. Metal homeostasis regulators suppress FRDA phenotypes in a *Drosophila* model of the disease (Soriano *et al*., sent for publication)

Metal homeostasis regulators suppress FRDA phenotypes in a *Drosophila* model of the disease.

Sirena Soriano[1,2], Pablo Calap-Quintana[1], José Vicente Llorens[1,#], Ismael Al-Ramahi[2], Lucía Gutiérrez[3], María José Martínez-Sebastián[1], Juan Botas[2], and María Dolores Moltó[1,4,§]

[1] Department of Genetics, University of Valencia, Burjassot, Valencia, Spain

[2] Department of Molecular and Human Genetics, Baylor College of Medicine, Houston, Texas, USA

[3] Department of Biomaterials and Bioinspired Materials, Instituto de Ciencia de Materiales de Madrid/CSIC, Madrid, Spain

[4] CIBERSAM, INCLIVA, Valencia, Spain

[#] Current Address: Evolutionary Biology Center, Uppsala University, Uppsala, Sweden

[§] dmolto@uv.es

Abstract

Friedreich's ataxia (FRDA), the most commonly inherited ataxia among Caucasians, is a neurodegenerative disorder caused by a decrease in frataxin levels. One of the hallmarks of the disease is the accumulation of iron in several tissues including the brain, and frataxin has been proposed to play a key role in iron homeostasis. We found that the levels of zinc, copper, manganese and aluminum were also increased in a *Drosophila* model of FRDA, and that copper and zinc chelation improve their impaired motor performance. By means of a candidate genetic screen, we identified that genes implicated in iron, zinc and copper transport and metal detoxification can restore frataxin deficiency-induced phenotypes. Taken together, these results demonstrate that the metal dysregulation in FRDA includes other metals besides iron, therefore providing a new set of potential therapeutic targets.

Keywords

Friedreich's ataxia, *Drosophila*, metal imbalance, iron, copper, zinc, oxidative stress

1. Introduction

Friedreich's ataxia (FRDA) is a neurodegenerative disorder caused by an intronic GAA expansion within *FXN,* the gene encoding frataxin [1]. Unstable GAA expansions in both alleles of this gene [2] inhibit transcription, therefore causing a reduction in frataxin protein levels [3,4]. FRDA is the most commonly inherited ataxia among Caucasians [5] and is characterized by progressive gait and limb ataxia, tendon areflexia, muscle weakness and peripheral sensory neuropathy occurring at early adulthood. Non-neurological manifestations include hypertrophic cardiomyopathy leading to morbidity, diabetes mellitus or carbohydrate intolerance [6]. Affected individuals are wheelchair-bound during later stages of disease, and early death may occur at the fourth to fifth decade of life.

Frataxin deficiency results in several biochemical disturbances including impaired iron-sulphur cluster biogenesis, dysfunction of respiratory chain complexes and aconitase, accumulation of mitochondrial iron coupled to cytosolic iron depletion and increased oxidative stress sensitivity (reviewed in [7]). Although frataxin function is not fully elucidated, it is accepted that frataxin is critical for iron homeostasis [8] and marked accumulation of iron has been reported in several tissues of FRDA patients. Iron appears to accumulate in myocardium [9–11], and in liver and spleen as well as in the dentate nucleus of the cerebellum [9,12]. Iron chelation was therefore promptly proposed as therapeutic approach for the disease and data from pre-clinical studies [13,14] were promising. However, early-phase clinical trials with the iron chelator deferiprone have not lead to conclusive results and indicate a possible improvement only in some aspects of FRDA pathogenesis [15,16].

In addition to iron, redistribution of copper and zinc was also described in the dentate nucleus of FRDA patients [17], as well as changes in the cellular localization of the zinc transporter Zip14 in the dorsal root ganglia [18]. These findings presented a novel perspective of FRDA pathophysiology by suggesting that metal dysregulation extends

beyond iron accumulation. Interestingly, there is extensive evidence of metal content imbalance in other neurodegenerative disorders such as Alzheimer's (AD), Parkinson's and Huntington's diseases as well as amyotrophic lateral sclerosis. Copper, zinc, aluminum and manganese appear to play an important role in these pathologies, and are known to induce oxidative stress, protein misfolding and aggregation or neuroinflamation, leading eventually to neurodegeneration (reviewed in [19]).

Based on the potential role of metal imbalance in FRDA pathogenesis, we set out to test whether genetic modification of key pathways regulating metal content and distribution would improve FRDA phenotypes by restoring metal homeostasis. To test a broad range of components within these pathways in a high-throughput manner, we utilized *Drosophila* as a model of FRDA [20–22] in a genetic screen of potential modifiers. By focusing on a candidate pathway screening approach, we report several novel genetic modifiers of eye morphology and motor dysfunction in the FRDA fly model. These data provide further support for the notion that disruptions in metal homeostasis may be a primary contributor to FRDA disease pathogenesis.

2. Materials and Methods

2.1. *Drosophila melanogaster* strains

Two lines that knockdown *fh*, the homolog of *FXN* in *Drosophila*, were used in this study: (1) UDIR2 [21], from Dr. Phillips from University of Guelph, Canada, and (2) UAS-*fh*IR [22] previously generated in our laboratory. Both lines have been renamed in the text and figures as *fh*RNAi-1 and *fh*RNAi-2 respectively, as in [23]. When expressed ubiquitously, *fh*RNAi-1 induced a strong interference with a 90% reduction of frataxin expression that resulted in adult lethality, whereas *fh*RNAi-2 produced a 70% reduction compatible with a normal development. w^{1118} strain was used as control in all the experiments. The driver lines *GMR*-GAL4 and *actin*-GAL4, which promote expression in the eye and in a ubiquitous pattern respectively were obtained from the Bloomington Stock Center (BSC, Indiana University, http://flystocks.bio.indiana.edu). For the genetic screen, we used shRNA lines from the Vienna Drosophila Resource Center (VDRC, http://stocks.vdrc.at) and loss-of-function and overexpression lines from BSC, except for tub-MTF-1 [24] that was kindly provided by Dr. Burke from University of Monash, Australia.

2.2. Culture conditions, metal chelation and climbing assay

Drosophila stocks were maintained at 25ºC on standard cornmeal agar medium. The standard medium was supplemented with the copper chelators Tetrathiomolybdate (TTM) at 10 μM dissolved in 0.1% dimethylsulfoxide (DMSO) and Bathocuproine disulphonate (BCS) at 300 μM in H_2O, and with the zinc chelator N,N,N',N'-tetrakis (2-pyridinylmethyl)-1,2-ethanediamine (TPEN) at 10 μM in EtOH/PBS. All chemicals were purchased from Sigma-Aldrich. Crosses were conducted at 25ºC in the supplemented medium or the vehicle medium containing the dissolving agent but not the chelator. The F_1 adults of appropriate genotype were transferred to fresh vials with the supplemented or vehicle medium every two days. We evaluated the effect of the metal chelators on the climbing ability as described in [25]. The results are expressed as a percentage, taking as 100% the mean climbing speed of control flies in the vehicle medium.

2.3. Genetic screen

External eye structure and motor performance phenotypes were used for the identification of genetic modifiers of frataxin depletion. For the eye screen, UAS-*fh*RNAi-1; *GMR*-GAL4 flies were crossed at 27ºC with the candidate lines, and the external eye structure of the F1 flies with appropriate genotype was observed with a Nikon light microscope. For the motor performance assays, we used the UAS-*fh*RNAi-2; *actin*-GAL4 line and both the crosses and the experimental individuals were maintained at 28ºC. These assays were performed as previously described in [26]. We recorded the number of flies that climbed to a height of 11.5 cm and the mean percentage of 10 observations was plotted for each day. Two replicates of 15 individuals were tested in parallel for each genotype. Data was analyzed by one-way ANOVA followed by Dunnett's post hoc.

2.4. Measurement of metals and MDA + HAE levels

Inductively Coupled Plasma – Atomic Emission Spectroscopy (ICP-AES) was used to measure the levels of iron, zinc, copper, manganese and aluminum calibrated against standard solutions in an OPTIME 2100DV from Perkin Elmer. Previously, whole flies were lyophilized, weighed and digested with nitric acid (1 h at 90 ºC) and hydrogen peroxide (1h at 90 ºC). These assays were conducted in triplicate with 600 adult males

per replicate. The concentration of malondialdehyde (MDA) + 4-hydroxyalkenals (HAE) was determined as described in [25].

2.5. Statistical analysis

All statistical analyses were carried out with the GraphPad Prism 6 software. For comparison of means, we performed unpaired nonparametric Student's t test or one-way ANOVA. In all cases, values of $P<0.05$ were considered statistically significant.

3. Results and Discussion

3.1. Frataxin deficiency in *Drosophila* leads to metal accumulation

Given that copper and zinc dysregulation has been suggested in FRDA [17,18], we hypothesized that ubiquitous reduction of frataxin driven by the *fh*RNAi-2 allele might cause a global alteration in metal content. Interestingly, atomic emission spectroscopic analysis revealed indeed that the levels of zinc, copper, manganese and aluminum were increased in the FRDA flies relative to control animals (Fig. 1A).

To investigate whether the increase in metal levels is implicated in the pathophysiology of FRDA, we asked whether metal chelation improves the climbing phenotype of the frataxin deficient flies reported by [22]. Previously, we showed that the iron chelator deferiprone rescued several phenotypes of the FRDA fly model, including the motor impairment [14]. In this case, the zinc chelator TPEN was effective in inducing a significant recovery of the climbing ability of the FRDA animals (Fig. 1B). The copper chelators TTM and BCS also ameliorated the climbing ability up to control levels (Fig. 1B). Taken together, these data indicate that the FRDA fly model recapitulates an imbalance in metal content, reminiscent of the human condition, and suggest that zinc and specially copper chelators might be of potential therapeutic interest for the treatment of the disease.

3.2. Modifying key regulators of iron homeostasis suppresses FRDA fly phenotypes

To determine whether targeted alterations of pathways involved in metal homeostasis are sufficient to improve FRDA fly phenotypes, we systematically evaluated the effect of decreasing or increasing the expression of metal-associated genes using two different and independent assays in the FRDA *Drosophila* model. We reasoned that utilizing a tiered strategy of first evaluating modifiers of eye morphology followed by evaluating modifiers of motor performance would provide high confidence genetic modifiers of these disease phenotypes. For our primary screen of external eye morphology, we evaluated modifiers of a mild rough eye phenotype induced by specific expression of the *fh*RNAi-1 allele in the developing eye. We then used a milder frataxin knockdown system (*actin*-GAL4>*fh*RNAi-2, enables systemic frataxin reduction compatible with adult survival) to determine whether these modifiers were also able to improve the impairment in motor performance reported in FRDA flies [22].

Given the central role of iron in FRDA pathogenesis, we first investigated whether genes implicated in iron homeostasis modify FRDA fly model phenotypes. Among the tested genes implicated in iron homeostasis, we found a total of 5 suppressors of both the eye and the motor performance phenotypes (Fig. 2A and B). Genotypes of the *Drosophila* strains corresponding to these genetic interactors are shown in Supplementary Table 1.

Of the five suppressor genes, three genes function as iron transporters. Knockdown of Malvolio (*Mvl*), the *Drosophila* homolog of the mammalian *Divalent metal transporter-1* (*DMT1*) [27], improved both the eye and motor performance phenotypes caused by frataxin deficiency (Fig. 2A and B). Similarly, genetic reduction of *Tsf1* and *Tsf3,* the *Drosophila* homologs of the iron transport carrier Transferrin [28], improved the phenotypes of the FRDA *Drosophila* model (Fig. 2A and B). *Tsf1* is abundant in the fly hemolymph and there is evidence that it plays a role in immune response [29,30]. However whether it serves as an iron transporter between cells similarly to mammalian transferrin still remains unclear (reviewed in [31]). Even less is known about *Tsf3*, also homolog of transferrin, which has not been characterized yet. Interestingly, the identification of both *Tsf1* and *Tsf3* as suppressors for FRDA provides indirect evidence supporting their role in iron metabolism in *Drosophila*.

In addition to altering genes encoding iron transporters, we found that altering key regulators of iron homeostasis can also improve the eye morphology and motor performance phenotypes of FRDA model flies. Iron absorption and metabolism are regulated by the IRP/IRE system. When the cells are iron depleted, Iron Regulatory Proteins (IRPs) bind to Iron Responsive Elements (IREs) on the 5'UTR and 3'UTR mRNAs of their target proteins. Specifically, binding of IRPs inhibit the translation of the L and H chains of ferritin, the iron exporter FPN1 and the mitochondrial aconitase, among others, whereas it increases the transferrin receptor TfR1 and DMT1 (reviewed in [32]). Knocking down the homologs of the IRPs in *Drosophila*, *Irp-1A* and *Irp-1B* [33], in the FRDA model fly rescued the eye structure and the motor performance impairment (Fig. 2A and B). An increase in IRP binding activity has been described in FRDA patient lymphoblasts and a cardiac mouse model [34,35], and it has been suggested to lead to a cytosolic iron depletion that contrasts with the mitochondrial iron overload. *fh*RNAi-2 animals show a reduced expression of *Irp-1A* in iron overload conditions that has been suggested to represent a cellular response against the prolonged IRP binding [36]. Similarly, the reduction in gene expression of the *Drosophila* homologs of the *IRP* and their targets transferrin and *DMT1* that we induced in the FRDA fly model might confer a protective effect counteracting the cytosolic iron overload. Taken together, these data demonstrate that modulating the expression of critical genes within key pathways in iron homeostasis is sufficient to suppress FRDA phenotypes in *Drosophila*.

3.3. Knockdown of zinc transporters and copper chaperones ameliorate FRDA fly phenotypes

As we were able to identify suppressors of FRDA phenotypes from our candidate genetic modifier analysis of iron-associated genes, we then evaluated whether pathways also implicated in disease pathogenesis, such as zinc and copper homeostasis [17], may also modify eye and motor performance in the FRDA *Drosophila* model.

Zinc is essential as a structural or catalytic co-factor in hundreds of proteins such as the zinc finger transcription factors. Zinc transport across membranes is mainly mediated by two conserved gene families of zinc transporters: (1) the Zip family (Zrt-/Irt-like, solute carrier family 39, SLC39A) function in zinc influx from the extracellular medium

or vesicular organelles into the cytoplasm, and (2) the ZnT family (Cation diffusion facilitator, CDF, SLC30A) that mediate zinc efflux or compartmentalization. Members of both zinc transporter families have been implicated in neurodegenerative diseases such as AD [37]. Among the orthologous Zip and ZnT transporters in *Drosophila* [38], we found that shRNA against *Zip42C.1*, *Zip42C.2* and *Zip88E* and *ZnT35C*, *ZnT41F* and *ZnT63C* improved both phenotypes of FRDA model flies (Fig. 3A and B).

In contrast to zinc, copper is part of a considerably lower number of proteins. However, the mechanisms for regulation of copper uptake, distribution, detoxification and efflux [39], are tightly regulated and evolutionarily conserved due to the redox properties of copper that, when disrupted, may lead to the generation of free radicals. Regarding copper associated-genes, we found that reducing the levels of *Atox1*, a chaperone that delivers copper to ATP7 transporters located in the trans-Golgi network [40], suppressed FRDA phenotypes in *Drosophila* (Fig. 3A and B). In addition, *dCutC*, a member of the Cut protein family associated with uptake, storage, delivery and efflux of copper [41] was also able to suppress eye degeneration and poor motor performance (Fig. 3A and B). Taken together, these findings related to both zinc and copper pathways suggest that altering the expression of genes that regulate the balance of metals other than iron may also be beneficial in FRDA.

3.4. MTF-1 overexpression suppress FRDA *Drosophila* model phenotypes

Cells have developed conserved mechanisms to protect themselves from the toxic effects of metals. Under stress conditions, notably metal overload and oxidative stress, the zinc-finger protein Metal-responsive Transcription Factor-1 (MTF-1) translocates to the nucleus and binds to metal response elements (MREs) located in the regulatory regions of its targets genes, such as the metal-sequestering metallothioneins (MT) [42]. MTs are small cysteine rich proteins that bind transition metals with high affinity, thus maintaining low levels of intracellular free metal [43].

In this study we found that MTF-1 is a modifier of FRDA fly model phenotypes, as an enhancer of the motor impairment by loss-of-function and a suppressor when overexpressed (Fig 4B). Similarly, *MTF-1* overexpression in *Drosophila* has been shown to rescue the toxicity induced by oxidative stress [24], the expression of human

Aβ42 peptide and a parkin null mutation [44,45]. Contrary to what we expected, knocking down *MtnA*, *MtnB* and *MtnC* (Fig 4A) suppress the eye phenotype of the frataxin deficient animals, as well as the motor performance for *MtnA* (Fig 4B). *MtnB* and *MtnC* knockdown alleles could not be tested for motor performance as their ubiquitous expression driven by *actin*-GAL4 resulted in adult lethality.

3.5. Suppression of FRDA *Drosophila* model phenotypes is mediated by reducing iron content and oxidative stress

We found that altering the expression of genes involved in iron transport, absorption and metabolism ameliorated eye degeneration and motor performance in the FRDA fly model (Fig. 2). To determine whether phenotype amelioration was correlated with changes in iron content, we measured the levels of iron in the FRDA model flies expressing the modifier alleles for iron-related genes. We found that four alleles corresponding to suppressors implicated in iron metabolism normalized the levels of this metal as measured by atomic emission spectroscopy, indicating that rescue of FRDA phenotypes can indeed be improved by reducing iron abundance and restoring iron homeostasis (Fig. 5A).

In addition, several members of the Zip family have been shown to transport not only zinc but also iron [46–48]. Therefore, we tested whether the improvement in the eye and motor phenotypes in these lines was mediated by a reduction in the iron accumulation displayed by the FRDA flies, independently of their role in zinc transport (Fig. 5B). We found that reducing the levels of the Zip transporters *ZnT41F* and *fear-of intimacy* (*foi)* reduced the iron content in FRDA flies. The loss-of-function of *foi* ameliorated the motor impairment of the FRDA flies (data not shown). According to these results, a reduced expression of at least some of the zinc transporters is sufficient to normalize iron content. We also found that overexpression of *MTF-1* improves the iron accumulation phenotype as well. In contrast, knocking down *MtnA* had no effect on the iron content (Fig 5B).

MTs have been broadly proposed to play a role in antioxidant response [49,50]. However there is evidence indicating that in some cases such as in presence of H_2O_2 they can generate hydroxyl radicals [51–53]. To determine the effect of altering the

metal detoxification pathway on the levels of oxidative stress of the FRDA flies, we measured the levels of malondialdehyde (MDA) + 4- hydroxyalkenals (HAE). Similar to previous findings [25], we confirmed that the amount of MDA + HAE is indeed higher in *fh*RNAi flies in comparison with controls (Fig. 5C). Interestingly, we found that overexpressing *MTF-1* was sufficient to normalize oxidative stress levels (Fig. 5C). Reducing the expression of MTs in FRDA flies also improved the oxidative stress phenotype, indirectly supporting their possible role as prooxidants, at least in a frataxin deficient scenario. Taking together the results on the iron and oxidative stress levels, the beneficial effect of overexpressing *MTF-1* may not be mediated by the MTs but most probably through reducing the iron accumulation.

In conclusion, these findings together with the rescue data related to iron-associated suppressors (Fig. 2) demonstrate that reducing the iron accumulation through a genetic strategy in FRDA model flies has potential therapeutic benefit. Although direct reduction in iron levels by the use of iron chelators has been only relatively successful in patients [15,16], our results support the notion that improvements in FRDA phenotypes can be mediated directly through pathways regulating iron homeostasis. We also show for the first time that alteration of genes implicated in copper and zinc homeostasis and metal detoxification, as well as copper and zinc chelation also constitute potential therapeutic targets for the disease. Overall, these findings provide the framework for future studies focused on improving metal not only iron homeostasis, either genetically or pharmacologically, in FRDA animal models.

Acknowledgements

The authors would like to thank Mª Carmen García González, Carolina Chaparro Ronda and María del Puerto Morales (ICMM) for their help with metal measurements, Dr. Richard Burke (University of Monash, Australia) for providing fly stains, and Dr. Rodney Samaco (Baylor College of Medicine) for critical reading of the manuscript.

This work was supported by grants from the European Community's Seventh Framework Program FP7/2007-2013 [grant agreement no. 242193 EFACTS], the Fundació la Marató TV3 of Spain [exp 101932] and the Prometeo Program from Generalitat Valenciana [PROMETEOII/2014/067]. Work in the Botas laboratory was

supported by the R01-NS42179 NIH grant. S.S. was a recipient of a fellowship from Ministerio de Ciencia e Innovación of Spain; P.C.-Q. is a recipient of a fellowship from Generalitat Valenciana of Spain, J.V.L. was supported by a research contract from the European Community's Seventh Framework Program FP7/2007-2013 [grant agreement no. 242193 EFACTS] and L.G. is the beneficiary of a postdoctoral grant from the AXA Research Fund.

Figure legends

Fig. 1. Metal accumulation in FRDA flies. A. Total zinc, copper, manganese and aluminum levels measured by atomic emission spectroscopy are increased in *fh*RNAi flies (*actin*-GAL4>UAS-*fh*RNAi-2) *vs* controls (w^{1118}; *actin*-GAL4). B. Zinc chelator TPEN and copper chelators BCS and TTM improve the climbing ability of *fh*RNAi flies (*actin*-GAL4>UAS-*fh*RNAi-2) compared to vehicle medium (EtOH/PBS, H_2O and DMSO 0.1%, respectively). n.s.: non-significant, *P<0.05, **P<0.01, ***P<0.001.

Fig. 2. Improvement of the eye morphology and the motor performance phenotypes of FRDA flies by decreased expression of genes implicated in iron homeostasis. A. Light microscope images of the external eye of control (w^{1118}; *GMR*-GAL4), *fh*RNAi (*GMR*-GAL4>UAS-*fh*RNAi-1) and *fh*RNAi/modifier flies (*GMR*-GAL4>UAS-*fh*RNAi-1 additionally carrying the corresponding allele of the modifier) B. Motor performance expressed as the percentage of flies that climbed passed a height of 11.5 cm. Control: w^{1118}; *actin*-GAL4. *fh*RNAi: *actin*-GAL4>UAS-*fh*RNAi-2. *fh*RNAi/modifier: *actin*-GAL4>UAS-*fh*RNAi-2 ; modifier allele. Asterisks represent the statistical significance between *fh*RNAi and *fh*RNAi/modifier for each day. *P<0.05, **P<0.01, ***P<0.001. Error bars represent SEM. shRNA: knockdown allele. LOF: loss of function allele.

Fig. 3. Improvement of the eye morphology and the motor performance phenotypes of FRDA flies by decreased expression of genes implicated in zinc and copper homeostasis. A. Light microscope images of the external eye of control (w^{1118}; *GMR*-GAL4), *fh*RNAi (*GMR*-GAL4>UAS-*fh*RNAi-1) and *fh*RNAi/modifier flies (*GMR*-GAL4>UAS-*fh*RNAi-1 additionally carrying the corresponding allele of the modifier) B. Motor performance expressed as the percentage of flies that climbed passed a height of 11.5 cm. Control: w^{1118}; *actin*-GAL4. *fh*RNAi: *actin*-GAL4>UAS-*fh*RNAi-2.

*fh*RNAi/modifier: *actin*-GAL4>UAS-*fh*RNAi-2 ; modifier allele. Asterisks represent the statistical significance between *fh*RNAi and *fh*RNAi/modifier for each day. *P<0.05, **P<0.01, ***P<0.001. Error bars represent SEM. shRNA: knockdown allele.

Fig. 4. Modification of the eye morphology and the motor performance phenotypes of FRDA flies by altered expression of genes implicated in metal detoxification. A. Light microscope images of the external eye of control (w^{1118}; *GMR*-GAL4), *fh*RNAi (*GMR*-GAL4>UAS-*fh*RNAi-1) and *fh*RNAi/modifier flies (*GMR*-GAL4>UAS-*fh*RNAi-1 additionally carrying the corresponding allele of the modifier) B. Motor performance expressed as the percentage of flies that climbed passed a height of 11.5 cm. Control: w^{1118}; *actin*-GAL4. *fh*RNAi: *actin*-GAL4>UAS-*fh*RNAi-2. *fh*RNAi/modifier: *actin*-GAL4>UAS-*fh*RNAi-2 ; modifier allele. Asterisks represent the statistical significance between *fh*RNAi and *fh*RNAi/modifier for each day. *P<0.05, **P<0.01, ***P<0.001. Error bars represent SEM. shRNA: knockdown allele. LOF: loss of function allele. OE: overexpression allele.

Fig. 5. Genetic modifiers of the FRDA phenotypes reduce iron content and oxidative stress. A and B. Increased iron levels are rescued by modification of genes implicated in iron (A) and zinc homeostasis and metal detoxification (B). Total iron content was measured by atomic emission spectroscopy and expressed in percentage relative to the controls. C. Reduction of the increased levels of malondialdehyde + 4-hydroxyalkenals by metal detoxification genes. Control: w^{1118}; *actin*-GAL4. *fh*RNAi: *actin*-GAL4>UAS-*fh*RNAi-2. *fh*RNAi/modifier: *actin*-GAL4>UAS-*fh*RNAi-2 ; modifier allele. n.s.: non-significant, *P<0.05, **P<0.01, ***P<0.001. Error bars represent SD. shRNA: knockdown allele. LOF: loss of function allele. OE: overexpression allele. qMtn*: loss of function of the four metallothioneins MtnA, MtnB, MtnC, MtnD.

References

[1] V. Campuzano, L. Montermini, M.D. Moltò, L. Pianese, M. Cossée, F. Cavalcanti, et al., Friedreich's ataxia: autosomal recessive disease caused by an intronic GAA triplet repeat expansion, Science. 271 (1996) 1423–1427.

[2] E. Monrós, M.D. Moltó, F. Martínez, J. Cañizares, J. Blanca, J.J. Vílchez, et al., Phenotype correlation and intergenerational dynamics of the Friedreich ataxia GAA trinucleotide repeat, Am. J. Hum. Genet. 61 (1997) 101–110.
[3] E. Soragni, D. Herman, S.Y.R. Dent, J.M. Gottesfeld, R.D. Wells, M. Napierala, Long intronic GAA*TTC repeats induce epigenetic changes and reporter gene silencing in a molecular model of Friedreich ataxia, Nucleic Acids Res. 36 (2008) 6056–6065. doi:10.1093/nar/gkn604.
[4] R.D. Wells, DNA triplexes and Friedreich ataxia, FASEB J. 22 (2008) 1625–1634. doi:10.1096/fj.07-097857.
[5] F. Palau, C. Espinós, Autosomal recessive cerebellar ataxias, Orphanet J Rare Dis. 1 (2006) 47. doi:10.1186/1750-1172-1-47.
[6] M.B. Delatycki, L.A. Corben, Clinical features of Friedreich ataxia, J. Child Neurol. 27 (2012) 1133–1137. doi:10.1177/0883073812448230.
[7] S. Schmucker, H. Puccio, Understanding the molecular mechanisms of Friedreich's ataxia to develop therapeutic approaches, Hum. Mol. Genet. 19 (2010) R103–110. doi:10.1093/hmg/ddq165.
[8] C.M. Gomes, R. Santos, Neurodegeneration in Friedreich's ataxia: from defective frataxin to oxidative stress, Oxid Med Cell Longev. 2013 (2013) 487534. doi:10.1155/2013/487534.
[9] J.L. Bradley, J.C. Blake, S. Chamberlain, P.K. Thomas, J.M. Cooper, A.H. Schapira, Clinical, biochemical and molecular genetic correlations in Friedreich's ataxia, Hum. Mol. Genet. 9 (2000) 275–282.
[10] J.B. Lamarche, M. Côté, B. Lemieux, The cardiomyopathy of Friedreich's ataxia morphological observations in 3 cases, Can J Neurol Sci. 7 (1980) 389–396.
[11] G. Sanchez-Casis, M. Cote, A. Barbeau, Pathology of the heart in Friedreich's ataxia: review of the literature and report of one case, Can J Neurol Sci. 3 (1976) 349–354.
[12] D. Waldvogel, P. van Gelderen, M. Hallett, Increased iron in the dentate nucleus of patients with Friedrich's ataxia, Ann. Neurol. 46 (1999) 123–125.
[13] O. Kakhlon, H. Manning, W. Breuer, N. Melamed-Book, C. Lu, G. Cortopassi, et al., Cell functions impaired by frataxin deficiency are restored by drug-mediated iron relocation, Blood. 112 (2008) 5219–5227. doi:10.1182/blood-2008-06-161919.
[14] S. Soriano, J.V. Llorens, L. Blanco-Sobero, L. Gutiérrez, P. Calap-Quintana, M.P. Morales, et al., Deferiprone and idebenone rescue frataxin depletion phenotypes in a Drosophila model of Friedreich's ataxia, Gene. 521 (2013) 274–281. doi:10.1016/j.gene.2013.02.049.
[15] N. Boddaert, K.H. Le Quan Sang, A. Rötig, A. Leroy-Willig, S. Gallet, F. Brunelle, et al., Selective iron chelation in Friedreich ataxia: biologic and clinical implications, Blood. 110 (2007) 401–408. doi:10.1182/blood-2006-12-065433.
[16] M. Pandolfo, J. Arpa, M.B. Delatycki, K.H. Le Quan Sang, C. Mariotti, A. Munnich, et al., Deferiprone in Friedreich ataxia: a 6-month randomized controlled trial, Ann. Neurol. 76 (2014) 509–521. doi:10.1002/ana.24248.
[17] A.H. Koeppen, R.L. Ramirez, D. Yu, S.E. Collins, J. Qian, P.J. Parsons, et al., Friedreich's ataxia causes redistribution of iron, copper, and zinc in the dentate nucleus, Cerebellum. 11 (2012) 845–860. doi:10.1007/s12311-012-0383-5.
[18] A.H. Koeppen, E.C. Kuntzsch, S.T. Bjork, R.L. Ramirez, J.E. Mazurkiewicz, P.J. Feustel, Friedreich ataxia: metal dysmetabolism in dorsal root ganglia, Acta Neuropathol Commun. 1 (2013) 26. doi:10.1186/2051-5960-1-26.

[19] K.A. Jellinger, The relevance of metals in the pathophysiology of neurodegeneration, pathological considerations, Int. Rev. Neurobiol. 110 (2013) 1–47. doi:10.1016/B978-0-12-410502-7.00002-8.
[20] P.R. Anderson, K. Kirby, W.C. Orr, A.J. Hilliker, J.P. Phillips, Hydrogen peroxide scavenging rescues frataxin deficiency in a Drosophila model of Friedreich's ataxia, Proc. Natl. Acad. Sci. U.S.A. 105 (2008) 611–616. doi:10.1073/pnas.0709691105.
[21] P.R. Anderson, K. Kirby, A.J. Hilliker, J.P. Phillips, RNAi-mediated suppression of the mitochondrial iron chaperone, frataxin, in Drosophila, Hum. Mol. Genet. 14 (2005) 3397–3405. doi:10.1093/hmg/ddi367.
[22] J.V. Llorens, J.A. Navarro, M.J. Martínez-Sebastián, M.K. Baylies, S. Schneuwly, J.A. Botella, et al., Causative role of oxidative stress in a Drosophila model of Friedreich ataxia, FASEB J. 21 (2007) 333–344. doi:10.1096/fj.05-5709com.
[23] J.A. Navarro, E. Ohmann, D. Sanchez, J.A. Botella, G. Liebisch, M.D. Moltó, et al., Altered lipid metabolism in a Drosophila model of Friedreich's ataxia, Hum. Mol. Genet. 19 (2010) 2828–2840. doi:10.1093/hmg/ddq183.
[24] S. Bahadorani, S. Mukai, D. Egli, A.J. Hilliker, Overexpression of metal-responsive transcription factor (MTF-1) in Drosophila melanogaster ameliorates life-span reductions associated with oxidative stress and metal toxicity, Neurobiol. Aging. 31 (2010) 1215–1226. doi:10.1016/j.neurobiolaging.2008.08.001.
[25] P. Calap-Quintana, S. Soriano, J.V. Llorens, I. Al-Ramahi, J. Botas, M.D. Moltó, et al., TORC1 Inhibition by Rapamycin Promotes Antioxidant Defences in a Drosophila Model of Friedreich's Ataxia, PLoS ONE. 10 (2015) e0132376. doi:10.1371/journal.pone.0132376.
[26] J. Park, I. Al-Ramahi, Q. Tan, N. Mollema, J.R. Diaz-Garcia, T. Gallego-Flores, et al., RAS-MAPK-MSK1 pathway modulates ataxin 1 protein levels and toxicity in SCA1, Nature. 498 (2013) 325–331. doi:10.1038/nature12204.
[27] V. Rodrigues, P.Y. Cheah, K. Ray, W. Chia, malvolio, the Drosophila homologue of mouse NRAMP-1 (Bcg), is expressed in macrophages and in the nervous system and is required for normal taste behaviour, EMBO J. 14 (1995) 3007–3020.
[28] B. Dunkov, T. Georgieva, Insect iron binding proteins: insights from the genomes, Insect Biochem. Mol. Biol. 36 (2006) 300–309. doi:10.1016/j.ibmb.2006.01.007.
[29] F. Levy, D. Rabel, M. Charlet, P. Bulet, J.A. Hoffmann, L. Ehret-Sabatier, Peptidomic and proteomic analyses of the systemic immune response of Drosophila, Biochimie. 86 (2004) 607–616. doi:10.1016/j.biochi.2004.07.007.
[30] T. Yoshiga, T. Georgieva, B.C. Dunkov, N. Harizanova, K. Ralchev, J.H. Law, Drosophila melanogaster transferrin. Cloning, deduced protein sequence, expression during the life cycle, gene localization and up-regulation on bacterial infection, Eur. J. Biochem. 260 (1999) 414–420.
[31] K. Mandilaras, T. Pathmanathan, F. Missirlis, Iron absorption in Drosophila melanogaster, Nutrients. 5 (2013) 1622–1647. doi:10.3390/nu5051622.
[32] M.W. Hentze, M.U. Muckenthaler, B. Galy, C. Camaschella, Two to tango: regulation of Mammalian iron metabolism, Cell. 142 (2010) 24–38. doi:10.1016/j.cell.2010.06.028.
[33] M. Muckenthaler, N. Gunkel, D. Frishman, A. Cyrklaff, P. Tomancak, M.W. Hentze, Iron-regulatory protein-1 (IRP-1) is highly conserved in two invertebrate species--characterization of IRP-1 homologues in Drosophila melanogaster and Caenorhabditis elegans, Eur. J. Biochem. 254 (1998) 230–237.

[34] K. Li, E.K. Besse, D. Ha, G. Kovtunovych, T.A. Rouault, Iron-dependent regulation of frataxin expression: implications for treatment of Friedreich ataxia, Hum. Mol. Genet. 17 (2008) 2265–2273. doi:10.1093/hmg/ddn127.
[35] M. Whitnall, Y.S. Rahmanto, R. Sutak, X. Xu, E.M. Becker, M.R. Mikhael, et al., The MCK mouse heart model of Friedreich's ataxia: Alterations in iron-regulated proteins and cardiac hypertrophy are limited by iron chelation, PNAS. 105 (2008) 9757–9762. doi:10.1073/pnas.0804261105.
[36] J.A. Navarro, J.A. Botella, C. Metzendorf, M.I. Lind, S. Schneuwly, Mitoferrin modulates iron toxicity in a Drosophila model of Friedreich′s ataxia, Free Radic. Biol. Med. 85 (2015) 71–82. doi:10.1016/j.freeradbiomed.2015.03.014.
[37] M. Lang, L. Wang, Q. Fan, G. Xiao, X. Wang, Y. Zhong, et al., Genetic inhibition of solute-linked carrier 39 family transporter 1 ameliorates aβ pathology in a Drosophila model of Alzheimer's disease, PLoS Genet. 8 (2012) e1002683. doi:10.1371/journal.pgen.1002683.
[38] J.C. Lye, C.D. Richards, K. Dechen, D. Paterson, M.D. de Jonge, D.L. Howard, et al., Systematic functional characterization of putative zinc transport genes and identification of zinc toxicosis phenotypes in Drosophila melanogaster, J. Exp. Biol. 215 (2012) 3254–3265. doi:10.1242/jeb.069260.
[39] K. Balamurugan, W. Schaffner, Copper homeostasis in eukaryotes: teetering on a tightrope, Biochim. Biophys. Acta. 1763 (2006) 737–746. doi:10.1016/j.bbamcr.2006.05.001.
[40] J.M. Walker, R. Tsivkovskii, S. Lutsenko, Metallochaperone Atox1 transfers copper to the NH2-terminal domain of the Wilson's disease protein and regulates its catalytic activity, J. Biol. Chem. 277 (2002) 27953–27959. doi:10.1074/jbc.M203845200.
[41] Y. Li, J. Du, P. Zhang, J. Ding, Crystal structure of human copper homeostasis protein CutC reveals a potential copper-binding site, J. Struct. Biol. 169 (2010) 399–405. doi:10.1016/j.jsb.2009.10.012.
[42] R. Heuchel, F. Radtke, O. Georgiev, G. Stark, M. Aguet, W. Schaffner, The transcription factor MTF-1 is essential for basal and heavy metal-induced metallothionein gene expression, EMBO J. 13 (1994) 2870–2875.
[43] T.D. Rae, P.J. Schmidt, R.A. Pufahl, V.C. Culotta, T.V. O'Halloran, Undetectable intracellular free copper: the requirement of a copper chaperone for superoxide dismutase, Science. 284 (1999) 805–808.
[44] H. Hua, L. Münter, A. Harmeier, O. Georgiev, G. Multhaup, W. Schaffner, Toxicity of Alzheimer's disease-associated Aβ peptide is ameliorated in a Drosophila model by tight control of zinc and copper availability, Biol. Chem. 392 (2011) 919–926. doi:10.1515/BC.2011.084.
[45] N. Saini, O. Georgiev, W. Schaffner, The parkin mutant phenotype in the fly is largely rescued by metal-responsive transcription factor (MTF-1), Mol. Cell. Biol. 31 (2011) 2151–2161. doi:10.1128/MCB.05207-11.
[46] J.P. Liuzzi, F. Aydemir, H. Nam, M.D. Knutson, R.J. Cousins, Zip14 (Slc39a14) mediates non-transferrin-bound iron uptake into cells, PNAS. 103 (2006) 13612–13617. doi:10.1073/pnas.0606424103.
[47] C.-Y. Wang, S. Jenkitkasemwong, S. Duarte, B.K. Sparkman, A. Shawki, B. Mackenzie, et al., ZIP8 Is an Iron and Zinc Transporter Whose Cell-surface Expression Is Up-regulated by Cellular Iron Loading, J. Biol. Chem. 287 (2012) 34032–34043. doi:10.1074/jbc.M112.367284.

[48] G. Xiao, Z. Wan, Q. Fan, X. Tang, B. Zhou, The metal transporter ZIP13 supplies iron into the secretory pathway in Drosophila melanogaster, Elife. 3 (2014) e03191. doi:10.7554/eLife.03191.
[49] P.J. Thornalley, M. Vasák, Possible role for metallothionein in protection against radiation-induced oxidative stress. Kinetics and mechanism of its reaction with superoxide and hydroxyl radicals, Biochim. Biophys. Acta. 827 (1985) 36–44.
[50] A. Viarengo, B. Burlando, N. Ceratto, I. Panfoli, Antioxidant role of metallothioneins: a comparative overview, Cell. Mol. Biol. (Noisy-Le-Grand). 46 (2000) 407–417.
[51] J.P. Fabisiak, L.L. Pearce, G.G. Borisenko, Y.Y. Tyhurina, V.A. Tyurin, J. Razzack, et al., Bifunctional anti/prooxidant potential of metallothionenin: redox signaling of copper binding and release, Antioxid. Redox Signal. 1 (1999) 349–364.
[52] Z.E. Suntres, E.M.K. Lui, Prooxidative effect of copper--metallothionein in the acute cytotoxicity of hydrogen peroxide in Ehrlich ascites tumour cells, Toxicology. 217 (2006) 155–168. doi:10.1016/j.tox.2005.09.004.
[53] K.T. Suzuki, M. Rui, J. Ueda, T. Ozawa, Production of hydroxyl radicals by copper-containing metallothionein: roles as prooxidant, Toxicol. Appl. Pharmacol. 141 (1996) 231–237.

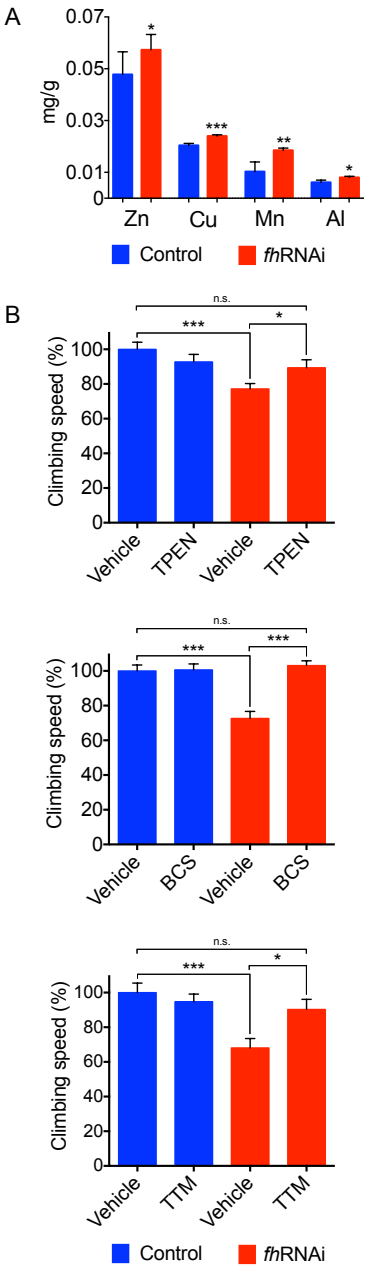
A
0.07
0.05
0.03
0.01
0
mg/g
*
***
**
*
Zn
Cu
Mn
Al
Control
fhRNAi
B
n.s.
***
*
Climbing speed (%)
100
80
60
40
20
0
Vehicle
TPEN
Vehicle
TPEN
n.s.
***
***
Climbing speed (%)
Vehicle
BCS
Vehicle
BCS
n.s.
***
*
Climbing speed (%)
Vehicle
TTM
Vehicle
TTM
Control
fhRNAi

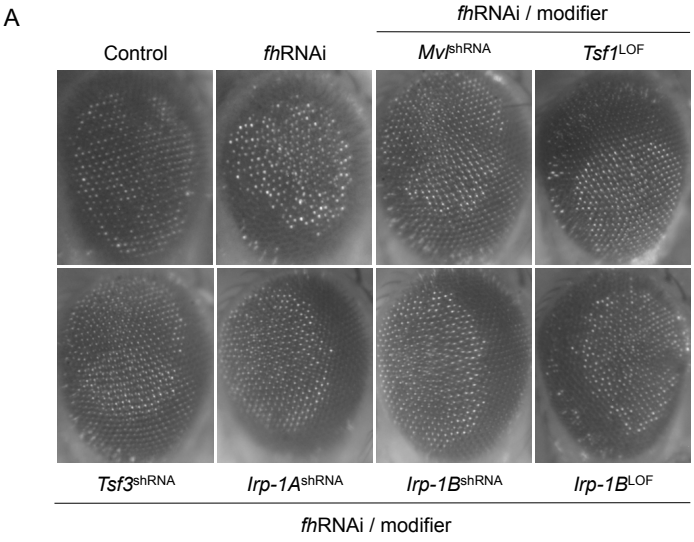
A
fhRNAi / modifier
Control
fhRNAi
Mvl shRNA
Tsf1 LOF
Tsf3 shRNA
Irp-1A shRNA
Irp-1B shRNA
Irp-1B LOF
fhRNAi / modifier

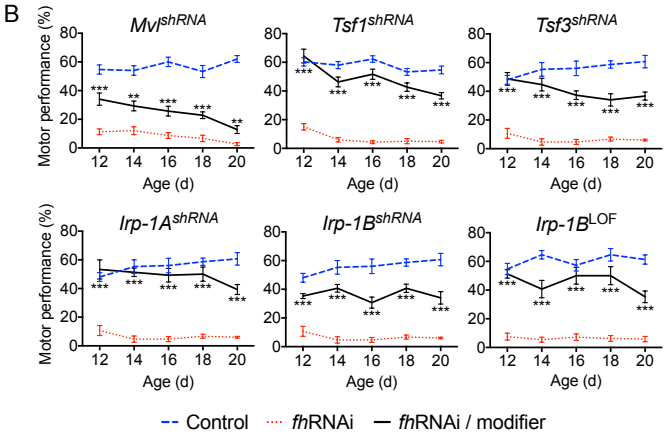
B
Mvl shRNA
Tsf1 shRNA
Tsf3 shRNA
Irp-1A shRNA
Irp-1B shRNA
Irp-1B LOF
Motor performance (%)
Age (d)
Control
fhRNAi
fhRNAi / modifier

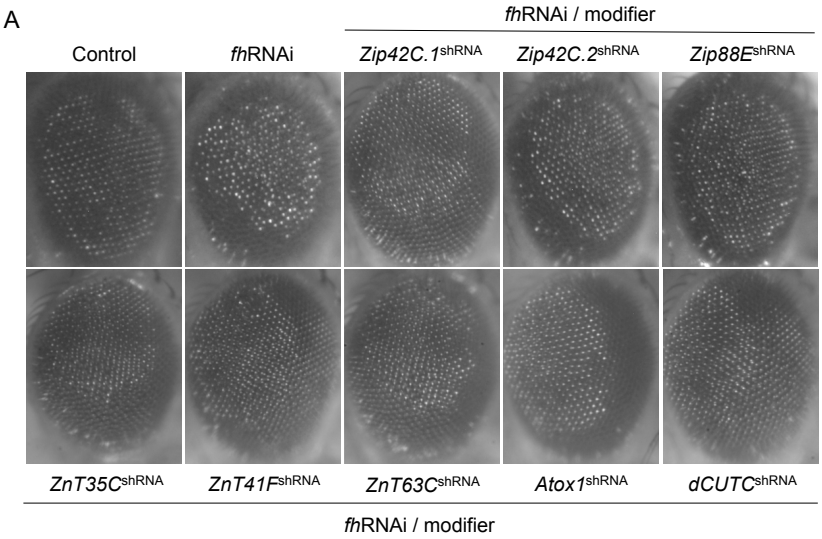
A
fhRNAi / modifier
Control
fhRNAi
Zip42C.1shRNA
Zip42C.2shRNA
Zip88EshRNA
ZnT35CshRNA
ZnT41FshRNA
ZnT63CshRNA
Atox1shRNA
dCUTCshRNA
fhRNAi / modifier

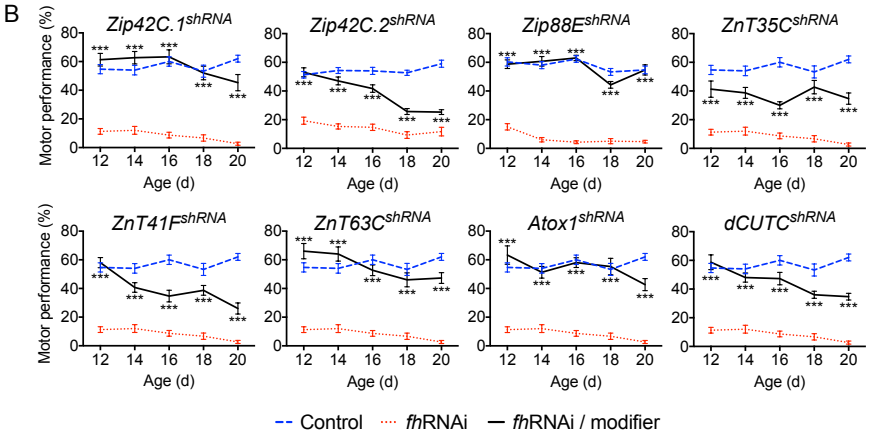
B
Zip42C.1shRNA
Zip42C.2shRNA
Zip88EshRNA
ZnT35CshRNA
ZnT41FshRNA
ZnT63CshRNA
Atox1shRNA
dCUTCshRNA
Motor performance (%)
Age (d)
Control
fhRNAi
fhRNAi / modifier

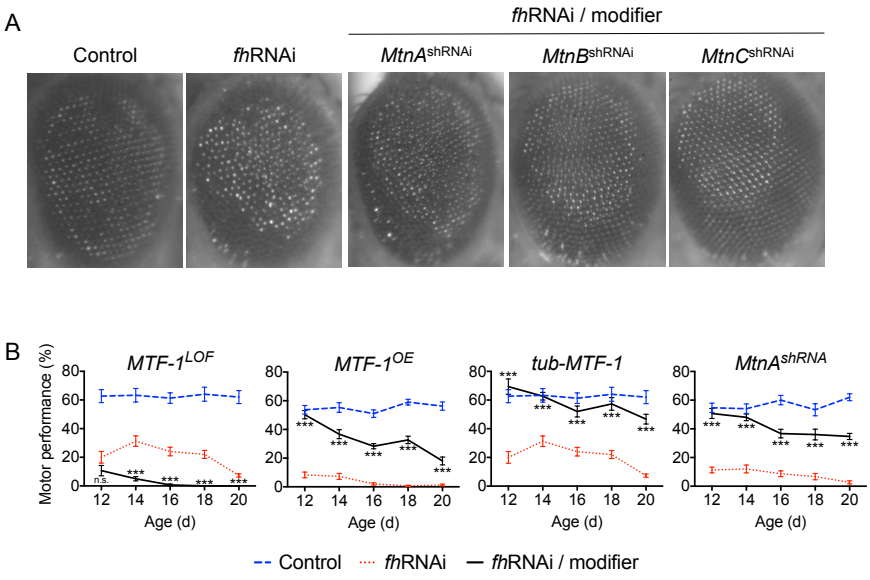
A
fhRNAi / modifier
Control
fhRNAi
MtnA shRNAi
MtnB shRNAi
MtnC shRNAi
B
MTF-1 LOF
MTF-1 OE
tub-MTF-1
MtnA shRNA
Motor performance (%)
Age (d)
Control
fhRNAi
fhRNAi / modifier

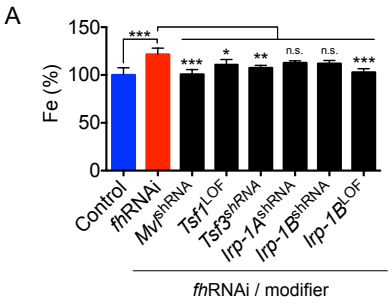
A
Fe (%)
150
100
50
0
***
***
*
**
n.s.
n.s.
***
Control
fhRNAi
MvshRNA
Tsf1LOF
Tsf3shRNA
Irp-1AshRNA
Irp-1BshRNA
Irp-1BLOF
fhRNAi / modifier

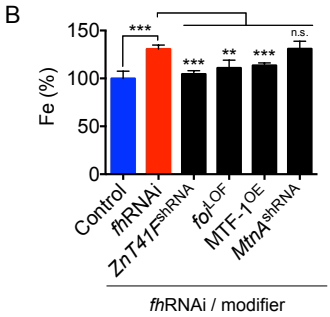
B
Fe (%)
150
100
50
0
***
***
**
***
n.s.
Control
fhRNAi
ZnT41FshRNA
folLOF
MTF-1OE
MtnAshRNA
fhRNAi / modifier

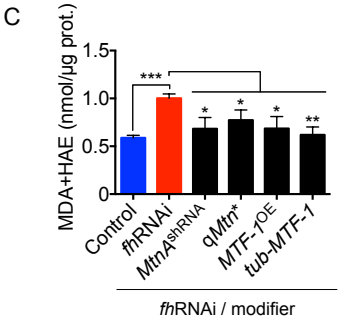
C
MDA+HAE (nmol/µg prot.)
1.5
1.0
0.5
0
***
*
*
*
**
Control
fhRNAi
MtnAshRNA
qMtn*
MTF-1OE
tub-MTF-1
fhRNAi / modifier

Supplementary Table 1. Genotypes of the *Drosophila* strains corresponding to genetic interactors implicated in metal homeostasis.

Strain	Genotype	Effect
Mvl^{shRNA}	P{KK108406}VIE-260B	Knockdown
Tsf1^{LOF}	w^{1118} PBac{WH}Tsf1^{f05108}	Loss of function
Tsf1^{shRNA}	P{KK103815}VIE-260B	Knockdown
Tsf3^{shRNA}	P{KK109853}VIE-260B	Knockdown
Irp-1A^{shRNA}	P{KK105828}VIE-260B	Knockdown
Irp-1B^{shRNA}	P{KK108179}VIE-260B	Knockdown
Irp-1B^{LOF}	y^{1} w^{67c23}; P{Mae-UAS.6.11}DP00726	Loss of function
Zip42C.1^{shRNA}	P{KK108319}VIE-260B	Knockdown
Zip42C.2^{shRNA}	P{KK104365}VIE-260B	Knockdown
Zip88E^{shRNA}	P{KK110168}VIE-260B	Knockdown
foi^{LOF}	y^{1} w*; Mi{MIC}foi^{MI00610}/TM3, Sb^{1} Ser^{1}	Loss of function
ZnT35C^{shRNA}	P{KK112697}VIE-260B	Knockdown
ZnT41F^{shRNA}	P{KK111282}VIE-260B	Knockdown
ZnT63C^{shRNA}	P{KK102261}VIE-260B	Knockdown
Atox1^{shRNA}	P{KK108811}VIE-260B	Knockdown
dCutC^{shRNA}	P{KK108196}VIE-260B	Knockdown
MtnA^{shRNAi}	P{KK112833}VIE-260B	Knockdown
MtnB^{shRNAi}	P{KK112935}VIE-260B	Knockdown
MtnC^{shRNAi}	P{KK114800}VIE-260B	Knockdown
MTF-1^{LOF}	MTF-1$^{140\text{-}1R}$	Loss of function
MTF-1^{OE}	y^{1} w^{67c23}; P{EPgy2}EY03895 [54]	Overexpression
tub-MTF-1^{LOF}	[24]	Loss of function
q*Mtn**	*MtnA*$^{\Delta ATG}$ *MtnC*$^{\Delta ATG}$ *MtnB*$^{\Delta ATG}$ *MtnD** [55]	Loss of function

Supplementary References

[54] D. Egli, A. Selvaraj, H. Yepiskoposyan, B. Zhang, E. Hafen, O. Georgiev, et al., Knockout of "metal-responsive transcription factor" MTF-1 in Drosophila by homologous recombination reveals its central role in heavy metal homeostasis, EMBO J. 22 (2003) 100–108. doi:10.1093/emboj/cdg012.

[55] D. Egli, J. Domènech, A. Selvaraj, K. Balamurugan, H. Hua, M. Capdevila, et al., The four members of the Drosophila metallothionein family exhibit distinct yet overlapping roles in heavy metal homeostasis and detoxification, Genes Cells. 11 (2006) 647–658. doi:10.1111/j.1365-2443.2006.00971.x.

Results and discussion

1. Functional equivalence of human and *Drosophila* frataxins (Navarro *et al*. 2011, figures 4 and 5)

Frataxin is a protein highly conserved throughout evolution and it is present from bacteria to humans (Gibson *et al*. 1996). The homolog of frataxin in *Drosophila melanogaster* shows a high similarity with the other frataxin orthologs, in both gene and protein sequence and structure (Cañizares *et al*. 2000). It also shares the mitochondrial subcellular localization found in eukaryotes (Llorens *et al*. 2007). Knocking down frataxin in *Drosophila* recapitulated relevant behavioral and biochemical features of FRDA, suggesting an equivalent function for the fly and the human frataxins (Anderson *et al*. 2005, Llorens *et al*. 2007).

In order to provide direct evidence of the functional equivalence of both proteins, we studied whether the human protein could functionally replace the endogenous frataxin in *Drosophila*. For that purpose, the UAS-*FXN* transgene was generated, with the coding region of *FXN* cDNA placed under the control of the UAS promoter. Then, a double transgenic fly strain was obtained by combining the UAS-*FXN* construct with the frataxin knockdown allele UAS-*fh*RNAi-1). It is worth mentioned that ubiquitous expression of *fh*RNAi-1 induced a 90% reduction of frataxin levels and produced pre-adult lethality (Anderson *et al*. 2005).

Due to their sequence similarity, we suspected that the RNAi directed against the endogenous *fh* transcript might also target the *FXN* mRNA in the double transgenic. We discarded that possibility by finding equivalent amounts of human frataxin by Western Blot in *actin*-GAL4>UAS-fhRNAi-1; UAS-FXN compared with *actin*-GAL4>UAS-FXN larvae [Figure 5 b in Navarro *et al*. 2011].

The decrease in aconitase activity is one of the hallmarks of FRDA that is reproduced in the *Drosophila* models (Anderson *et al*. 2005, Llorens *et al*. 2007). We measured the aconitase activity in larvae simultaneously and ubiquitously expressing *fh*RNA-1 and *FXN* with the *actin*-GAL4 driver [Figure 4 a in Navarro *et al*. 2011]. We reproduced the reduction in aconitase activity induced by frataxin depletion previously described (Anderson *et al*. 2005) and

we found that it was reverted up to control levels by the expression of *FXN*. This result indicates that human frataxin can replace the endogenous protein in the *fh*-knockdown flies and therefore that both proteins are functionally equivalent. In previous studies, human and yeast (Cavadini *et al*. 2000) and human and mouse (Lim *et al*. 2007) frataxins had been shown to be functionally interchangeable. Expressing *FXN* in the *yfh1*Δ yeast knockout mutant (*yfh1*Δ [*FXN*]) prevented mitochondrial iron overload and oxidative stress damage. Similarly to our results in *Drosophila*, the impaired aconitase activity of the *yfh1*Δ mitochondria was also rescued by expression of *FXN* to levels comparable to those of *yfh1*Δ [YFH1], in which the endogenous yeast frataxin has been reintroduced (Cavadini *et al*. 2000). A gene rescue experiment was performed as well in a conditional FRDA mouse model. In those loxP[frda] animals, the expression of the human frataxin cDNA with an HSV-1 amplicon vector improved their motor coordination deficit (Lim *et al*. 2007).

Noteworthy is that the expression of *FXN* in *Drosophila* by itself produces a reduction in aconitase activity similar to the situation found for the frataxin deficiency [Figure 4 a in Navarro *et al*. 2011]. Overexpression of the *Drosophila* frataxin in the fly had already been reported to decrease aconitase activity, among other detrimental phenotypes (Llorens *et al*. 2007). An increase in frataxin oligomerization had been proposed to explain the impairment in Fe-S cluster formation and aconitase and SDH activity in yeast overexpressing *Yfh* (Seguin *et al*. 2009). Considering the possibility that the human frataxin was producing oligomers or toxic aggregates leading to a reduction in the level of functional frataxin, we performed a gel filtration assay [Figure 5 a in Navarro *et al*. 2011]. However, the human protein expressed in *Drosophila* was recovered only in the monomeric form. Therefore the *FXN* overexpression phenotypes and probably also the *fh* overexpression phenotypes that we found in *Drosophila*, cannot be explained by frataxin aggregation. It is possible that frataxin amounts above a certain threshold may overwhelm the system or sequester frataxin interactor proteins. Our data indicates that frataxin levels must be considered in therapy strategies based on increasing the amounts of this protein.

2. Deferiprone and idebenone rescue FRDA phenotypes in *Drosophila* (Soriano *et al*. 2013)

Reports of mitochondrial iron accumulation in heart, liver, spleen and brain of FRDA patients (Waldvogel *et al*. 1999; Bradley *et al*. 2000) provided the rationale for the use of iron chelators for the treatment of the disease. Deferiprone (DFP) is a blood-barrier permeable molecule that chelates iron (Sohn *et al*. 2008). Given that DFP had provided promising results in frataxin deficient cells and in patients (Boddaert *et al*. 2007; Kakhlon *et al*. 2008), we tested the effect of this iron chelator in the FRDA flies, in order to validate our model for drug screening. Two concentrations of DFP (60 and 163 µM) and two drug regimens (early and adult treatments) were assayed.

Ubiquitous expression of the allele *fh*RNAi-2 induced a moderate interference with a 70% reduction in frataxin levels that was compatible with normal adult development (Llorens *et al*. 2007; Navarro *et al*. 2010). *actin*-Gal4> *fh*RNAi-2 individuals show a shortened lifespan and an impaired motor ability. Food supplementation from the larval stage with DFP improved both the survival and the motor phenotypes. Overall, the highest concentration of DFP used was more effective in all cases. Using this dose, *fh*RNAi-2 flies extended the life span from 60 to 80 days, very close to the controls values. Similarly, the climbing of the *fh*RNAi-2 flies is impaired when the reduction in frataxin expression is limited to the peripheral nervous system (PNS), which is particularly affected in FRDA patients, using the *neur*-GAL4 driver. Treatment with 163 µM of DFP improved as well the motor ability of the *neur*-Gal4> *fh*RNAi-2 flies.

Next, we investigated the effect that the chelator DFP was having on the iron pool of the FRDA *Drosophila* model. In order to do that, we first characterized the iron content of the *actin*-Gal4> *fh*RNAi-2 flies. We found that although the mitochondrial iron was increased compared to controls, there was a reduction in soluble iron in the form of ferrous ions, which might be indicating the existence of insoluble iron aggregates. It was unexpected to find that the mitochondrial iron levels were further increased after treating the FRDA animals with DFP. However DFP increased the soluble ferrous iron back

to control levels and relatively increased the soluble ferric iron. We interpreted these results as the DFP binding the ferric iron before it accumulates into a toxic insoluble form.

In addition to iron accumulation, oxidative stress has been highlighted as a major pathological feature of FRDA and therefore the use of antioxidants was proposed as a therapeutic strategy for the treatment of the disease. The coenzyme Q10 analog idebenone (IDE) seemed to stabilize the neurological function in a clinical trial with pediatric FRDA patients (Meier *et al*. 2012). In the FRDA *Drosophila* model, we tested two concentrations of IDE (7 and 15 µM). IDE improved the lifespan of the *actin*-Gal4> *fh*RNAi-2 and the motor ability either when the frataxin deficiency was ubiquitous or directed to the PNS. Here, the two concentrations of IDE used were effective although IDE 7µM showed better results than 15 µM.

To evaluate the antioxidant effect of IDE on the FRDA flies, we used the aconitase activity as a marker of oxidative stress levels. We had already found that the activity of this enzyme was reduced in hyperoxia in the *fh*RNAi-2 flies (Llorens *et al*. 2007). Treatment with IDE recovered the aconitase activity in hyperoxic conditions up to control levels. Altogether we have shown that the iron chelator DFP and the antioxidant IDE ameliorate the FRDA phenotypes in *Drosophila*, and these results validated the use of our model for the screen of therapeutic molecules.

DFP and IDE were among the first compounds included in clinical trials for FRDA. However, both have been recently discarded after initial testing since there is not a consensus regarding their efficacy in the neurological conditions of the patients and because contradictory results regarding their usefulness have been reported (http://www.curefa.org/pipeline). In this context, our *Drosophila* model constitutes a powerful tool for the screening of novel therapeutic molecules.

3. Screen of genetic modifiers of FRDA phenotypes in *Drosophila*

One of the reasons explaining the success of *Drosophila melanogaster* as a model organism is its power for high-throughput genetic screening of the genes implicated in a biological process (reviewed in Jonhston *et al*. 2002). Taking advantage of this feature, we designed a genetic screen of modifiers of the FRDA pathogenesis, based on a candidate approach.

First, we elaborated a list of 198 candidate genes to be tested [Supplementary table 1] including: (1) pathways known to be implicated in FRDA, including metal homeostasis, oxidative stress and autophagy; (2) hits from an unpublished proteomic study comparing the expression profiles of the *fh*RNAi-2 flies *vs* controls; and (3) hits from genetic screens in *Drosophila* models of other neurodegenerative diseases. Then, we selected 452 fly strains commercially available, carrying mutant alleles affecting the genes in the list. Knockdown shRNAi lines were obtained from the Vienna Drosophila Resource Center, and loss-of-function and overexpression lines from the Bloomington Stock Center.

The impaired motor activity displayed by the *actin*-GAL4> *fh*RNAi-2 flies (Llorens *et al*. 2007) was a suitable screening phenotype as: (i) it is quantifiable and (ii) it had been proved to be modifiable for instance by pharmacological treatments as we described in the previous section. Considering the high number of crosses to be performed, we needed to obtain the desired F1 offspring to be tested out of a single step cross. Therefore we generated a parental strain carrying simultaneously the *actin*-GAL4 driver and the UAS-*fh*RNAi-2 transgene [Supplementary table 2]. We also introduced the GAL80 repressor of GAL4 in order to ensure the healthy maintenance of the stock. The resulting UAS-*fh*RNAi-2/CyO; *actin*-GAL4/TM6B-GAL80 strain was crossed with each of the mutant fly strains or w^{118} as control and the F1 individuals of appropriate genotypes were selected for the motor performance assay.

The motor tests were performed in a semi-automated setup, in the laboratory of Dr. Juan Botas (Baylor College of Medicine, Houston, U.S.A.). Two replicates of fifteen virgin females were tested for each genotype. Each group

was placed in a transparent vial and tapped down. The percentage of them that passed a sensor located at a height of 11.5 cm after 16 seconds was recorded. The values of ten repetitions were averaged for each time point, from day 8 to day 20 after eclosion from the puparium. Ten vials could be tested simultaneously in every round of tapping/recording. Several combinations of sensor heights and recording times were tested and these particular conditions were selected as they provided a clear separation between the FRDA individuals and the controls, and the values obtained for the model flies allowed both improvement to identify suppressors and worsening to identify enhancers.

According to the results of the motor performance tests, the mutant alleles were classified as not changing, enhancers or suppressors of the motor performance phenotype. Network analysis revealed enrichment in members of the TOR (Target of Rapamycin) pathway and metal homeostasis among the hits of the genetic screen, and therefore they were selected for further study.

3.1. The TORC1 pathway genetically interacts with frataxin (Calap-Quintana *et al*. 2015, figure 1)

The TORC1 (Target of Rapamycin Complex 1) pathway integrates intracellular and extracellular signals of nutrient availability and serves as a central regulator of cell metabolism, growth, proliferation and survival. TORC1 is a complex with kinase activity that phosphorylates substrates that promote anabolic processes including mRNA translation and lipid synthesis, and limit catabolic processes such as autophagy. TORC1 promotes protein synthesis by activating eIF-4E (eukaryotic translation initiation factor 4E) and the protein kinase S6K. Upstream TORC1, most inputs converge into the TSC1 (Tuberous Sclerosis Complex 1)/TSC2 (Tuberous Sclerosis Complex 2) complex that inhibits the TORC1 stimulator Rheb (the Ras homolog enriched in brain ortholog).

Four genes from the TORC1 pathway were identified as genetic modifiers of the FRDA phenotype in the *Drosophila* model [Figure 1 in Calap-Quintana *et al*., 2015]. Knockdown of *Tsc1* induced semi-lethality when combined with

frataxin deficiency but not on control flies. A constitutively active allele of *S6K* was also an enhancer by inducing semi-lethality, whereas a dominant negative allele was a suppressor improving the motor performace of the model flies. Loss of function of *eIF-4E* and knockdown of *Lrrk* (Leucine-rich repeat kinase), an activator of *eIF-4E*, were suppressors of the motor phenotype too. Taken together these results indicate that genetic inhibition of the TORC1 pathway ameliorates FRDA related phenotypes in *Drosophila*.

At this point, we formulated several hypotheses to explain the beneficial effect of the inhibition of TORC1 pathway in the context of frataxin depletion and the subsequent biochemical pathogenesis. Downregulation of TOR is known to lead to an extension of the lifespan (Vellai *et al*. 2003; Kapahi *et al*. 2004; Kaeberlein *et al*. 2005; Harrison *et al*. 2009) and shows a protective effect against aging and neurodegeneration. Inhibition of the negative regulator of autophagy TOR would induce autophagic degradation of protein aggregates and clearance of damaged organelles, and has been proposed for the treatment of neurodegenerative disorders such as Huntington disease, Alzheimer's disease or Parkinson's disease (reviewed in Nixon 2013). Furthermore, TOR signaling pathway is a sensor for different types of stress including oxidative insults and inhibition of the pathway provides resistance to oxidative stress (Tettweiler *et al*. 2005; Patel and Tamanoi 2006) and increases the expression of genes participating in free radical scavenging (Kofman *et al*. 2012; Robida-Stubbs *et al*. 2012).

The initial identification of TORC1 as a genetic interactor in FRDA led to further investigating its role in the disease pathogenesis and the therapeutic use of inhibitors of the pathway such as rapamycin in the *Drosophila* model (Calap-Quintana *et al*. 2015).

3.2. Metal homeostasis pathways genetically interact with frataxin (Soriano *et al*., sent for publication)

Due to the involvement of iron in the pathophysiology of the FRDA, genes implicated in metal homeostasis were included in the candidate list for the genetic screen [Supplementary table 1]. In this work, we evaluated an

additional phenotype for the identification of modifiers, which was a defective external eye development in the *GMR*-GAL4>UAS-*fh*RNA-1 flies. Supplementary table 2 shows the crosses established in order to obtain this strain used for the genetic screen. After evaluating the eye phenotype, we tested the motor performance of *actin*-Gal4>UAS-*fh*RNA-2 flies to identify high confidence modifiers.

Reduced expression of the Iron Regulatory Proteins Irp-1A and Irp-1B rescued the eye and the motor performance phenotypes of the FRDA fly model. The iron transporters *Malvolio* (*Mvl*) and the transferrins *Tsf1* and *Tsf3* are regulated by the IRPs and were also suppressors of both phenotypes when their expression was reduced. It has been proposed that the mitochondrial iron overload in FRDA is coupled with a cytosolic iron depletion due to an increase in IRP binding activity (Li *et al*. 2008). We suggest that this toxic effect might be suppressed by the reduced expression of the IRPs or their downstream targets. This is in agreement with the reduction in Irp-1A expression in iron overload conditions found on the fhRNAi-2 model, which was explained as cellular response against the prolonged IRP binding (Navarro *et al*. 2015).

Interestingly, we identified suppressors involved in the homeostasis of other metals besides iron. Knockdown of six zinc transporters (*Zip42C.1*, *Zip42C.2*, *Zip88E*, *ZnT35C*, *ZnT41F* and *ZnT63C*) as well as a copper chaperone (*Atox1*) and a copper transporter (*dCutC*) ameliorated the FDRA phenotypes. The Metal-responsive Transcription Factor-1 (*MTF-1*), a master transcriptional regulator of metal detoxification, also improved the eye and motor deficits by overexpression. However, the metallothioneins *MtnA*, *MtnB* and *MtnC* that are target genes of MTF-1, were identified as suppressors when their expression was reduced. This indicates that the recovery induced by overexpression of MTF-1 is mediated by transcriptional targets different from the metallothioneins, and might support the pro-oxidant effect that has been suggested for this protein family (Suzuki *et al*. 1996).

As a result of the genetic screen, we also showed a novel participation of zinc and copper transporters as suppressors of FRDA phenotypes. This finding

was followed by the study of the metal levels and the effect of zinc and copper chelators in the *Drosophila* model.

4. Metal accumulation in the FRDA model in *Drosophila* (Soriano *et al*., sent for publication)

Changes in the distribution of iron, copper and zinc were characterized in the dentate nucleus of FRDA post-mortem brain samples (Koeppen *et al*. 2012). Although Koeppen *et al.* did not find a significant increase in the levels of metals in the dentate nucleus or the dorsal root ganglia of patients (Koeppen *et al*. 2012; Koeppen *et al*. 2013), the total levels of iron, zinc, copper and manganese are increased in the *actin*-GAL4>*fh*RNAi-2 flies. Furthermore, the zinc chelator TPEN (N,N,N',N'-tetrakis(2-pyridinylmethyl)-1,2-ethanediamine) and the copper chelators TTM (Tetrathiomolybdate) and BCS (Bathocuproine disulphonate) improved the climbing ability of the FRDA model flies.

Finally, we investigated the mechanisms by which the genes implicated in metal homeostasis identified in the genetic screen were suppressing the FRDA phenotypes. In order to do that, we studied their effect on the iron accumulation displayed by the *fh*RNAi flies. Genetic reduction of *Mvl*, *Tsf1*, *Tsf3* and *Irp1B* that improved the defects in the eye morphology and the motor impairment, also induced a reduction of the total iron levels. We also found that reduced expression of the zinc transporters *ZnT41F* and *fear of intimacy* (*foi*) and overexpression of MTF-1 rescued the iron accumulation, whereas knocking-down *MtnA* had no effect. As the metallothioneins had been proposed to generate hydroxyl radicals in oxidative stress conditions (Suzuki *et al*. 1996), we hypothesized that the rescue of the FRDA phenotypes induced by knockdown of the *Mtn* could be explained by a reduction in the increased levels of oxidative stress of the *fh*RNAi flies. The levels of MDA+HAE, indicators of oxidative stress, were indeed reduced by *MtnA* knockdown and by *MTF-1* overexpression.

Taking these findings together with the results of the genetic screen, we have identified metal homeostasis as a pathway implicated in FRDA pathogenesis and zinc and copper chelation as potential disease treatments. The transcription factor MTF-1 appears to be an interesting therapeutic target for FRDA as it recovers several phenotypes including the motor performance, the iron accumulation and the increase in oxidative stress in the *Drosophila* model.

The *Drosophila* models of FRDA used in this work had been previously generated and their initial characterization showed that they could reproduce a variety of aspects of the disease, at the molecular, cellular, tissue and behavioral levels (Anderson *et al*. 2005; Llorens *et al*. 2007). The model established in our laboratory is of special relevance since it closer to the situation encountered in the patients with frataxin levels that are compatible with adult viability. In subsequent publications, the FRDA models in *Drosophila* provided further insight on the function of frataxin and the pathogenesis of the disease (Anderson *et al*. 2008; Navarro *et al*. 2010; Soriano *et al*. 2013; Calap-Quintana *et al*. 2015; Navarro *et al*. 2015).

Specifically, the candidate-based genetic screen presented here identifies the TORC1 pathway and metal homeostasis to be implicated in FRDA. The exact role of frataxin and how its deficiency produces the pathological features of the disease are not yet fully understood [Introduction, sections 3.2 and 4]. In this context, the identification of interacting pathways can shed some light for its clarification, in addition to revealing new therapeutic targets. In that sense, our results suggest possible treatments for FRDA in the form of inhibition of TOR with rapamycin or other rapalogs, and copper and zinc chelation.

More generally, we have validated the use of the *Drosophila* models of FRDA for drug discovery by reproducing the positive effects of idebenone and deferiprone seen in patients. Although at present there is no cure or effective treatment for the disease, there are several treatments in different phases of pre-clinical research and clinical trials [Introduction, section 5]. However, compounds that yielded promising results in the initial clinical tests for FRDA

had to be later discarded due to a lack of consistency of the results. Moreover, the lack of frataxin triggers a high number of molecular disturbances and a complex pathophysiology that give rise to both neurological and non-neurological symptoms. The drugs developed for the treatment of FRDA are frequently directed to a single molecular feature of the disease and the effect on the patients is far from being a cure, and in most cases consists in stabilizing, slowing the progression or slightly improving some of the symptoms. Similarly to other diseases of equal complexity, we can anticipate that the treatment for FRDA will probably come in the form of combined therapy. In any case, it is crucial to continue with the identification of new therapeutic compounds for FRDA and we propose that the models in *Drosophila* constitute a valuable tool for this process.

Drosophila is in an exceptional situation among the model organisms [Introduction, section 7.1]. The fly has a complex nervous system contrary to the cellular models, and a faster generation time and lower maintenance cost than the murine models. These features together with the variety of genetic tools available enable the design of large-scale screens. The present work takes advantage for the first time of this feature of *Drosophila* in order to carry out a candidate-based genetic screen in the fly models of FRDA, and validates their use for future large-scale unbiased genetic and drug screens. However, the findings generated in the *Drosophila* models have to be taking cautiously as the jump up to humans is still big in terms of genetic, molecular and physiological complexity. This is especially true for the drug discovery process in which going from the first pre-clinical discoveries in lower organisms to a treatment available for the patients has a very low success rate and may take decades.

Supplementary table 1: *Drosophila* strains used in the genetic screen.

Gene anotation	Gene symbol	Gene name	Stock number
CG1081	Rheb	Ras homolog enriched in brain ortholog	B16873
			B22248
			B9688
			B9690
CG1107	aux	auxilin	V103426
CG1210	Pdk1	Phosphoinositide-dependent kinase 1	V18736
CG1216	mri	mrityu	V101345
CG1227	CG1227		V105610
CG1241	Atg2	Autophagy-related 2	V108447
CG1275			B17162
CG1417	slgA	sluggish A	V101449
			B27907
			B42153
CG1469	Fer2LCH	Ferritin 2 light chain homologue	V14491
			V106960
CG1516	PCB	Pyruvate carboxylase	V41577
			V105936
			B35985
CG1594	hop	hopscotch	V102830
CG1643	Atg5	Autophagy-related 5	V104461
CG1721	Pglym78	Phosphoglyceromutase	B30063
CG1765	EcR	Ecdysone receptor	V37058
CG1848	LIMK1	LIM-kinase1	V25343
			B17491
			B9116
			B9117
			B9240
CG1886	ATP7	ATP7	B10114
			B16866
			V108159
			V8315

CG1951	CG1951		V33431
CG2056	spirit	Serine Protease Inmune Response Integrator	V107936
CG2171	Tpi	Triose phosphate isomerase	V25643
			B16563
CG2177	Zip102B	Zinc/iron regulated transporter-related protein 102B	V51083
CG2216	Fer1HCH	Ferritin 1 heavy chain homologue	V49536
			V102406
CG2286	ND-75	NADH dehydrogenase (ubiquinone) 75 kDa subunit	V52047
			V100733
CG2330	Neuroch ondrin	Neurochondrin	V46555
			V109002
CG2621	sgg	shaggy	V101538
CG2720	Hop	Hsp70/Hsp90 organizing protein homolog	V41696
			V105658
			B17166
CG2846	CG2846		V100266
CG3051	AMPKα	AMP-activated protein kinase α subunit	V106200
CG3127	Pgk	Phosphoglycerate kinase	V33798
			B15113
			B14487
CG3143	foxo	forkhead box, sub-group O	B20279
			B32699
			B9575
			B38644
			B42220
			B42221
			B43633
			B44214
CG3200	Reg-2	Rhythmically expressed gene 2	V14125
			V107185
			B29999
CG3481	Adh	Alcohol dehydrogenase	V50970
			B13997
			B12535

CG3609	CG3609		V52600
			V108742
			B27094
			B18024
			B18037
CG3666	Tsf3	Transferrin 3	V108470
CG3671	Mvl	Malvolio	B14419
			B19886
			B5151
			V109434
			V44000
CG3738	Cks30A	Cyclin-dependent kinase subunit 30A	V108401
CG3743	MTF-1	Metal response element-binding Transcription Factor-1	B16580
			B9241
			V107124
			tub-MTF-1*
CG3821	Aats-asp	Aspartyl-tRNA synthetase	V7750
			B5552
			B13265
CG3837	Sdr	Secreted decoy of InR	V105549
CG3861	kdn	knockdown	V26302
			V107642
			B38093
			B14436
CG3915	Drl-2	Derailed-2	V102192
CG3964	CG3964		V38983
			V102197
			B12450
CG3977	Ctr1A	Copper transporter 1A	B11243
			B29641
			V46757
CG3994	ZnT35C	Zinc transporter 35C	B26138
			V103263
			V3836
CG4001	Pfk	Phosphofructokinase	V105666

CG4006	Akt1	Akt1	B50758
			V103703
CG4035	eIF-4E	Eukaryotic initiation factor 4E	B2470
			B8648
			B8650
			B8654
			B8655
			B8710
CG4141	Pi3K92E	Pi3K92E	V107390
			V38985
CG4157	Rpn12	Regulatory particle non-ATPase 12	V21799
			B20583
CG4205	Fdx1	Ferredoxin 1	V104499
			V24497
CG4217	TFAM	mitochondrial transcription factor A	V37819
			V107191
			B10713
CG4225	Hmt-1	Heavy metal tolerance factor 1	B22259
			V108877
			V37356
CG4233	Got2	Glutamate oxaloacetate transaminase 2	V26452
			V106120
			B4002
			B4003
CG4312	MtnB	Metallothionein B	V106118
CG4334	Zip88E	Zinc/iron regulated transporter-related protein 88E	B20270
			V106785
			V49329
CG4349	Fer3HCH	Ferritin 3 heavy chain homologue	V40505
CG4379	Pka-C1	Protein kinase, cAMP-dependent, catalytic subunit 1	V101524
CG4460	Hsp22	Heat shock protein 22	V43632
			B20055
CG4900	Irp-1A	Iron regulatory protein 1A	B30181
			V105583
CG4926	Ror	Ror	V29930

CG4963	mfrn	mitoferrin	B19811
			V12342
CG4973	mdlc	midlife crisis	V42015
			V110421
CG5025	Sps2	Selenophosphate synthetase 2	V105268
CG5092	Tor	Target of rapamycin	B11218
			B7014
			B25363
			B7012
			B7013
CG5097	MtnC	Metallothionein C	V109945
			V35817
CG5122	CG5122		V27358
CG5130	ZnT77C	Zinc transporter 77C	B20726
			V5390
CG5165	Pgm	phosphoglucose mutase	V34954
			V105820
			B4039
			B22244
CG5373	Pi3k59F	Phosphotidylinositol 3 kinase 59F	V100296
CG5429	Atg6	Autophagy-related 6	B11487
			V110197
			V22123
CG5483	Lrrk	Leucine-rich repeat kinase	B34750
			V22139
			V105630
CG5489	Atg7	Autophagy-related 7	B17635
			V45558
CG5671	Pten	Phosphatase and tensin homolog	V101475
			V35731
CG5730	AnxB9	Annexin B9	V106867
			B16880
CG5733	Nup75	Nucleoporin 75kD	V27495
CG5959	MCO3	multicopper oxidase 3	B16349
			V43288

CG5974	pll	pelle	V103774
CG6030	ATPsynD	ATP synthase, subunit D	V104353
			B16696
			B35060
CG6042	Cyp12a4	Cyp12a4	V49492
			V107088
			B18342
CG6058	Ald	Aldolase	V47667
			B20862
			B34186
			V101339
CG6092	Dak1	Dak1	V104861
CG6114	sff	sugar-free frosting	V100717
CG6136	(CutC)		B18087
			B22000
			V109421
			V22238
CG6147	Tsc1	Tsc1	B18488
			V110811
			V22252
CG6186	Tsf1	Transferrin 1	V106479
			V14666
			B18838
CG6194	Atg4b	Autophagy-related 4b	V108299
			V22294
CG6297	JIL-1	JIL-1 kinase	V107001
CG6342	Irp-1B	Iron regulatory protein 1B	B14849
			B21822
			V110637
			V30153
CG6543	CG6543		V27658
			B20026
CG6672	ZnT86D	Zinc transporter 86D	V107388
CG6803	Mf	Myofilin	V34186
			V102458

CG6817	foi	fear-of-intimacy	B10171
			B17838
			B34103
			V10102
CG6877	Atg3	Autophagy-related 3	V22455
CG6898	Zip89B	Zinc/iron regulated transporter-related protein 89B	B15505
			B32954
CG6975	gig	gigas	B26386
			B27142
			V103417
			V6313
CG6998	ctp	cut up	V109084
CG7010	l(1)G0334	lethal (1) G0334	V40410
			V107209
			B14513
CG7028	CG7028		V107042
CG7094	CG7094		V108273
CG7176	Idh	Isocitrate dehydrogenase	V42915
			V100554
			B20183
			B4019
			B4020
			B12211
CG7331	Atg13	Autophagy-related 13	B30169
			V103381
			V27956
CG7390	smp-30	Senescence marker protein-30	V35230
			V103377
CG7445	fln	flightin	V46153
			V101988
CG7459	Ctr1B	Copper transporter 1B	B21959
			B29019
			B29020
			V5804
			UAS-Ctr1B*

CG7470	CG7470		V38955
			V101476
CG7478	Act79B	Actin 79B	V102588
CG7524	Src64b	Src oncogene at 64b	V35252
CG7610	ATPsynγ	ATP synthase, γ subunit	V16539
			B15641
CG7816	Zip99C	Zinc/iron regulated transporter-related protein 99C	B10395
			B18311
			B18595
			V1362
CG7920	CG7920		B15298
			B15648
CG7986	Atg18a	Autophagy-related 18a	B13945
			V105366
			V22643
CG8094	Hex-C	Hexokinase C	V35388
CG8193	PPO2	Prophenoloxidase 2	V26941
			V107772
			B25223
CG8251	Pgi	Phosphoglucose isomerase	B17595
CG8256	Gpo-1	Glycerophosphate oxidase-1	V19565
			B4902
			B10577
			B22315
CG8363	Papss	PAPS synthetase	V35904
CG8454	Vps16A	Vacuolar protein sorting 16A	V23769
CG8632	ZnT49B	Zinc transporter 49B	B29476
			V108929
			V4654
CG8846	Thor	Thor	B11481
			B24854
			B8649
			B9147
			B9558
			B9559

CG8866	CG8866		V103725
CG8885	Scox	Synthesis of cytochrome c oxidase	B16652
			B29505
			V100005
			V7861
CG8893	Gapdh2	Glyceraldehyde 3 phosphate dehydrogenase 2	V50351
			B19967
			B19295
CG8967	otk	off-track	V104688
CG9065	(Cox17)		B32633
			V108483
			V29839
CG9244	Acon	aconitase	V11767
			V103809
CG9285	Dip-B	Dipeptidase B	V6296
			B20098
CG9391	CG9391		V23725
			B16929
CG9428	Zip42C.1	Zinc/iron regulated transporter-related protein 42C.1	V107309
			V3987
CG9430	Zip42C.2	Zinc/iron regulated transporter-related protein 42C.2	V110047
			V7338
CG9470	MtnA	Metallothionein A	V105011
			V46119
CG9475	Rpt3R	Regulatory particle triple-A ATPase 3-related	V110309
			B16849
CG9746	Vps15	Vacuolar protein sorting 15	V110706
CG9765	tacc	transforming acidic coiled-coil protein	V110633
			B15521
			B16881
			B37343
CG9914	CG9914		V29322
			V106649
			B26582
CG9961	CG9961		V101702

CG10006	Zip71B	Zinc/iron regulated transporter-related protein 71B	B13470
			V44538
CG10026	CG10026		V46016
			V107452
			B19177
CG10260	PI4KIIIα	Phosphatidylinositol 4-kinase III α	V105614
CG10449	Catsup	Catecholamines up	B10572
			B3987
			V100095
CG10505	CG10505		V107842
			V6593
CG10539	S6K	Ribosomal protein S6 kinase	B11713
			B6911
			B6914
			V104369
CG10572	Cdk8	Cyclin-dependent kinase 8	V107187
CG10620	Tsf2	Transferrin 2	B13452
			V5236
CG10691	l(2)37Cc	lethal (2) 37Cc	V12360
			B16326
			B3395
			B5389
			B5390
			B5391
CG10861	Atg12	Autophagy-related 12	V29791
CG10863	CG10863		V48618
			V103433
			B13483
			B20108
			B33288
CG10967	Atg1	Autophagy-related 1	B11494
			V16133
CG10992	CtsB1	Cathepsin B1	V45345
			V108315
			B15434

CG11059	Cals	Calsyntenin-1	V37291
			V105111
			B11279
CG11143	Inos	Inos	V5617
			V100763
			B14921
CG11154	ATPsynβ	ATP synthase, β subunit	V37812
			B14642
CG11163	ZnT41F	Zinc transporter 41F	B13098
			B19952
			B38183
			V107931
			V13311
CG11221	CG11221		V100163
CG11299	Sesn	Sestrin	V38481
CG11324	homer	homer	V18061
			V100271
			B17027
			B9564
CG11489	Srpk79D	Serine-arginine protein kinase at 79D	V102632
CG11491	br	broad	V104648
CG11660	RIOK	RIO kinase 1	
CG11821	Cyp12a5	Cyp12a5	B41082
			V103961
			V26796
CG12055	Gapdh1	Glyceraldehyde 3 phosphate dehydrogenase 1	B26984
CG12101	Hsp60	Heat shock protein 60	V100697
			B15361
			B4686
			B4689
CG12140	Etf-QO	Electron transfer flavoprotein-ubiquinone oxidoreductase	V15508
			V110540
			B18892
CG12147	CG12147		V101875

CG12230	car	carnation	V110756
			V4548
CG12244	lic	licorne	V106822
CG12295	stj	straightjacket	V108569
			B34109
			B11004
CG12362	CG12362		V31746
			V103218
			B42404
CG12375	CG12375		V45309
			V108253
			B27449
CG13189	Zip48C	Zinc/iron regulated transporter-related protein 48C	V105650
CG13850	CG13850		V100863
CG13922	mRpL46	mitochondrial ribosomal protein L46	V41516
			V110327
			B29676
CG14217	Tao	Tao	V107645
			V17432
CG14895	Pak3	Pak3	V107260
CG14992	Ack	Activated Cdc42 kinase	V39857
CG15224	CkIIβ	Casein kinase II β subunit	V106845
CG15551	Ctr1C	Copper transporter 1C	V102136
			V10263
CG17256	Nek2	Nek2	V103408
CG17534	GstE9	Glutathione S transferase E9	V32947
CG17645	Pglym87	Pglym87	V41658
CG17698	CG17698		V105884
CG17723	ZnT63C	Zinc transporter 63C	B10496
			B31851
			B37196
			V105145
			V7461
CG17753	Ccs	Copper chaperone for superoxide dismutase	B14068
			B24755

CG17753	Ccs	Copper chaperone for superoxide dismutase	V108665
			V20536
CG18734	Fur2	Furin 2	V101242
CG30021	metro	menage a trois	V29965
CG31038	CG31038		V25655
			V110531
CG31431	CG31431		V104697
CG31860	ZnT33D	Zinc transporter 33D	B26425
			V103398
			V7688
CG32180	Eip74EF	Ecdysone-induced protein 74EF	V105301
CG32315	dlt	discs lost	V41876
			V103709
			B10160
CG32446	Atox1		B18361
			B21158
			B34166
			V104437
			V23057
CG32592	hiw	highwire	V36085
CG32672	Atg8a	Autophagy-related 8a	B10107
			B14639
CG32703	Erk7	Extracellularly regulated kinase 7	V33522
CG33138	AGBE	1,4-Alpha-Glucan Branching Enzyme	V43781
			B17488
CG33338	p38c	p38c MAP kinase	V105173
CG33970	CG33970		V33090
			V101855
			B22850
			B37666
CG34123	trpm	Transient receptor potential cation channel, subfamily M	B15365
			B38037
			V107537
			V30610
CG34384	CG34384		V102481

CG43286	cnc	cap-n-collar	B13550
			B17502
			B38631
	Mtn A, B, C, D	Metallothioneins	qMT*

*Strains kindly provided by Dr. Burke from University of Monash, Australia. Stock numbers starting with “V” were obtained from the Vienna Drosophila Resource Center and the ones starting with “B” from the Bloomington Stock Center, Indiana University.

Supplementary table 2: Diagram of the crosses established to obtain the lines used in the genetic screens.

I – Screen with motor performance phenotype			
P_{1A}	♀ *fh*RNAi-2 / *fh*RNAi-2 ; + / +	X	♂ *Gla Bc* / CyO ; TM2 / TM6B
F_{1A}	Selection of ♂ *fh*RNAi-2 / *Gla Bc* ; TM2 / +		
P_{1B}	♀ + / + ; *actin*-GAL4 / +	X	♂ *Gla Bc* / CyO ; TM2 / TM6B
F_{1B}	Selection of ♀ CyO / + ; *actin*-GAL4 / TM6B		
F_{1A} X F_{1B}	♀ CyO / + ; *actin*-GAL4 / TM6B	X	♂ *fh*RNAi-2 / *Gla Bc* ; TM2 / +
F_{2A}	Selection of ♂ *fh*RNAi-2 / CyO ; *actin*-GAL4 / TM2		
P_{2B}	♀ CyO / + ; TM6B , tub-GAL80 / +	X	♂ *fh*RNAi-2 / *fh*RNAi-2 ; + / +
F_{2B}	Selection of ♀ *fh*RNAi-2 / CyO ; TM6B , tub-GAL80 / +		
F_{2A} X F_{2B}	♀ *fh*RNAi-2 / CyO ; TM6B , tub-GAL80 / +	X	♂ *fh*RNAi-2 / CyO ; *actin*-GAL4 / TM2
F_3 X F_3	Selection of ♀ and ♂ *fh*RNAi-2 / *fh*RNAi-2 ; *actin*-GAL4 / TM6B , tub-GAL80 that are crossed in order to establish the line		
II – Screen with rough eye phenotype			
P_1	♀ *GMR*-GAL4 / *GMR*-GAL4	X	♂ *fh*RNAi-1 / *fh*RNAi-1
F_1	Selection of ♀ *fh*RNAi-1 / *GMR*-GAL4		
P_2	♀ *fh*RNAi-1 / *GMR*-GAL4	X	♂ w^{118} / ¬ ; + / +
F_2	Selection of recombinant ♂ *fh*RNAi-1 ::: *GMR*-GAL4 / + with rough eye phenotype		
P_3	♀ *fh*RNAi-1 ::: *GMR*-GAL4 / +	X	♂ CyO / +
F_3	Selection of ♀ and ♂ *fh*RNAi-1 ::: *GMR*-GAL4 / CyO that are crossed in order to establish the line		

Conclusions

1. Expression of human FXN rescues the impaired aconitase activity produced by the loss of endogenous frataxin in *Drosophila*, indicating a functional equivalence for both proteins.

2. The iron chelator Deferiprone improves frataxin knockdown phenotypes (lifespan and motor capabilities) in the *Drosophila* model of FRDA by chelating mitochondrial iron.

3. The antioxidant Idebenone improves FRDA-like phenotypes in the *Drosophila* model and recovers the reduction of aconitase activity under hyperoxia.

4. The levels of zinc, copper, manganese and aluminum are increased in the *Drosophila* model of FRDA, and zinc and copper chelation ameliorate the motor performance phenotype induced by frataxin knockdown.

5. Genetic reduction of iron, zinc and copper transport and overexpression of the transcription factor MTF-1 improve FRDA phenotypes in the *Drosophila* model.

6. Members of the TOR pathway Tsc1, S6K, Lrrk and eIF-4E genetically interact with frataxin, indicating that a genetic reduction in TORC1 signaling activity suppresses the impaired motor performance of the FRDA flies.

References

Acquaviva F, Castaldo I, Filla A, Giacchetti M, Marmolino D, Monticelli A, Pinelli M, Saccà F, Cocozza S. 2008. Recombinant human erythropoietin increases frataxin protein expression without increasing mRNA expression. Cerebellum Lond. Engl. 7:360–365.

Acquaviva F, De Biase I, Nezi L, Ruggiero G, Tatangelo F, Pisano C, Monticelli A, Garbi C, Acquaviva AM, Cocozza S. 2005. Extra-mitochondrial localisation of frataxin and its association with IscU1 during enterocyte-like differentiation of the human colon adenocarcinoma cell line Caco-2. J. Cell Sci. 118:3917–3924.

Adamec J, Rusnak F, Owen WG, Naylor S, Benson LM, Gacy AM, Isaya G. 2000. Iron-dependent self-assembly of recombinant yeast frataxin: implications for Friedreich ataxia. Am. J. Hum. Genet. 67:549–562.

Adams MD, Celniker SE, Holt RA, Evans CA, Gocayne JD, Amanatides PG, Scherer SE, Li PW, Hoskins RA, Galle RF, et al. 2000. The Genome Sequence of Drosophila melanogaster. Science 287:2185–2195.

Adinolfi S, Iannuzzi C, Prischi F, Pastore C, Iametti S, Martin SR, Bonomi F, Pastore A. 2009. Bacterial frataxin CyaY is the gatekeeper of iron-sulfur cluster formation catalyzed by IscS. Nat. Struct. Mol. Biol. 16:390–396.

Adinolfi S, Trifuoggi M, Politou AS, Martin S, Pastore A. 2002. A structural approach to understanding the iron-binding properties of phylogenetically different frataxins. Hum. Mol. Genet. 11:1865–1877.

Al-Mahdawi S, Pinto RM, Varshney D, Lawrence L, Lowrie MB, Hughes S, Webster Z, Blake J, Cooper JM, King R, et al. 2006. GAA repeat expansion mutation mouse models of Friedreich ataxia exhibit oxidative stress leading to progressive neuronal and cardiac pathology. Genomics 88:580–590.

Anderson PR, Kirby K, Hilliker AJ, Phillips JP. 2005. RNAi-mediated suppression of the mitochondrial iron chaperone, frataxin, in Drosophila. Hum. Mol. Genet. 14:3397–3405.

Anderson PR, Kirby K, Orr WC, Hilliker AJ, Phillips JP. 2008. Hydrogen peroxide scavenging rescues frataxin deficiency in a Drosophila model of Friedreich's ataxia. Proc. Natl. Acad. Sci. U. S. A. 105:611–616.

Anjomani Virmouni S, Ezzatizadeh V, Sandi C, Sandi M, Al-Mahdawi S, Chutake Y, Pook MA. 2015. A novel GAA-repeat-expansion-based mouse model of Friedreich's ataxia. Dis. Model. Mech. 8:225–235.

Auchère F, Santos R, Planamente S, Lesuisse E, Camadro J-M. 2008. Glutathione-dependent redox status of frataxin-deficient cells in a yeast model of Friedreich's ataxia. Hum. Mol. Genet. 17:2790–2802.

Babcock M, de Silva D, Oaks R, Davis-Kaplan S, Jiralerspong S, Montermini L, Pandolfo M, Kaplan J. 1997. Regulation of mitochondrial iron accumulation by Yfh1p, a putative homolog of frataxin. Science 276:1709–1712.

Bayot A, Santos R, Camadro J-M, Rustin P. 2011. Friedreich's ataxia: the vicious circle hypothesis revisited. BMC Med. 9:112.

Bencze KZ, Kondapalli KC, Cook JD, McMahon S, Millán-Pacheco C, Pastor N, Stemmler TL. 2006. The structure and function of frataxin. Crit. Rev. Biochem. Mol. Biol. 41:269–291.

Bodai L, Pallos J, Thompson LM, Marsh JL. 2003. Altered protein acetylation in polyglutamine diseases. Curr. Med. Chem. 10:2577–2587.

Boddaert N, Le Quan Sang KH, Rötig A, Leroy-Willig A, Gallet S, Brunelle F, Sidi D, Thalabard J-C, Munnich A, Cabantchik ZI. 2007. Selective iron chelation in Friedreich ataxia: biologic and clinical implications. Blood 110:401–408.

Boesch S, Nachbauer W, Mariotti C, Sacca F, Filla A, Klockgether T, Klopstock T, Schöls L, Jacobi H, Büchner B, et al. 2014. Safety and tolerability of carbamylated erythropoietin in Friedreich's ataxia. Mov. Disord. Off. J. Mov. Disord. Soc. 29:935–939.

Boesch S, Sturm B, Hering S, Scheiber-Mojdehkar B, Steinkellner H, Goldenberg H, Poewe W. 2008. Neurological effects of recombinant human erythropoietin in Friedreich's ataxia: a clinical pilot trial. Mov. Disord. Off. J. Mov. Disord. Soc. 23:1940–1944.

Bolinches-Amorós A, Mollá B, Pla-Martín D, Palau F, González-Cabo P. 2014. Mitochondrial dysfunction induced by frataxin deficiency is associated with cellular senescence and abnormal calcium metabolism. Front. Cell. Neurosci. 8:124.

Bradley JL, Blake JC, Chamberlain S, Thomas PK, Cooper JM, Schapira AH. 2000. Clinical, biochemical and molecular genetic correlations in Friedreich's ataxia. Hum. Mol. Genet. 9:275–282.

Brand AH, Perrimon N. 1993. Targeted gene expression as a means of altering cell fates and generating dominant phenotypes. Dev. Camb. Engl. 118:401–415.

Bridwell-Rabb J, Fox NG, Tsai C-L, Winn AM, Barondeau DP. 2014. Human frataxin activates Fe-S cluster biosynthesis by facilitating sulfur transfer chemistry. Biochemistry (Mosc.) 53:4904–4913.

Bulteau A-L, O'Neill HA, Kennedy MC, Ikeda-Saito M, Isaya G, Szweda LI. 2004. Frataxin acts as an iron chaperone protein to modulate mitochondrial aconitase activity. Science 305:242–245.

Bulteau AL, Planamente S, Jornea L, Dur A, Lesuisse E, Camadro JM, Auchère F. 2012. Changes in mitochondrial glutathione levels and protein thiol oxidation in Δyfh1 yeast cells and the lymphoblasts of patients with Friedreich's ataxia. Biochim. Biophys. Acta 1822:212–225.

Calap-Quintana P, Soriano S, Llorens JV, Al-Ramahi I, Botas J, Moltó MD, Martínez-Sebastián MJ. 2015. TORC1 Inhibition by Rapamycin Promotes Antioxidant Defences in a Drosophila Model of Friedreich's Ataxia. PloS One 10:e0132376.

Calmels N, Schmucker S, Wattenhofer-Donzé M, Martelli A, Vaucamps N, Reutenauer L, Messaddeq N, Bouton C, Koenig M, Puccio H. 2009. The first cellular models based on frataxin missense mutations that reproduce spontaneously the defects associated with Friedreich ataxia. PloS One 4:e6379.

Campuzano V, Montermini L, Lutz Y, Cova L, Hindelang C, Jiralerspong S, Trottier Y, Kish SJ, Faucheux B, Trouillas P, et al. 1997. Frataxin is reduced in Friedreich ataxia patients and is associated with mitochondrial membranes. Hum. Mol. Genet. 6:1771–1780.

Campuzano V, Montermini L, Moltò MD, Pianese L, Cossée M, Cavalcanti F, Monros E, Rodius F, Duclos F, Monticelli A, et al. 1996. Friedreich's ataxia: autosomal recessive disease caused by an intronic GAA triplet repeat expansion. Science 271:1423–1427.

Cañizares J, Blanca JM, Navarro JA, Monrós E, Palau F, Moltó MD. 2000. dfh is a Drosophila homolog of the Friedreich's ataxia disease gene. Gene 256:35–42.

Cavadini P, Gellera C, Patel PI, Isaya G. 2000. Human frataxin maintains mitochondrial iron homeostasis in Saccharomyces cerevisiae. Hum. Mol. Genet. 9:2523–2530.

Cavadini P, O'Neill HA, Benada O, Isaya G. 2002. Assembly and iron-binding properties of human frataxin, the protein deficient in Friedreich ataxia. Hum. Mol. Genet. 11:217–227.

Chan PK, Torres R, Yandim C, Law PP, Khadayate S, Mauri M, Grosan C, Chapman-Rothe N, Giunti P, Pook M, et al. 2013. Heterochromatinization induced by GAA-repeat hyperexpansion in Friedreich's ataxia can be reduced upon HDAC inhibition by vitamin B3. Hum. Mol. Genet. 22:2662–2675.

Chen OS, Hemenway S, Kaplan J. 2002. Inhibition of Fe-S cluster biosynthesis decreases mitochondrial iron export: evidence that Yfh1p affects Fe-S cluster synthesis. Proc. Natl. Acad. Sci. U. S. A. 99:12321–12326.

Clark IE, Dodson MW, Jiang C, Cao JH, Huh JR, Seol JH, Yoo SJ, Hay BA, Guo M. 2006. Drosophila pink1 is required for mitochondrial function and interacts genetically with parkin. Nature 441:1162–1166.

Condò I, Malisan F, Guccini I, Serio D, Rufini A, Testi R. 2010. Molecular control of the cytosolic aconitase/IRP1 switch by extramitochondrial frataxin. Hum. Mol. Genet. 19:1221–1229.

Condò I, Ventura N, Malisan F, Rufini A, Tomassini B, Testi R. 2007. In vivo maturation of human frataxin. Hum. Mol. Genet. 16:1534–1540.

Condò I, Ventura N, Malisan F, Tomassini B, Testi R. 2006. A pool of extramitochondrial frataxin that promotes cell survival. J. Biol. Chem. 281:16750–16756.

Coppola G, Choi S-H, Santos MM, Miranda CJ, Tentler D, Wexler EM, Pandolfo M, Geschwind DH. 2006. Gene expression profiling in frataxin deficient mice: microarray evidence for significant expression changes without detectable neurodegeneration. Neurobiol. Dis. 22:302–311.

Cossée M, Dürr A, Schmitt M, Dahl N, Trouillas P, Allinson P, Kostrzewa M, Nivelon-Chevallier A, Gustavson KH, Kohlschütter A, et al. 1999. Friedreich's ataxia: point mutations and clinical presentation of compound heterozygotes. Ann. Neurol. 45:200–206.

Cossée M, Puccio H, Gansmuller A, Koutnikova H, Dierich A, LeMeur M, Fischbeck K, Dollé P, Koenig M. 2000. Inactivation of the Friedreich ataxia mouse gene leads to early embryonic lethality without iron accumulation. Hum. Mol. Genet. 9:1219–1226.

Cossée M, Schmitt M, Campuzano V, Reutenauer L, Moutou C, Mandel JL, Koenig M. 1997. Evolution of the Friedreich's ataxia trinucleotide repeat expansion: founder effect and premutations. Proc. Natl. Acad. Sci. U. S. A. 94:7452–7457.

De Biase I, Rasmussen A, Monticelli A, Al-Mahdawi S, Pook M, Cocozza S, Bidichandani SI. 2007. Somatic instability of the expanded GAA triplet-repeat sequence in Friedreich ataxia progresses throughout life. Genomics 90:1–5.

Del Gaizo V, MacKenzie JA, Payne RM. 2003. Targeting proteins to mitochondria using TAT. Mol. Genet. Metab. 80:170–180.

Dhe-Paganon S, Shigeta R, Chi YI, Ristow M, Shoelson SE. 2000. Crystal structure of human frataxin. J. Biol. Chem. 275:30753–30756.

Di Prospero NA, Baker A, Jeffries N, Fischbeck KH. 2007. Neurological effects of high-dose idebenone in patients with Friedreich's ataxia: a randomised, placebo-controlled trial. Lancet Neurol. 6:878–886.

Dürr A, Cossee M, Agid Y, Campuzano V, Mignard C, Penet C, Mandel JL, Brice A, Koenig M. 1996. Clinical and genetic abnormalities in patients with Friedreich's ataxia. N. Engl. J. Med. 335:1169–1175.

Evans-Galea MV, Lockhart PJ, Galea CA, Hannan AJ, Delatycki MB. 2014. Beyond loss of frataxin: the complex molecular pathology of Friedreich ataxia. Discov. Med. 17:25–35.

Feany MB, Bender WW. 2000. A Drosophila model of Parkinson's disease. Nature 404:394–398.

Fernandez-Funez P, Nino-Rosales ML, de Gouyon B, She WC, Luchak JM, Martinez P, Turiegano E, Benito J, Capovilla M, Skinner PJ, et al. 2000. Identification of genes that modify ataxin-1-induced neurodegeneration. Nature 408:101–106.

Ferrante RJ, Kubilus JK, Lee J, Ryu H, Beesen A, Zucker B, Smith K, Kowall NW, Ratan RR, Luthi-Carter R, et al. 2003. Histone deacetylase inhibition by sodium butyrate chemotherapy ameliorates the neurodegenerative phenotype in Huntington's disease mice. J. Neurosci. Off. J. Soc. Neurosci. 23:9418–9427.

Finelli A, Kelkar A, Song H-J, Yang H, Konsolaki M. 2004. A model for studying Alzheimer's Abeta42-induced toxicity in Drosophila melanogaster. Mol. Cell. Neurosci. 26:365–375.

Fleming J, Spinoulas A, Zheng M, Cunningham SC, Ginn SL, McQuilty RC, Rowe PB, Alexander IE. 2005. Partial correction of sensitivity to oxidant stress in Friedreich ataxia patient fibroblasts by frataxin-encoding adeno-associated virus and lentivirus vectors. Hum. Gene Ther. 16:947–956.

Fossgreen A, Brückner B, Czech C, Masters CL, Beyreuther K, Paro R. 1998. Transgenic Drosophila expressing human amyloid precursor protein show gamma-secretase activity and a blistered-wing phenotype. Proc. Natl. Acad. Sci. U. S. A. 95:13703–13708.

Foury F, Pastore A, Trincal M. 2007. Acidic residues of yeast frataxin have an essential role in Fe-S cluster assembly. EMBO Rep. 8:194–199.

Gakh O, Adamec J, Gacy AM, Twesten RD, Owen WG, Isaya G. 2002. Physical evidence that yeast frataxin is an iron storage protein. Biochemistry (Mosc.) 41:6798–6804.

Gavin BA, Dolph MJ, Deleault NR, Geoghegan JC, Khurana V, Feany MB, Dolph PJ, Supattapone S. 2006. Accelerated accumulation of misfolded prion protein and spongiform degeneration in a Drosophila model of Gerstmann-Sträussler-Scheinker syndrome. J. Neurosci. Off. J. Soc. Neurosci. 26:12408–12414.

Gerber J, Mühlenhoff U, Lill R. 2003. An interaction between frataxin and Isu1/Nfs1 that is crucial for Fe/S cluster synthesis on Isu1. EMBO Rep. 4:906–911.

Ghelli A, Porcelli AM, Zanna C, Martinuzzi A, Carelli V, Rugolo M. 2008. Protection against Oxidant-Induced Apoptosis by Exogenous Glutathione in Leber Hereditary Optic Neuropathy Cybrids. Investig. Opthalmology Vis. Sci. 49:671.

Gibson TJ, Koonin EV, Musco G, Pastore A, Bork P. 1996. Friedreich's ataxia protein: phylogenetic evidence for mitochondrial dysfunction. Trends Neurosci. 19:465–468.

Golic KG, Lindquist S. 1989. The FLP recombinase of yeast catalyzes site-specific recombination in the Drosophila genome. Cell 59:499–509.

Gomez-Sebastian S, Gimenez-Cassina A, Diaz-Nido J, Lim F, Wade-Martins R. 2007. Infectious delivery and expression of a 135 kb human FRDA genomic DNA locus complements Friedreich's ataxia deficiency in human cells. Mol. Ther. J. Am. Soc. Gene Ther. 15:248–254.

Goncalves S, Paupe V, Dassa EP, Rustin P. 2008. Deferiprone targets aconitase: implication for Friedreich's ataxia treatment. BMC Neurol. 8:20.

González-Cabo P, Bolinches-Amorós A, Cabello J, Ros S, Moreno S, Baylis HA, Palau F, Vázquez-Manrique RP. 2011. Disruption of the ATP-binding cassette B7 (ABTM-1/ABCB7) induces oxidative stress and premature cell death in Caenorhabditis elegans. J. Biol. Chem. 286:21304–21314.

González-Cabo P, Vázquez-Manrique RP, García-Gimeno MA, Sanz P, Palau F. 2005. Frataxin interacts functionally with mitochondrial electron transport chain proteins. Hum. Mol. Genet. 14:2091–2098.

Grabczyk E, Usdin K. 2000. The GAA*TTC triplet repeat expanded in Friedreich's ataxia impedes transcription elongation by T7 RNA polymerase in a length and supercoil dependent manner. Nucleic Acids Res. 28:2815–2822.

Greene E, Entezam A, Kumari D, Usdin K. 2005. Ancient repeated DNA elements and the regulation of the human frataxin promoter. Genomics 85:221–230.

Greene JC, Whitworth AJ, Kuo I, Andrews LA, Feany MB, Pallanck LJ. 2003. Mitochondrial pathology and apoptotic muscle degeneration in Drosophila parkin mutants. Proc. Natl. Acad. Sci. U. S. A. 100:4078–4083.

Greeve I, Kretzschmar D, Tschäpe J-A, Beyn A, Brellinger C, Schweizer M, Nitsch RM, Reifegerste R. 2004. Age-dependent neurodegeneration and Alzheimer-amyloid plaque formation in transgenic Drosophila. J. Neurosci. Off. J. Soc. Neurosci. 24:3899–3906.

Harrison DE, Strong R, Sharp ZD, Nelson JF, Astle CM, Flurkey K, Nadon NL, Wilkinson JE, Frenkel K, Carter CS, et al. 2009. Rapamycin fed late in life extends lifespan in genetically heterogeneous mice. Nature 460:392–395.

Herman D, Jenssen K, Burnett R, Soragni E, Perlman SL, Gottesfeld JM. 2006. Histone deacetylase inhibitors reverse gene silencing in Friedreich's ataxia. Nat. Chem. Biol. 2:551–558.

He Y, Alam SL, Proteasa SV, Zhang Y, Lesuisse E, Dancis A, Stemmler TL. 2004. Yeast frataxin solution structure, iron binding, and ferrochelatase interaction. Biochemistry (Mosc.) 43:16254–16262.

Hick A, Wattenhofer-Donzé M, Chintawar S, Tropel P, Simard JP, Vaucamps N, Gall D, Lambot L, André C, Reutenauer L, et al. 2013. Neurons and cardiomyocytes derived from induced pluripotent stem cells as a model for mitochondrial defects in Friedreich's ataxia. Dis. Model. Mech. 6:608–621.

Hockly E, Richon VM, Woodman B, Smith DL, Zhou X, Rosa E, Sathasivam K, Ghazi-Noori S, Mahal A, Lowden PAS, et al. 2003. Suberoylanilide hydroxamic acid, a histone deacetylase inhibitor, ameliorates motor deficits in a mouse model of Huntington's disease. Proc. Natl. Acad. Sci. U. S. A. 100:2041–2046.

Hsu T-C, Wang C-K, Yang C-Y, Lee L-C, Hsieh-Li H-M, Ro L-S, Chen C-M, Lee-Chen G-J, Su M-T. 2014. Deactivation of TBP contributes to SCA17 pathogenesis. Hum. Mol. Genet. 23:6878–6893.

Huang ML-H, Lane DJR, Richardson DR. 2011. Mitochondrial Mayhem: The Mitochondrion as a Modulator of Iron Metabolism and Its Role in Disease. Antioxid. Redox Signal. 15:3003–3019.

Iannuzzi C, Adinolfi S, Howes BD, Garcia-Serres R, Clémancey M, Latour J-M, Smulevich G, Pastore A. 2011. The role of CyaY in iron sulfur cluster assembly on the E. coli IscU scaffold protein. PloS One 6:e21992.

Iijima K, Liu H-P, Chiang A-S, Hearn SA, Konsolaki M, Zhong Y. 2004. Dissecting the pathological effects of human Abeta40 and Abeta42 in Drosophila: a potential model for Alzheimer's disease. Proc. Natl. Acad. Sci. U. S. A. 101:6623–6628.

International Human Genome Sequencing Consortium. 2004. Finishing the euchromatic sequence of the human genome. Nature 431:931–945.

Isaya G, O'Neill HA, Gakh O, Park S, Mantcheva R, Mooney SM. 2004. Functional studies of frataxin. Acta Paediatr. Oslo Nor. 1992 Suppl. 93:68–71; discussion 72–73.

Isnard R, Kalotka H, Dürr A, Cossée M, Schmitt M, Pousset F, Thomas D, Brice A, Koenig M, Komajda M. 1997. Correlation between left ventricular hypertrophy and GAA trinucleotide repeat length in Friedreich's ataxia. Circulation 95:2247–2249.

Jackson GR, Salecker I, Dong X, Yao X, Arnheim N, Faber PW, MacDonald ME, Zipursky SL. 1998. Polyglutamine-expanded human huntingtin transgenes induce degeneration of Drosophila photoreceptor neurons. Neuron 21:633–642.

Jackson GR, Wiedau-Pazos M, Sang T-K, Wagle N, Brown CA, Massachi S, Geschwind DH. 2002. Human wild-type tau interacts with wingless pathway components and produces neurofibrillary pathology in Drosophila. Neuron 34:509–519.

Jackson SM, Whitworth AJ, Greene JC, Libby RT, Baccam SL, Pallanck LJ, La Spada AR. 2005. A SCA7 CAG/CTG repeat expansion is stable in Drosophila melanogaster despite modulation of genomic context and gene dosage. Gene 347:35–41.

Jauslin ML, Meier T, Smith RAJ, Murphy MP. 2003. Mitochondria-targeted antioxidants protect Friedreich Ataxia fibroblasts from endogenous oxidative stress more effectively than untargeted antioxidants. FASEB J. Off. Publ. Fed. Am. Soc. Exp. Biol. 17:1972–1974.

Jin P, Zarnescu DC, Zhang F, Pearson CE, Lucchesi JC, Moses K, Warren ST. 2003. RNA-mediated neurodegeneration caused by the fragile X premutation rCGG repeats in Drosophila. Neuron 39:739–747.

Kaeberlein M, Powers RW, Steffen KK, Westman EA, Hu D, Dang N, Kerr EO, Kirkland KT, Fields S, Kennedy BK. 2005. Regulation of yeast replicative life span by TOR and Sch9 in response to nutrients. Science 310:1193–1196.

Kakhlon O, Manning H, Breuer W, Melamed-Book N, Lu C, Cortopassi G, Munnich A, Cabantchik ZI. 2008. Cell functions impaired by frataxin deficiency are restored by drug-mediated iron relocation. Blood 112:5219–5227.

Kapahi P, Zid BM, Harper T, Koslover D, Sapin V, Benzer S. 2004. Regulation of lifespan in Drosophila by modulation of genes in the TOR signaling pathway. Curr. Biol. CB 14:885–890.

Kim H-J, Raphael AR, LaDow ES, McGurk L, Weber RA, Trojanowski JQ, Lee VM-Y, Finkbeiner S, Gitler AD, Bonini NM. 2014. Therapeutic modulation of eIF2α phosphorylation rescues TDP-43 toxicity in amyotrophic lateral sclerosis disease models. Nat. Genet. 46:152–160.

Koeppen AH. 2013. Nikolaus Friedreich and degenerative atrophy of the dorsal columns of the spinal cord. J. Neurochem. 126 Suppl 1:4–10.

Koeppen AH, Kuntzsch EC, Bjork ST, Ramirez RL, Mazurkiewicz JE, Feustel PJ. 2013. Friedreich ataxia: metal dysmetabolism in dorsal root ganglia. Acta Neuropathol. Commun. 1:26.

Koeppen AH, Ramirez RL, Yu D, Collins SE, Qian J, Parsons PJ, Yang KX, Chen Z, Mazurkiewicz JE, Feustel PJ. 2012. Friedreich's ataxia causes redistribution of iron, copper, and zinc in the dentate nucleus. Cerebellum Lond. Engl. 11:845–860.

Kofman AE, McGraw MR, Payne CJ. 2012. Rapamycin increases oxidative stress response gene expression in adult stem cells. Aging 4:279–289.

Kondapalli KC, Kok NM, Dancis A, Stemmler TL. 2008. Drosophila frataxin: an iron chaperone during cellular Fe-S cluster bioassembly. Biochemistry (Mosc.) 47:6917–6927.

Koutnikova H, Campuzano V, Foury F, Dollé P, Cazzalini O, Koenig M. 1997. Studies of human, mouse and yeast homologues indicate a mitochondrial function for frataxin. Nat. Genet. 16:345–351.

Koutnikova H, Campuzano V, Koenig M. 1998. Maturation of wild-type and mutated frataxin by the mitochondrial processing peptidase. Hum. Mol. Genet. 7:1485–1489.

Kumari D, Biacsi RE, Usdin K. 2011. Repeat expansion affects both transcription initiation and elongation in friedreich ataxia cells. J. Biol. Chem. 286:4209–4215.

Ku S, Soragni E, Campau E, Thomas EA, Altun G, Laurent LC, Loring JF, Napierala M, Gottesfeld JM. 2010. Friedreich's ataxia induced pluripotent stem cells model intergenerational GAA·TTC triplet repeat instability. Cell Stem Cell 7:631–637.

Latouche M, Lasbleiz C, Martin E, Monnier V, Debeir T, Mouatt-Prigent A, Muriel M-P, Morel L, Ruberg M, Brice A, et al. 2007. A conditional pan-neuronal Drosophila model of spinocerebellar ataxia 7 with a reversible adult phenotype suitable for identifying modifier genes. J. Neurosci. Off. J. Soc. Neurosci. 27:2483–2492.

Lavara-Culebras E, Muñoz-Soriano V, Gómez-Pastor R, Matallana E, Paricio N. 2010. Effects of pharmacological agents on the lifespan phenotype of Drosophila DJ-1beta mutants. Gene 462:26–33.

Lawal HO, Terrell A, Lam HA, Djapri C, Jang J, Hadi R, Roberts L, Shahi V, Chou M-T, Biedermann T, et al. 2014. Drosophila modifier screens to identify novel neuropsychiatric drugs including aminergic agents for the possible treatment of Parkinson's disease and depression. Mol. Psychiatry 19:235–242.

Lee MG, Cho SJ, Yang JK, Song HK, Suh SW. 2000. Crystallization and preliminary X-ray crystallographic analysis of Escherichia coli CyaY, a structural homologue of human frataxin. Acta Crystallogr. D Biol. Crystallogr. 56:920–921.

Lee Y-K, Ho PW-L, Schick R, Lau Y-M, Lai W-H, Zhou T, Li Y, Ng K-M, Ho S-L, Esteban MA, et al. 2014. Modeling of Friedreich ataxia-related iron overloading cardiomyopathy using patient-specific-induced pluripotent stem cells. Pflüg. Arch. Eur. J. Physiol. 466:1831–1844.

Li DS, Ohshima K, Jiralerspong S, Bojanowski MW, Pandolfo M. 1999. Knock-out of the cyaY gene in Escherichia coli does not affect cellular iron content and sensitivity to oxidants. FEBS Lett. 456:13–16.

Li K, Besse EK, Ha D, Kovtunovych G, Rouault TA. 2008. Iron-dependent regulation of frataxin expression: implications for treatment of Friedreich ataxia. Hum. Mol. Genet. 17:2265–2273.

Lill R. 2009. Function and biogenesis of iron-sulphur proteins. Nature 460:831–838.

Li L, Voullaire L, Sandi C, Pook MA, Ioannou PA, Delatycki MB, Sarsero JP. 2013. Pharmacological screening using an FXN-EGFP cellular genomic reporter assay for the therapy of Friedreich ataxia. PloS One 8:e55940.

Lim F, Palomo GM, Mauritz C, Giménez-Cassina A, Illana B, Wandosell F, Díaz-Nido J. 2007a. Functional recovery in a Friedreich's ataxia mouse model by frataxin gene transfer using an HSV-1 amplicon vector. Mol. Ther. J. Am. Soc. Gene Ther. 15:1072–1078.

Lim F, Palomo GM, Mauritz C, Giménez-Cassina A, Illana B, Wandosell F, Díaz-Nido J. 2007b. Functional Recovery in a Friedreich's Ataxia Mouse Model by Frataxin Gene Transfer Using an HSV-1 Amplicon Vector. Mol. Ther. 15:1072–1078.

Liu J, Verma PJ, Evans-Galea MV, Delatycki MB, Michalska A, Leung J, Crombie D, Sarsero JP, Williamson R, Dottori M, et al. 2011. Generation of induced pluripotent stem cell lines from Friedreich ataxia patients. Stem Cell Rev. 7:703–713.

Liu Z, Wang X, Yu Y, Li X, Wang T, Jiang H, Ren Q, Jiao Y, Sawa A, Moran T, et al. 2008. A Drosophila model for LRRK2-linked parkinsonism. Proc. Natl. Acad. Sci. U. S. A. 105:2693–2698.

Llorens JV, Navarro JA, Martínez-Sebastián MJ, Baylies MK, Schneuwly S, Botella JA, Moltó MD. 2007. Causative role of oxidative stress in a Drosophila model of Friedreich ataxia. FASEB J. Off. Publ. Fed. Am. Soc. Exp. Biol. 21:333–344.

Lodi R, Cooper JM, Bradley JL, Manners D, Styles P, Taylor DJ, Schapira AH. 1999. Deficit of in vivo mitochondrial ATP production in patients with Friedreich ataxia. Proc. Natl. Acad. Sci. U. S. A. 96:11492–11495.

Loría F, Díaz-Nido J. 2015. Frataxin knockdown in human astrocytes triggers cell death and the release of factors that cause neuronal toxicity. Neurobiol. Dis. 76:1–12.

Lu C, Schoenfeld R, Shan Y, Tsai H-J, Hammock B, Cortopassi G. 2009. Frataxin deficiency induces Schwann cell inflammation and death. Biochim. Biophys. Acta 1792:1052–1061.

Manservigi R, Argnani R, Marconi P. 2010. HSV Recombinant Vectors for Gene Therapy. Open Virol. J. 4:123–156.

Martelli A, Napierala M, Puccio H. 2012. Understanding the genetic and molecular pathogenesis of Friedreich's ataxia through animal and cellular models. Dis. Model. Mech. 5:165–176.

Martelli A, Puccio H. 2014. Dysregulation of cellular iron metabolism in Friedreich ataxia: from primary iron-sulfur cluster deficit to mitochondrial iron accumulation. Drug Metab. Transp. 5:130.

McGurk L, Berson A, Bonini NM. 2015. Drosophila as an In Vivo Model for Human Neurodegenerative Disease. Genetics 201:377–402.

Meier T, Perlman SL, Rummey C, Coppard NJ, Lynch DR. 2012. Assessment of neurological efficacy of idebenone in pediatric patients with Friedreich's ataxia: data from a 6-month controlled study followed by a 12-month open-label extension study. J. Neurol. 259:284–291.

Menzies FM, Yenisetti SC, Min K-T. 2005. Roles of Drosophila DJ-1 in survival of dopaminergic neurons and oxidative stress. Curr. Biol. CB 15:1578–1582.

Meulener M, Whitworth AJ, Armstrong-Gold CE, Rizzu P, Heutink P, Wes PD, Pallanck LJ, Bonini NM. 2005. Drosophila DJ-1 mutants are selectively sensitive to environmental toxins associated with Parkinson's disease. Curr. Biol. CB 15:1572–1577.

Miranda CJ, Santos MM, Ohshima K, Smith J, Li L, Bunting M, Cossée M, Koenig M, Sequeiros J, Kaplan J, et al. 2002. Frataxin knockin mouse. FEBS Lett. 512:291–297.

Monrós E, Moltó MD, Martínez F, Cañizares J, Blanca J, Vílchez JJ, Prieto F, de Frutos R, Palau F. 1997. Phenotype correlation and intergenerational dynamics of the Friedreich ataxia GAA trinucleotide repeat. Am. J. Hum. Genet. 61:101–110.

Montermini L, Richter A, Morgan K, Justice CM, Julien D, Castellotti B, Mercier J, Poirier J, Capozzoli F, Bouchard JP, et al. 1997. Phenotypic variability in Friedreich ataxia: role of the associated GAA triplet repeat expansion. Ann. Neurol. 41:675–682.

Morgan TH. 1915. Localization of the Hereditary Material in the Germ Cells. Proc. Natl. Acad. Sci. U. S. A. 1:420–429.

Musco G, Stier G, Kolmerer B, Adinolfi S, Martin S, Frenkiel T, Gibson T, Pastore A. 2000. Towards a structural understanding of Friedreich's ataxia: the solution structure of frataxin. Struct. Lond. Engl. 1993 8:695–707.

Mutsuddi M, Marshall CM, Benzow KA, Koob MD, Rebay I. 2004. The spinocerebellar ataxia 8 noncoding RNA causes neurodegeneration and associates with staufen in Drosophila. Curr. Biol. CB 14:302–308.

Nair M, Adinolfi S, Pastore C, Kelly G, Temussi P, Pastore A. 2004. Solution structure of the bacterial frataxin ortholog, CyaY: mapping the iron binding sites. Struct. Lond. Engl. 1993 12:2037–2048.

Napoli E, Morin D, Bernhardt R, Buckpitt A, Cortopassi G. 2007. Hemin rescues adrenodoxin, heme a and cytochrome oxidase activity in frataxin-deficient oligodendroglioma cells. Biochim. Biophys. Acta 1772:773–780.

Navarro JA, Botella JA, Metzendorf C, Lind MI, Schneuwly S. 2015. Mitoferrin modulates iron toxicity in a Drosophila model of Friedreich's ataxia. Free Radic. Biol. Med. 85:71–82.

Navarro JA, Llorens JV, Soriano S, Botella JA, Schneuwly S, Martínez-Sebastián MJ, Moltó MD. 2011. Overexpression of human and fly frataxins in Drosophila provokes deleterious effects at biochemical, physiological and developmental levels. PloS One 6:e21017.

Navarro JA, Ohmann E, Sanchez D, Botella JA, Liebisch G, Moltó MD, Ganfornina MD, Schmitz G, Schneuwly S. 2010. Altered lipid metabolism in a Drosophila model of Friedreich's ataxia. Hum. Mol. Genet. 19:2828–2840.

Nixon RA. 2013. The role of autophagy in neurodegenerative disease. Nat. Med. 19:983–997.

Obis È, Irazusta V, Sanchís D, Ros J, Tamarit J. 2014. Frataxin deficiency in neonatal rat ventricular myocytes targets mitochondria and lipid metabolism. Free Radic. Biol. Med. 73:21–33.

Palau F, Espinós C. 2006. Autosomal recessive cerebellar ataxias. Orphanet J. Rare Dis. 1:47.

Pandolfo M, Arpa J, Delatycki MB, Le Quan Sang KH, Mariotti C, Munnich A, Sanz-Gallego I, Tai G, Tarnopolsky MA, Taroni F, et al. 2014. Deferiprone in

Friedreich ataxia: a 6-month randomized controlled trial. Ann. Neurol. 76:509–521.

Pandolfo M, Hausmann L. 2013. Deferiprone for the treatment of Friedreich's ataxia. J. Neurochem. 126:142–146.

Parkinson MH, Boesch S, Nachbauer W, Mariotti C, Giunti P. 2013. Clinical features of Friedreich's ataxia: classical and atypical phenotypes. J. Neurochem. 126 Suppl 1:103–117.

Park J, Al-Ramahi I, Tan Q, Mollema N, Diaz-Garcia JR, Gallego-Flores T, Lu H-C, Lagalwar S, Duvick L, Kang H, et al. 2013. RAS-MAPK-MSK1 pathway modulates ataxin 1 protein levels and toxicity in SCA1. Nature 498:325–331.

Park J, Kim SY, Cha G-H, Lee SB, Kim S, Chung J. 2005. Drosophila DJ-1 mutants show oxidative stress-sensitive locomotive dysfunction. Gene 361:133–139.

Park J, Lee SB, Lee S, Kim Y, Song S, Kim S, Bae E, Kim J, Shong M, Kim J-M, et al. 2006. Mitochondrial dysfunction in Drosophila PINK1 mutants is complemented by parkin. Nature 441:1157–1161.

Pastore A, Puccio H. 2013. Frataxin: a protein in search for a function. J. Neurochem. 126 Suppl 1:43–52.

Pastore A, Tozzi G, Gaeta LM, Bertini E, Serafini V, Di Cesare S, Bonetto V, Casoni F, Carrozzo R, Federici G, et al. 2003. Actin glutathionylation increases in fibroblasts of patients with Friedreich's ataxia: a potential role in the pathogenesis of the disease. J. Biol. Chem. 278:42588–42595.

Patel PH, Tamanoi F. 2006. Increased Rheb-TOR signaling enhances sensitivity of the whole organism to oxidative stress. J. Cell Sci. 119:4285–4292.

Perdomini M, Belbellaa B, Monassier L, Reutenauer L, Messaddeq N, Cartier N, Crystal RG, Aubourg P, Puccio H. 2014. Prevention and reversal of severe mitochondrial cardiomyopathy by gene therapy in a mouse model of Friedreich's ataxia. Nat. Med. 20:542–547.

Pianese L, Cavalcanti F, Michele GD, Filla A, Campanella G, Calabrese O, Castaldo I, Monticelli A, Cocozza S. 1997. The effect of parental gender on the GAA dynamic mutation in the FRDA gene. Am. J. Hum. Genet. 60:460.

Pianese L, Tammaro A, Turano M, De Biase I, Monticelli A, Cocozza S. 2002. Identification of a novel transcript of X25, the human gene involved in Friedreich ataxia. Neurosci. Lett. 320:137–140.

Piemonte F, Pastore A, Tozzi G, Tagliacozzi D, Santorelli FM, Carrozzo R, Casali C, Damiano M, Federici G, Bertini E. 2001. Glutathione in blood of patients with Friedreich's ataxia. Eur. J. Clin. Invest. 31:1007–1011.

Pineda M, Arpa J, Montero R, Aracil A, Domínguez F, Galván M, Mas A, Martorell L, Sierra C, Brandi N, et al. 2008. Idebenone treatment in paediatric and adult patients with Friedreich ataxia: long-term follow-up. Eur. J. Paediatr. Neurol. EJPN Off. J. Eur. Paediatr. Neurol. Soc. 12:470–475.

Pollard LM, Sharma R, Gómez M, Shah S, Delatycki MB, Pianese L, Monticelli A, Keats BJB, Bidichandani SI. 2004. Replication-mediated instability of the GAA triplet repeat mutation in Friedreich ataxia. Nucleic Acids Res. 32:5962–5971.

Pook MA, Al-Mahdawi S, Carroll CJ, Cossée M, Puccio H, Lawrence L, Clark P, Lowrie MB, Bradley JL, Cooper JM, et al. 2001. Rescue of the Friedreich's ataxia knockout mouse by human YAC transgenesis. Neurogenetics 3:185–193.

Puccio H, Simon D, Cossée M, Criqui-Filipe P, Tiziano F, Melki J, Hindelang C, Matyas R, Rustin P, Koenig M. 2001. Mouse models for Friedreich ataxia exhibit cardiomyopathy, sensory nerve defect and Fe-S enzyme deficiency followed by intramitochondrial iron deposits. Nat. Genet. 27:181–186.

Radisky DC, Babcock MC, Kaplan J. 1999. The yeast frataxin homologue mediates mitochondrial iron efflux. Evidence for a mitochondrial iron cycle. J. Biol. Chem. 274:4497–4499.

Rea SL, Ventura N, Johnson TE. 2007. Relationship between mitochondrial electron transport chain dysfunction, development, and life extension in Caenorhabditis elegans. PLoS Biol. 5:e259.

Reiter LT, Potocki L, Chien S, Gribskov M, Bier E. 2001. A systematic analysis of human disease-associated gene sequences in Drosophila melanogaster. Genome Res. 11:1114–1125.

Ristow M, Mulder H, Pomplun D, Schulz TJ, Müller-Schmehl K, Krause A, Fex M, Puccio H, Müller J, Isken F, et al. 2003. Frataxin deficiency in pancreatic islets causes diabetes due to loss of beta cell mass. J. Clin. Invest. 112:527–534.

Robida-Stubbs S, Glover-Cutter K, Lamming DW, Mizunuma M, Narasimhan SD, Neumann-Haefelin E, Sabatini DM, Blackwell TK. 2012. TOR signaling and rapamycin influence longevity by regulating SKN-1/Nrf and DAF-16/FoxO. Cell Metab. 15:713–724.

Romero E, Cha G-H, Verstreken P, Ly CV, Hughes RE, Bellen HJ, Botas J. 2008. Suppression of neurodegeneration and increased neurotransmission caused by expanded full-length huntingtin accumulating in the cytoplasm. Neuron 57:27–40.

Rötig A, de Lonlay P, Chretien D, Foury F, Koenig M, Sidi D, Munnich A, Rustin P. 1997. Aconitase and mitochondrial iron-sulphur protein deficiency in Friedreich ataxia. Nat. Genet. 17:215–217.

Rubin GM. 2000. Biological annotation of the Drosophila genome sequence. Novartis Found. Symp. 229:79–82; discussion 82–83.

Rubin GM, Spradling AC. 1982. Genetic transformation of Drosophila with transposable element vectors. Science 218:348–353.

Runko AP, Griswold AJ, Min K-T. 2008. Overexpression of frataxin in the mitochondria increases resistance to oxidative stress and extends lifespan in Drosophila. FEBS Lett. 582:715–719.

Saccà F, Piro R, De Michele G, Acquaviva F, Antenora A, Carlomagno G, Cocozza S, Denaro A, Guacci A, Marsili A, et al. 2011. Epoetin alfa increases frataxin production in Friedreich's ataxia without affecting hematocrit. Mov. Disord. Off. J. Mov. Disord. Soc. 26:739–742.

Sakamoto N, Chastain PD, Parniewski P, Ohshima K, Pandolfo M, Griffith JD, Wells RD. 1999. Sticky DNA: self-association properties of long GAA.TTC repeats in R.R.Y triplex structures from Friedreich's ataxia. Mol. Cell 3:465–475.

Sandi C, Sandi M, Jassal H, Ezzatizadeh V, Anjomani-Virmouni S, Al-Mahdawi S, Pook MA. 2014. Generation and Characterisation of Friedreich Ataxia YG8R Mouse Fibroblast and Neural Stem Cell Models. PLoS ONE 9:e89488.

Santos MM, Ohshima K, Pandolfo M. 2001. Frataxin deficiency enhances apoptosis in cells differentiating into neuroectoderm. Hum. Mol. Genet. 10:1935–1944.

Sarsero JP, Li L, Wardan H, Sitte K, Williamson R, Ioannou PA. 2003. Upregulation of expression from the FRDA genomic locus for the therapy of Friedreich ataxia. J. Gene Med. 5:72–81.

Satterfield TF, Jackson SM, Pallanck LJ. 2002. A Drosophila homolog of the polyglutamine disease gene SCA2 is a dosage-sensitive regulator of actin filament formation. Genetics 162:1687–1702.

Saveliev A, Everett C, Sharpe T, Webster Z, Festenstein R. 2003. DNA triplet repeats mediate heterochromatin-protein-1-sensitive variegated gene silencing. Nature 422:909–913.

Schiavi A, Maglioni S, Palikaras K, Shaik A, Strappazzon F, Brinkmann V, Torgovnick A, Castelein N, De Henau S, Braeckman BP, et al. 2015. Iron-Starvation-Induced Mitophagy Mediates Lifespan Extension upon Mitochondrial Stress in C. elegans. Curr. Biol. CB 25:1810–1822.

Schiavi A, Torgovnick A, Kell A, Megalou E, Castelein N, Guccini I, Marzocchella L, Gelino S, Hansen M, Malisan F, et al. 2013. Autophagy induction extends lifespan and reduces lipid content in response to frataxin silencing in C. elegans. Exp. Gerontol. 48:191–201.

Schmucker S, Argentini M, Carelle-Calmels N, Martelli A, Puccio H. 2008. The in vivo mitochondrial two-step maturation of human frataxin. Hum. Mol. Genet. 17:3521–3531.

Schmucker S, Martelli A, Colin F, Page A, Wattenhofer-Donzé M, Reutenauer L, Puccio H. 2011. Mammalian frataxin: an essential function for cellular viability through an interaction with a preformed ISCU/NFS1/ISD11 iron-sulfur assembly complex. PloS One 6:e16199.

Schulz JB, Dehmer T, Schöls L, Mende H, Hardt C, Vorgerd M, Bürk K, Matson W, Dichgans J, Beal MF, et al. 2000. Oxidative stress in patients with Friedreich ataxia. Neurology 55:1719–1721.

Schulz JB, Di Prospero NA, Fischbeck K. 2009. Clinical experience with high-dose idebenone in Friedreich ataxia. J. Neurol. 256 Suppl 1:42–45.

Seguin A, Bayot A, Dancis A, Rogowska-Wrzesinska A, Auchère F, Camadro J-M, Bulteau A-L, Lesuisse E. 2009. Overexpression of the yeast frataxin homolog (Yfh1): contrasting effects on iron-sulfur cluster assembly, heme synthesis and resistance to oxidative stress. Mitochondrion 9:130–138.

Seyer L, Greeley N, Foerster D, Strawser C, Gelbard S, Dong Y, Schadt K, Cotticelli MG, Brocht A, Farmer J, et al. 2015. Open-label pilot study of interferon gamma-1b in Friedreich ataxia. Acta Neurol. Scand. 132:7–15.

Seznec H, Simon D, Bouton C, Reutenauer L, Hertzog A, Golik P, Procaccio V, Patel M, Drapier J-C, Koenig M, et al. 2005. Friedreich ataxia: the oxidative stress paradox. Hum. Mol. Genet. 14:463–474.

Sharma R, Bhatti S, Gomez M, Clark RM, Murray C, Ashizawa T, Bidichandani SI. 2002. The GAA triplet-repeat sequence in Friedreich ataxia shows a high level of somatic instability in vivo, with a significant predilection for large contractions. Hum. Mol. Genet. 11:2175–2187.

Shidara Y, Hollenbeck PJ. 2010. Defects in Mitochondrial Axonal Transport and Membrane Potential without Increased Reactive Oxygen Species Production in a Drosophila Model of Friedreich Ataxia. J. Neurosci. 30:11369–11378.

Simon D, Seznec H, Gansmuller A, Carelle N, Weber P, Metzger D, Rustin P, Koenig M, Puccio H. 2004. Friedreich Ataxia Mouse Models with Progressive Cerebellar and Sensory Ataxia Reveal Autophagic Neurodegeneration in Dorsal Root Ganglia. J. Neurosci. 24:1987–1995.

Sohn Y-S, Breuer W, Munnich A, Cabantchik ZI. 2008. Redistribution of accumulated cell iron: a modality of chelation with therapeutic implications. Blood 111:1690–1699.

Soriano S, Llorens JV, Blanco-Sobero L, Gutiérrez L, Calap-Quintana P, Morales MP, Moltó MD, Martínez-Sebastián MJ. 2013. Deferiprone and idebenone rescue frataxin depletion phenotypes in a Drosophila model of Friedreich's ataxia. Gene 521:274–281.

Steffan JS, Bodai L, Pallos J, Poelman M, McCampbell A, Apostol BL, Kazantsev A, Schmidt E, Zhu YZ, Greenwald M, et al. 2001. Histone deacetylase inhibitors arrest polyglutamine-dependent neurodegeneration in Drosophila. Nature 413:739–743.

Stehling O, Elsässer H-P, Brückel B, Mühlenhoff U, Lill R. 2004. Iron-sulfur protein maturation in human cells: evidence for a function of frataxin. Hum. Mol. Genet. 13:3007–3015.

Sturm B, Bistrich U, Schranzhofer M, Sarsero JP, Rauen U, Scheiber-Mojdehkar B, de Groot H, Ioannou P, Petrat F. 2005. Friedreich's ataxia, no changes in mitochondrial labile iron in human lymphoblasts and fibroblasts: a decrease in antioxidative capacity? J. Biol. Chem. 280:6701–6708.

Sturm B, Helminger M, Steinkellner H, Heidari MM, Goldenberg H, Scheiber-Mojdehkar B. 2010. Carbamylated erythropoietin increases frataxin independent from the erythropoietin receptor. Eur. J. Clin. Invest. 40:561–565.

Sturm B, Stupphann D, Kaun C, Boesch S, Schranzhofer M, Wojta J, Goldenberg H, Scheiber-Mojdehkar B. 2005. Recombinant human erythropoietin: effects on frataxin expression in vitro. Eur. J. Clin. Invest. 35:711–717.

Suzuki KT, Rui M, Ueda J, Ozawa T. 1996. Production of hydroxyl radicals by copper-containing metallothionein: roles as prooxidant. Toxicol. Appl. Pharmacol. 141:231–237.

Tettweiler G, Miron M, Jenkins M, Sonenberg N, Lasko PF. 2005. Starvation and oxidative stress resistance in Drosophila are mediated through the eIF4E-binding protein, d4E-BP. Genes Dev. 19:1840–1843.

Thackray AM, Muhammad F, Zhang C, Di Y, Jahn TR, Landgraf M, Crowther DC, Evers JF, Bujdoso R. 2012. Ovine PrP transgenic Drosophila show reduced locomotor activity and decreased survival. Biochem. J. 444:487–495.

Tomassini B, Arcuri G, Fortuni S, Sandi C, Ezzatizadeh V, Casali C, Condò I, Malisan F, Al-Mahdawi S, Pook M, et al. 2012. Interferon gamma upregulates frataxin and corrects the functional deficits in a Friedreich ataxia model. Hum. Mol. Genet. 21:2855–2861.

Tricoire H, Palandri A, Bourdais A, Camadro J-M, Monnier V. 2014. Methylene blue rescues heart defects in a Drosophila model of Friedreich's ataxia. Hum. Mol. Genet. 23:968–979.

Tsai C-L, Barondeau DP. 2010. Human frataxin is an allosteric switch that activates the Fe-S cluster biosynthetic complex. Biochemistry (Mosc.) 49:9132–9139.

Vaubel RA, Isaya G. 2013. Iron-sulfur cluster synthesis, iron homeostasis and oxidative stress in Friedreich ataxia. Mol. Cell. Neurosci. 55:50–61.

Vázquez-Manrique RP, González-Cabo P, Ros S, Aziz H, Baylis HA, Palau F. 2006. Reduction of Caenorhabditis elegans frataxin increases sensitivity to oxidative stress, reduces lifespan, and causes lethality in a mitochondrial complex II mutant. FASEB J. Off. Publ. Fed. Am. Soc. Exp. Biol. 20:172–174.

Vellai T, Takacs-Vellai K, Zhang Y, Kovacs AL, Orosz L, Müller F. 2003. Genetics: influence of TOR kinase on lifespan in C. elegans. Nature 426:620.

Venken KJT, He Y, Hoskins RA, Bellen HJ. 2006. P[acman]: a BAC transgenic platform for targeted insertion of large DNA fragments in D. melanogaster. Science 314:1747–1751.

Ventura N, Rea S, Henderson ST, Condo I, Johnson TE, Testi R. 2005. Reduced expression of frataxin extends the lifespan of Caenorhabditis elegans. Aging Cell 4:109–112.

Vyas PM, Tomamichel WJ, Pride PM, Babbey CM, Wang Q, Mercier J, Martin EM, Payne RM. 2011 Nov 23. A TAT-Frataxin fusion protein increases lifespan and cardiac function in a conditional Friedreich's Ataxia mouse model. Hum. Mol. Genet.:ddr554.

Waldvogel D, van Gelderen P, Hallett M. 1999. Increased iron in the dentate nucleus of patients with Friedrich's ataxia. Ann. Neurol. 46:123–125.

Warrick JM, Morabito LM, Bilen J, Gordesky-Gold B, Faust LZ, Paulson HL, Bonini NM. 2005. Ataxin-3 suppresses polyglutamine neurodegeneration in Drosophila by a ubiquitin-associated mechanism. Mol. Cell 18:37–48.

Warrick JM, Paulson HL, Gray-Board GL, Bui QT, Fischbeck KH, Pittman RN, Bonini NM. 1998. Expanded polyglutamine protein forms nuclear inclusions and causes neural degeneration in Drosophila. Cell 93:939–949.

Wells RD. 2008. DNA triplexes and Friedreich ataxia. FASEB J. Off. Publ. Fed. Am. Soc. Exp. Biol. 22:1625–1634.

Wittmann CW, Wszolek MF, Shulman JM, Salvaterra PM, Lewis J, Hutton M, Feany MB. 2001. Tauopathy in Drosophila: neurodegeneration without neurofibrillary tangles. Science 293:711–714.

Wong A, Yang J, Cavadini P, Gellera C, Lonnerdal B, Taroni F, Cortopassi G. 1999. The Friedreich's ataxia mutation confers cellular sensitivity to oxidant stress which is rescued by chelators of iron and calcium and inhibitors of apoptosis. Hum. Mol. Genet. 8:425–430.

Xia H, Cao Y, Dai X, Marelja Z, Zhou D, Mo R, Al-Mahdawi S, Pook MA, Leimkühler S, Rouault TA, et al. 2012. Novel frataxin isoforms may contribute to the pathological mechanism of Friedreich ataxia. PloS One 7:e47847.

Yang Y, Gehrke S, Haque ME, Imai Y, Kosek J, Yang L, Beal MF, Nishimura I, Wakamatsu K, Ito S, et al. 2005. Inactivation of Drosophila DJ-1 leads to impairments of oxidative stress response and phosphatidylinositol 3-kinase/Akt signaling. Proc. Natl. Acad. Sci. U. S. A. 102:13670–13675.

Yang Y, Gehrke S, Imai Y, Huang Z, Ouyang Y, Wang J-W, Yang L, Beal MF, Vogel H, Lu B. 2006. Mitochondrial pathology and muscle and dopaminergic neuron degeneration caused by inactivation of Drosophila Pink1 is rescued by Parkin. Proc. Natl. Acad. Sci. U. S. A. 103:10793–10798.

Ye Y, Fortini ME. 1999. Apoptotic activities of wild-type and Alzheimer's disease-related mutant presenilins in Drosophila melanogaster. J. Cell Biol. 146:1351–1364.

Yoon T, Cowan JA. 2003. Iron-sulfur cluster biosynthesis. Characterization of frataxin as an iron donor for assembly of [2Fe-2S] clusters in ISU-type proteins. J. Am. Chem. Soc. 125:6078–6084.

Yoon T, Cowan JA. 2004. Frataxin-mediated iron delivery to ferrochelatase in the final step of heme biosynthesis. J. Biol. Chem. 279:25943–25946.

Zarse K, Schulz TJ, Birringer M, Ristow M. 2007. Impaired respiration is positively correlated with decreased life span in Caenorhabditis elegans models of Friedreich Ataxia. FASEB J. Off. Publ. Fed. Am. Soc. Exp. Biol. 21:1271–1275.